

International
Progress Report

IPR-00-16

Äspö Hard Rock Laboratory

Äspö Task Force on Modelling of Grounwater Flow and Transport of Solutes

Proceedings from the 13th task force meeting
at Carlsbad, NM, USA, February 8-11, 2000

Part 2 of 2: Task 5 contributions

Mansueto Morosini

Svensk Kärnbränslehantering AB

May 2000

Svensk Kärnbränslehantering AB

Swedish Nuclear Fuel
and Waste Management Co
Box 5864
SE-102 40 Stockholm Sweden
Tel 08-459 84 00
+46 8 459 84 00
Fax 08-661 57 19
+46 8 661 57 19



**Äspö Hard Rock
Laboratory**

Äspö Hard Rock Laboratory

Äspö Task Force on Modelling of Groundwater Flow and Transport of Solutes

**Proceedings from the 13th task force meeting
at Carlsbad, NM, USA, February 8-11, 2000**

Part 2 of 2: Task 5 contributions

Mansueto Morosini

Svensk Kärnbränslehantering AB

May 2000

Keywords: Groundwater flow, solute transport, tracer test, fractured rock, underground laboratory, radionuclide, stochastic modelling, deterministic modelling.

This report concerns a study which was conducted for SKB. The conclusions and viewpoints presented in the report are those of the author(s) and do not necessarily coincide with those of the client.

Appendix B – Task 5 Modelling results

- Groundwater mixing and geochemical reactions – an inverse modelling approach. A. Luukkonen, VTT
- M3 predictions of the groundwater changes associated with the construction of Äspö HRL M. Laaksoharju, INTERA
- The origin and composition of groundwater leaking into the Äspö tunnel. U. Svensson, CFE
- Integration of hydrogeology and hydrochemistry at the Äspö site. J. Molinero, ULC
- A hydraulic transport model of the large-scale fracture system in the Äspö Hard Rock Laboratory consisting of ten intersecting macro-elements L. Liedtke, BGR
- Geochemical Modelling Plan and Preliminary Results T. Hasegawa, CRIEPI
- Executive summary of Task 5 modelling W. Dershowitz, Golder
- Modelling work of CEA/DMT for Task 5 C. Grenier, CEA
- Task 5 modelling J. Wendling, ANTEA
- Task 5 Modelling, Executive Summary D. Billaux, ITASCA
- Comments on predictions I. Rhén, VBB-VIAK
- Comments by appointed Task 5 reviewer. A. Bath, IntelliSci.

Modelling of the REDOX Zone experiment J. Molinero, ULC

**Groundwater mixing and geochemical reactions -
an inverse modelling approach**

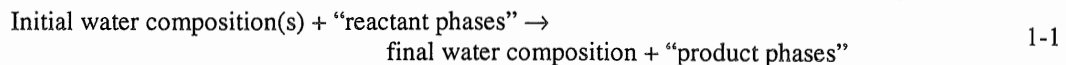
A Luukkonen (VTT)

GROUNDWATER MIXING AND GEOCHEMICAL REACTIONS – AN INVERSE-MODELLING APPROACH

Ari Luukkonen, VTT Communities & Infrastructure

The inverse-modelling method

The inverse-modelling method is a combination of speciation modelling and mole-balance modelling. Speciation modelling, petrographic observations, reactions expected to dominate in a groundwater system, and isotopic data available provide constraints for inverse studies. In accordance with these constraints, mole-balance modelling produces quantitative geochemical reactions that reproduce the compositions of the samples and are consistent with any constraints on the reactant phase (e.g. Parkhurst & Plummer 1993, Runnells 1993, Plummer et al. 1994, Parkhurst 1997, Parkhurst & Appelo 1999). The processes of dissolution and precipitation of minerals, gases, and organic matter in addition to ion exchange and oxidation/reduction processes can be presented with the following mole-balance formula:



Calculation constraints

The geochemical mole-transfer reactions, considered here, are dissolution/precipitation of calcite, consumption of organic matter (CH₂O), dissolution of goethite, precipitation of pyrite, and in detail undefined ion exchange processes among pairs Na-Ca, Na-Mg and Na-Fe. Mole-balance calculations are applicable only for steady-state conditions. In the undisturbed conditions it can be assumed that all above reactions are active, even the slow dissolution of goethite coupled with reduction of iron. In the disturbed conditions hydrological transport is considered to be so fast that goethite dissolution is not possible.

From *the analytical data delivered*, reported values on pH, Na, Ca, Mg, Fe_{tot}, HCO₃, Cl, SO₄, and δ¹⁸O for each sample were used for modellings. In the inverse calculations Cl- and ¹⁸O-concentrations are considered as conservative parameters, i.e. these two parameters essentially define mixing fractions among one, two or three initial water samples.

Based on the interpretations of the geochemical data a simplified history of the Äspö site was constructed (Fig. 1). *The recent reference water types* (Fig. 1d) considered, are the currently recharging meteoric water and the seawater recharging into the bedrock from the present Baltic Sea. *The Litorina stage* (Fig. 1c - begun about 7,500–7,000 BP) preceding the present stage is characterised with samples contaminated significantly with the Litorina Sea and postglacial altered marine water. Both of these reference water types have higher salinities than the present Baltic Sea and high δ¹⁸O values. During *the glacial stage* (Fig. 1b) melt water from the Pleistocene ice sheet is considered as the dominant source of water recharging into bedrock (cf. Pitkänen et al. 1999). *The preglacial stage* (Fig. 1a) is the oldest water-recharging period currently considered.

The clear signs of the “preglacial altered” water type are not found and its composition is based on reasoning of the Quaternary history of the Äspö region, and on argumentation of the estimated glacial melt composition and the most glacial type samples analysed from the Äspö Island.

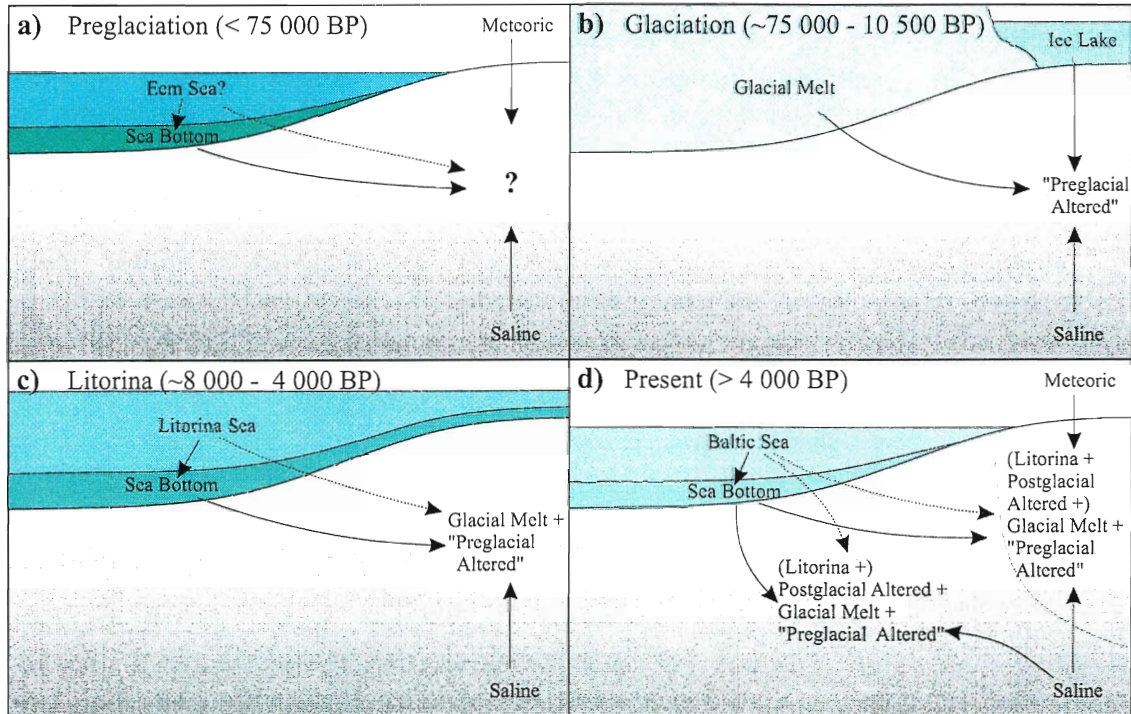


Figure 1. Schematic Quaternary history of the Äspö area. The interpretation is based on the analyses of geochemical data and on the other interpretations of the Quaternary history of the Fennoscandian Shield (e.g. Eronen 1988, Laaksoharju & Wallin 1997). Only periods considered significant for groundwater evolution in the Äspö site have been presented.

Calculation method

The inverse calculations are done in steps assuming that the steady-state assumption of chemical reactions is valid. In practice this means that a final water composition can be produced from a realistic set of initial water samples with small, moderate or otherwise feasible mole-transfers. The directions of dissolution/precipitation reactions form an important basis for judgement of acceptability of the steady state condition. Judgements depend strongly on what kind of initial water samples are being mixed together. Say for example, if in the initial sample set the fresh seawater is the dominating member, we have to assume that the reactions taking place in the sea bottom sediments contribute strongly to net mole-transfers to be calculated (cf. Canfield et al. 1993, Wang & Van Chapellen 1996). In this case, strong consumption of organic matter, dissolution of calcite, dissolution of Ca and Fe from CaX_2 and FeX_2 /goethite, precipitation of Na and Mg to NaX and MgX_2 , and precipitation of pyrite can be expected.

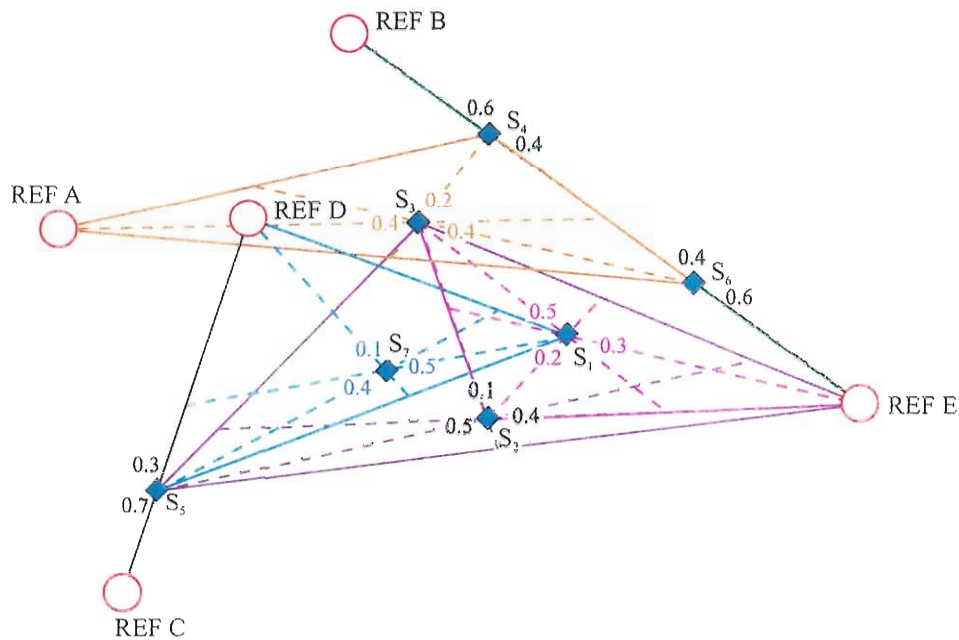


Figure 2. Diagrammatic presentation on stepwise calculation of reference water-type mixing fractions in given water samples. Samples used as initial waters for certain final water are related together with solid tie-lines. The broken lines illustrate approximate euclidean distance of initial waters from a final water sample. Solid and broken lines, and given mixing fractions, related to same final water sample, are presented with same colour.

The idea of the calculation process is presented in Figure 2. In the diagram, there are five reference water types (REF A ... REF E) and 7 water samples. The choice of steady-state steps is based on the identification of the geochemical affinities for each sample, and finding suitable initial water assemblage for each of these 7 samples (usually one or two suitable initial water samples exhibit somehow chemically kindred character towards final water). According to Figure 2, following steady-state steps are defined for the samples:

$S_1 = 0.2*S_2 + 0.5*S_3 + 0.3*REF E$	1-2
$S_2 = 0.1*S_3 + 0.5*S_5 + 0.4*REF E$	1-3
$S_3 = 0.2*S_4 + 0.4*S_6 + 0.4*REF A$	1-4
$S_4 = 0.6*REF B + 0.4*REF E$	1-5
$S_5 = 0.7*REF C + 0.3*REF D$	1-6
$S_6 = 0.4*REF B + 0.6*REF E$	1-7
$S_7 = 0.5*S_1 + 0.4*S_5 + 0.1*REF D$	1-8

The calculation of mixing fractions of reference water types for each sample from equations 1-2...1-8 becomes straightforward. For all samples the results are:

$S_1 = 0.20 \cdot \text{REF A} + 0.15 \cdot \text{REF B} + 0.07 \cdot \text{REF C} + 0.03 \cdot \text{REF D} + 0.55 \cdot \text{REF E}$	1-9
$S_2 = 0.04 \cdot \text{REF A} + 0.03 \cdot \text{REF B} + 0.35 \cdot \text{REF C} + 0.15 \cdot \text{REF D} + 0.43 \cdot \text{REF E}$	1-10
$S_3 = 0.40 \cdot \text{REF A} + 0.28 \cdot \text{REF B} + 0.32 \cdot \text{REF E}$	1-11
$S_4 = 0.60 \cdot \text{REF B} + 0.40 \cdot \text{REF E}$	1-12
$S_5 = 0.70 \cdot \text{REF C} + 0.30 \cdot \text{REF D}$	1-13
$S_6 = 0.40 \cdot \text{REF B} + 0.60 \cdot \text{REF E}$	1-14
$S_7 = 0.10 \cdot \text{REF A} + 0.07 \cdot \text{REF B} + 0.32 \cdot \text{REF C} + 0.24 \cdot \text{REF D} + 0.27 \cdot \text{REF E}$	1-15

Results

Undisturbed conditions

The undisturbed samples, considered, have been sampled before January 1, 1991. In all, reference water mixing-fractions and mole-transfers of reacting phases have been calculated for 25 undisturbed samples. The present summary, however, outlines only how the mole-transfer reactions and reference water mixing-fractions are evaluated for the sample KAS03/-348.6m (day -868), and to the intermediate samples in the calculation chain towards the reference water types. A graphical illustration of the calculation chain is presented in Figure 3.

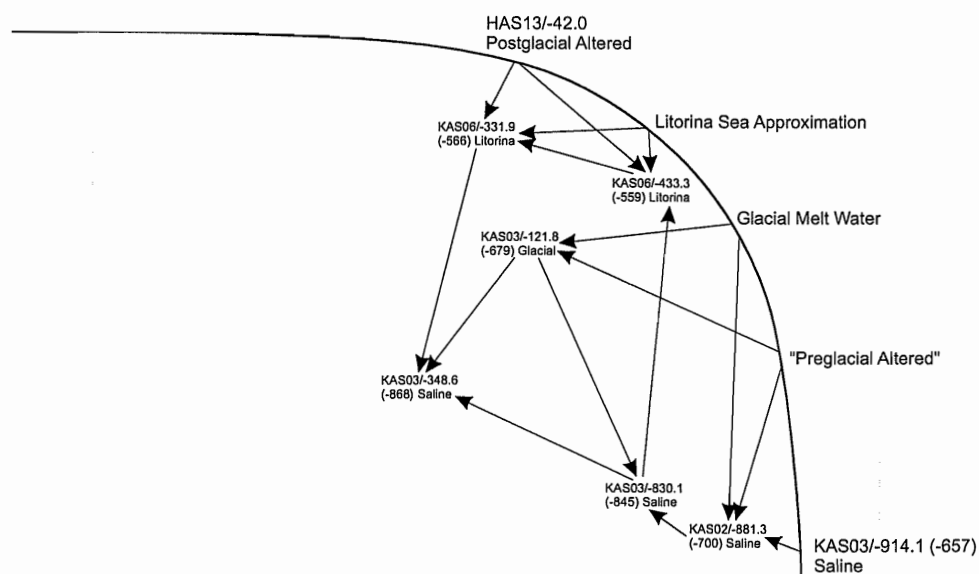


Figure 3. Hypothetical flow paths used in modelling of the sample KAS03/-348.6 (-868). The arch separates reference water types from the rest of the data and describes roughly the apparent age of reference water types.

The chained calculation starts by finding suitable set of initial water samples for the sample KAS03/-348.6, and continues by finding new sets of initial water samples for previous initial water samples, and so on. The steps are ultimately extended to the reference water types, and then the reference water mixing fractions for all samples in the chain can be solved. The results of the calculations among the chain leading to sample KAS03/-348.6 are presented in Tables 1 and 2.

Table 1. Summary of mole-transfer results leading to sample KAS03/-348.6 (-868). The reference days given with the sample ID indicate the sampling date and refer to date Jan. 1, 1991. The upper part shows mixing fractions of initial water samples for each final water. All mole- and redox-transfers are in mmol/l. A negative value indicates precipitation/cation uptake and a positive value of dissolution/cation release. The minimum and maximum fractions and mole-transfers possible within given analytical uncertainties are denoted after the representative values.

		Final Water																		
Sample		KAS06/-331.9			KAS06/-433.3			KAS03/-121.8			KAS02/-881.3			KAS03/-830.1			KAS03/348.6			
Day		-566			-559			-679			-700			-845			-868 (a)			
Initial Water	Litorina Sea	0.10	0.03	0.14	0.23	0.15	0.31													
	KAS06/-331.9	-566															0.09	0.06	0.10	
	KAS06/-433.3	-559	0.64	0.45	0.71															
	HAS13/-42.0	-547	0.26	0.16	0.51	0.50	0.36	0.59												
	Glacial Melt Water							0.68	0.68	0.68	0.10	0.03	0.14							
	KAS03/-121.8	-679										0.19	0.17	0.19	0.39	0.33	0.42			
	"Preglacial Altered"							0.32	0.32	0.32	0.07	0.00	0.14							
	KAS03/-914.1	-657										0.83	0.76	0.97						
	KAS02/-881.3	-700													0.81	0.81	0.83			
	KAS03/-830.1	-845				0.27	0.22	0.34										0.52	0.48	0.60
Transfers (mmol/l)																				
	Calcite	-0.03	-2.06	-0.03	-0.82	-4.37	-0.43	0.04	0.04	0.04	-0.28	-5.86	-0.15	-1.23	-2.31	-0.81	-0.46	-3.37	-0.37	
	CH ₂ O	0.00	0.00	2.10	0.12	0.06	3.71	0.02	0.02	0.03	0.04	0.02	5.82	1.09	0.65	2.15	0.07	0.05	2.99	
	NaX	2.59	0.62	6.44				1.15	0.83	1.49	0.00	0.0	8.2	0.00	0.0	1.4	0.53	0.43	3.7	
	CaX ₂				4.44	2.60	7.89				0.93	0.00	4.12	0.00	0.00	0.81				
	MgX ₂	-1.29	-2.74	-0.29	-3.93	-5.76	-2.19	-0.57	-0.74	-0.41	-0.75	-1.16	-0.36	0.66	0.43	0.87				
	Goethite	0.00	0.00	1.59	0.49	0.24	3.24				0.18	0.10	4.51	0.90	0.58	1.74	0.27	0.21	2.51	
	FeX ₂	0.00	-1.14	0.00	-0.51	-2.42	-0.25				-0.18	-3.17	-0.10	-0.66	-1.24	-0.43	-0.27	-1.83	-0.21	
	Pyrite	0.00	-0.49	0.00	0.00	-0.83	0.00	-0.01	-0.01	-0.01	0.00	-1.34	0.00	-0.25	-0.49	-0.14	0.00	-0.68	0.00	
Redox (mmol/l)																				
	Fe(3)	0.00			0.49			0.00			0.18			0.90			0.27			
	H(0)	0.00			0.00			-0.01			0.00			0.00			0.00			
	S(-2)													-0.49						

a) $\Delta^{18}\text{O} = 0.2$ in final

Table 2. Reference water type mixing fractions (in percent) in the calculation chain of undisturbed Äspö water samples leading to sample KAS03/-348.6 (-868). The sampling dates given refer to date 01.01.91. Estimated minimum and maximum fractions are noted after each representative value.

Sample	Day	Meteoric	Baltic Sea	Postgl. Alt.	Litorina Sea	Glacial Melt	"Pregl. Alt."	Saline	Sum					
KAS06/-331.9	-566			58.0	32.5 92.7	24.5	10.0 35.6	3.6	1.4 5.8	2.0	0.5 4.2	11.8	6.1 19.3	100.0
KAS06/-433.3	-559			49.7	36.4 59.1	23.1	15.2 30.9	5.7	3.1 8.1	3.2	1.2 5.9	18.4	13.5 27.0	100.0
KAS03/-121.8	-679							68.4	68.3 68.4	31.6	31.6 31.7			100.0
KAS02/-881.3	-700							9.9	3.2 13.8	7.1	0.0 14.0	83.0	75.7 96.8	100.0
KAS03/-830.1	-845							20.8	14.3 24.1	11.6	5.4 17.5	67.6	61.6 80.3	100.0
KAS03/-348.6	-868			5.5	2.0 9.4	2.3	0.6 3.6	37.6	29.5 43.6	18.4	13.1 24.2	36.2	30.0 50.0	100.0

Disturbed conditions

The effects of tunnel construction were monitored with many control points. Figure 4 shows an example how two control points in boreholes KAS03 and KAS07 plot in the Cl-¹⁸O field. According to Figure 4 samples from KAS03 seem to contain significant amounts glacial related water types, and there is also considerable variation of water composition in time. On the other hand, compositions in the KAS07 control point seem to remain stable with time. The reference water mixing fractions in the control points are solved utilising neighbouring undisturbed samples in the Cl-¹⁸O field. Undisturbed samples KAS03/-121.8, KAS02/-199.8, KAS03/-239.0, KAS03/-602.5 and KAS03/-830.1 have been used for solving mixing fractions and mole-transfers for KAS03 control point samples. In the case of KAS07 control point samples, undisturbed KAS06/-284.4, KAS02/-523.0, KAS03/-602.5 and KAS03/-830.1 samples have been used (cf. Fig. 4). The results of reference water mixing fraction calculations as a function of sampling date are shown in Figure 5.

Inverse calculations of disturbed samples produce a data set of mole-transfers that can be studied as a function of reference water mixing fractions. Figure 6 shows the mole-transfer processes in the samples with high fraction (over 50%) of fresh Baltic Sea water. As the fresh seawater fraction gets higher, increasing and significant mole-transfer reactions are needed. The extensive, organic activity driven, redox reactions are bound to happen mostly in the sea bottom sediments where the organic activity is strong enough.

Chemical reactions in hydrological simulations

The mixing fraction results of reference water types are considered as water conservative parameters similarly as for example Cl- or ¹⁸O-concentrations in groundwater. Mixing fractions can be transported like conservative parameters in hydrological simulations and mole-transfer results detected in the inverse calculations may be coupled indirectly to hydrological transport. The conservative transport results are corrected with trends (net mole-transfer vs. dominant reference water-type fraction) that have been solved earlier with known sample set.

As an example, we may assume that a hydrological simulation predicts 70% fresh Baltic Sea, 6% meteoric, 10% postglacial altered, 4% fresh Litorina Sea, 5% glacial melt, 3% "preglacial altered" and 2% saline reference water to a location in the hydrogeological model. By knowing the reference water compositions, an "uncorrected conservative water composition" can be calculated in accordance with percentages. Since the fresh seawater clearly dominates the simulated composition, Figure 6 can be used to correct the simulated "conservative water composition".

As a summary, *forward* groundwater mixing and transport modelling is based on two steps. The first step is conservative mixing and transport, and the second is a single net reaction step based on earlier inverse-modelling calculation results.

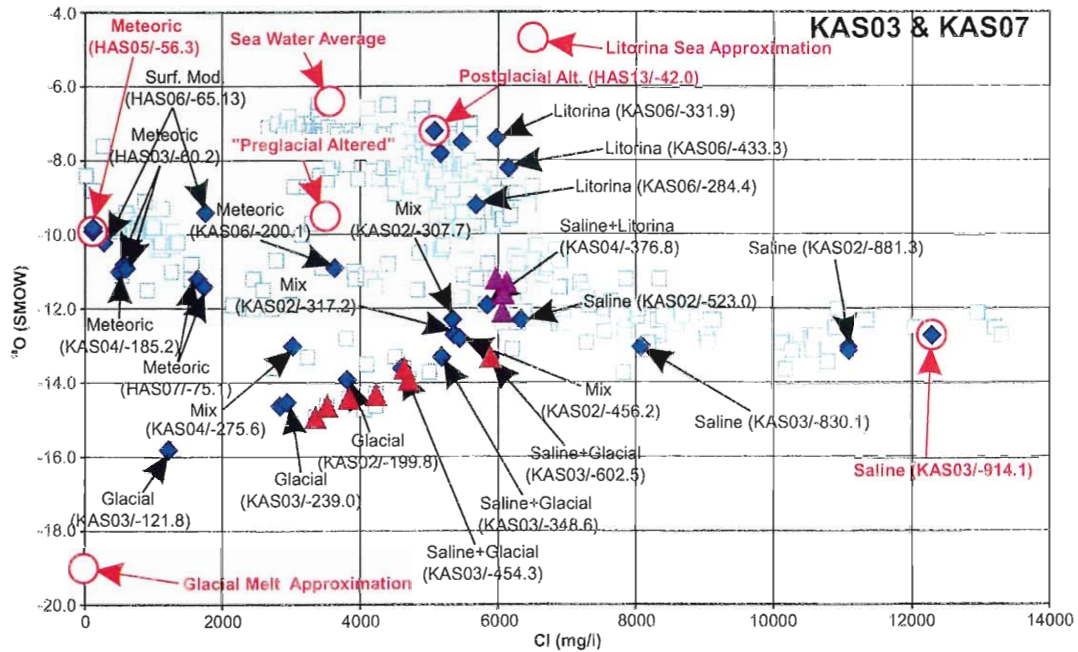


Figure 4. Disturbed KAS03 (red triangles), and KAS07 (purple triangles) samples in the Cl-¹⁸O field. Undisturbed samples are shown with blue diamonds and disturbed samples not considered with grey squares.

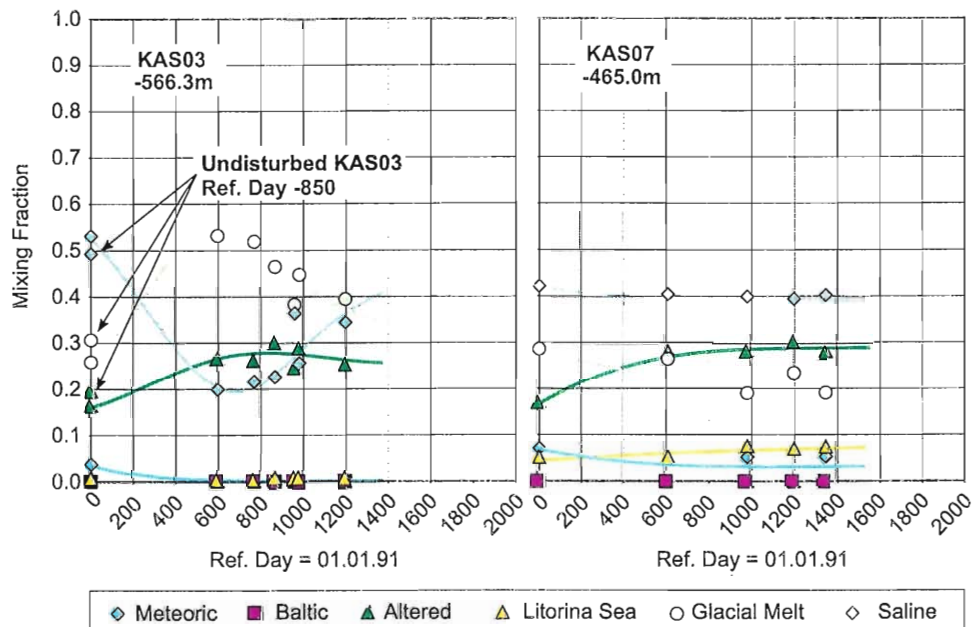


Figure 5. Reference water type mixing fractions in control points KAS03 and KAS07 as a function of time. Regressions drawn in diagrams are visual approximations.

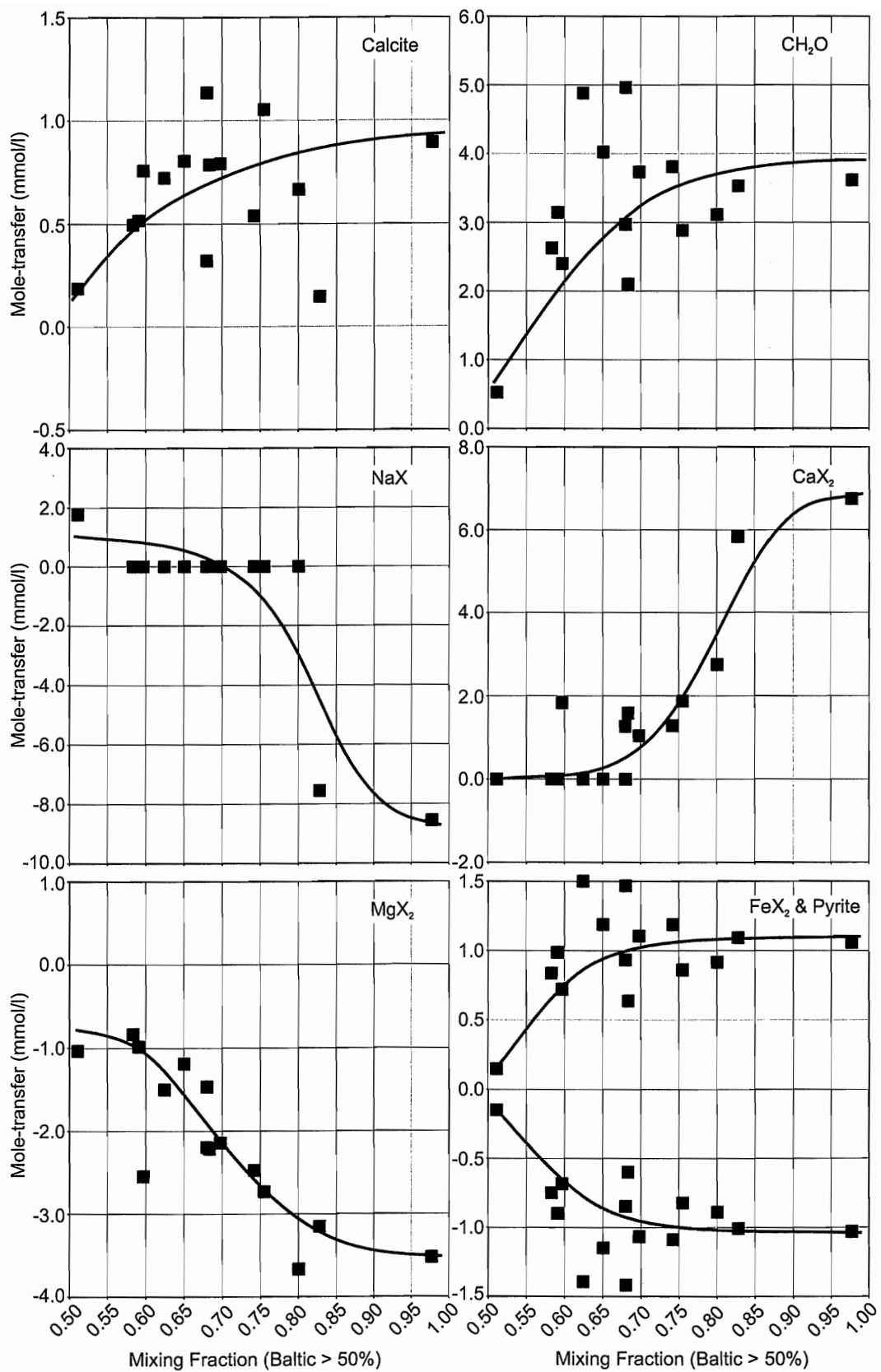


Figure 6. Mole-transfers as a function of fresh Baltic Sea fraction in samples containing over 50% of seawater. Drawn regressions are visual approximations. Pyrite mole-transfers are shown with brown squares.

References

- Canfield, D.E., Thamdrup, B. & Hansen, J.W., 1993. The anaerobic degradation of organic matter in Danish coastal sediments: Iron reduction, manganese reduction and sulfate reduction. *Geochimica et Cosmochimica Acta* 57, 3867–3883.
- Eronen, M., 1988. A scrutiny of the late Quaternary history of the Baltic Sea. Geological Survey of Finland, Espoo. Special Paper 6, 11–18.
- Laaksoharju, M. & Wallin, B. (eds.), 1997. Evolution of the groundwater chemistry at the Äspö Hard Rock Laboratory. Proceedings of the second Äspö International Geochemistry Workshop, June 6-7, 1995. Swedish Nuclear Fuel and Waste Management Co. (SKB), Stockholm. International Cooperation Report 97-04.
- Parkhurst, D.L., 1997. Geochemical mole-balance modeling with uncertain data. *Water Resources Research* 33, 1957-1970.
- Parkhurst, D.L. & Appelo, C.A.J., 1999. User's guide to PHREEQC (Version 2) – A computer program for speciation, batch-reaction, one dimensional transport, and inverse geochemical calculations. U.S. Geological Survey, Denver. Water-Resources Investigations Report 99-4259. 312 p.
- Parkhurst, D.L. & Plummer, L.N., 1993. Geochemical models. In: (ed. Allen, W.M.) Regional ground-water quality. Van Nostrand Reinhold, New York, 199–225.
- Pitkänen, P., Luukkonen, A., Ruotsalainen, P., Leino-Forsman, H. & Vuorinen, U., 1999. Geochemical modelling of groundwater evolution and residence time at the Olkiluoto site. Posiva Oy, Helsinki. Report POSIVA 98-10. 184 p.
- Plummer, L.N., Prestemon, E.C., and Parkhurst, D.L., 1994, An interactive code (NETPATH) for modeling NET geochemical reactions along a flow PATH. Version 2.0. U.S. Geological Survey, Reston. Water-Resources Investigations Report 94-4169. 130 p.
- Runnells, D.D., 1993. Inorganic chemical processes and reactions. In: (ed. Allen, W.M.) Regional ground-water quality. Van Nostrand Reinhold, New York. 131–153.
- Wang, Y. & Van Cappellen, P., 1996. A multicomponent reactive transport model of early diagenesis: Application to redox cycling in coastal marine sediments. *Geochimica et Cosmochimica Acta* 60, 2993–3014.

**M3 predictions of the groundwater changes
associated with the construction of Äspö HRL**

M Laaksoharju, I Gurban and C Andersson (INTERA KB)

**CHEMICAL
MODELLING
WITH M3**

**HYDRODYNAMIC
MODELLING**

Mixing proportions
in observed points

Flow distribution

Interpolation of
mixing proportions

Mixing proportion
distribution in the
modelled domain

Origin and processes
in specific features

Backtracking

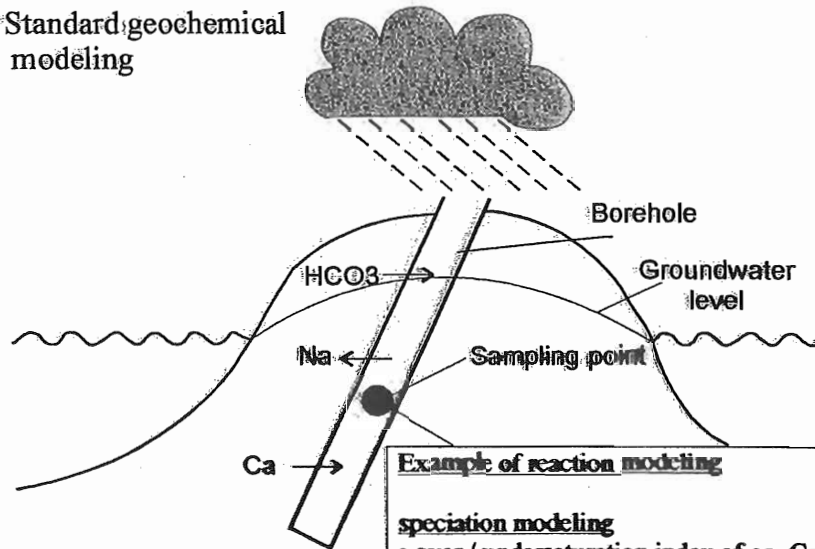
M3 on control point
data >2900 m

Prediction
2900-3600m

Boundary
conditions
Comparison
no calibration

Comparison
no calibration

a) Standard geochemical modeling



Example of reaction modeling

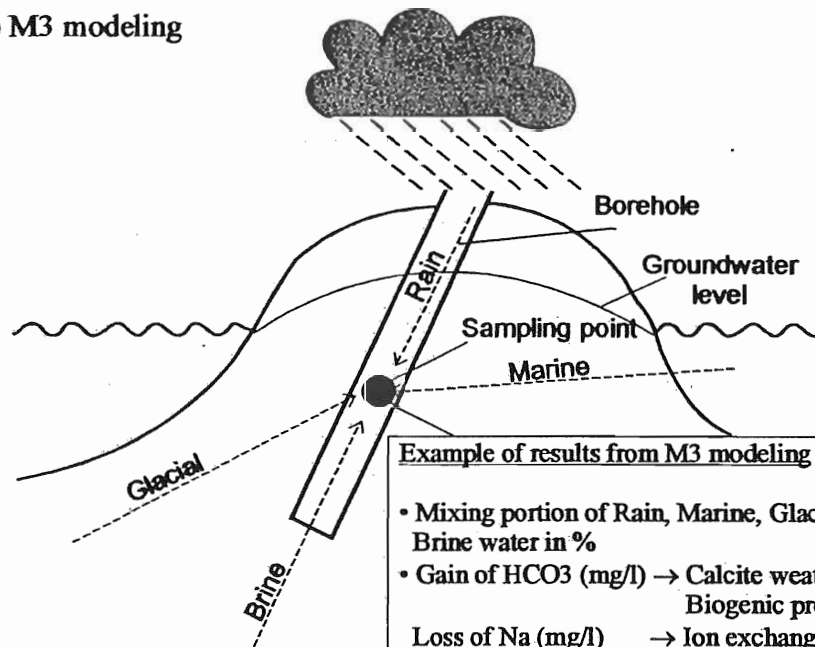
speciation modeling

- over / undersaturation index of eg. Calcite

massbalance modeling

- mixing portion (%) of samples in the same fracture zone / flow path
- extent of Calcite solution / precipitation
- extent of Na/Ca ion exchange

b) M3 modeling



Example of results from M3 modeling

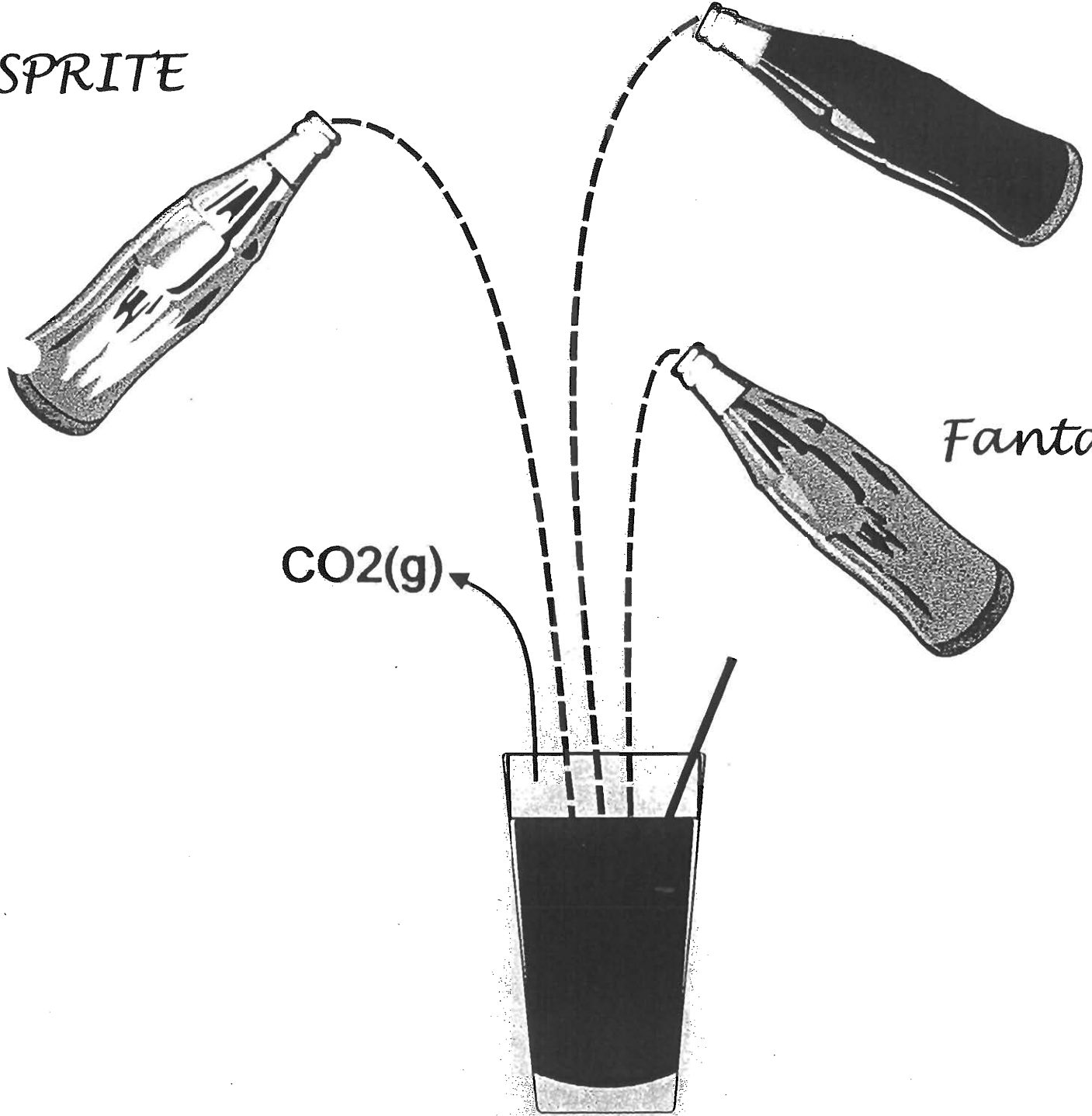
- Mixing portion of Rain, Marine, Glacial and Brine water in %
- Gain of HCO₃ (mg/l) → Calcite weathering
Biogenic processes
- Loss of Na (mg/l) → Ion exchange
- Gain of Ca (mg/l)

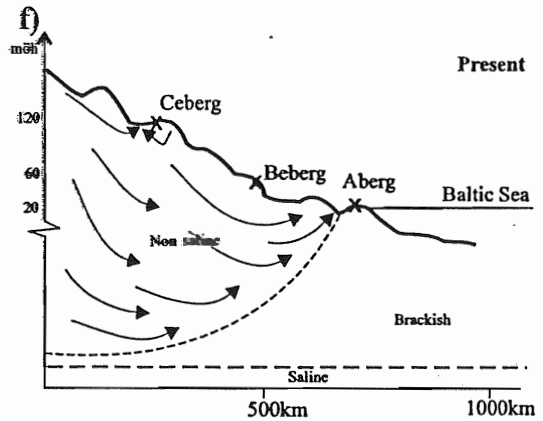
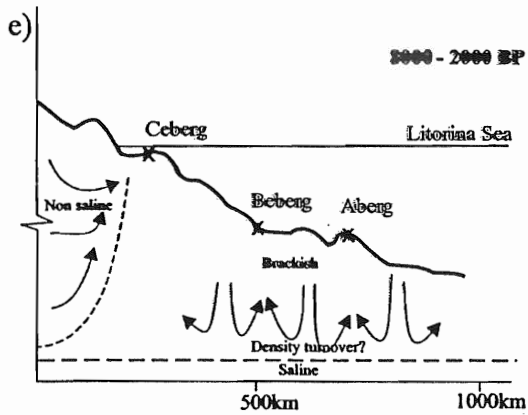
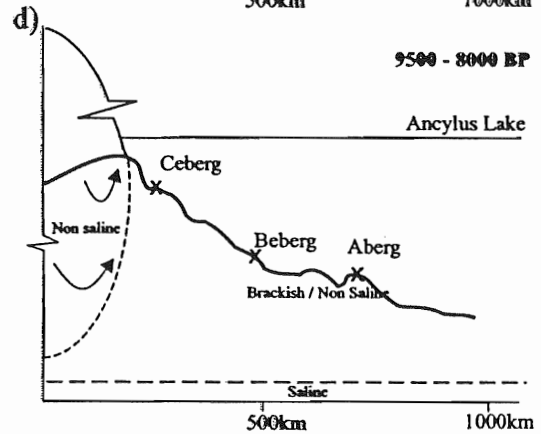
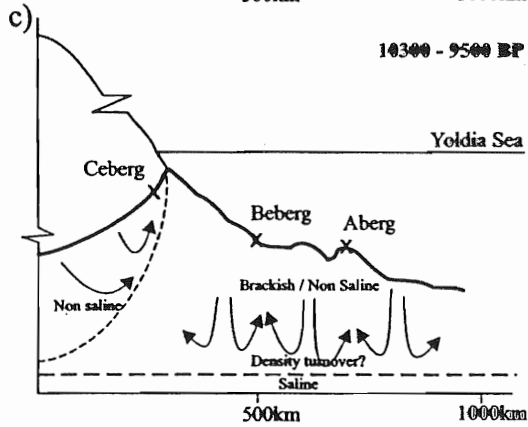
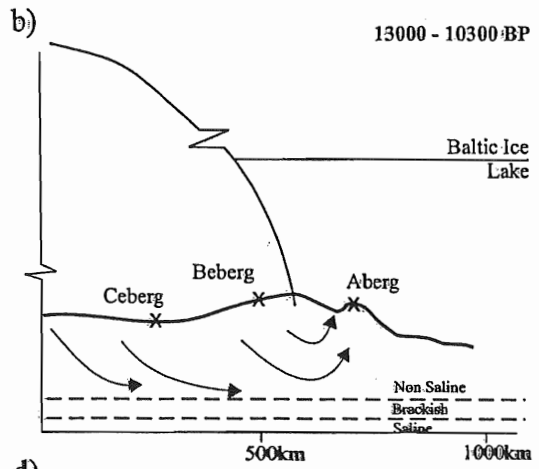
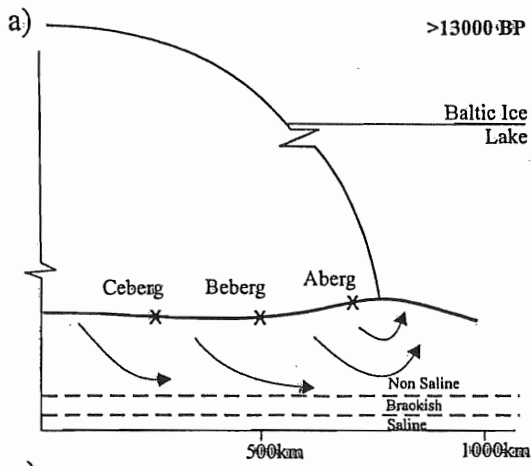
SPRITE

Coca Cola

Fanta

CO₂(g)

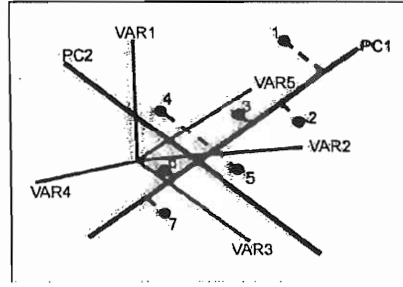




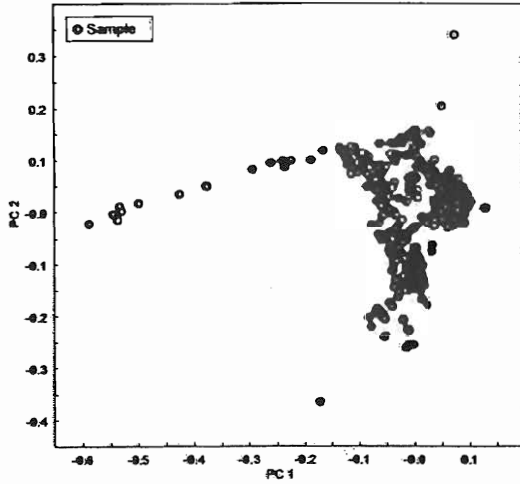
a)

Sample no	Variable 1	Variable 2	Variable 3	Variable 4	Variable 5
1	8500	45.5	19300	2.12	14.1
2	818	24	162	21	161
3	1980	95	937	234	99
4	115	23	154	1.9	163
5	2140	351	504	195	786
6	3020	73	4380	49.5	11
7	0	70	0	0	3
8	3179.8	1541	152.0	379.6	148.0
9	0	0	0	0	7
10	2184	91.8	163	256	793
11	2320	28	618	217	227
12	2250	28	741	244	219
13	385	14	80	38	235
14	388	12	87	39	235
15	228	4	27	4	373

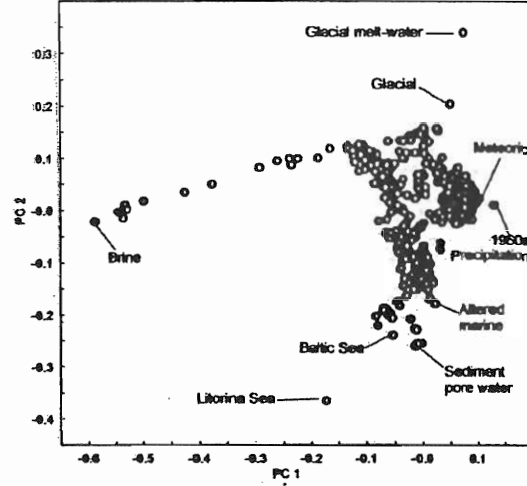
b)



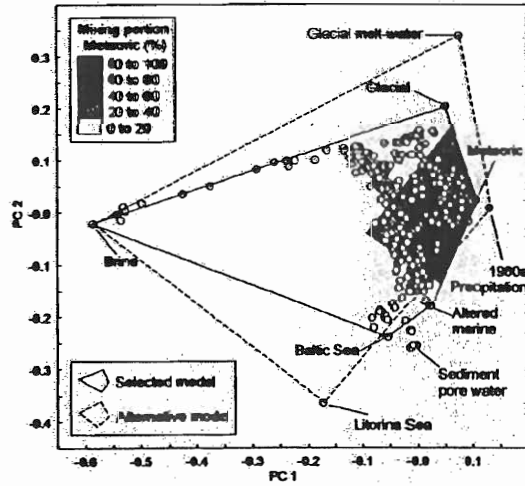
c)



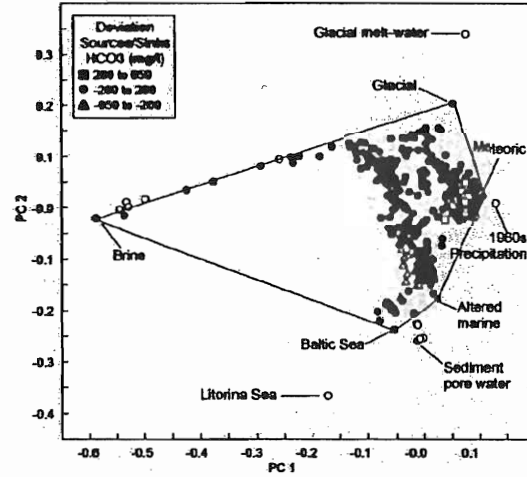
d)



e)



f)



Äspö Simulation Mixing Portions

Horizontal layer elevation - 650 m

Interpolated time 1995.65

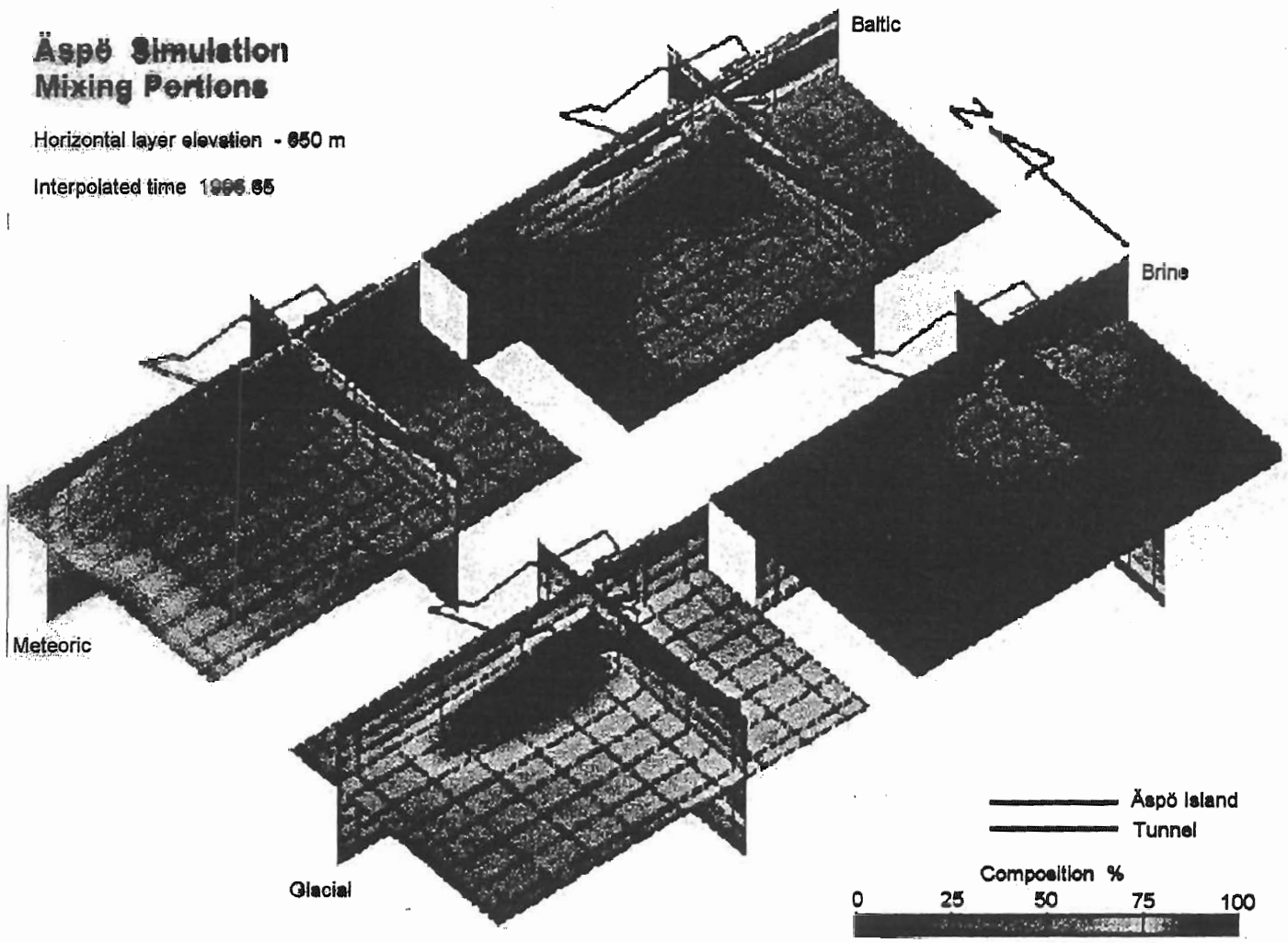
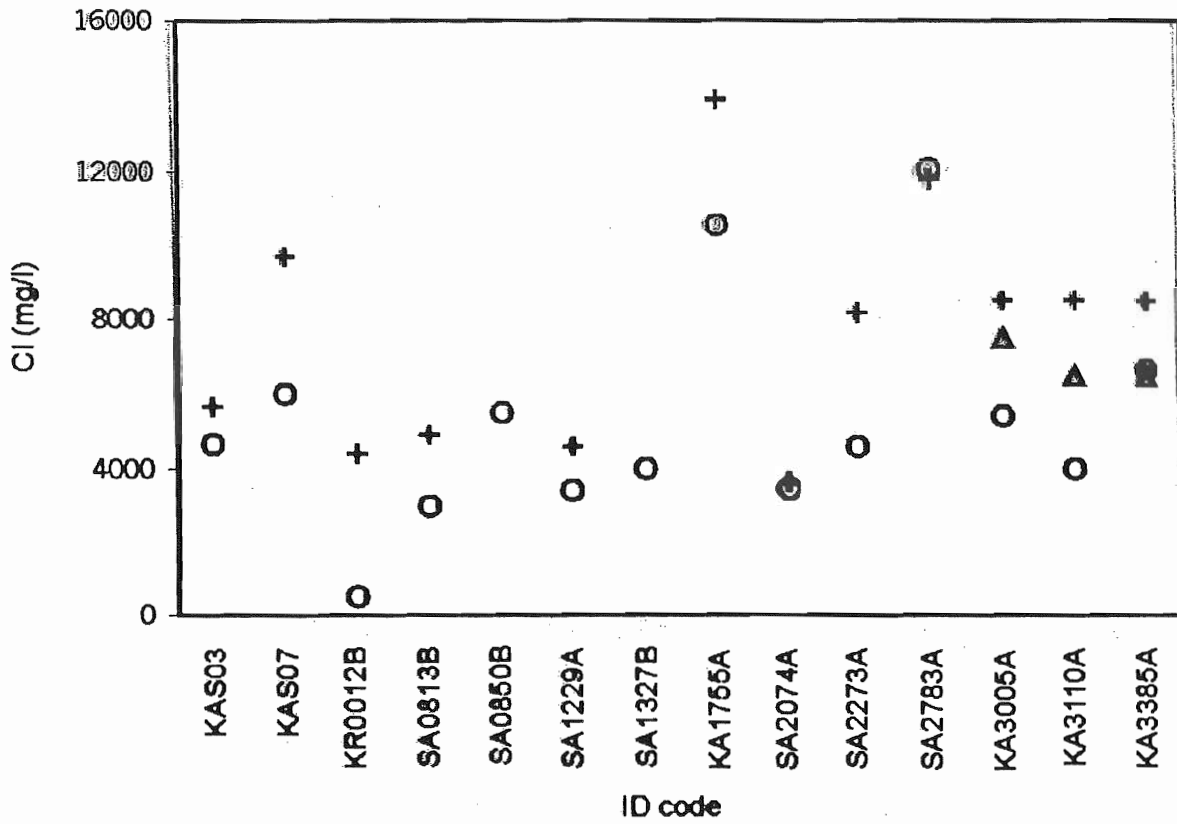


figure x-4

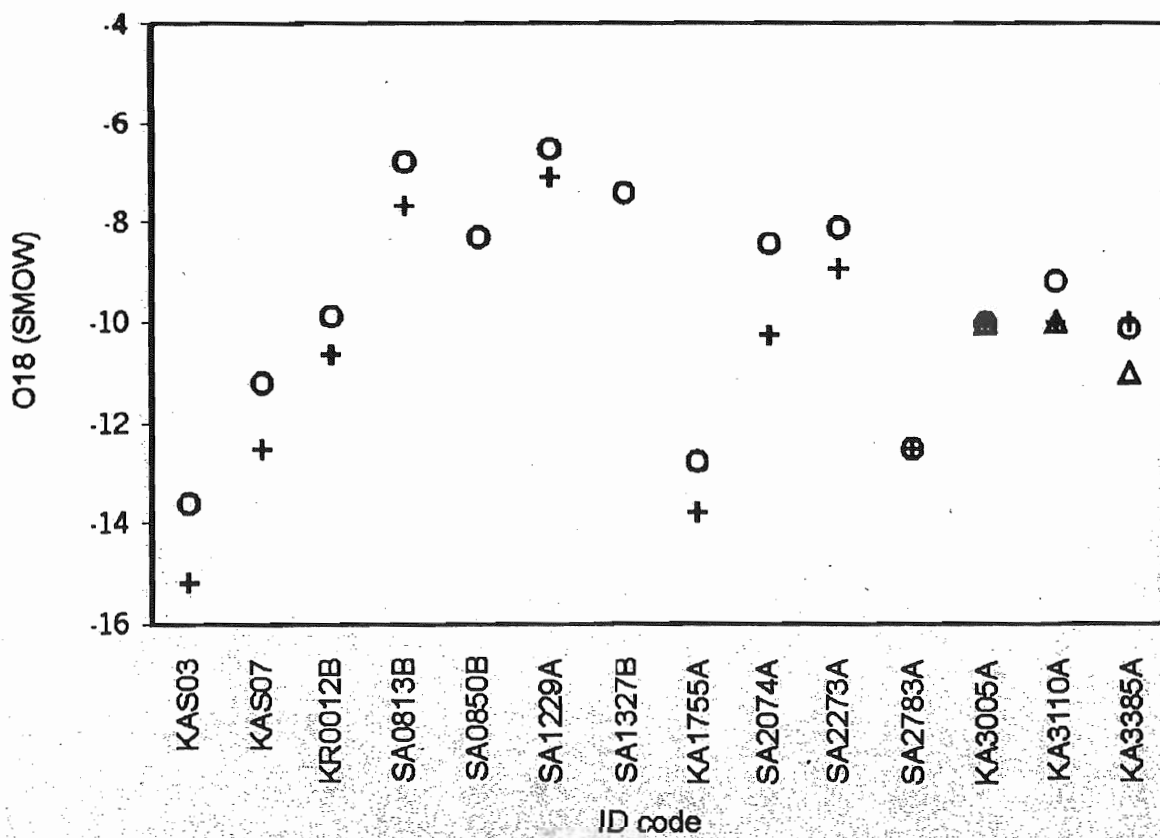
Reactions to consider within TASK#5

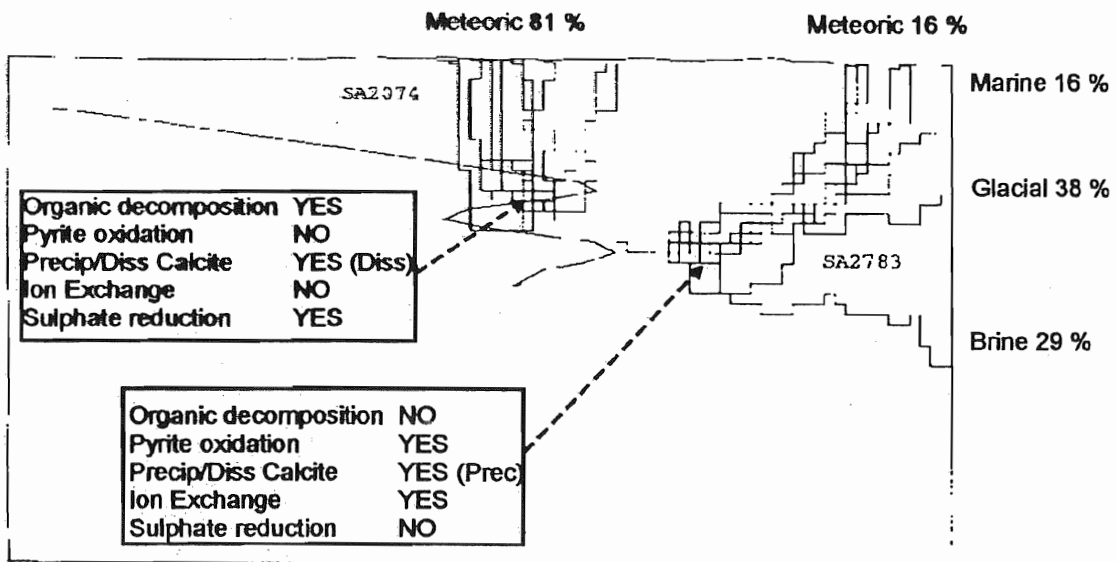
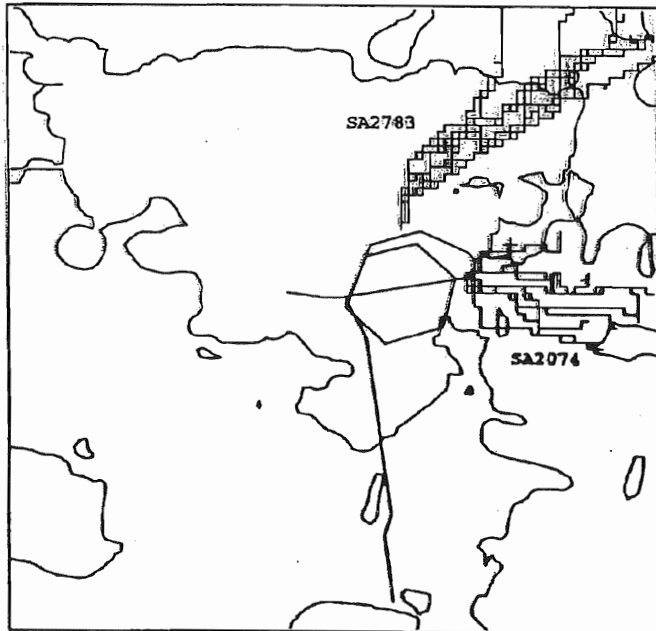
- 1) **Organic decomposition:** $O_2 + CH_2O \rightarrow CO_2 + H_2O$
M3 reports a gain of HCO_3^- as a result of this reaction.
- 2) **Inorganic redox reaction:** $HS^- + 2O_2 \rightarrow SO_4^{2-} + H^+$.
M3 reports a gain of SO_4 as a result of this reaction.
- 3) **Dissolution and precipitation of calcite:** $CO_2 + CaCO_3 \rightarrow Ca^{2+} + 2HCO_3^-$. M3 reports a gain or a loss of Ca and HCO_3^- as a result of this reaction.
- 4) **Ion exchange:** $Na_2X_{(s)} + Ca^{2+} \rightarrow CaX_{(s)} + 2Na^+$, where X is a solid substrate such as a clay mineral. M3 reports a change in the Na/Ca ratios as a result of this reaction.
- 5) **Sulphate reduction:** $SO_4^{2-} + 2(CH_2O) + OH^- \rightarrow HS^- + 2HCO_3^- + H_2O$. M3 reports a loss of SO_4 and a gain of HCO_3^- as a result of this reaction.

○ Measured + M3 predicted △ Voxel interpolated



○ Measured + M3 predicted △ Voxel interpolation





**The origin and composition of groundwater leaking
into the Äspö tunnel**

U Svensson (CFE)

My Task#5 History

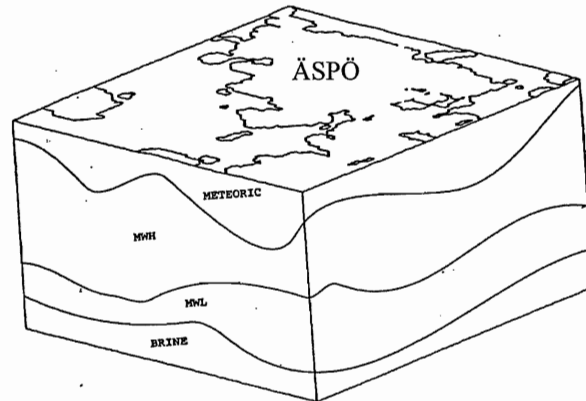
- **Aug. -98: Basic techniques tested**
- **Jan. -99: Prediction report**
 - **Techniques ok**
 - **Points to conceptual problems: Water too easily exchanged (Porosity, Connectivity, Conductivity, Dispersion)**
- **1999: New methods to generate conductivity fields developed (SKB TR, 99-24,99-25).**
- **Dec. -99: Small project on porosity concepts.**
- **Jan. -00: Include new developments in Task#5 simulations.**
- **Feb. -00: Problem with routine for unsaturated zone!!**
- **TF13 -meeting: Results presented somewhat uncertain. Final results in March.**

Outline of presentation

- **Basic conceptual assumptions**
- **New developments**
- **Calibration**
- **Predictions, Jan -99, Jan -00**
- **Conclusions**

Basic conceptual assumptions

Boundary Conditions

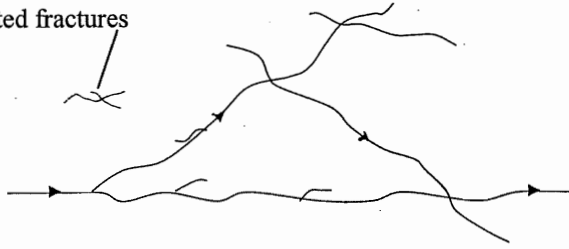


- **Top of domain: On land we use a boundary condition of 100% Meteoric water and for the bottom of the Baltic Sea we assume 100% Baltic water.**
- **Bottom of domain: 100% Brine**
- **Vertical boundaries:**
 - **If s (Salinity) $\leq 0.1\%$ we assume that the water is of Meteoric origin.**
 - **If $s \leq 2\%$ it is assumed that the water type is Brine.**
 - **If $0.1 < s \leq 1.2\%$ we call this water type "Mixed Water High" (MWH).**
 - **If $1.2 < s < 2.0\%$ we call this water type "Mixed Water Low" (MWL).**
- **MWH. Composition based on field data from borehole KLX01: 10% Baltic, 37% Meteoric, 43% Glacial and 10% Brine.**
- **MWL. 50% Glacial and 50% Brine. This is to some degree supported by measurements in KLX02, at a depth with a salinity of 1.5%.**

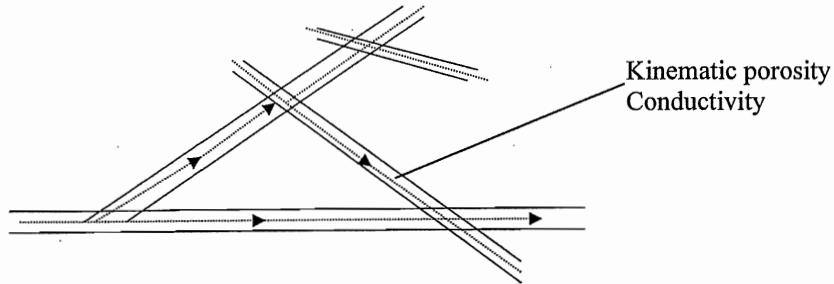
Initial conditions obtained from a steady state solution for natural conditions.

New developments

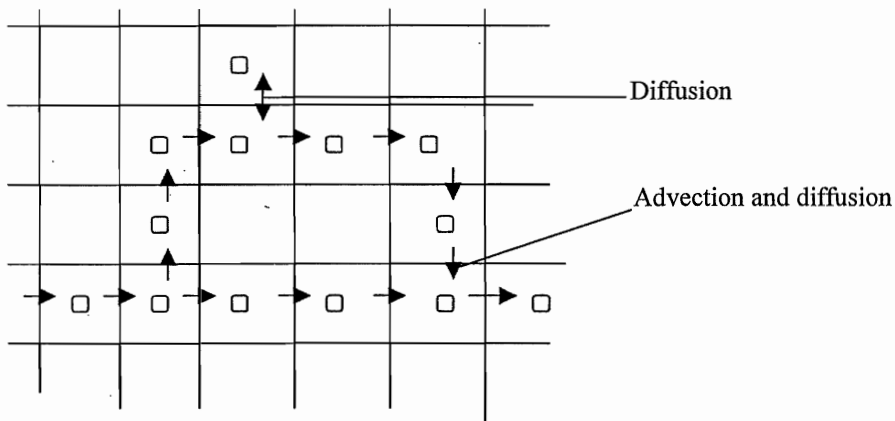
Isolated fractures



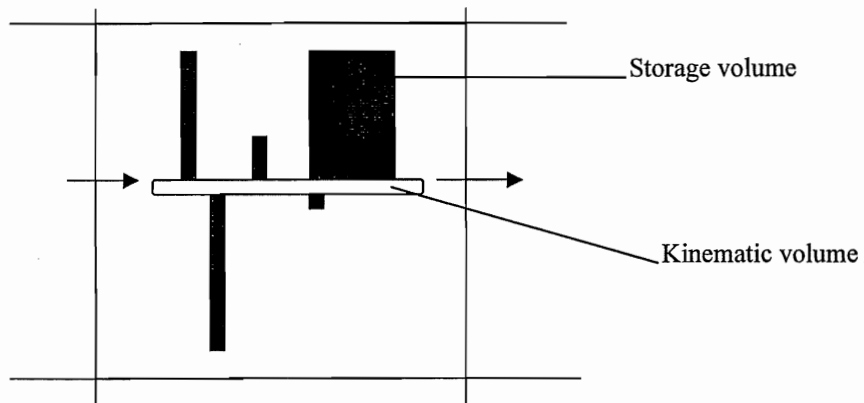
"Real World" fracture system



Representation as conductive blocks



Representation on the grid



Computational cell with storage volumes

New developments

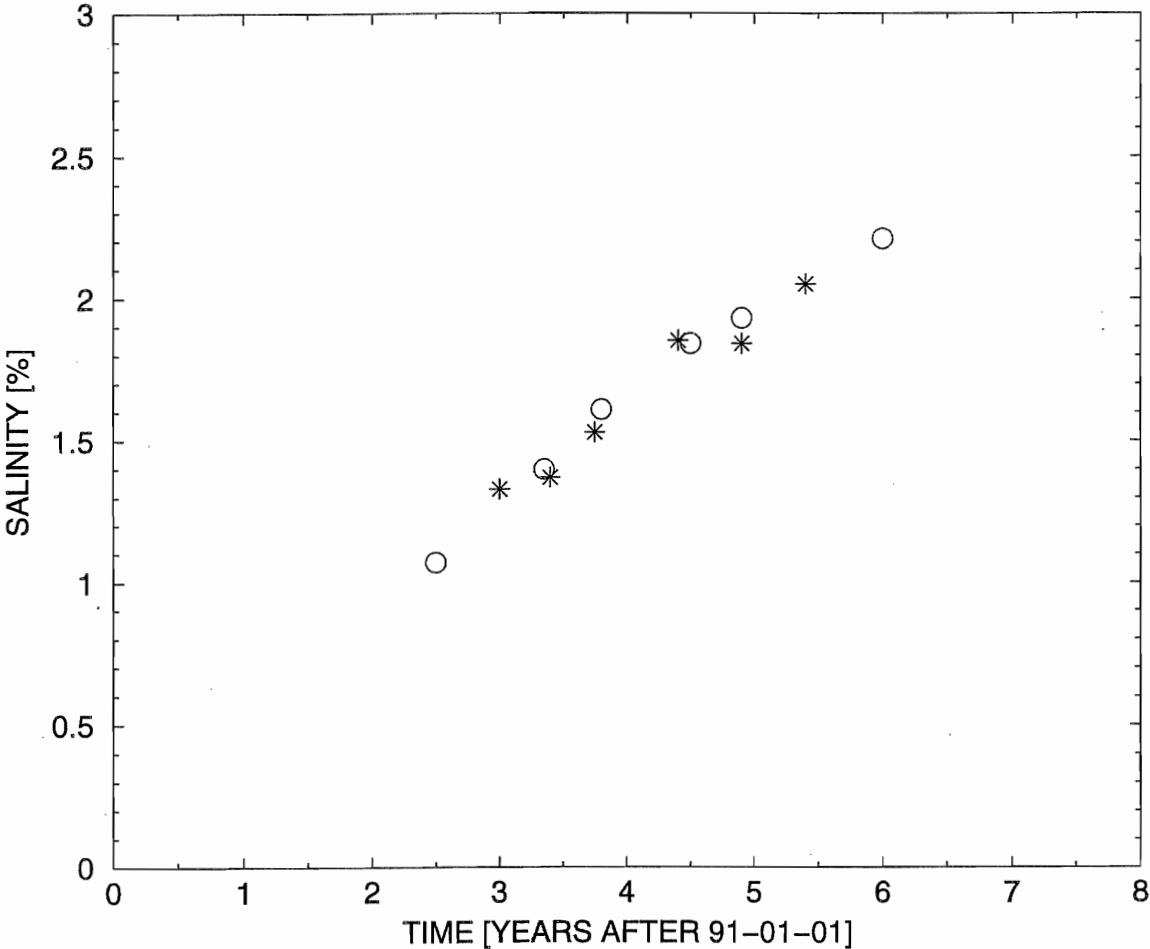


Illustration of porosity (top) and flow fields. Depth interval shown is 400 to 500 metres below ground level. The flow is from west to east. View from south.

Calibration

- A. Flow model:**
- Natural conditions (groundwater table)
 - Tunnelfront at 2875 m (drawdowns)
- B. Transport model:** - Water composition for MWH and MWL adjusted to ensure agreement with measured composition in boreholes (initial conditions and tunnelfront at 2875 m).
- C. Result:**
- MWH: 30% Meteoric, 20% Baltic, 35% Glacial, 15% Brine.
- MWL: 50% Glacial, 50% Brine.
- Kinematic porosity: 5 times larger than the value based on flow aperture. ($\approx 10^{-3}$).

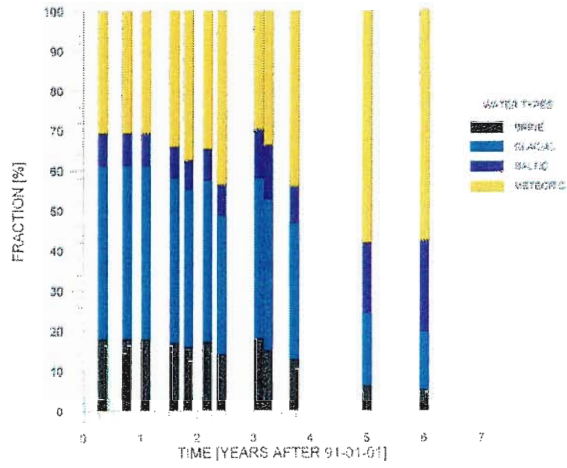
Upconing in SA2783



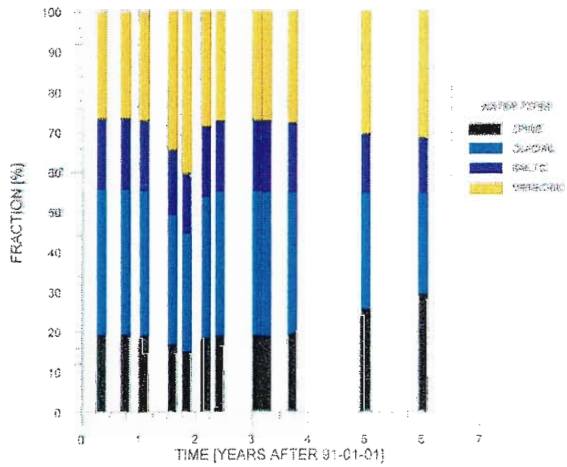
□ Measured
○ Simulated

Predictions. SA2783

Jan -99:



Jan -00:

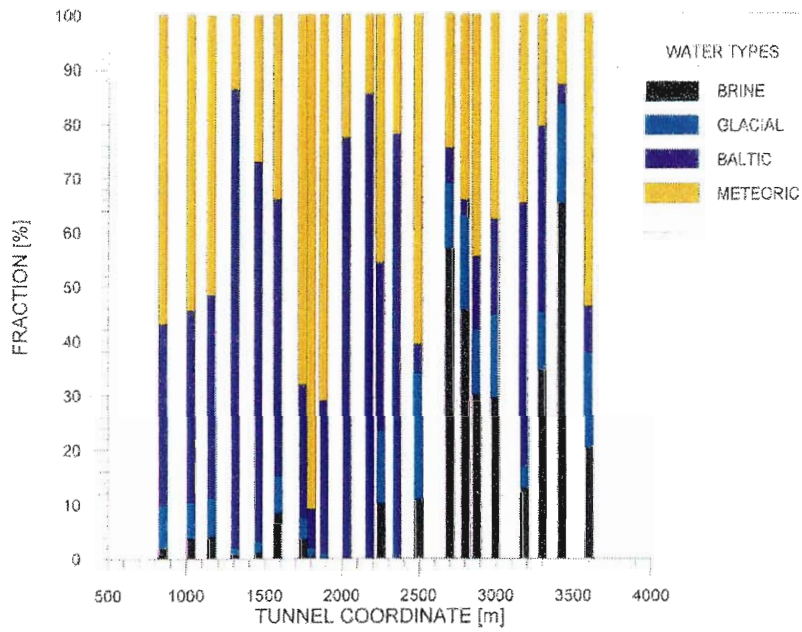


Measured:

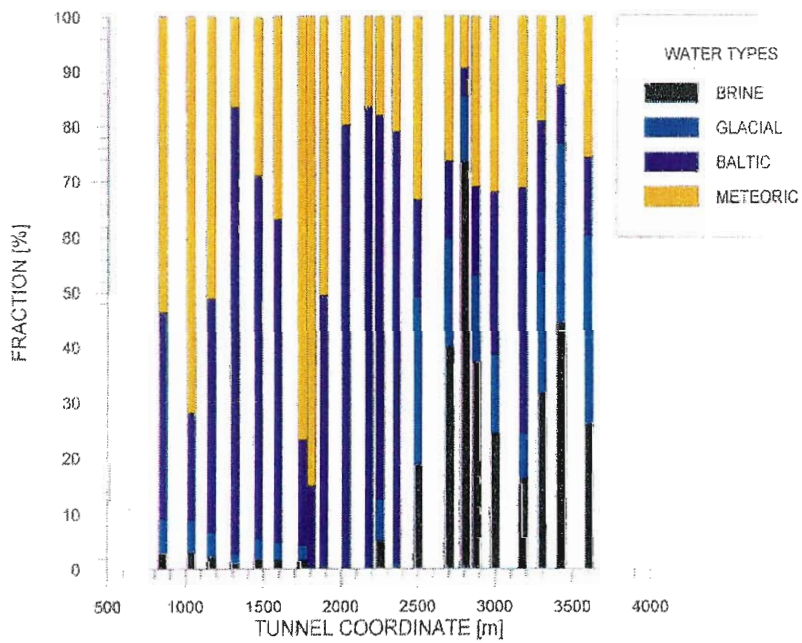


Predictions, completed tunnel (97-01-01)

Jan -99:



Jan -00:



Predictions, water composition

Initial conditions

Borehole depth [m]	Measured (top) and simulated water composition			
	Meteoric	Baltic	Glacial	Brine
KAS02C	30.1	14.8	40.4	14.8
300 m	30.9	17.8	34.5	16.8
KAS02D	26.9	15.0	43.0	15.0
440 m	25.7	17.0	37.0	20.4
KAS02E	17.9	17.9	44.7	19.6
520 m	25.9	17.1	36.9	20.1
KAS03D	20.2	14.7	50.3	14.7
340 m	34.9	18.6	32.6	14.0
KAS03E	22.6	12.8	51.7	12.8
440 m	30.3	19.6	34.9	15.3
KAS03F	16.0	16.0	50.9	17.1
600 m	25.8	16.9	37.0	20.3
KAS04C	24.9	17.3	40.5	17.3
360 m	27.1	17.5	36.3	19.1
KAS06C	34.5	35.4	15.1	15.1
320 m	28.0	18.3	35.9	17.7
KAS06D	33.7	31.3	17.6	17.6
420m	25.5	16.9	37.1	20.6
Average	25.2	19.4	39.4	16.0
	28.2	17.7	35.8	18.2

Tunnelfront at 3170 m

Borehole depth [m]	Measured (top) and simulated water composition			
	Meteoric	Baltic	Glacial	Brine
SA0813	48.0	41.0	5.5	5.5
100m	41.2	46.4	8.5	3.8
SA1229	40.0	51.0	4.5	4.5
160m	4.2	95.1	0.4	0.2
SA1420	54.0	28.0	9.0	9.0
200m	22.9	58.7	12.0	6.4
SA1641	48.0	16.0	20.0	16.0
220m	51.6	24.2	15.9	8.3
SA1696	35.0	18.0	29.0	18.0
220	47.6	16.6	23.6	12.2
SA1828	46.0	28.0	13.0	13.0
240	66.5	21.8	7.9	3.8
SA2074	47.0	29.0	12.0	12.0
280m	30.2	39.2	20.8	9.8
SA2175	39.0	39.0	11.0	11.0
280m	15.7	83.9	0.3	0.1
SA2273	41.0	41.0	9.0	9.0
300m	23.9	75.7	0.3	0.1
SA2600	32.0	19.0	29.0	20.0
340m	24.5	15.9	37.6	22.0
SA2783	20.0	20.0	39.0	21.0
360m	27.4	17.9	36.1	18.6
SA2834	19.0	19.0	37.0	25.0
360m	29.9	17.5	34.6	17.9
Average	39.1	29.1	18.2	13.7
	32.1	42.7	16.5	8.6

Completed tunnel (96-05)

Borehole depth [m]	Measured (top) and simulated water composition			
	Meteoric	Baltic	Glacial	Brine
SA2273	46.0	38.0	8.0	8.0
300m	15.5	84.4	0.1	0.1
Sa2600	48.0	20.0	16.0	16.0
340m	38.2	17.5	27.8	16.5
SA2783	17.0	17.0	37.0	29.0
360m	31.0	14.3	27.6	27.1
SA2880	18.0	18.0	34.0	31.0
380m	27.8	15.9	32.9	23.5
KA3005	54.0	21.0	13.0	13.0
400m	25.2	17.1	34.3	23.4
SA3067	18.0	18.0	43.0	21.0
400m	31.0	25.2	29.1	14.7
KA3110	47.0	37.0	8.0	8.0
400m	36.0	57.9	3.7	2.4
KA3385	38.0	18.0	25.0	18.0
440m	20.9	13.9	38.7	26.5
Average	35.8	23.4	23.0	18.0
	28.2	30.8	24.3	16.8

Conclusions

Task#5 generally:

- **Points to a number of shortcomings in traditional continuum models. How can we store Glacial water for 10 000 years at a depth of 200 metres? Measurements are likely to be from stagnant waters; models simulate the moving water.**
- **The task is a challenge computationally (3D, transient, tunnelpropagation, transport, backtracking, etc).**
- **The "presentation of chemistry" as four water types is useful for the exchange of information between hydrologists and chemists.**
- **Stimulates further discussions about porosity, connectivity, conductivity and dispersion.**

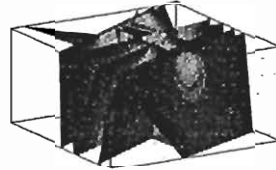
Present model

- **Good agreement with measured water composition in boreholes for initial conditions, tunnelfront at 3170 m and for the completed tunnel (date 1996-05).**
- **The upcoming measured in SA2783 provides a nice opportunity to calibrate the kinematic porosity.**
- **The model has been developed significantly during Task#5. The present version has more realistic conductivity and porosity fields than the model we started out with.**

**Integration of hydrogeology and hydrochemistry at
the Äspö site**

J Molinero, J Samper, R Juanes and L Buján (ULC)

INTEGRATION OF HYDROGEOLOGY AND HYDROCHEMISTRY AT THE ÄSPÖ SITE:

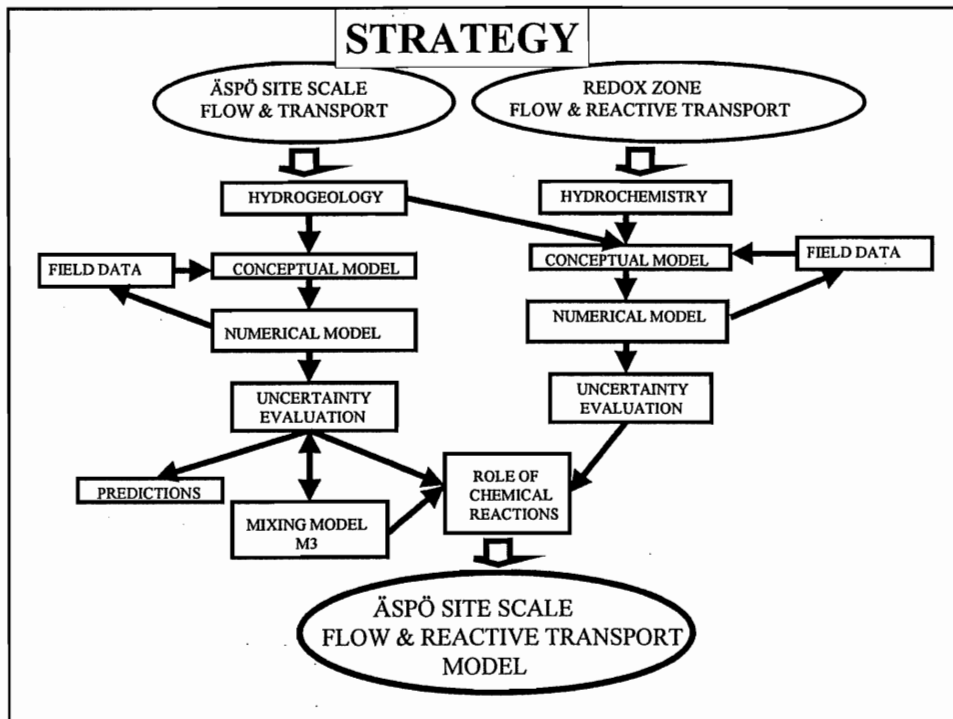


➤ Hydrodynamic numerical modeling of the impact of the tunnel construction and evaluation of the consistency with a hydrochemical mixing approach (M3 model).

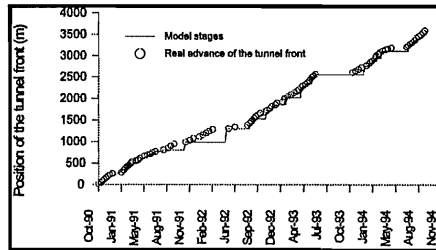
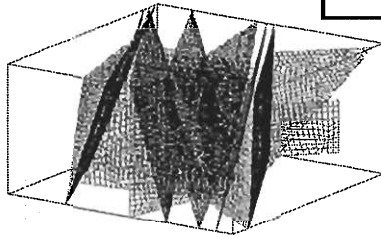
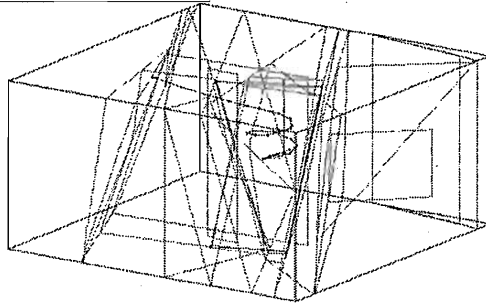
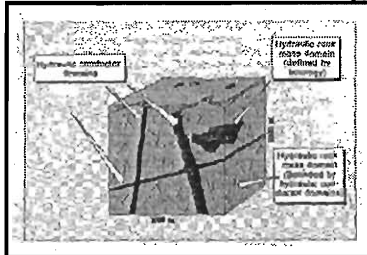
➤ Numerical modeling of groundwater flow and multicomponent reactive transport at the Redox Zone.

enresa

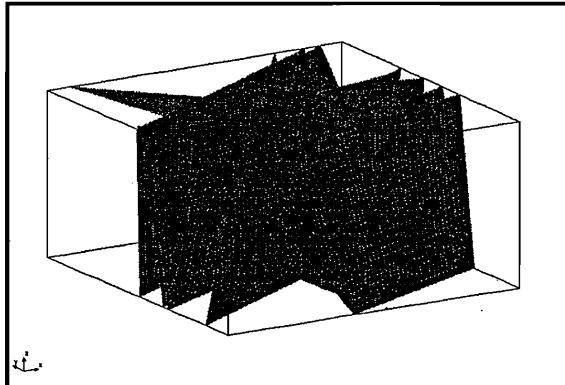
J. Molinero, J. Samper, R. Juanes & L. Buján



CONCEPTS & GEOMETRY

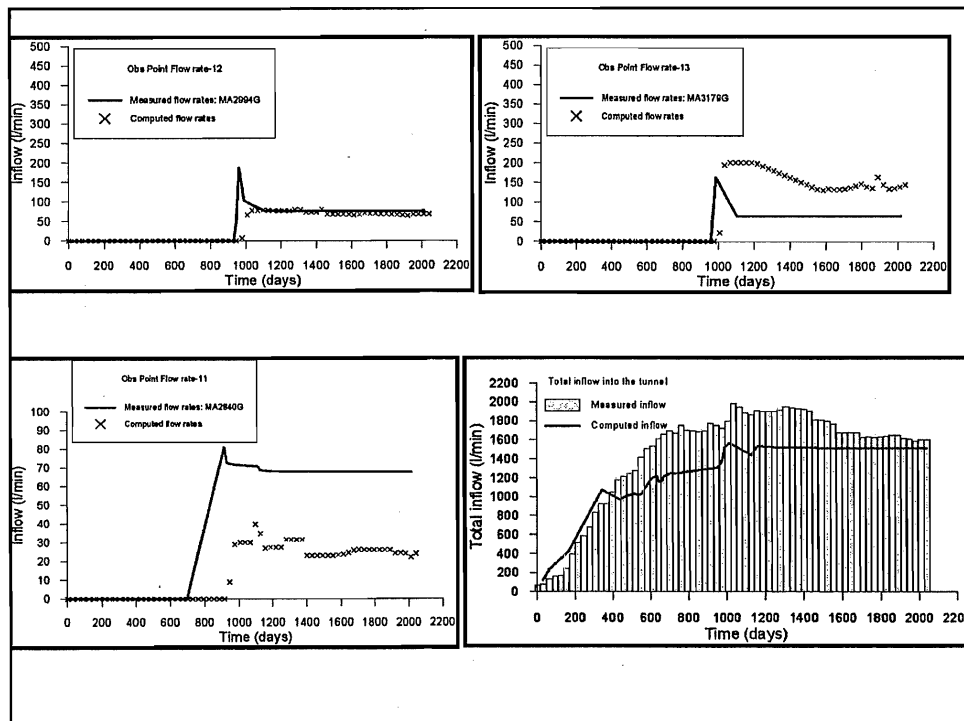
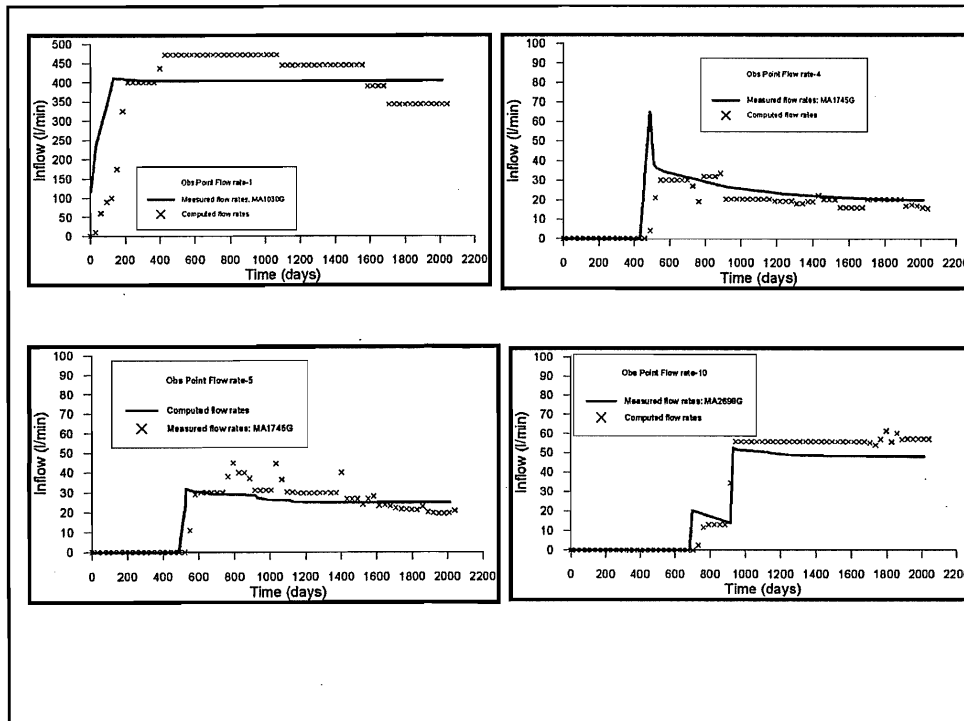


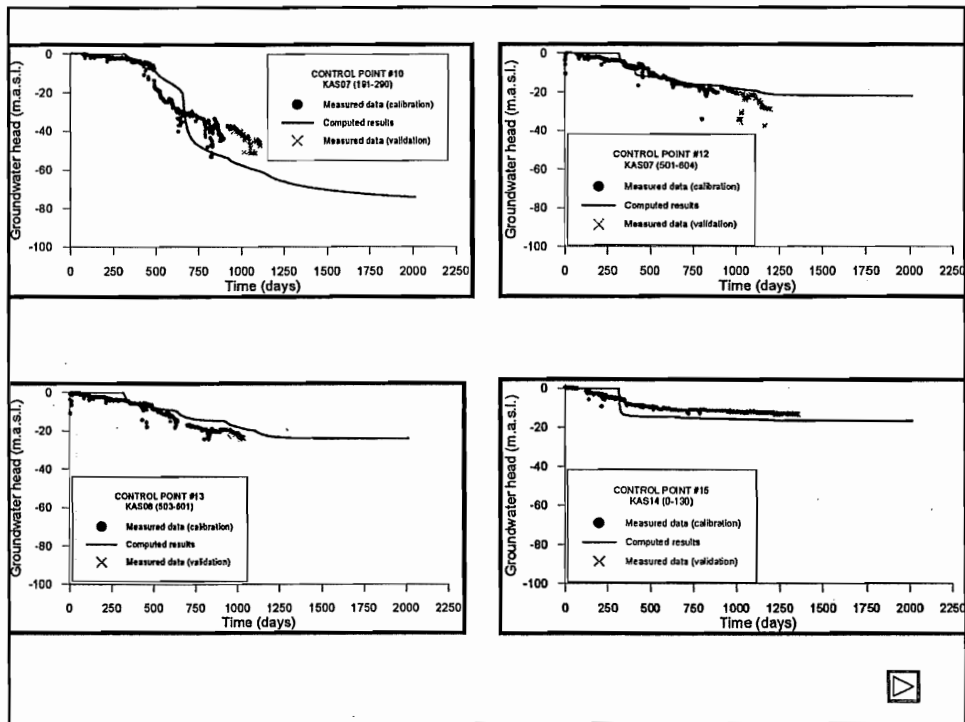
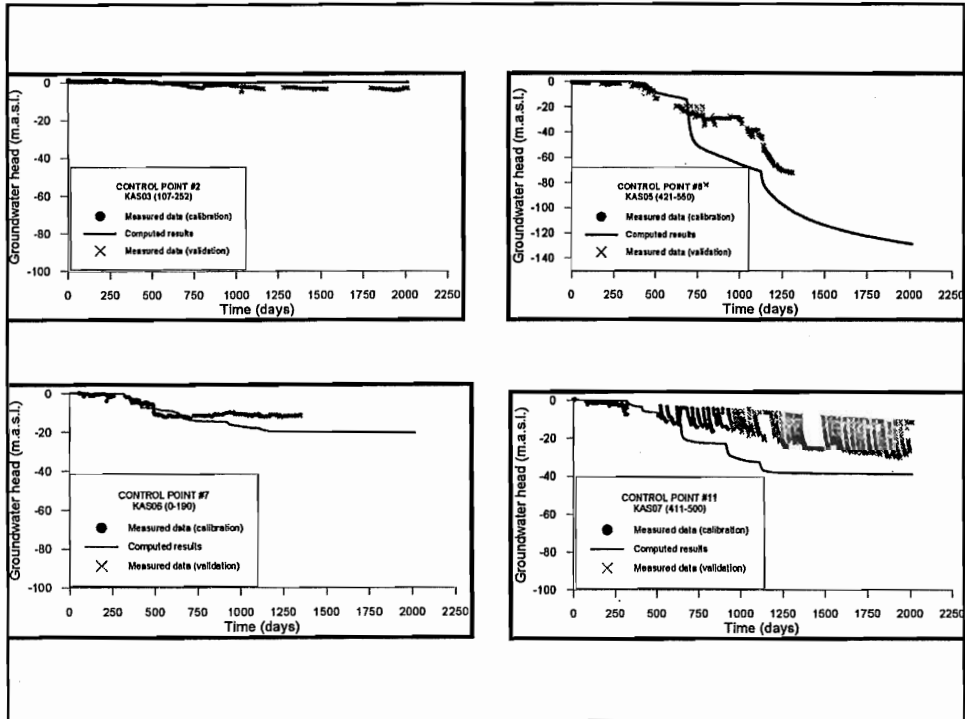
GROUNDWATER FLOW MODEL



STRONGLY CALIBRATED

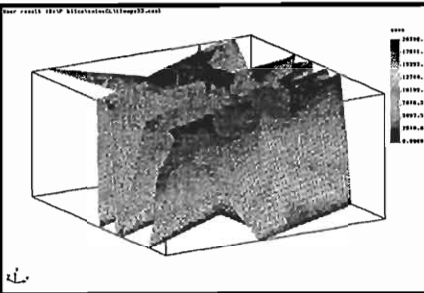
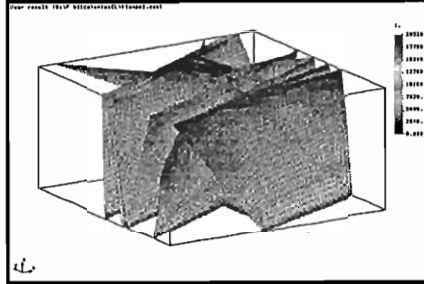
- INFLOWS INTO THE TUNNEL
- HEADS ON THE FRACTURE ZONES



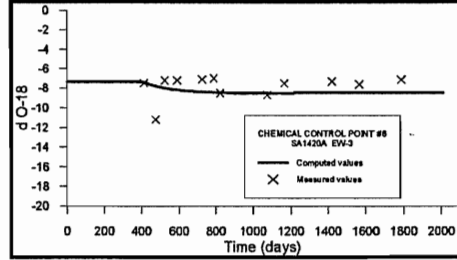
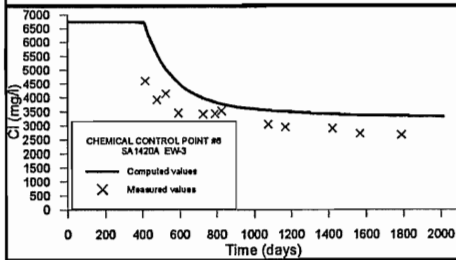
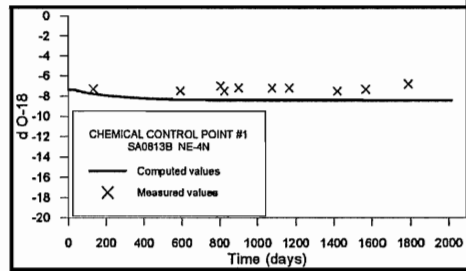
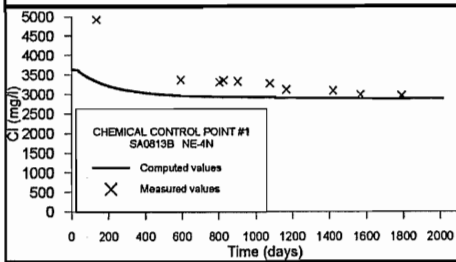
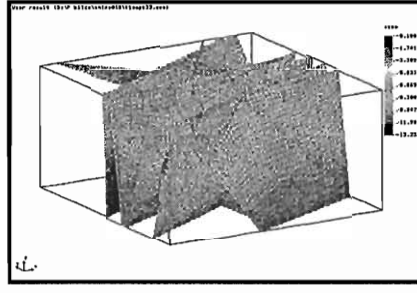
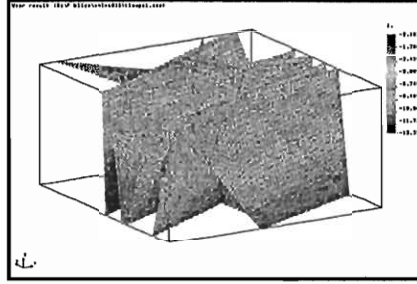


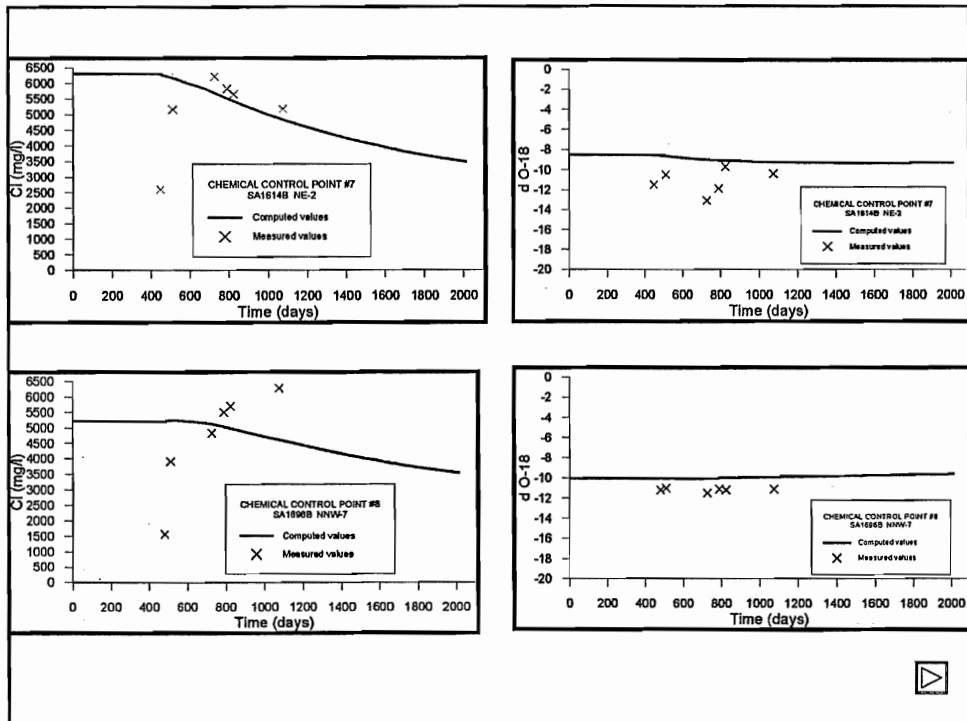
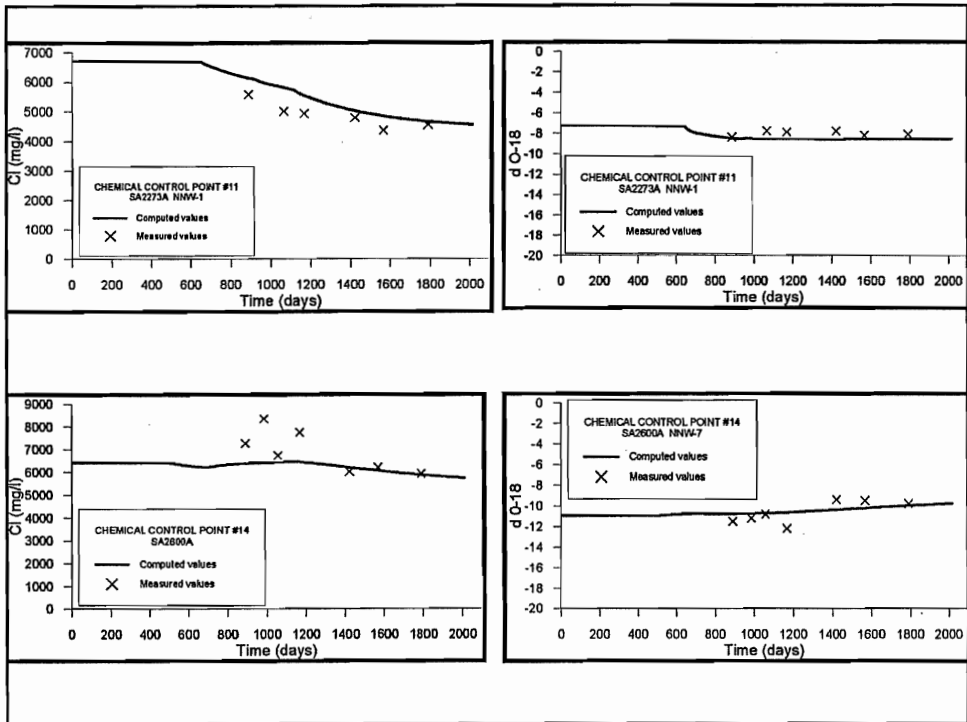
SOLUTE TRANSPORT MODEL

CHLORIDES

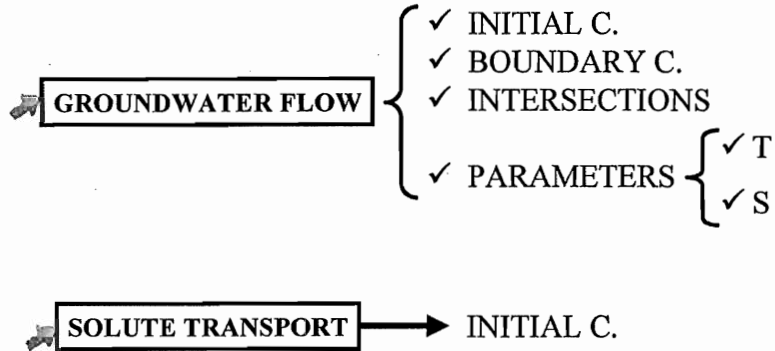


O-18



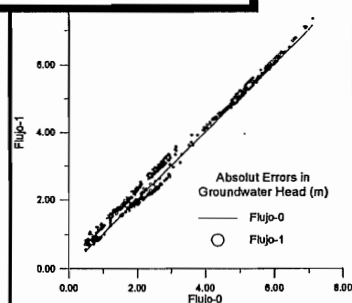


SENSITIVITY ANALISES

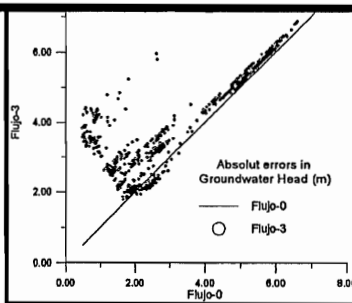


FLOW B&I CONDITIONS

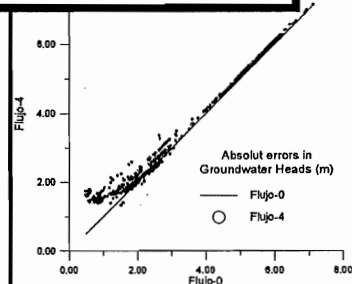
B. C.: REGIONAL MODEL



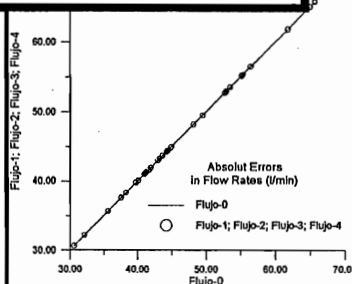
B. & I. C.: R.M. + SALINITY CORRECTION



B. & i. C.: REGIONAL MODEL

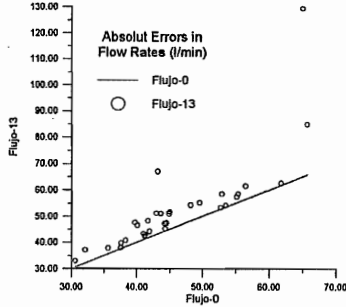
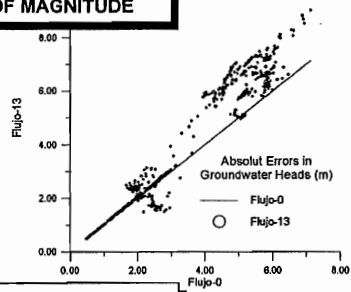


TUNNEL INFLOWS (4 RUNS)

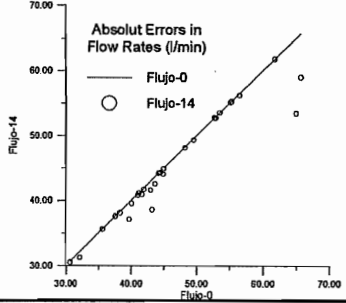
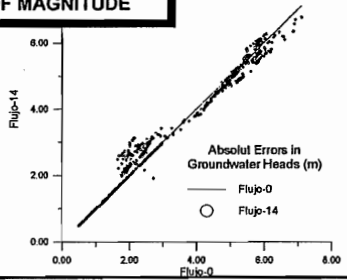


SPECIFIC STORAGE COEFFICIENTS

**AUMENTED:
1 ORDER OF MAGNITUDE**

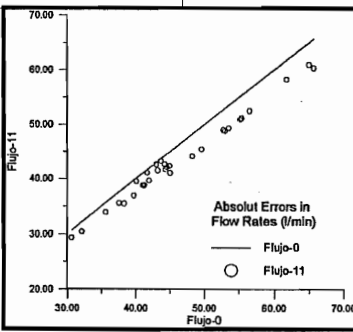
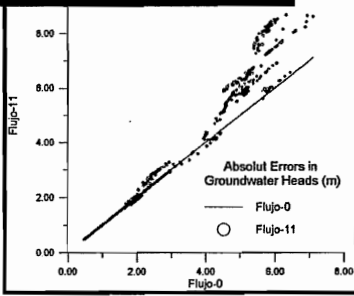


**REDUCED:
1 ORDER OF MAGNITUDE**

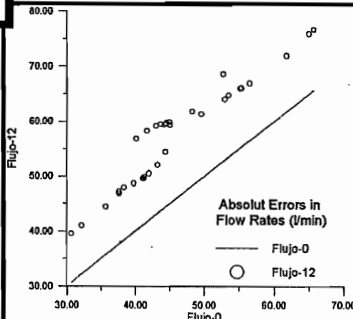
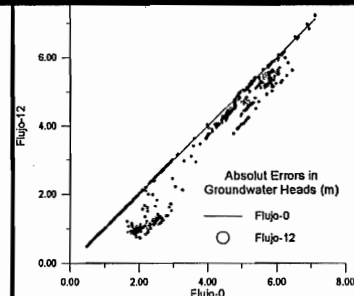


TRANSMISSIVITY

EW-1S: MINIMUM MEASURED VALUE

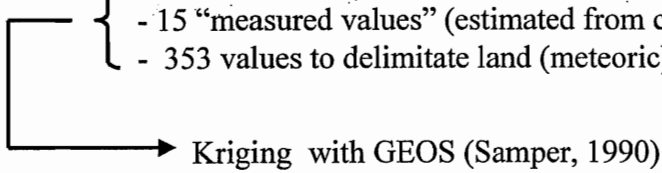


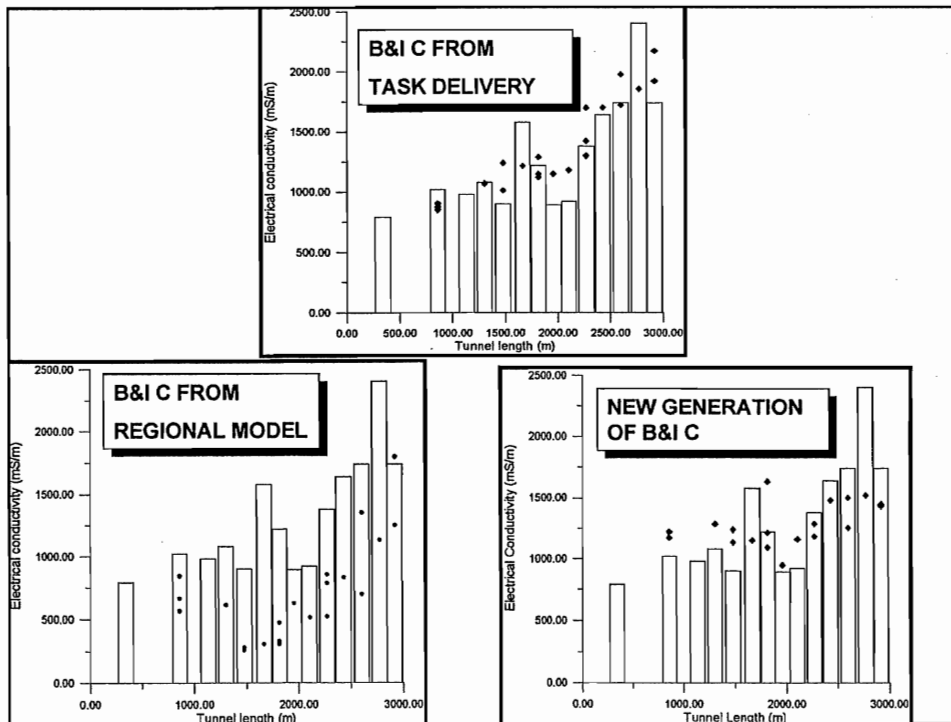
EN-1 & NNW-7: MINIMUM MEASURED VALUE

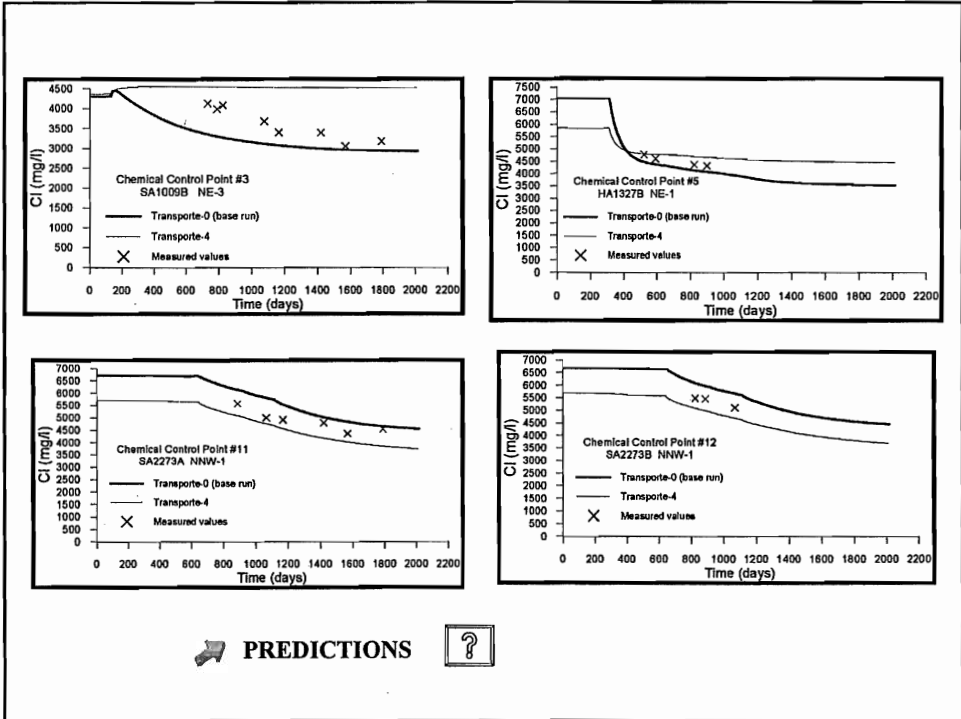
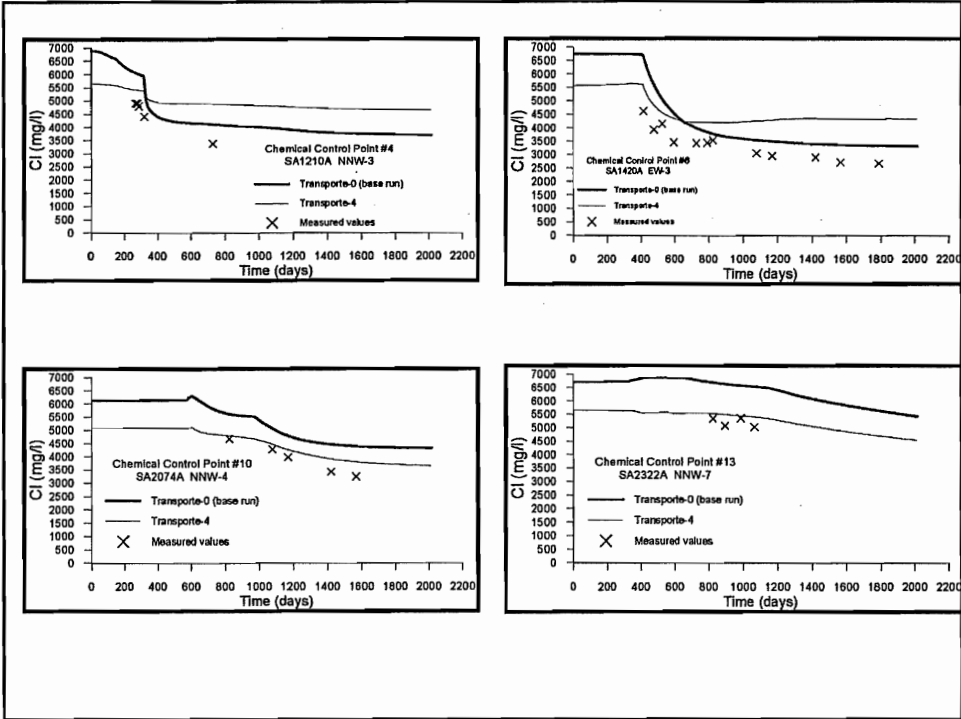


SOLUTE TRANSPORT I. & B. CONDITIONS

RUNS:

- 1- Transport I & B conditions from Regional Model
 - 2- Same than 1 with flow I & B conditions from Regional Model
 - 3- Base run with flow I & B conditions from Regional Model
 - 4- Alternative generation of transport B & I conditions:
 - 32 field measured values (undisturbed conditions)
 - 15 “measured values” (estimated from control points)
 - 353 values to delimitate land (meteoric) and sea (Baltic)
- 
 Kriging with GEOS (Samper, 1990)





 PREDICTIONS



PREDICTIONS

TUNNEL PREDICTION SECTION

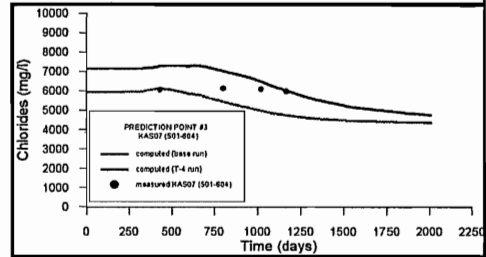
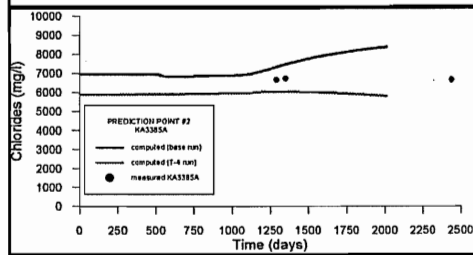
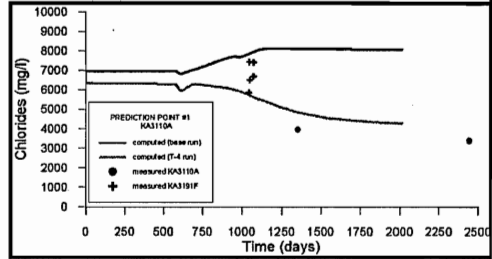
KA3005A ⇒ HRD

➤ KA3110A

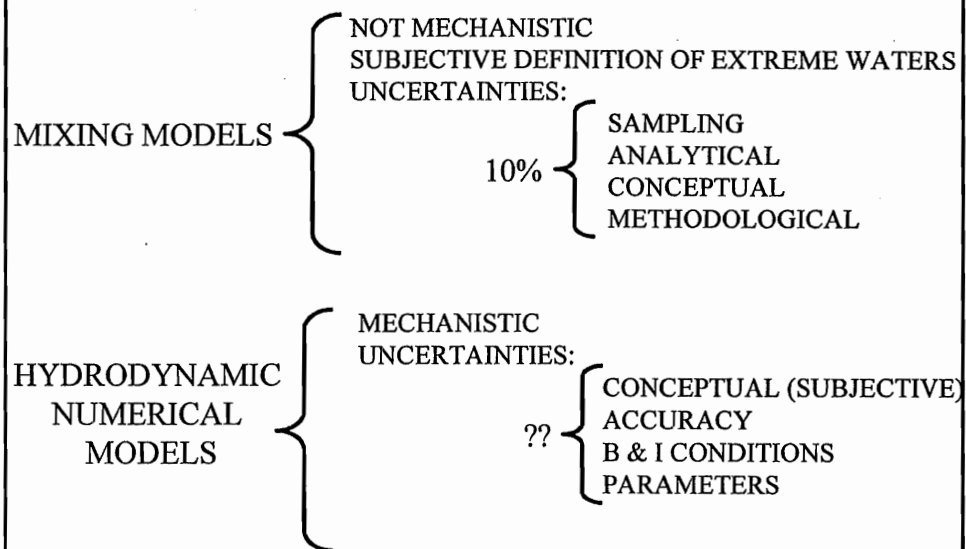
➤ KA3385A

C.P. OUTSIDE TUNNEL

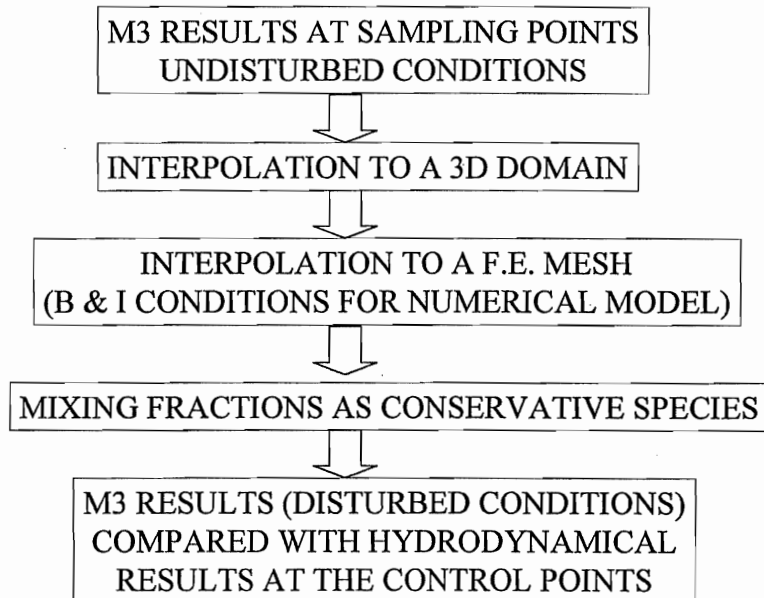
➤ KAS07(501-604)

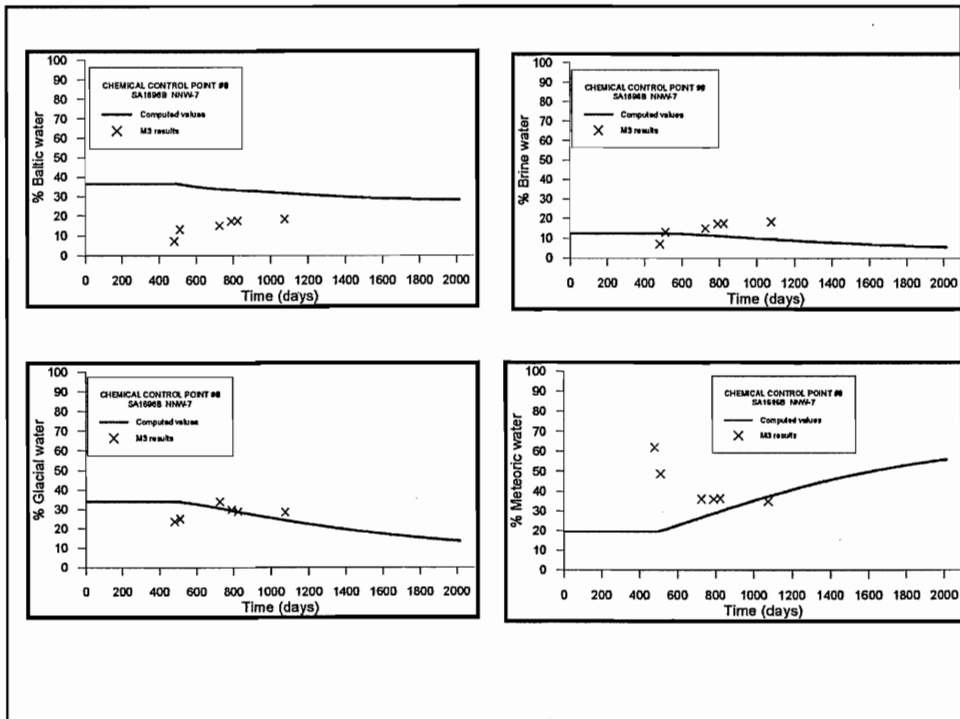
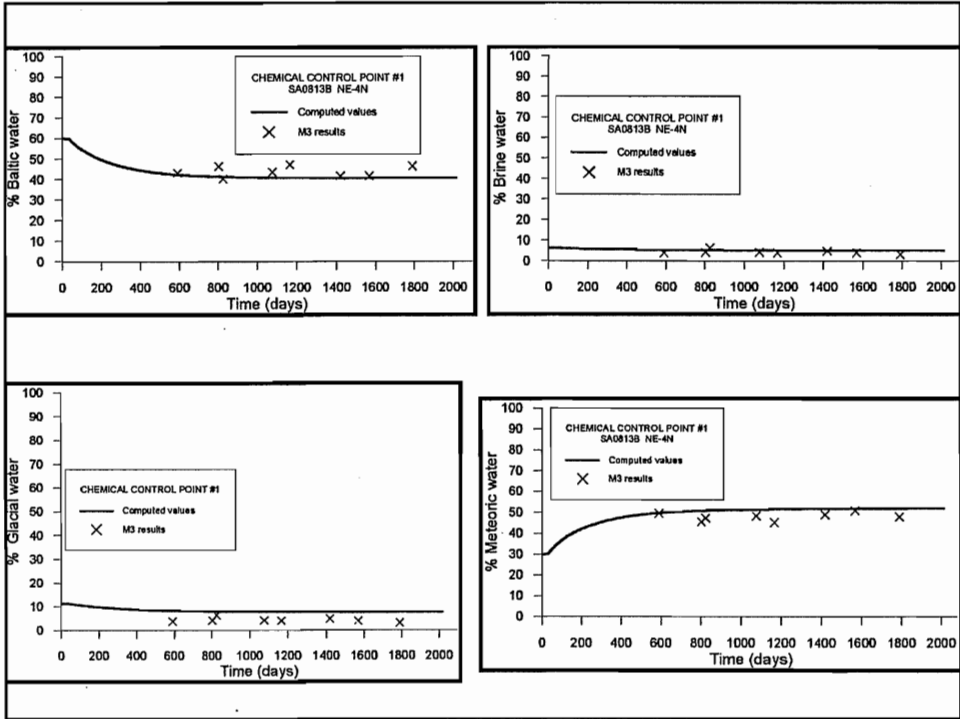


HYDRODYNAMIC vs. MIXING MODELS

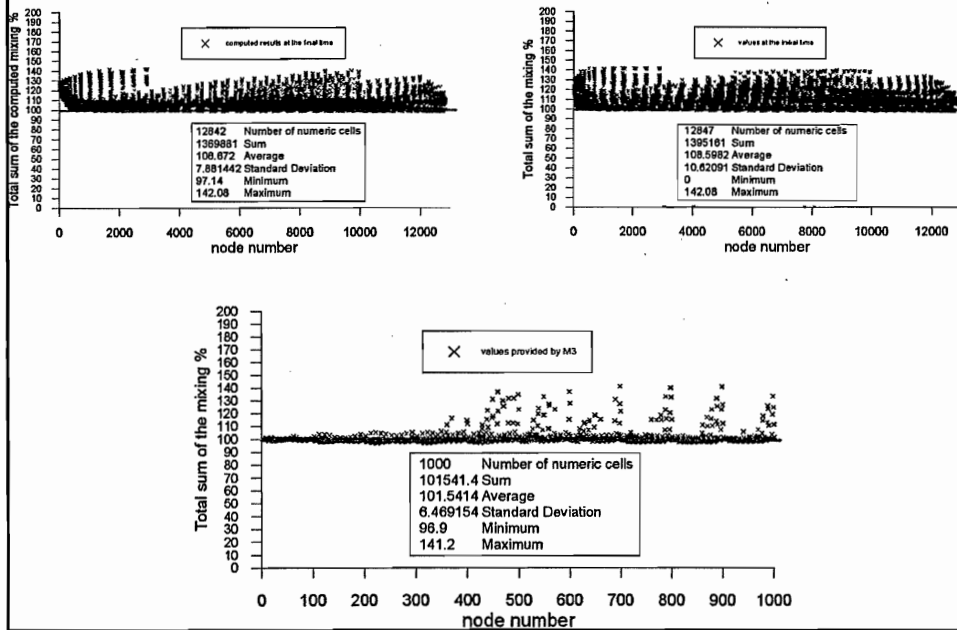


CONSISTENCY ASSESMENT

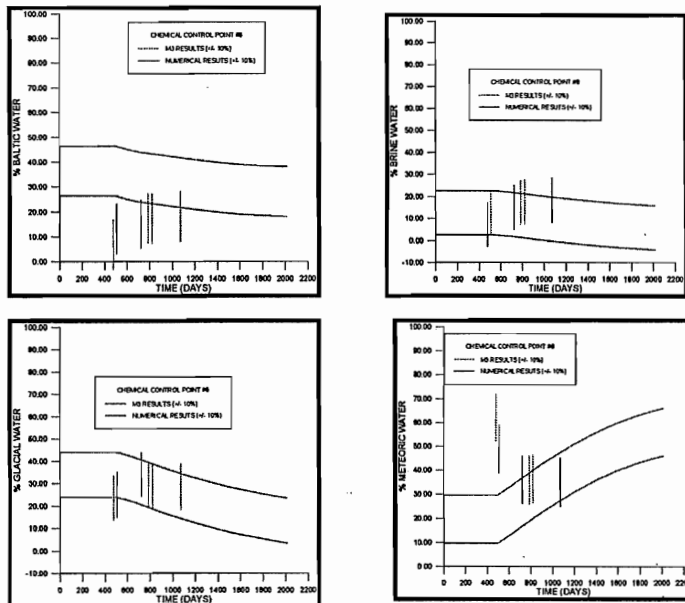


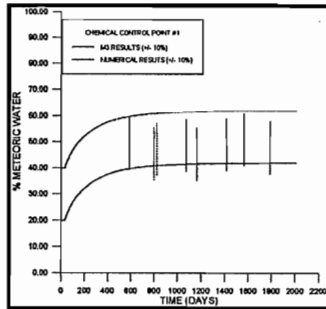
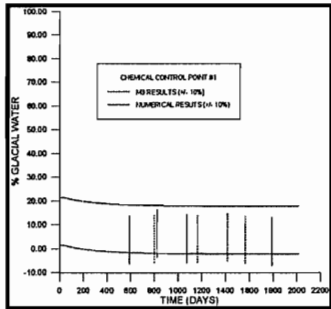
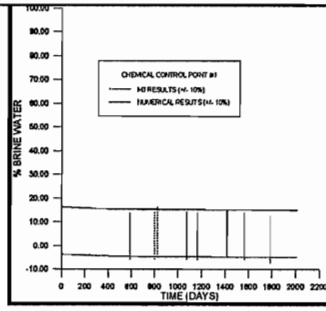
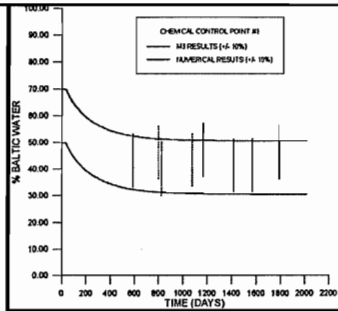


ERRORS IN THE NUMERICAL MODEL (?)



HOW MUCH IS THE CONSISTENCY?





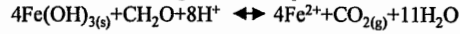
 The accuracy of the method is on the range of variations

ASSESSING THE ROLE OF THE CHEMICAL REACTIONS FROM A HYDROLOGICAL POINT OF VIEW

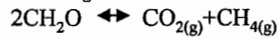
Calcite dissolution/precipitation:



Iron reduction through Carbon respiration:



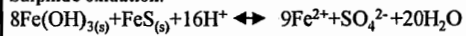
Methanogenesis:



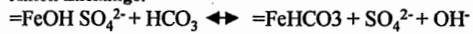
Cation Exchange:



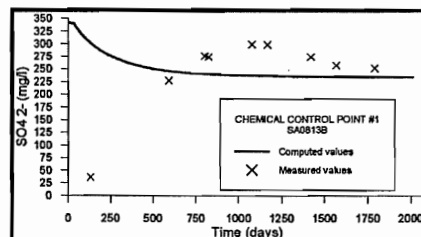
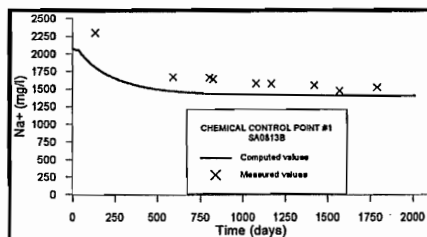
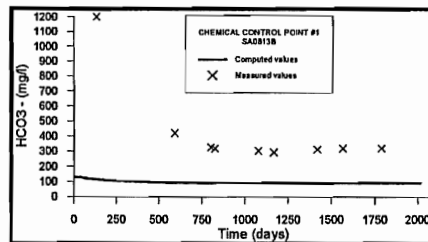
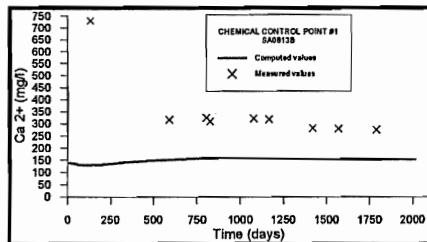
Sulphide oxidation:

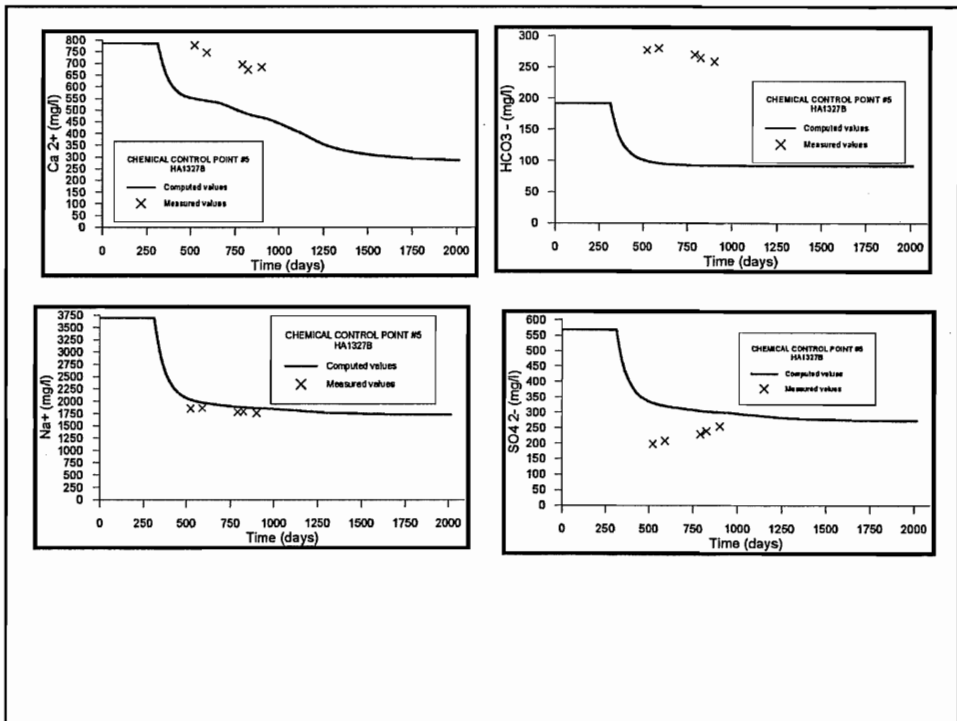
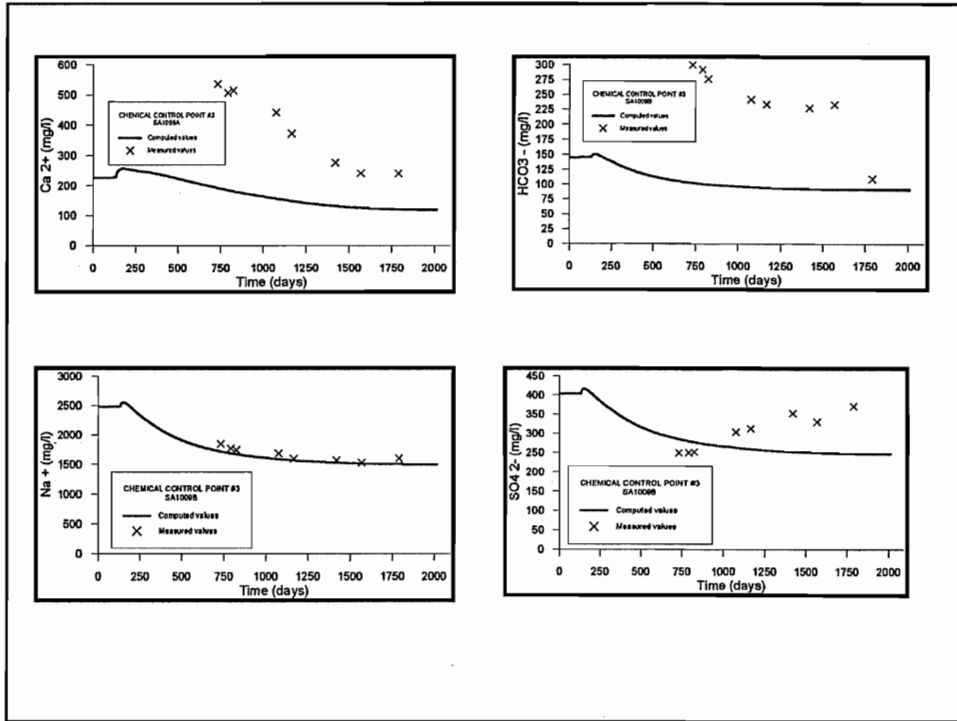


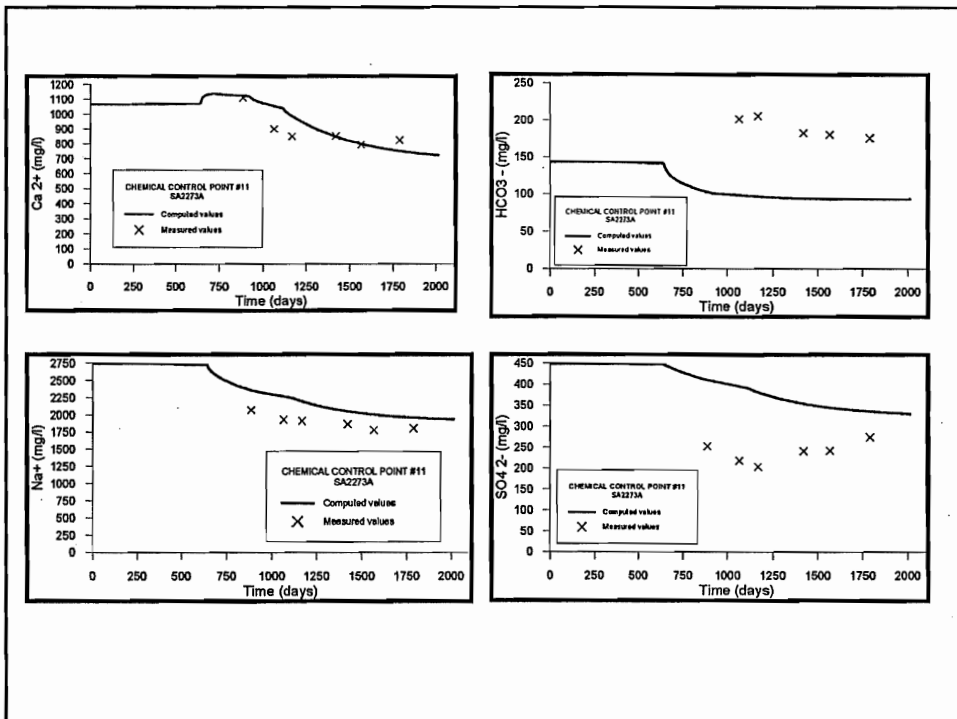
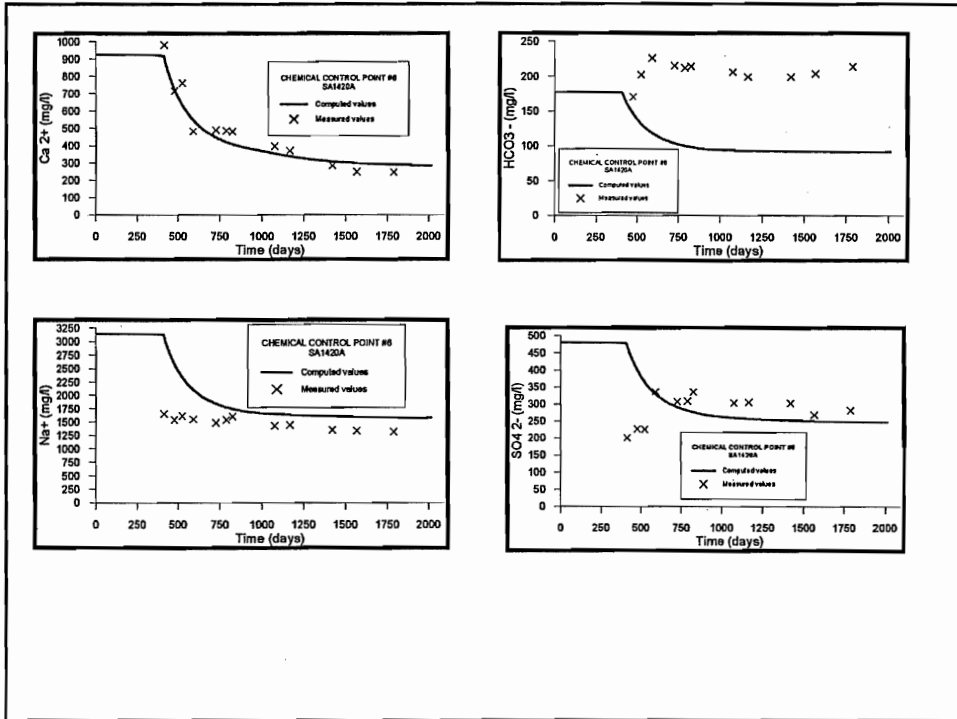
Anion Exchange:

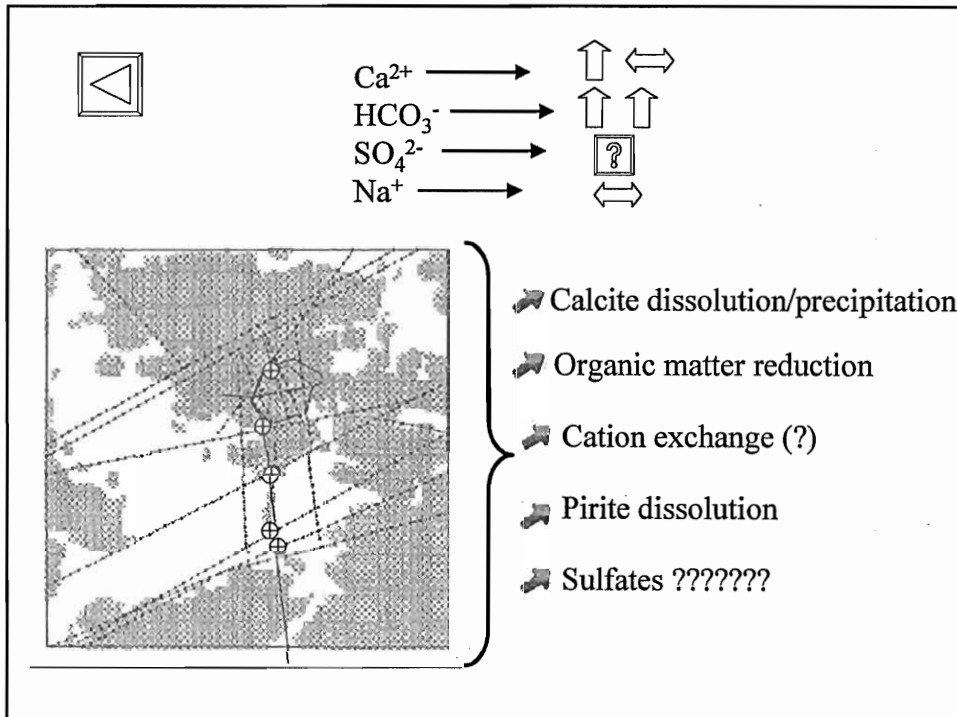


Conservative transport run with the "reactive" species:
 $\text{Na}^+, \text{Ca}^{2+}, \text{HCO}_3^-, \text{SO}_4^{2-}$









CONCLUSIONS I

Calibrated model provides an excellent solution for both inflows into the tunnel and heads at boreholes

With a strongly consistent flow model, the numerical model reproduces conservative species using available transport parameters

**Numerical model is very sensitive to flow parameters on HCD, and not sensitive to flow boundary conditions and parameters at the intersections
The main source of uncertainty is related with the initial field of concentrations**

The numerical model has been validated with additional data of heads and by predictions at selected points near the tunnel.

Predictions were made as a range defined by runs with alternative initial concentrations. Results computed with both runs provided a reliable prediction range, in agreement with field measurements

CONCLUSIONS II

A good agreement was found between the M3 model and the hydrodynamic numerical model. In general it can be said that there are consistency, but rigorously, the combination of uncertainties related with M3 method and the interpolation makes impossible to quantify this consistency.

M3 has been useful to shape some aspects of the Äspö site hydrogeology, specially, it provides a good conceptual-genetical model.

Hydrogeology has been found fundamental to understand the hydrochemistry

The role of chemical reactions has been evaluated and sources of bicarbonates and calcium has been detected. Sulfates behaviour remains unclear. Some hypothesis for hydrochemistry are formulated, which can be tested by coupled flow and reactive transport models.

A hydraulic transport model of the large-scale fracture system in the Äspö HRL consisting of ten intersection macro-elements

L Liedtke and N Klennert (BGR)

Task 5 - 13th Meeting of the Task Force on Modelling of Groundwater Flow and Transport of Solutes

February 8 - 11, 2000 - Sandia National Laboratories, Carlsbad, NM, USA

A hydraulic transport model of the large-scale fracture system in the Äspö Hard Rock Laboratory consisting of ten intersecting macro- elements

BGR

L. Liedtke & N. Klennert

ABSTRACT

This study deals with the influence of the tunnel construction on the groundwater system at the Äspö site concerning changes in the flow pattern as well as the disturbance of the chemical balance. A hydraulic and transport model was constructed to simulate the processes dominating the hydraulic and chemical systems in the investigated area with and without the spiral tunnel.

Flow and transport calculations were carried out for a multi fracture model including ten fracture zones. The conditions before, during and after the tunnel construction were simulated. Measured piezometric heads and the distribution of the four different water types at specific control points were compared to simulated values. Corresponding to the deviations, input parameters and boundary conditions were varied to achieve a better response of measured and simulated values.

The modelling confirmed the observed drawdown beneath the island of Äspö and the resulting change in the flow pattern and flow velocities. In contrast to initial conditions, the model indicates downward groundwater flow above the tunnel. This results in dilution of dissolved substances by meteoric water flowing into the aquifer. However, upward groundwater flow of brine water that increases the salinity is observed in the fractures beneath the tunnel.

Transport calculations demonstrate the changing distributions of the different water types at the Äspö site that can be compared to observed chemical compositions at specific control points. Nevertheless, chemical analyses of water samples at the control points show clear deviations in comparison to simulated concentrations that result from the mixing model. For this reason, a chemical program is used to identify chemical processes that helps to increase the understanding of the groundwater development.

OBJECTIVES

The aim of Task 5 is to compare and ultimately integrate hydrochemistry and hydrogeology. The general method is to compare the outcome of the hydrochemical models with the groundwater flow models. The Task 5 modelling will also be useful for a future assessment of the stability of the hydrodynamic and hydrochemical conditions at Äspö. This modelling approach could, if successful, then be used for any future repository site investigation and evaluation, especially in a crystalline bedrock environment. The objectives of this study arise from the general objectives stated for Task 5.

The specific objectives are:

- to assess the consistency of groundwater flow models and hydrochemical mixing-reaction models through integration and comparison of the hydraulic and chemical data obtained before, during and after tunnel construction
- to develop a procedure for integration of hydrological and hydrochemical information which could be used for an assessment of potential disposal sites.

SITE DESCRIPTION

The Äspö Hard Rock Laboratory is located about 2 km north of the Oskarshamn Nuclear Power Station on the island of Äspö. The access tunnel extends from the Simpevarp island, runs under the sea floor and reaches the spiral part of the HRL beneath the island. The total length of the tunnel amounts to 3600 metres and reaches a maximum depth of 450 metres below ground level.

The geology of the Äspö site is characterised by a Småland type medium grained porphyritic granite to quartz monzodiorite and in the south of the island by the red granite variety of Ävrö. Furthermore some intersections with fine-grained alkali granite, altered greenstone and dacitic metavolcanics occur as lenses and dikes. Figure 1 shows the major fracture zones in the investigated area in relation to the HRL tunnel. The structures modelled in this study using a part of the collected data set are pointed out.

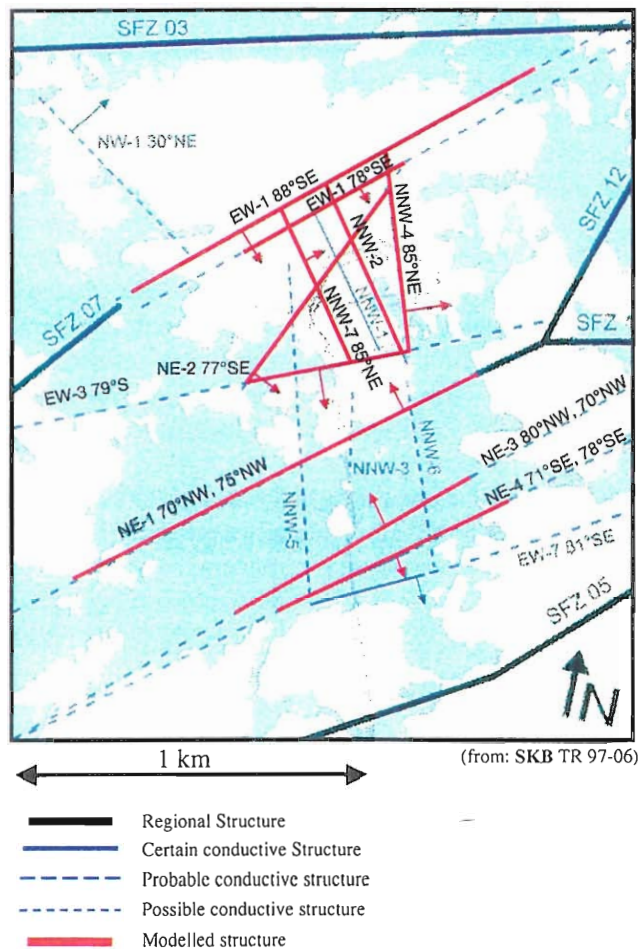


Fig. 1: Hydraulic conductors at the Äspö site.

BASIC APPROACH AND DATA

The 10 discrete fracture zones in the multi fracture model are mostly in hydraulic contact and demonstrate the complex connections between the major hydraulic discontinuities, see Figure 2. Some conductors were intersected by the tunnel several times and show a more significant change in the dynamic conditions than others. Non-steady-state flow was calculated and a detailed pressure model for the following transport calculations was constructed.

The considered fractures are controlled by the island of Äspö and the Baltic Sea and partly by the Hållö Island (fracture NE-4). Therefore, different boundary conditions influencing the dynamic system are to be considered. The modelled fractures are intersected by a number of boreholes in which pressure and chemical data were measured. Hydraulic head measurements from several surface drilled boreholes (KAS) were considered. The groundwater composition was compared with measured water samples taken from probing holes in the tunnel.

GEOMETRIC FRAMEWORK

The model includes the location and orientation of the hydraulic fracture zones NE-1, NE-2, NE-3, NE-4, NNW-2, NNW-4, NNW-7, EW-1 78°, EW-1 88°, and EW-3. They are assumed to be two-dimensional, planar fracture zones, see Figure 2.

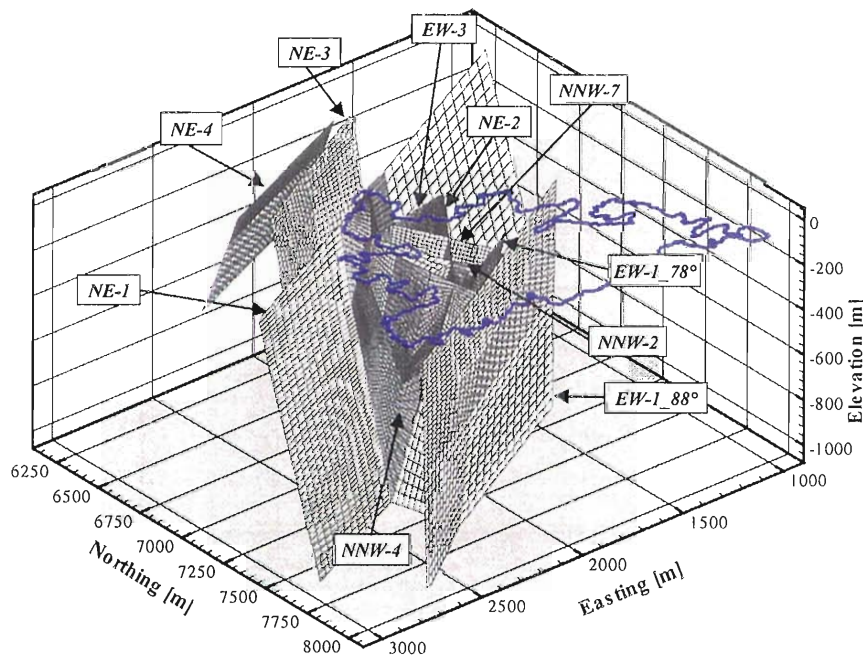


Fig. 2. Survey of the modelled structures.

Quadrilateral, two-dimensional finite elements are used to construct the mesh of the fracture zones. After a refining process of 144 macro-elements the modelled domain of the multi-fracture model includes 13761 nodes and 13536 two-dimensional elements. The edge lengths of the cells are between 8 and 86 metres. Considering the corner points of the computational domain the modelled fractures can be placed in a cube of 2000 m x 1800 m x 1000 m. During the construction of the FE-mesh the calculated corner points, points of intersection with the tunnel and intersections with each other were considered. The tunnel with the shafts as well as the coast of Äspö are represented by one-dimensional elements.

Table 1. Orientation of the fracture planes.

	NE-1	NE-2	NE-3	NE-4	EW-3
Dip [°]	72.5	77	74.3	74.7	79
Azimuth [°]	332.7	126	330	153.7	168.3

	EW-1 78°	EW-1 88°	NNW-2	NNW-4	NNW-7
Dip [°]	78.5	88.1	90	85	85
Azimuth [°]	150.7	150.7	66.3	82.8	65.2

MATERIAL PROPERTIES**Table 2 a. Material properties for the hydraulic conductor domains in the multi-fracture model.**

Fracture	Macroelements	Permeability K [m/s]	Fracture aperture b [m]
NE-1	me 1- 20	8E-7	35
NE-2	me 1; 2; 3; 4	5E-6	10
NE-2	me 5; 6; 7	5E-6	0.1
NE-2	me 8; 9	5E-6	1
NE-2	me 10; 11	5E-6	10
NE-2	me 12	5E-6	30
NE-3	me 1-4	1E-6	35
NE-4	me 1-4	5E-6	35
NNW-2	me 1-7	5E-6	10
NNW-4	me 1; 2; 3; 4	5E-6	20
NNW-4	me 5; 6; 7	5E-6	0.1
NNW-4	me 8; 9	5E-6	1.0
NNW-4	me 10; 11	5E-6	10
NNW-4	me 12	5E-6	30
NNW-7	me 1-8	5E-6	10
EW-1 78°	me 1-9	5E-6	10
EW-1 88°	me 1-9	5E-6	10
EW-3	me 1; 2; 3	5E-6	5
EW-3	me 4	5E-6	10
EW-3	me 5; 6; 7	5E-6	0.1
EW-3	me 8; 9	5E-6	1

Table 2 b.: Material properties for the hydraulic conductor domains in the multi-fracture model.

spec.storage coefficient [1/m]	effective Porosity [%]	longitudinal Dispersion [m]	transversal Dispersion [m]	Diffusion [m ² /s]	Tortuosity [-]
0.0001	25.0	25.0	2.5	1e-09	1

TIME DISCRETIZATION AND SPATIAL ASSIGNMENT METHOD

The modelling period for the flow and transport calculations starts with the beginning of the tunnel construction, representing natural initial conditions. The starting date is the 1st October 1990 (0 days); the modelling period ends after 3765 days. Time discretization of one day was chosen for the transport model which leads to a total of 3765 time steps. For the hydraulic model several flow fields were calculated representing the modelling period between the penetrations of the fractures by the tunnel. This approach depends on the position of the tunnel face during the excavation progress.

BOUNDARY AND INITIAL CONDITIONS

Initially the fractures are assumed to be completely water-filled. The boundary conditions for the vertical, bottom and the upper boundary (Baltic sea) of the flow model are constant pressure heads of zero (Dirichlet conditions) except for the intersection lines of some of the fracture zones. No boundary conditions were assigned to their vertical intersections and bottom boundaries. The recharge rate is assigned to each node of the upper boundary belonging to Äspö island. The initial rate is $7 \cdot 10^{-7} \text{ m}^3/\text{s}$; after the beginning of the drawdown it increases continuously following a defined time function and reaches a value of $2.4 \cdot 10^{-5} \text{ m}^3/\text{s}$ after the tunnel construction.

At the internal boundaries where the tunnel intersects the fractures, temporarily a prescribed head of zero is given until the tunnel reaches the fracture. After the penetration date a piezometric head corresponding to the geodetic height is assigned and a value for the inflow to the tunnel is calculated (Dirichlet conditions).

Initial conditions for transport calculations were interpolated according to the grid information available from data delivery 7 (GURBAN et al. 1998). Different distributions were assigned for the area below Äspö island and the Baltic Sea. The chemical concentrations of the model boundaries depend on the initial proportions of the different types of water. The upper boundary in the area of the Baltic Sea shows a concentration of 100 % of Baltic Sea water, the island of Äspö 100 % of meteoric water. The lower and side boundaries represent constant concentrations according to the initial conditions.

BASIC CHEMICAL ASSUMPTIONS

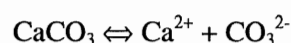
The chemical composition of water samples can for a large part be explained by mixing processes of the four main water types. Differences from analysed non-conservative elements are due to chemical reactions that take place as water-rock interactions, e.g. silicate alteration, solution/dissolution of calcite and gypsum and exchange processes. Possible chemical reactions have a different effective influence on the groundwater composition. This is a criterion to distinguish between important and less important interactions, see below. However, the major constituents are consistent with the known mineralogy at the Äspö site whereas chloride acts as a conservative tracer and does not take part in any of the assumed reactions.

- Most important ions in Äspö groundwater:



- Reactions to be taken into account, e.g.:

- dissolution / precipitation of carbonate:



- dissolution / precipitation of gypsum: $\text{CaSO}_4 \Leftrightarrow \text{Ca}^{2+} + \text{SO}_4^{2-}$
 - dissolution / precipitation of Mn(OH)_2 : $\text{Mn(OH)}_2 \Leftrightarrow \text{Mn}^{2+} + 2\text{OH}^-$
 - carbonate chemistry: $\text{H}_2\text{CO}_3 \Leftrightarrow \text{H}^+ + \text{HCO}_3^-$
 $\text{HCO}_3^- \Leftrightarrow \text{H}^+ + \text{CO}_3^{2-}$
 - sulphate chemistry: $\text{H}_2\text{SO}_4 \Leftrightarrow 2\text{H}^+ + \text{SO}_4^{2-}$
- Reactions, which may be neglected:
 - dissolution / precipitation of salt: $\text{NaCl} \Leftrightarrow \text{Na}^+ + \text{Cl}^-$
 (undersaturated in simulated area)
 - dissolution / precipitation of (iron-)sulphides
 (low concentrations of iron and sulphide)
 - dissolution / precipitation of flourides
 (low concentrations of flouride)
 - dissolution / precipitation of Ba-salts
 (barium not measured)

Mixing proportions of the water samples based on calculations with the M3 - Multivariate Mixing and Mass Balance Calculations approach (LAAKSOHARJU & WALLIN 1997) show significant differences compared to the measured element concentrations of the water samples (GURBAN et al. 1998). For a couple of water samples the chloride concentration shows a deviation of more than 50%. For this reason, the mixing proportions for the water samples were recalculated corresponding to the starting concentrations of the reference waters using chloride, sodium and 18-O as conservative tracers. In order to obtain more realistic initial conditions for further chemical modelling steps the mixing proportions were revised. The four groundwater types were distributed with regard to a better response of the concentrations in comparison to the measurements.

MAIN RESULTS

FLOW MODEL

Corresponding to the leakage rate into the tunnel a drawdown in the modelled area extends that has also been measured in several boreholes. It can be concluded that the intersection of the tunnel with the fractures causes an increase of the hydraulic gradients in the vicinity of the tunnel. The disturbed area around the extraction points extends with time as the tunnel reaches forward and the inflow in the tunnel increases. The observed drawdown reaches a maximum depth of 80 to 90 m below sea level in the central area of the HRL. Results of the simulated drawdown in several boreholes compared with measurements are shown in Figure 3. It includes the surface drilled boreholes KAS04, KAS06, KAS07, KAS08, KAS09, and KAS14. The selected control points represent a good fit compared to the measurements. Apart from this the computed heads generally indicate a drawdown that is too low. This is partly due to the inner boundary conditions where the tunnel penetrates the fractures (Dirichlet conditions). In this area the hydraulic gradient is very high and a control point that is very near to the flow out in the model reflects the pressure heads assigned to the extraction node. This effect can also be observed in Figure 4.

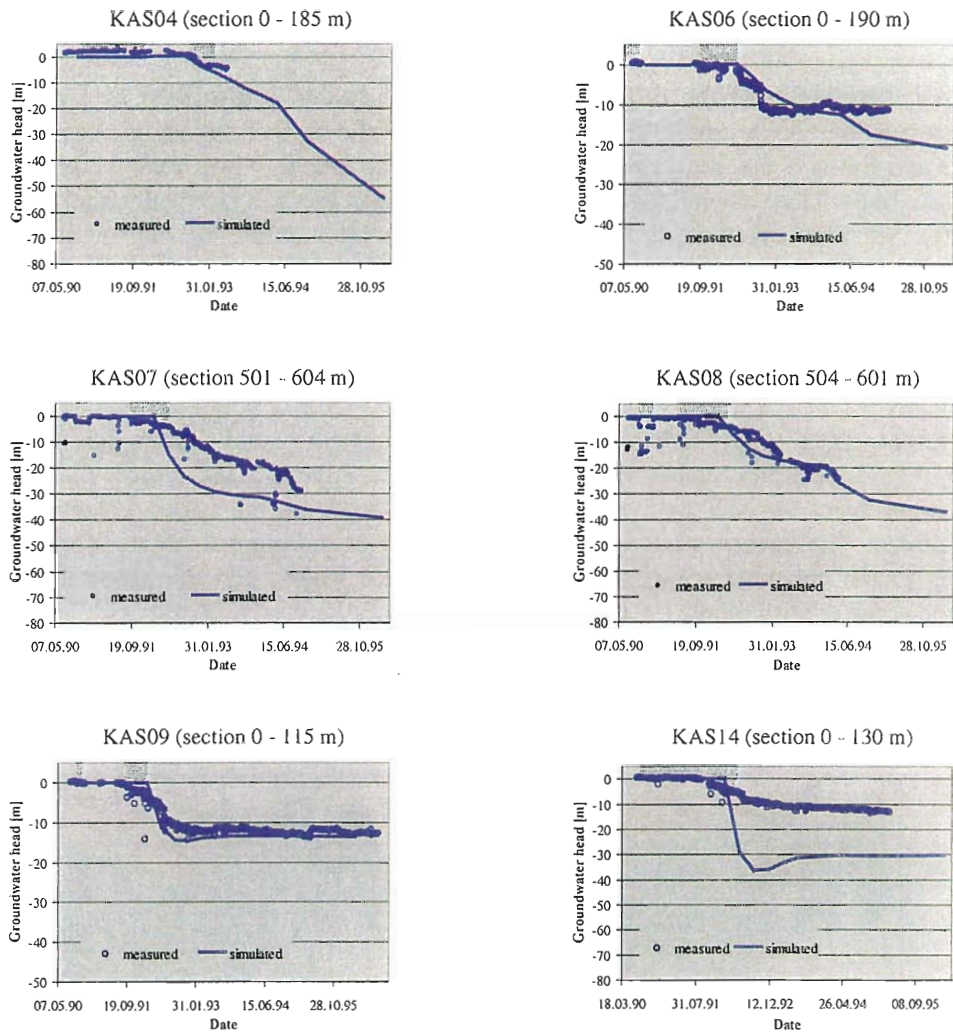


Fig. 3. Measured and simulated groundwater heads at selected control points.

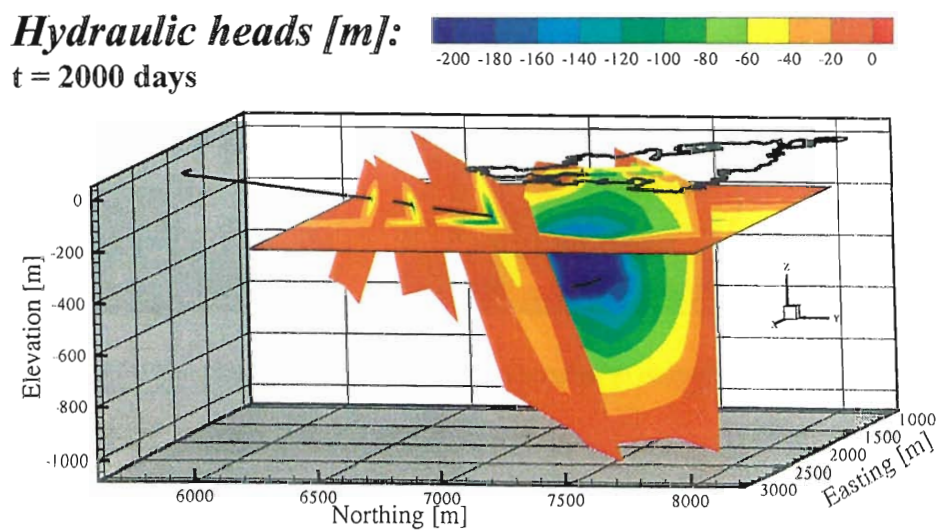


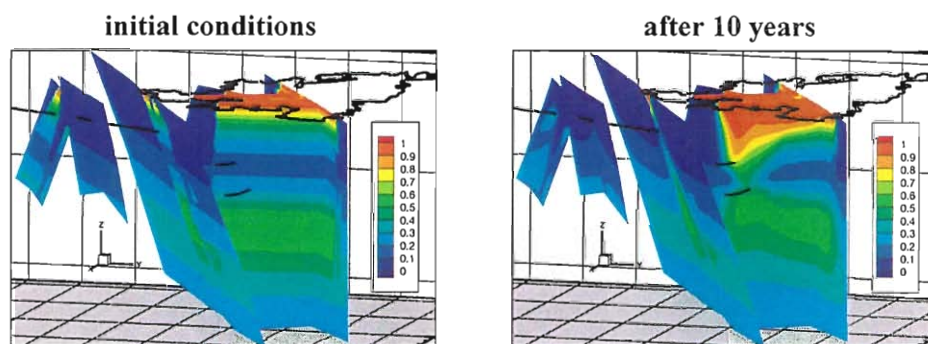
Fig. 4. Simulated hydraulic heads in the multi-fracture model.

TRANSPORT MODEL

The initial distribution of the different types of groundwater is disturbed as a result of the tunnel excavation. As a result of the disturbance of the flow field an increase mainly of meteoric and Baltic Sea water can be observed above the tunnel, which reflects the orientation of the flow lines. They extend downwards to the points in the tunnel where water is extracted constantly. Simultaneously an upconing of the contour lines below the intersections with the fractures is apparent, even if it is in the secondary meaning. However, this leads to an increase of glacial and brine proportions in the upper area. Nevertheless, the proportion of glacial water in general decreases with time. This effect can be explained by a glacial water lense which is slowly bleeding out and can not be refilled as it is a relict water.

The different types of groundwater (brine, glacial, meteoric and Baltic Sea water) were considered separately and treated as conservative tracers. Figures 5 and 6 show the distribution of two water types as well as a comparison of simulated and measured values at selected control points. The conservative species Cl and 18-O at the control points were calculated according to the chemical composition of the reference waters and the proportion of every water type at the control point.

Distribution of meteoric water:



Distribution of glacial water:

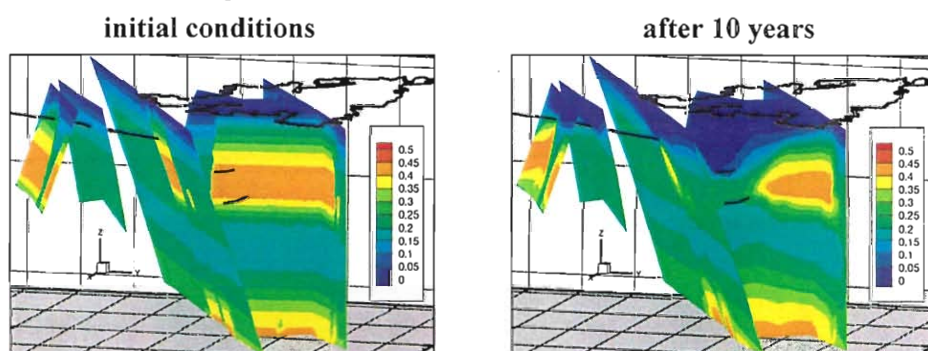


Fig. 5. *Distribution of meteoric and glacial water in the multi-fracture model.*

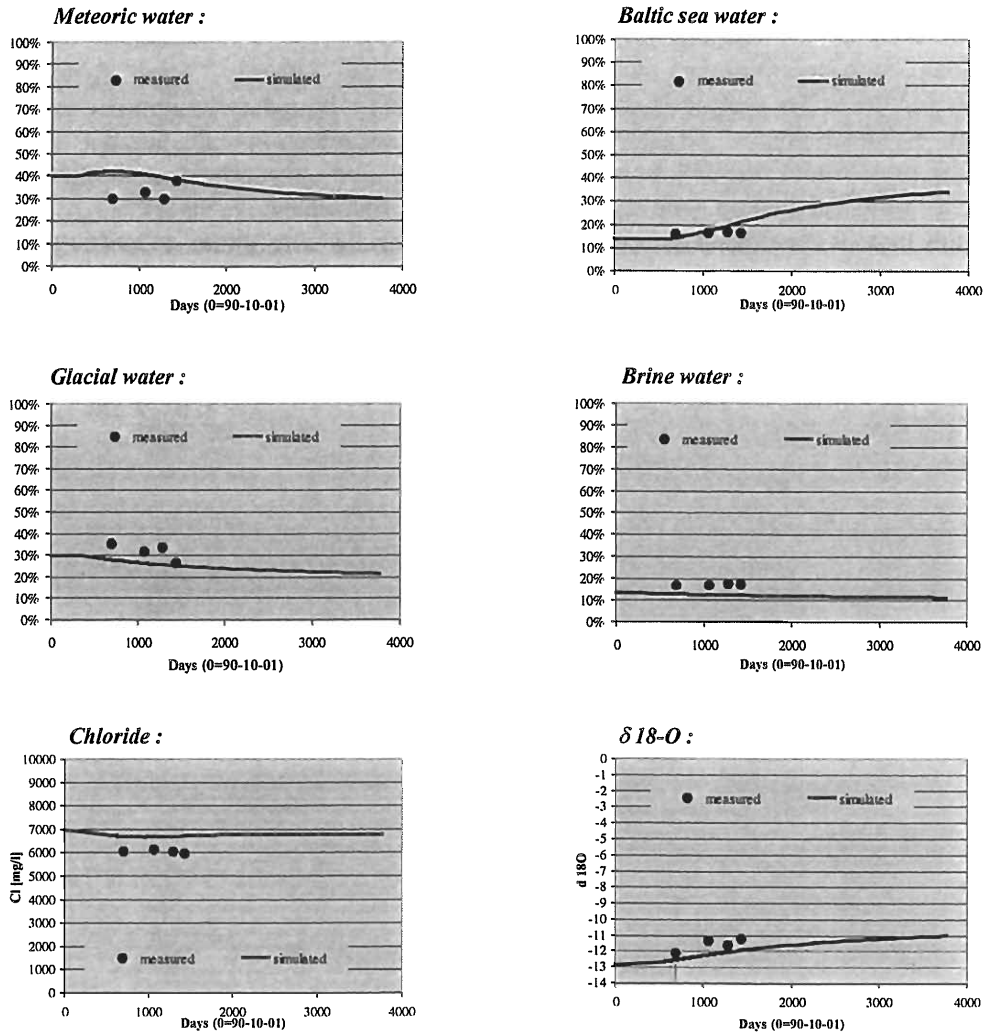


Fig. 6. Measured and simulated values of meteoric, Baltic sea, glacial, and brine water, chloride content, and $\delta^{18}\text{O}$ at borehole KAS07 (CP 11).

Chemical Model

As mentioned above the mixing proportions for some considered water samples given from the M3 approach were recalculated. In the following the procedure for recalculating the water proportions and for doing speciation calculations for the water sample, and mixing and equilibrium calculations for the recalculations with Phreeqc is to be described. The process was done to possibly reduce the deviations of a pure mixing model from measured element concentrations as they exist for conservative elements in the M3 model. In this way not only the conservative but also the non-conservative constituents should show a much better response. The element analyses of a water sample serves as basis for further calculations with Phreeqc (PARKHURST & APPELO 1999). For each water sample the proportions of the different groundwater types are calculated after a set of equations, whereby chloride, sodium and the oxygen isotope ^{18}O act as conservative tracers. Using the determined proportions of each reference water the concentrations of the remaining non-conservative elements can be determined. This is done by means of mixing calculations in Phreeqc. The initial compositions of the reference waters are given and mixed in the determined relation.

The mixture calculation leads to a composition for a specific water sample, whereby concentrations of the non-conservative elements deviate from the measured values. These deviations are to be minimized by equilibrium calculations. For this purpose first a speciation analysis for the water sample is done, that gives specific boundary conditions (SI of calcite, gypsum, dolomite, and CO₂(g)) for the following equilibration calculations. The element concentrations, which resulted from the mixing calculation, are defined as initial solution for the equilibrium calculation with appropriate pH and Eh values. As boundary conditions the saturation indices mentioned above as well as equilibrium with albite, k-feldspar and quartz (SI=0) serve. The element concentrations for borehole SA1828B resulting from the chemical approach are shown in Figure 7.

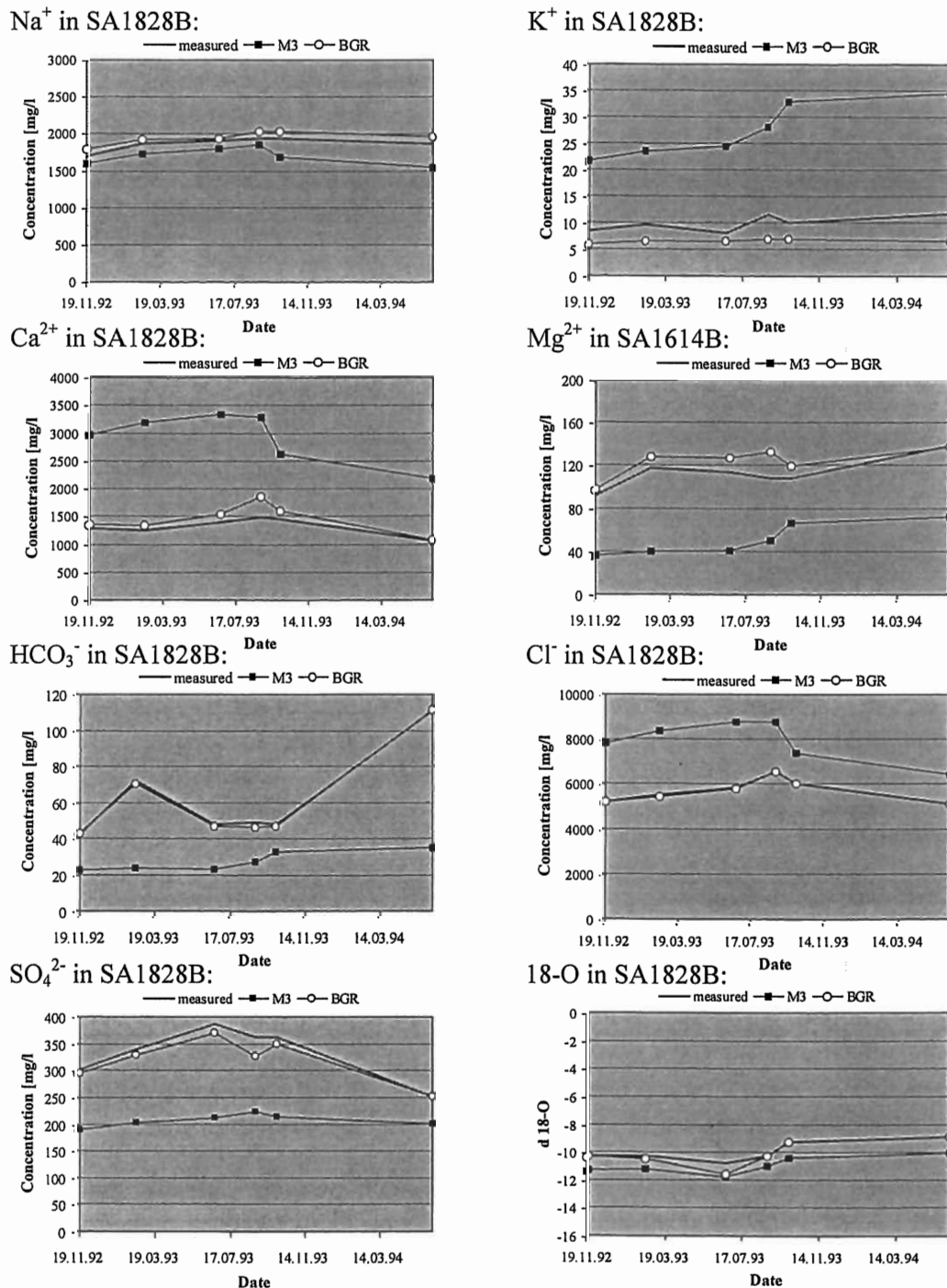


Fig. 7. Development of the measured element concentrations in borehole SA1828B compared to the M3 mixing model and the BGR mixing and equilibration approach.

REFERENCES

- Ittner T, Gustafsson E, 1995. Groundwater Chemical Composition and Transport of Solutes. Evaluation of the Fracture Zones NE-1, NE-2 and NNW-4 during Preinvestigation and Tunnel Construction. SKB PR HRL-96-03, Stockholm.
- Gurban I, Laaksoharju M, Andersson C, 1998. Influences of the Tunnel Construction on the Groundwater Chemistry at Äspö – Hydrochemical Initial and Boundary Conditions: WP D1, WP D2. SKB TN-98-17g, Stockholm.
- Laaksoharju M, Skarman C, 1995. Groundwater Sampling and Chemical Characterisation of the Äspö HRL Tunnel in Sweden. SKB PR 25-95-29, Stockholm.
- Laaksoharju M, Wallin B, 1997. Evolution of the Groundwater Chemistry at the Äspö Hard Rock Laboratory. Proceedings of the Second Äspö International Geochemistry Workshop, June 6-7, 1995. SKB ICR 97-04, Stockholm.
- Markström I, Erlström M, 1996. Äspö Hard Rock Laboratory. Overview of Documentation of Tunnel, Niches and Core Boreholes. SKB PR HRL-96-19, Stockholm.
- Mészáros F, 1996. Simulation of the Transient Hydraulic Effect of the Access Tunnel at Äspö. SKB ICR 96-06, Stockholm.
- Parkhurst D L, Appelo C A J, 1999. User's Guide to Phreeqc (Version 2) – A Computer Program for Speciation, Batch-Reaction, one-dimensional Transport, and Inverse Geochemical Calculations. U.S. Geol. Surv. Water Res. Inv. 99-4259, 312 pp; Denver, Colorado.
- Parkhurst D L, 1995. User's Guide to Phreeqc – A Computer Program for Speciation, Reaction-Path, Advective-Transport, and Inverse Geochemical Calculations. U.S. Geol. Surv. Water Res. Inv. 95-4227, 143 pp; Lakewood, Colorado.
- Rhén I, Stanfors R, 1993. Passage through Water-Bearing Fracture Zones. Evaluation of Investigations in Fracture Zones NE-1, EW-7 and NE-3. SKB PR 25-92-18, Stockholm.
- Rhén I, Stanfors R, 1995. Supplementary Investigations of Fracture Zones in Äspö Tunnel. SKB PR 25-95-20, Stockholm.
- Rhén I, Gustafson G, R Stanfors, P Wikberg, 1997. ÄSPÖ HRL - Geoscientific Evaluation 1997/5. Models Based on Site Characterisation 1986 - 1995. SKB TR 97-06, Stockholm.
- Rhén I, Magnusson J, Forsmark T, 1998. Äspö Task Force on Modelling of Groundwater Flow and Transport of Solutes - Task #5. Data Compilation: WP A3, WP A 4. SKB TN-98-06g, Stockholm.
- Wikberg P, 1998. Äspö Task Force on Modelling of Groundwater Flow and Transport of Solutes. Plan for Modelling Task # 5: Impact of the Tunnel Construction on the Groundwater System at Äspö, a Hydrological-Hydrochemical Model Assessment Exercise. SKB PR HRL-97-07, Stockholm.

Geochemical modelling plan and preliminary results

T Hasegawa and T Igarashi (CRIEPI)

1. Background

On Task#5, the mixing ratio of four end members, i.e. Meteoric, Baltic, Brine and Glacial water, was already obtained without considering geochemical reaction. The initial and boundary conditions of the calculation was based on the principle component analysis, which is called M3 (Multivariate Mixing and Mass balance calculations). In this study, the effect of geochemical reactions on the groundwater chemistry in the tunnel are evaluated by considering equilibrium reactions using PHREEQE.

2. Modeling Process

The concept of the geochemical modeling used in this study is shown in Fig.1. The modeling consists of three processes. First, the initial compositions of four end members are defined based on the measured chemical compositions (e.g. Brine and Glacial water). Second, the chemical properties of the mixed water are calculated from the mixing ratio predicted by the M3 results. In this step, chemical reactions are not taken into account. Finally, several equilibrium geochemical reactions are introduced to the calculated chemical compositions at the second step to identify the reaction that evolve groundwater chemistry. The HARPHRQ is used for the calculation, together with the geochemical database, HATCHES, which were developed by UKAEA. In addition, cation exchange reactions are also considered.

3. Geochemical reactions considered

Based on 'Groundwater reaction to consider within the Task 5 modeling', the following reactions were selected,

- 1) HCO_3^- production caused by decomposition of organic material in meteoric water
- 2) Consumption of dissolved oxygen in meteoric water by pyrite oxidation
- 3) Precipitation and dissolution of calcite
- 4) Cation exchange by clay minerals
- 5) Oxidation-reduction between HS^- and SO_4^{2-}

4. Assumptions

The chemical compositions of four end members were assumed in Table 1. The observed chemical compositions of groundwater samples at evaluation points are shown in Table 2.

Table 1 Representative chemical composition of four end members

Reference Water	Na	K	Ca	Mg	HCO ₃	Cl	SO ₄	D	Tr	O18
Brine	8500	45.5	19300	2.12	14.1	47200	906	-44.9	4.2	-8.9
Baltic Sea	1960	95	93.7	234	90	3760	325	-53.3	42	-5.9
Glacial	0.17	0.4	0.18	0.1	0.12	0.5	0.5	-158	0	-21
Meteoric	0.4	0.29	0.24	0.1	12.2	0.23	1.4	-80	100	-10.5

Unit D: (o/oo dev SMOW); Deuterium (o/oo) deviation from SMOW, Tr: (TU); Tritium, TU= Tritium units, O18: (o/oo dev SMOW); oxygen - 18 (o/oo) deviation from SMOW, Others: (mg/liter)

Table 2 Observed chemical condition at evaluation points

ID code	date	Brine	Glacial	Meteoric	Baltic Sea	Na	K	Ca	Mg	HCO ₃	Cl	SO ₄
KR0012B	960521	3.1%	3.1%	88.8%	4.9%	326.9	3.7	83.6	14.4	302	495.6	102
SA0813B	960521	3.0%	3.0%	47.8%	46.2%	1523	19.4	276	112	319	2964	252
SA1229A	960521	2.4%	2.4%	38.3%	56.8%	1640	28.0	413	137	303	3393	248
SA2074A	950518	7.6%	7.6%	53.9%	31.0%	1454	9.3	560	119	128	3414	262
SA2783A	960520	29.4%	37.7%	16.5%	16.5%	3053	10.9	4062	49	15	12054	616

Initial conditions of end members

Initial chemical conditions of four end members were assumed as follows,

- 1) The pH values range from 6 to 9, because the observed pH values at almost all of the monitoring points were within the range.
- 2) Considering the origin of the end members, meteoric water is oxic and the others are anoxic.
- 3) The solubility of calcium ion is restricted by the solubility product of calcite for brine and Baltic Sea water, because of high salinity of the two end members. The principal chemical forms of carbon and sulfur are HCO₃⁻ and SO₄²⁻, respectively. Appropriate pH and pe values are selected so that the chemical compositions of the end members could meet the initial conditions.
- 4) The evaluated pH and pe values are listed in Table 3. The values for glacial and meteoric waters are cited from the JNC Report.

Table 3 pH and pe for each end member

date	Brine	Glacial	Meteoric	Baltic Sea
pH	6.9	7.9	8.5	8.5
pe	-3.6	-4.4	-4.75	7.98

5. Geochemical reaction analysis

The following reactions are considered in this study, and the structure of the geochemical modeling is presented in Fig. 2.

(a) Mixing of different end members

The chemical compositions are evaluated by the mixing of different end members. No chemical reactions are considered.

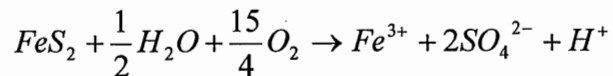
(b) Redox condition controlled by HS⁻/SO₄²⁻, and precipitation/dissolution of calcite

The redox controlled by HS⁻/SO₄²⁻ is assumed to keep the condition anoxic. In addition, the precipitation/dissolution reaction of calcite controls aqueous calcium concentration since calcite is very common fracture fillings.

(c) Consumption of dissolved oxygen in meteoric water by pyrite oxidation

(Considering redox condition controlled by HS⁻/SO₄²⁻ and precipitation/dissolution of calcite)

Pyrite is oxidized when it contacts with dissolved oxygen in groundwater. Therefore, the following reaction is considered for oxic meteoric water.



In this calculation, it is assumed that the meteoric water is saturated with dissolved oxygen in equilibrium with air and that all of the dissolved oxygen is consumed for the pyrite oxidation, producing Fe^{3+} and SO_4^{2-} .

(d) HCO_3^- production caused by decomposition of organic material in meteoric water (Considering redox condition controlled by HS^-/SO_4^{2-} and precipitation/dissolution of calcite)
The decomposition of organic material in the meteoric water is most promising process for the production of HCO_3^- . In the calculation, 20mmol of HCO_3^- is assumed to be supplied by the decomposition of organic material.

(e) Cation exchange between Ca and Na (Considering redox condition controlled by HS^-/SO_4^{2-} and precipitation/dissolution of calcite)
The following conditions related to cation exchange reactions are assumed; 1) the cation exchange reaction occurs on clay minerals, 2) the content of clay mineral is 20%, and 3) the clay minerals within 0.1mm in depth from fracture surfaces participate in the reaction. The geochemical data related to the reaction is determined based on those of bentonite in the JNC report.

6. Calculated results

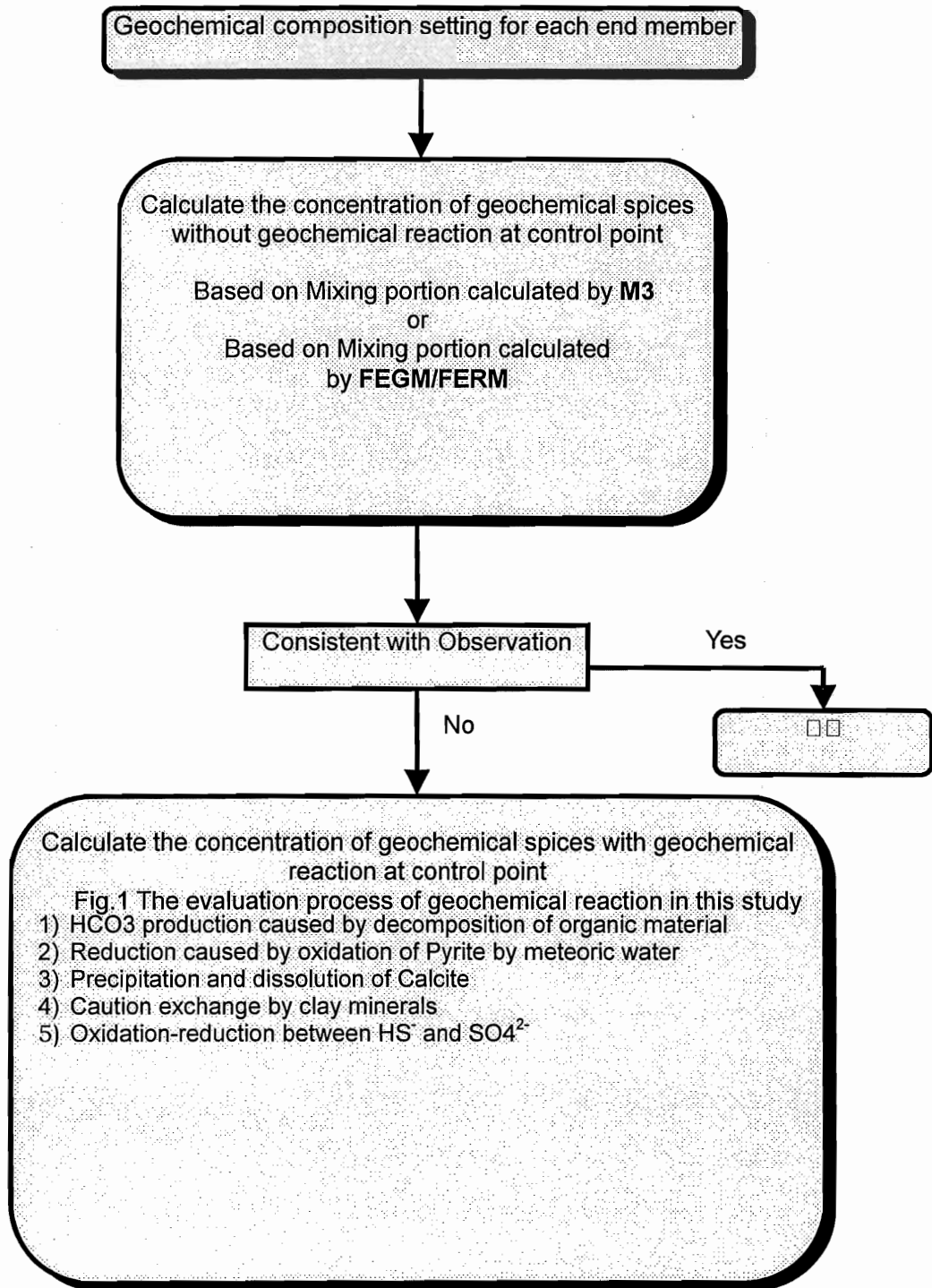
The calculated results are shown in Figs. 3 and 4. Figure 3 represents the predicted results based on the M3, whereas Fig. 4 represents the predicted ones based on the simulated results by FEGM/FERM.

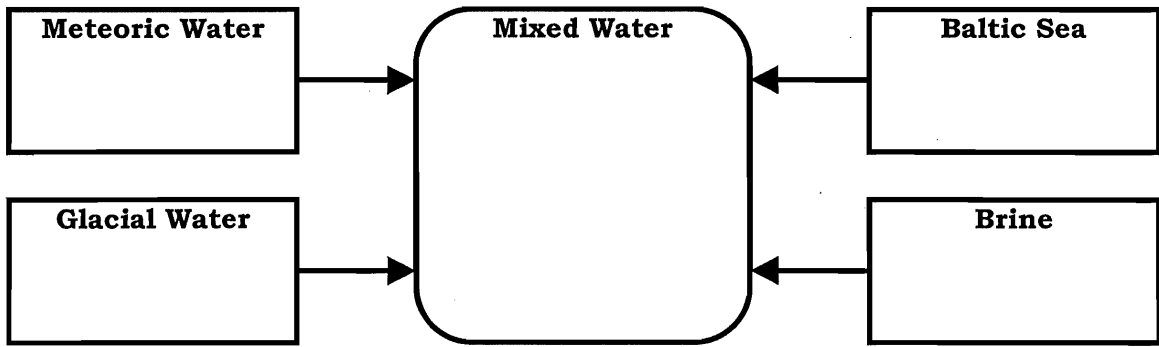
- 1) Decomposition of organic material is sensitive to the concentration of HCO_3^- . It indicates the decomposition of organic material controls the HCO_3^- concentration. However, it is necessary to examine the concentration of organic material. On the other hand, the simulated HCO_3^- concentrations at CP4 and 5 did not agree with the measured data. Much more different results from the measured ones were obtained by considering the decomposition of organic material. Further investigation is necessary to clarify the role of the decomposition of organic material.
- 2) Cation exchange reactions affected the concentration of cations. Better agreement between calculated results and observed ones was obtained by considering the reaction.
- 3) The effects of the redox condition controlled by HS^-/SO_4^{2-} , the precipitation/dissolution of calcite, and the oxidation of pyrite were not significant.

7. Future works

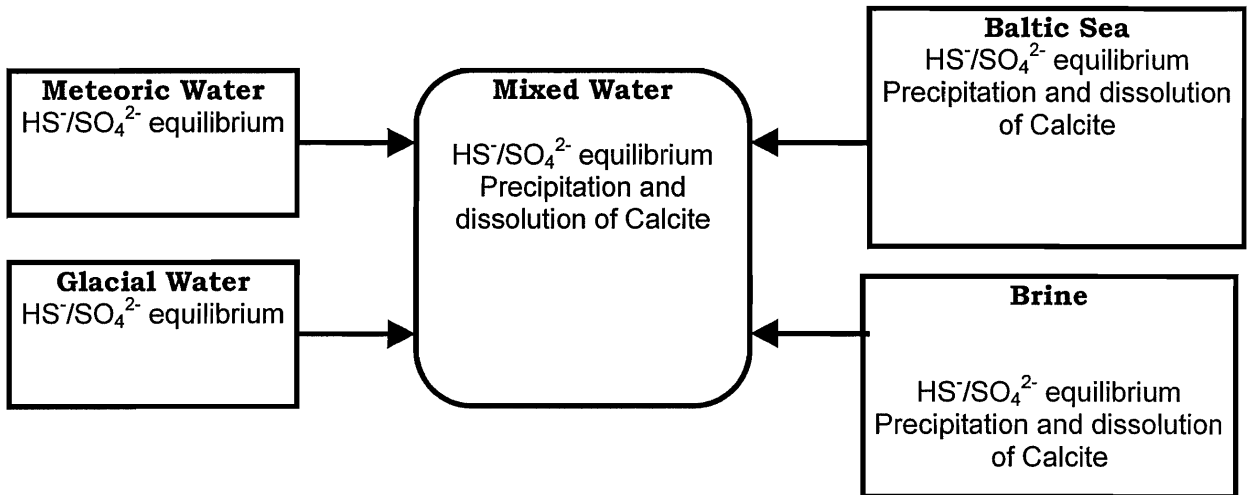
The following issues will be investigated for future study.

- 1) Initial compositions of end members (e.g., pH, pe, HS^- , Fe (II), Fe (III), TOC, DOC)
- 2) Clay minerals participating in the ion exchange reactions
- 3) Equilibrium/Non Equilibrium
- 4) Activity coefficient (e.g., beyond application of Davis's equation)
- 5) Temperature dependence
- 6) Errors of chemical reactions and mixing

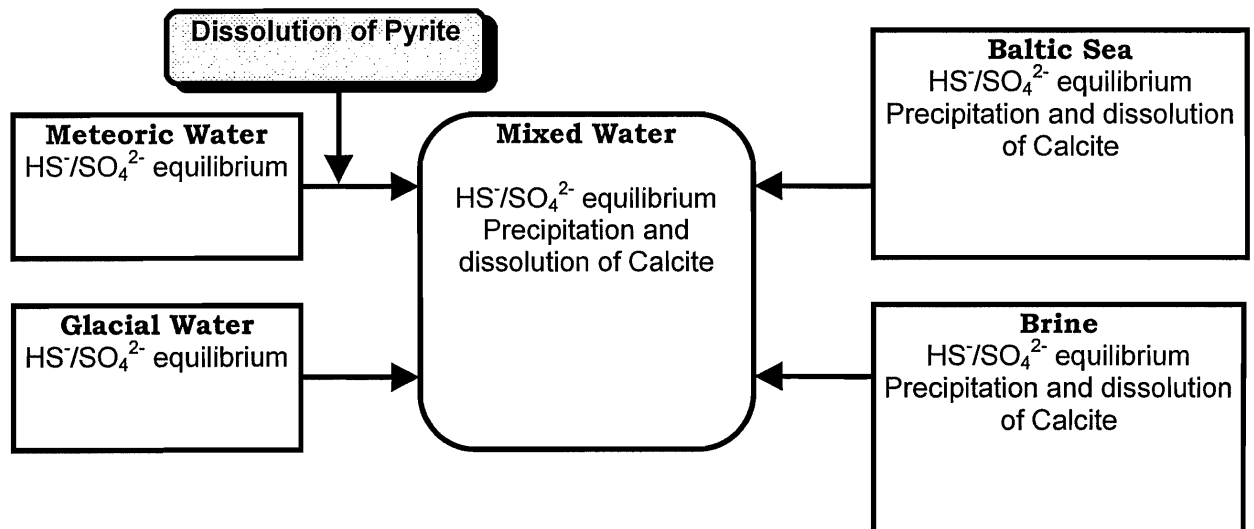




(A) Mixing of different end members

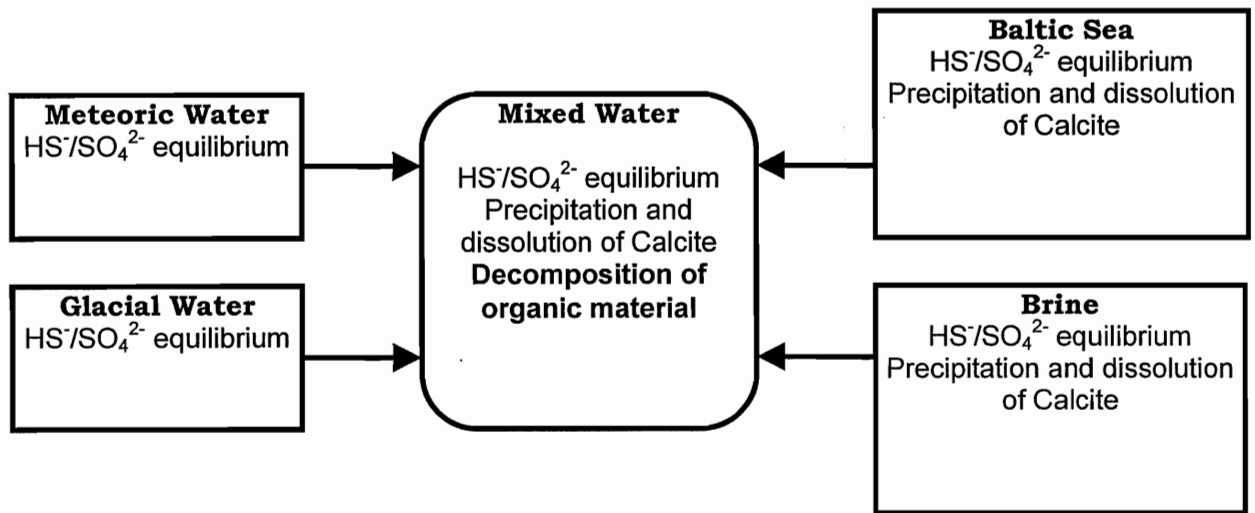


(b) HS⁻/SO₄²⁻ equilibrium, precipitation and dissolution of Calcite

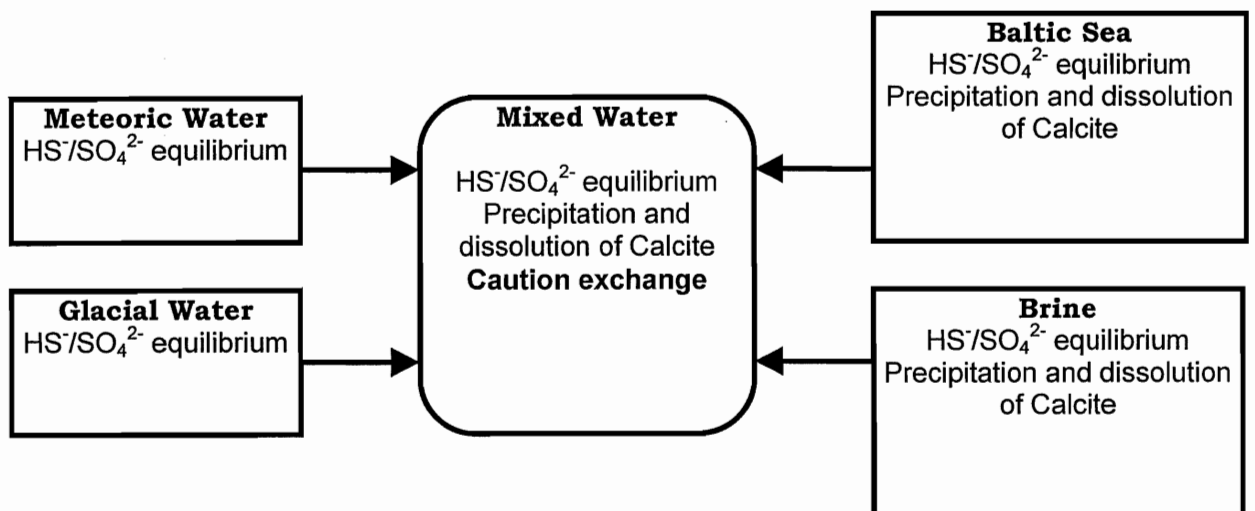


(c) Reduction caused by oxidation of Pyrite by meteoric water

Fig.2 □ Geochemical reaction models including this study (1/2)



(D) HCO₃ production caused by decomposition of organic material in meteoric water



(E) Cation exchange between Ca and Na

Fig.2 Geochemical reaction models including this study (2/2)

Executive summary of Task 5 modelling

W Dershowitz, M Uchida and D Shuttle (JNC/Golder)

Executive Summary of Task 5 Modelling
JNC/Golder
W. Dershowitz, M. Uchida, D. Shuttle
31 January 2000

Approach

The JNC/Golder team participated in Task 5 for a number of reasons, principally,

- to determine the value of geochemical data in hydrogeological modelling, models
- to demonstrate the use of geochemical data in hydrogeological model development and validation, and
- to assess the applicability of DFN pathways analysis at the 2 km scale.

To achieve these goals, the JNC/Golder team implemented two models. The first model "H" was based solely on geological and hydrogeological data. The second model "G" was further conditioned and calibrated based on geochemical data. Both model "H" and model "G" were then used in predictive simulations, and were evaluated by comparison to head and geochemical responses not included in the predictive simulations.

JNC/Golder modeling was carried out using the discrete feature network/channel network approach. In this approach, both major deterministic fracture zones and background fracturing was modeled explicitly as two dimensional discrete features using FracMan/FracWorks. Deterministic fracture zones were based on the zone specifications of Rhen (1999), with the addition of a northwest trending feature to explain the step drawdown responses observed during shaft construction.

Flow and transport were modelled by transforming the fracture network to a topologically equivalent pipe network using FracMan/PAWorks. Flow velocities were adjusted to account for the effect of salinity on density and flow.

Hydrological and geochemical initial conditions for the model were provided by SKB. All transport calculations were made using transport pathways defined by graph theory searches through the channel network model. Transport was expressed in terms of travel times and proportions of four geochemical end members: meteoric, glacial, marine, and brine. Oxygen-18 and Chloride were back calculated from the geochemical end members. The modeled period was from 1990 through 1996.

Head Predictions

Model predictions were prepared for drawdown (head) and geochemical endmembers at control points. Figures 1 through 4 present comparisons of typical head predictions against measurements. Figure 1 shows an example interval in which the predictive model (G4) provided an excellent prediction, even out to two years following the calibration stage. In contrast, the hydrogeologically based model had significantly more error during the calibration stage, and increasing error during the predictive stage.

Figure 2 shows an example prediction in which the model correctly predicts constant head at the control point during the predictive period. As a result, the level of error for the geochemical prediction at this control point remains constant throughout the

predictive period. This implies that the model is adequate for pathways connected to this control point, since it is not effected by activities during the predictive period.

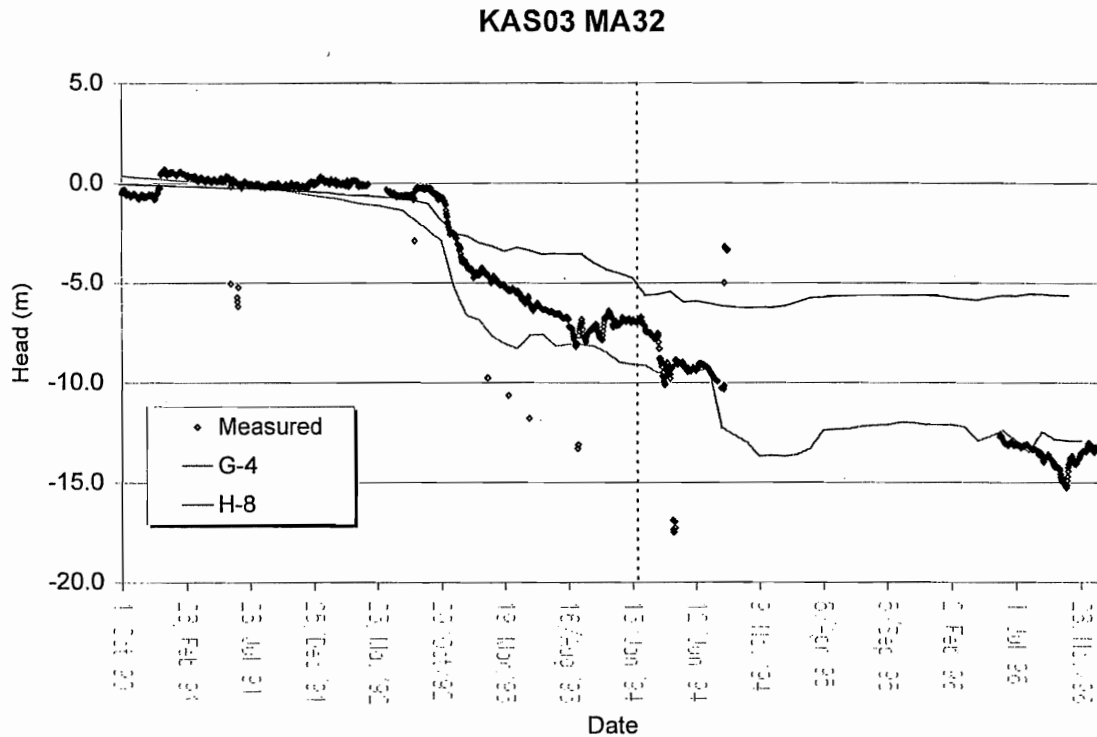


Figure 1: Head Prediction and Measurement for KAS03/MA32

In contrast, Figure 3 show a control point at which 25 meters of drawdown during the prediction period, even though tunnel advance has stopped. This cannot be explained by any of the boundary conditions in our model, and therefore it is a good thing that our model does not predict this occurrence. Thus, for our model to predict the observed behaviors at the control point, our model would require a different boundary condition.

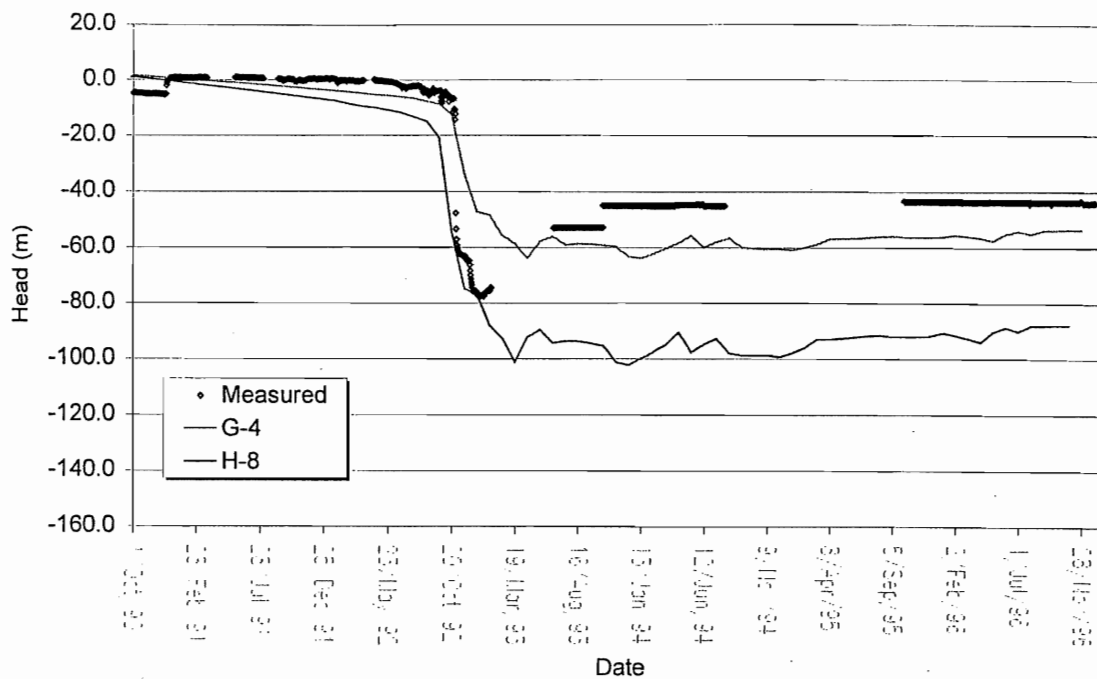


Figure 2: Head Prediction and Measurement for KAS02/MA25

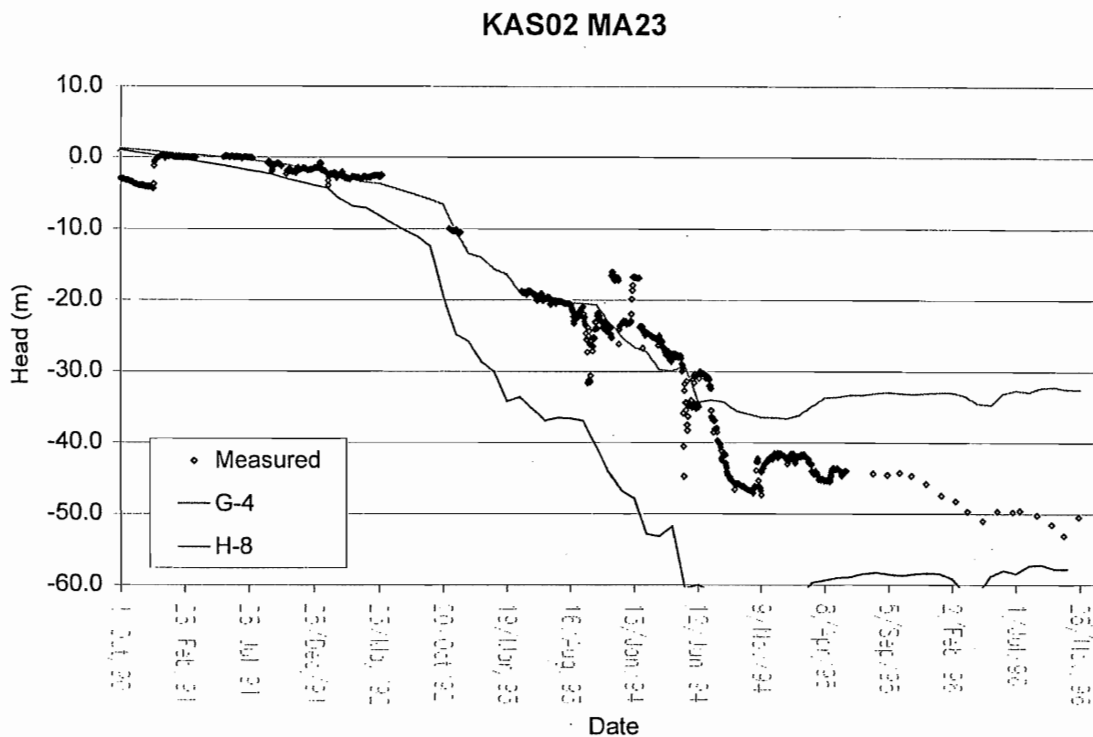


Figure 3 Head Prediction and Measurement for KAS02/MA23

Figures 4 and 5 present error measures dh and DH for the accuracy of the hydrologic geochemical model calibrations H8 and G4. The average error dh for model H8 is significantly higher than that for model G4. This is in part because defined structures assumed from the SKB hydrostructural model were not adjusted during the hydrogeologic calibration, which concentrated on boundary conditions, storativity, and

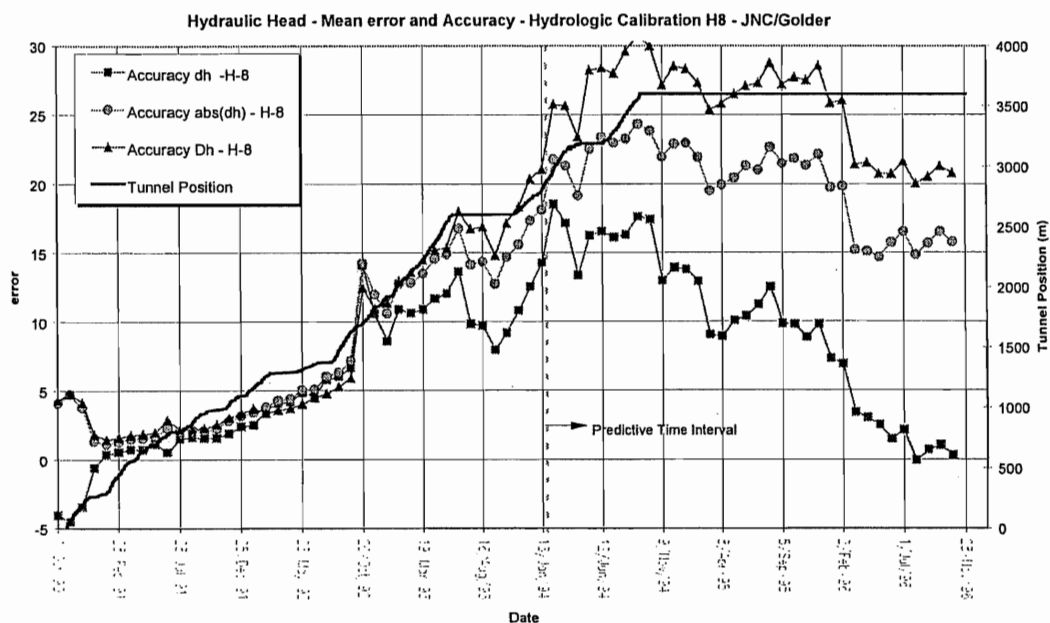
background fracture networks. Interestingly, the average error dh for the H8 model decreased significantly during the prediction period, from near 15 m down to 1 meter. This indicates that although the H8 model was not accurate while tunnel construction activities were ongoing, the model was better as the hydraulic transients in the system decreased.

In contrast, the dh error of the geochemical model G4 (Figure 5) is very small following calibration, and remains near zero for about the first two months following completion of construction. After that, however, the model on the average over-predicts drawdown and the dh error increases systematically from near zero to -4 m.

The systematic nature of this increase in error implies that activities being carried out during this period are not being captured in the model. Most activities carried out in the HRL should be captured by the model boundary conditions, which use measured tunnel inflow. As a result, the predictive error should not increase due to activities such as grouting and borehole installation unless they significantly change the flow pathways to the tunnels. An example of this type of activity might be for example installation of a borehole which provides depressurizes a local region but does not produce sufficient flow to produce a noticeable change to the tunnel inflow boundary condition.

The error measure Dh for the G4 model, however, remains fairly constant during the predictive period indicating that on average, the model continues to perform about as well during the predictive period as it did during the calibration period. Any model improvement for the average error dh might actually make Dh worse. The fact that the model error remained fairly constant for the first six months of the predictive period implies that more accurate prediction would have needed to include additional processes to describe activities in the tunnel during the period June 1994 to December 1996. However, this systematic increase in error for a time period during which no tunnel construction is taking place does not imply issues regarding the model pathways.

Figure 5: Average Predictive Error dh and dH for Hydrologic Calibration H8



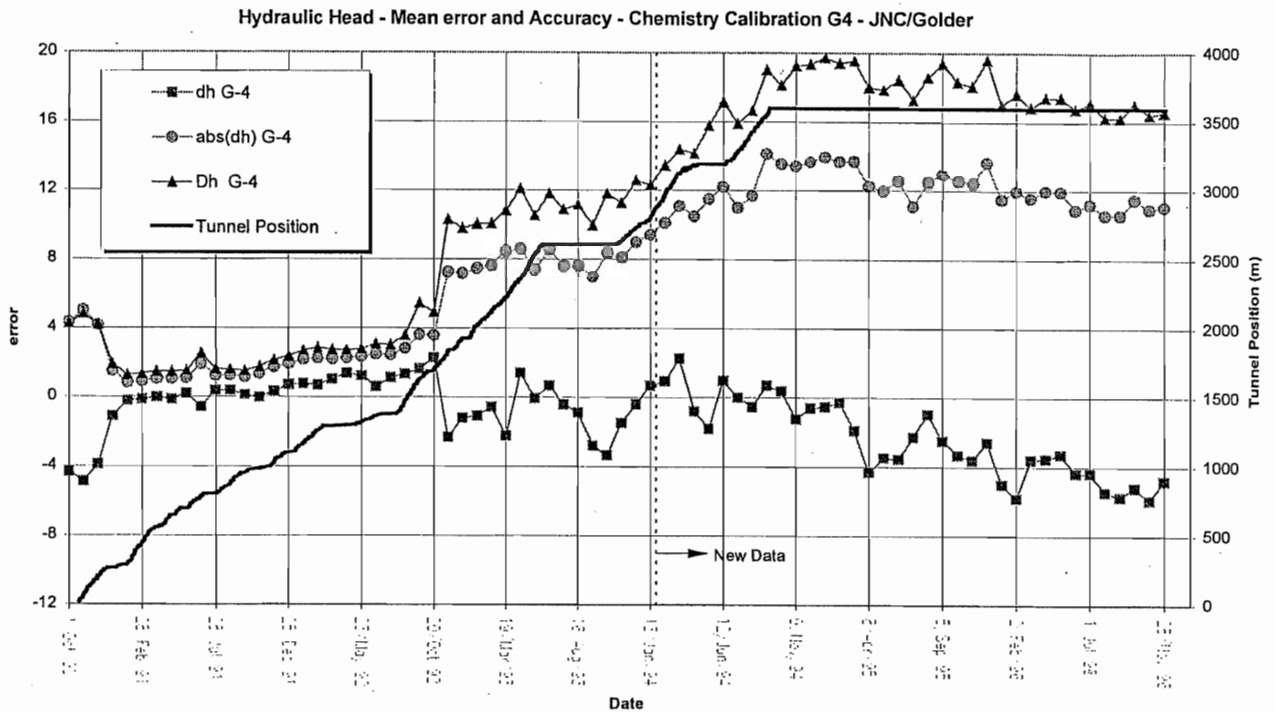


Figure 5: Average Predictive Error dh and dH for Geochemical Calibration G4

Geochemical Predictions

As in the case of geochemical predictions, there are cases in which the model predictions provided a good match, and other cases in which the match was less than inspiring. These latter cases fall into three basic categories.

- a) Cases where the model predicts no change, yet change does occur
- b) Cases where the model predicts change, yet the geochemistry remains stable, and
- c) Cases where the model calibration was poor, and remains poor during the prediction stage.

The comparison of our "H" series predictions to measurements based solely on hydrogeological data generally fall into category c) as shown in Figure 6. Figure 7 shows an example "H" prediction in which our model predicted a significant breakthrough of marine (Baltic) water through a strong pathway to the Baltic. This breakthrough did not occur at the control point, which remained essentially unchanged during the prediction time period.

Figure 8 illustrates a prediction from our geochemical model "G4" in which our model predicted (successfully) that geochemistry would remain essentially constant during the prediction period. Unfortunately, for this case the calibration was not very good, such that the geochemical end member mixture at the end of the calibration period did not provide a good match. Figure 9 presents an example in which our "G4" model did

provide a good match for measurements in the predictive period. However, since little dramatic occurs geochemically during the prediction period, it is hard to discern the effect of pathways connecting to model boundaries and other pathway properties

KA3110A

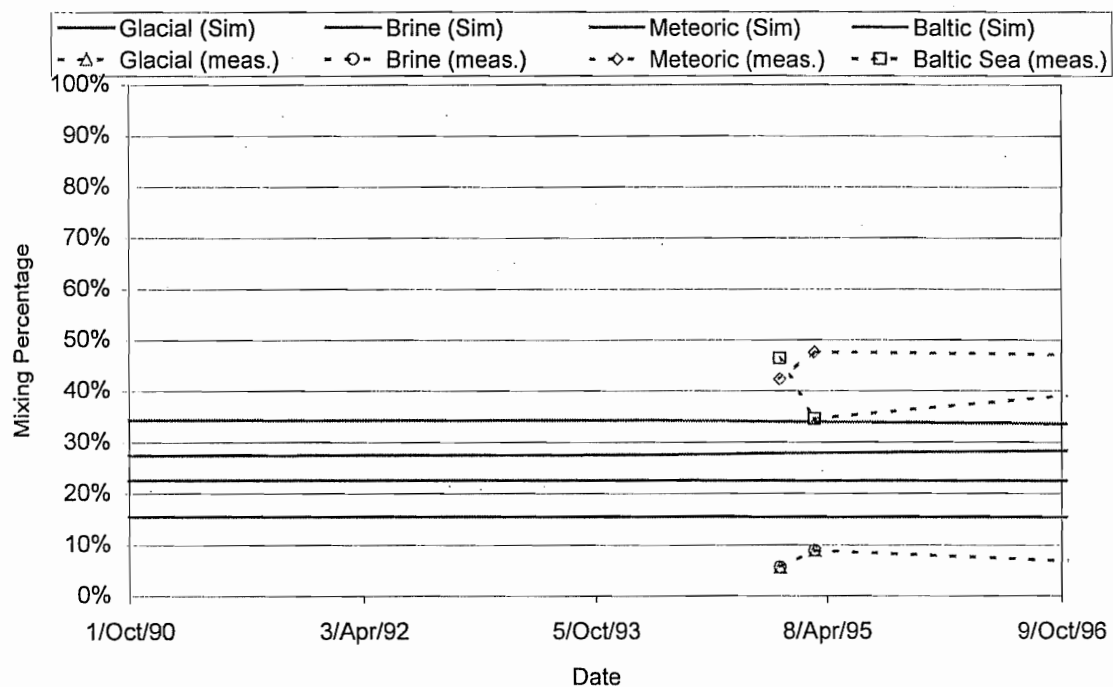


Figure 6: Comparison of Geochemical Predictions and Measurements, H8 Model

KA3385A

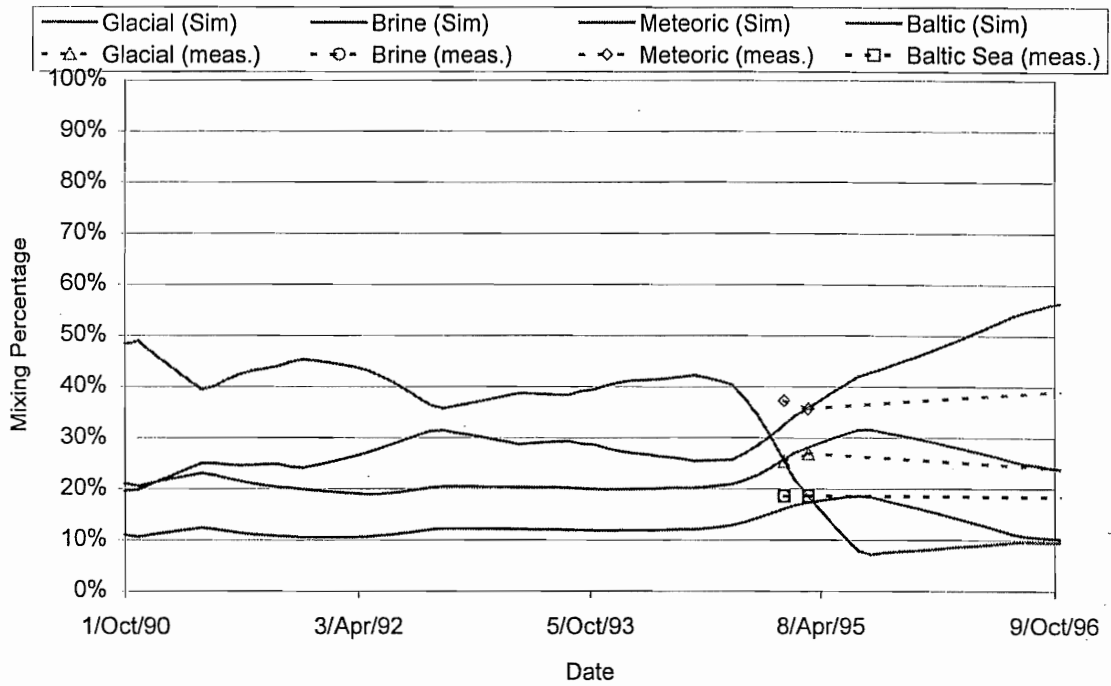


Figure 7: Comparison of Geochemical Predictions and Measurements, H8 Model

KA3005A - Prediction

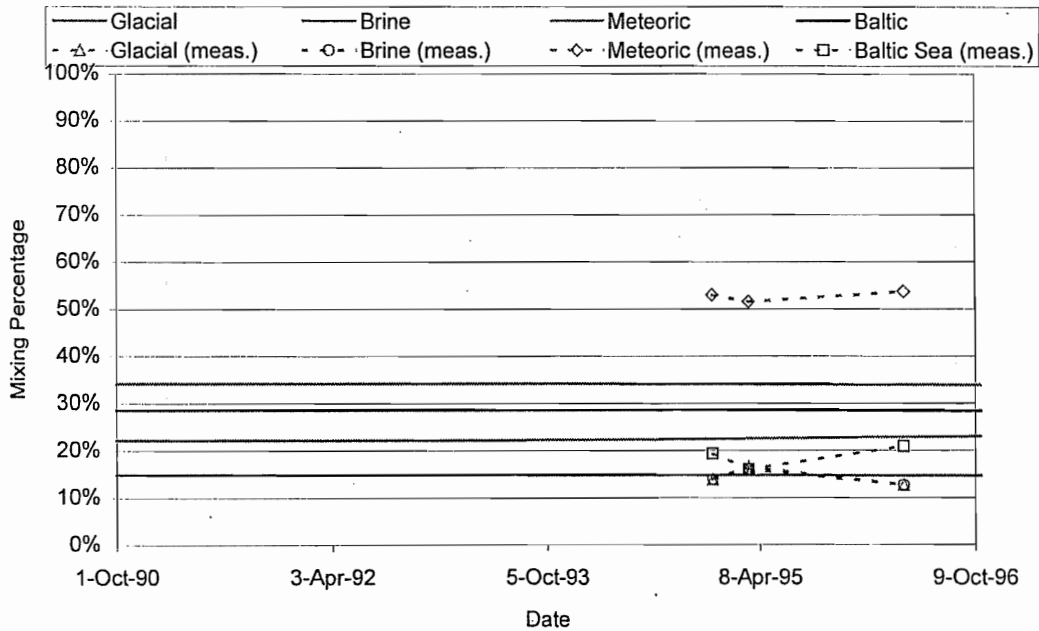


Figure 8: Comparison of Geochemical Predictions and Measurements, G4 Model

KA3385A - Prediction

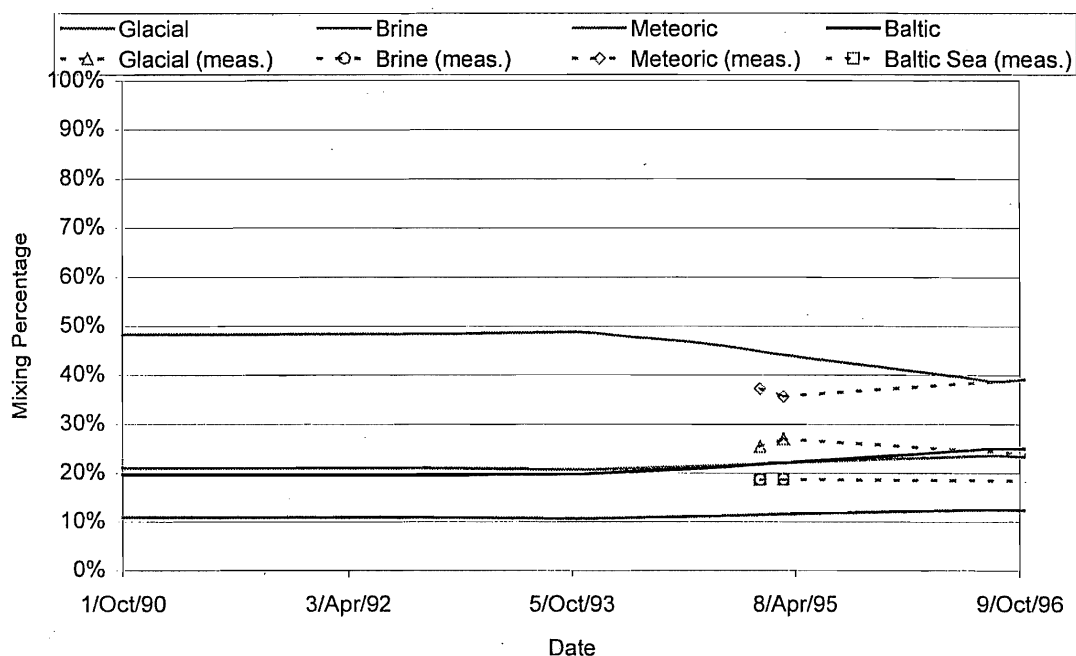


Figure 9: Comparison of Geochemical Predictions and Measurements, G4 Model

Pathway Visualizations

Example pathway visualizations for the hydrogeologic (H8) calibrated model and the geochemical (G4) model are provided in Figures 10 and 11. Figure 10 illustrates how in that model, despite the good match to hydraulic data, pathways are not available to bring Glacial water as measured at KAS2783B. Glacial waters are only available deep in the model, and to the North of Äspö. The geochemical calibration extended fracture connections to the north along the alignment of fracture zone NNW5 to provide a source for glacial water.

Another pathway visualization is shown in Figure 12. Figure 12 shows how model H8 includes overly circuitous paths which bring too much brine and glacial water to chemistry reference point dominated by Baltic and meteoric water. Reduction of the number of pathways included in the model decreases connectivity to sources of Baltic and Meteoric water, increasing the percentage delivery of Baltic water and improving the geochemical calibration.

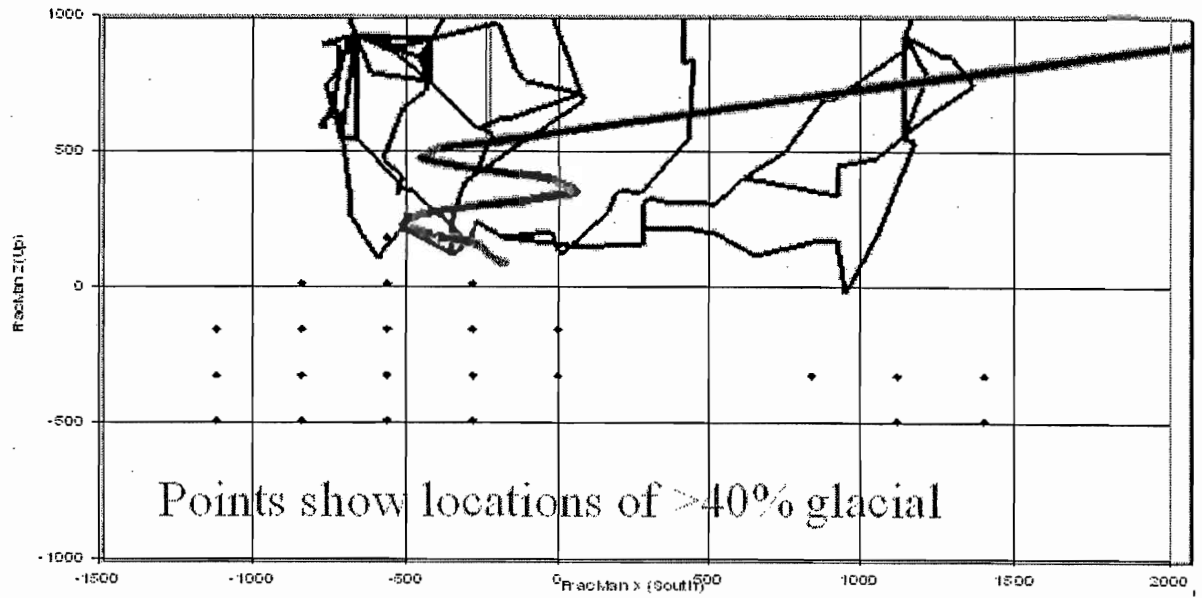


Figure 10: Pathways to SA2783 in H4 Model

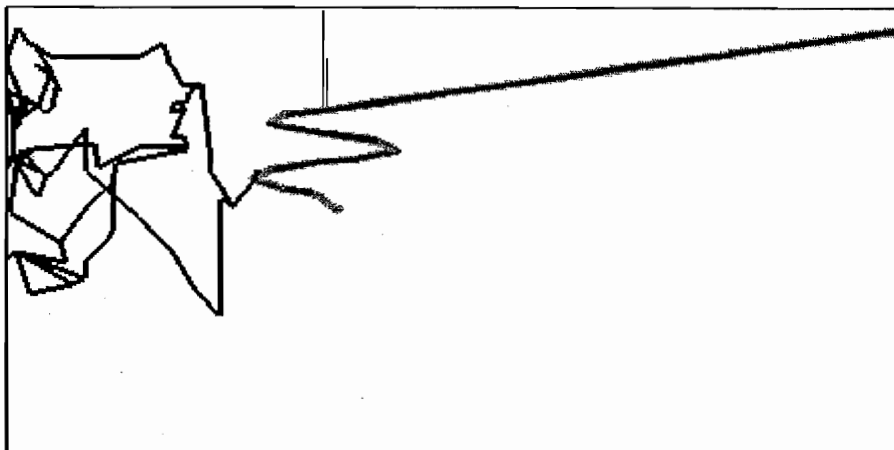


Figure 11: Pathways in H8 Model Connect to Glacial Waters at North of Äspö

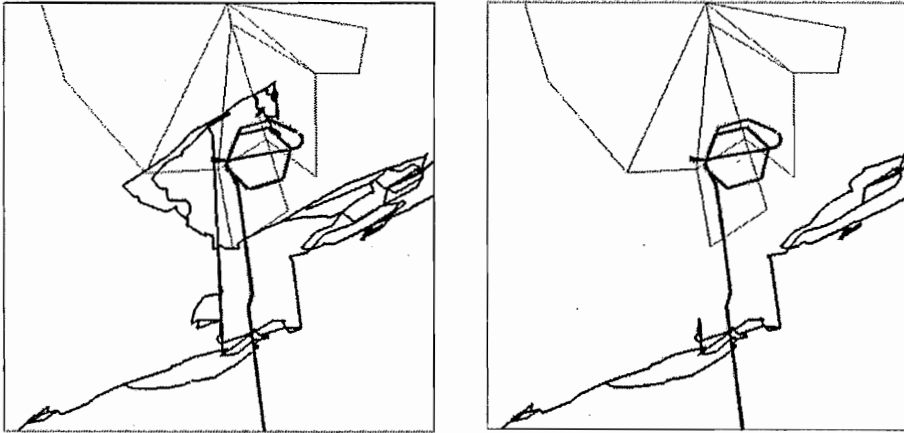


Figure 12: Plan View of Pathways at South of Äspö a) Model H8, and b) Model G4

Conclusions

The modelling carried out for Task 5 demonstrated the strengths and weakness of a forward modeling pathways approach.

1. Because the forward model is confined to physical parameters and structures, there are limited degrees of freedom for model calibration and improvement. In order to improve the geochemical model fit, for example, it was necessary to add structural features to the model which had not been characterized by SKB.
2. Further improvements to the pathways model could require incorporation of additional changes to the structural model to add or delete connections from the model. These changes would require geological or geophysical support.
3. The incorporation of background fractures significantly increased computation time without playing an important role in flow and transport pathways at the 2 km scale. These features could probably be eliminated from most of the model region and replaced by a small increase in transmissivity and storativity of fracture zones.
4. The pathways found by the pathways approach are considerably more complex and less "streamline" than would be expected. It would be useful to compare the pathways from the PAWorks pathway algorithm with streamline pathways through the same DFN model using particle tracking in the network of plate fractures.
5. Modelling and analysis assumed that end-members are accurate as assigned by the Task 5 team. Errors in geochemical end-member predictions are consistent with the level of accuracy of end-member evaluations.
6. The SKB structural model and properties provided a sufficient basis for decent flow and pathways analysis. The hydraulic storage aperture, which controls the travel time and flow rate along pathways, was not available in the structural model and needed to be derived essentially by calibration. This implies that pathways model development requires access to transient data to assess such parameters; steady state data by itself is not sufficient.
7. The hydrologic modelling indicates the importance of boundary conditions, such as the Baltic skin effect. Without any change to material properties inside the model,

changes to boundary conditions alone can modify pathway geometries, geochemical breakthroughs, and head responses.

8. Geochemical data significantly improves model development, both for understanding the geometric structure and pathways, and also for deriving material properties and appropriate boundary conditions.

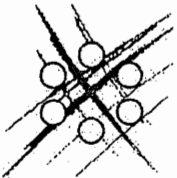
Modelling work of CEA/DMT for Task 5C

C Grenier and L-V Benet (CEA)

Modeling work of CEA/DMT for Task5

C. Grenier and L.-V. Benet

Carlsbad, New Mexico, february 2000



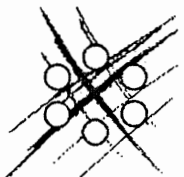
DMT/SEMT/MTMS



Grenier, february 2000 in Carlsbad

Overview

- Geometry and mesh generation
- Permanent flow field before excavation
- Unsteady flow field during excavation
 - ▷ Calibration phase (inflows and pressures)
- Transport and mixing of water types
 - ▷ Mixing proportions, travel times
 - ▷ Sensitivity / calibration elements
- Density effects
- ◇ No chemistry considered

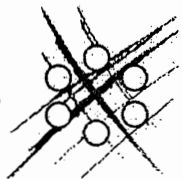


DMT/SEMT/MTMS



Geometry and mesh generation

- Geometrical features obtained by IDEAS (2D fractures and 3D blocks)
- Interface with CASTEM2000
- All features are transformed into 3D objects for future simulations

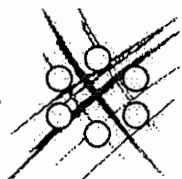


DMT/SEMT/MTMS



Geometrical features

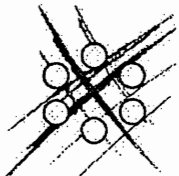
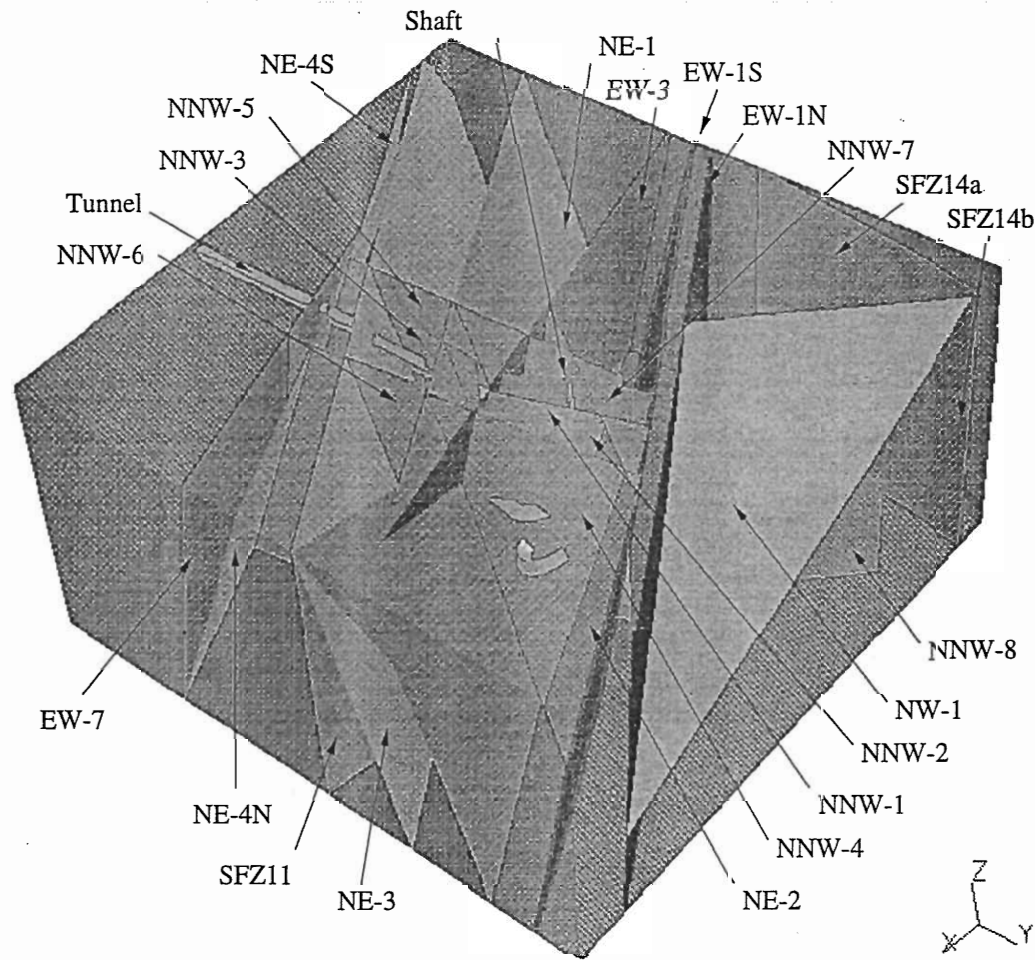
- Aspo 2km x 2km x 1km domain
- Preliminary work limited to hydraulic conductor domain
- Retain 16 pertinent features (6514 meshes), Tunnel (D=80m with triangle section + skin) and Shaft (D=10m with circular section)
- Complicated fracture intersections are not modeled geometrically but by means of continuity relations



DMT/SEMT/MTMS



Geometrical features (2km x 2km x 1km)

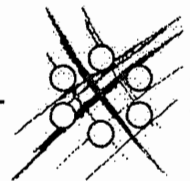
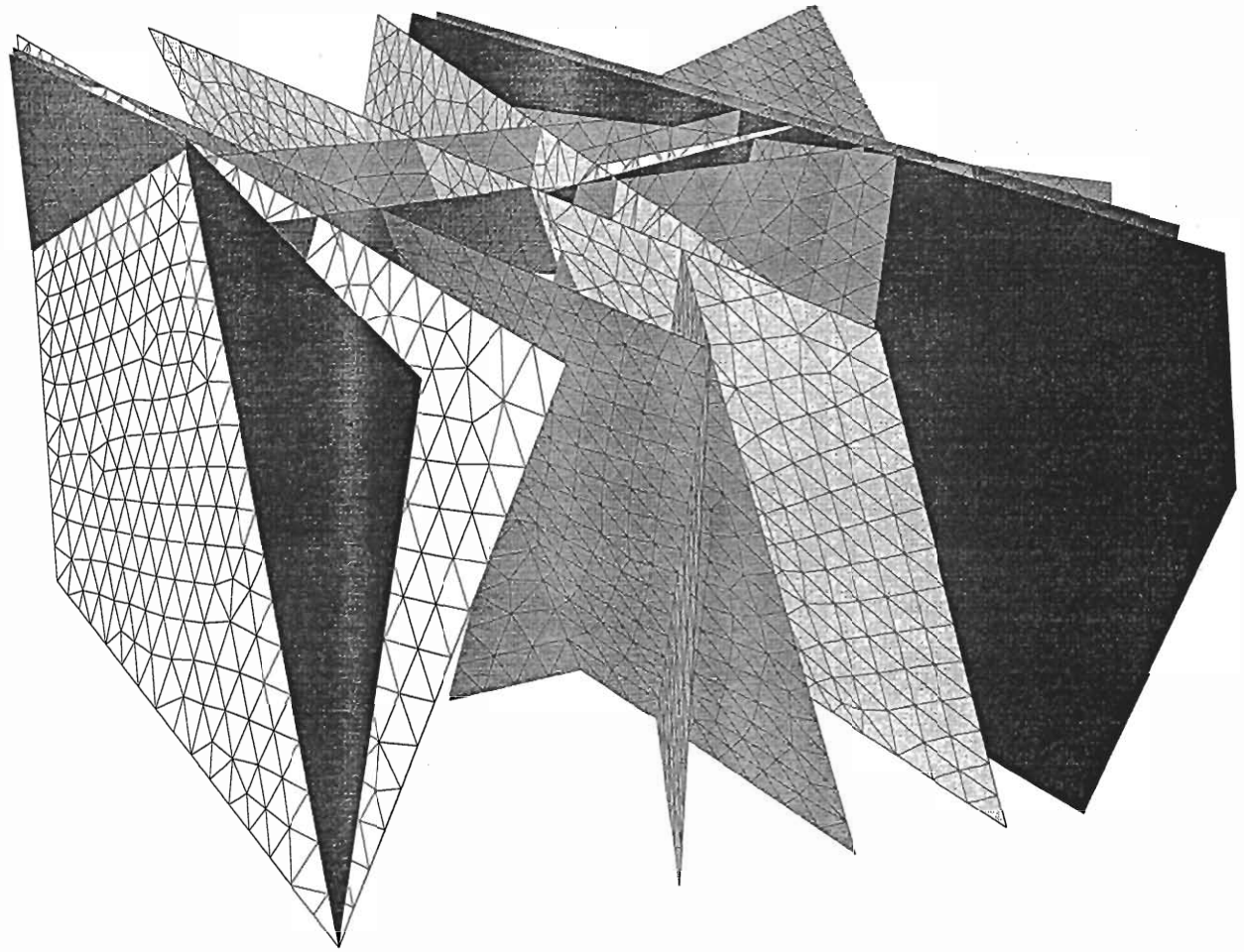


DMT/SEMT/MTMS



Grenier, february 2000 in Carlsbad

Hydraulic conductors (2km x 2km x 1km domain)



DMT/SEMT/MTMS



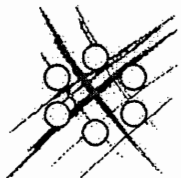
Grenier, february 2000 in Carlsbad

Flow model

▷ No density effect for calibration

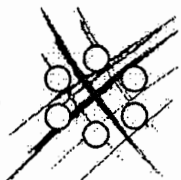
$$\begin{cases} \rho \vec{U} + \frac{K}{g} [\vec{\nabla} p + (\rho - \rho_0) g \vec{\nabla} z] = 0 \\ C_H \cdot \frac{\partial p}{\partial t} + \vec{\nabla} \cdot \rho \vec{U} = 0 \end{cases} \quad (1)$$

- Resolution by MHFE method
- 7000 meshes, 200 time steps



Flow model, boundary conditions for the excavation phase

- Imposed pressure : lateral sides and on top under Baltic sea.
- No flux : bottom and island (recharge)
- Initial pressures and density fields : from Svensson regional model
- Initial fields resulting from permanent calculation compared to the results by Svensson



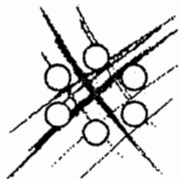
DMT/SEMT/MTMS



Hydraulic calibration phase

Using tunnel inflow and borehole pressures measurement :

- Change (constant) Transmissivity value associated to each conductor domain
 - Take grouting information into account (Rhen 97, P 159)
-
- ▷ Larger sensitivity of measured inflows than pressures
 - ▷ The best solution is retained
 - ▷ The model is fairly consistent over the data available



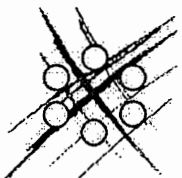
DMT/SEMT/MTMS



Hydraulic calibration results

Conductor domain	Transm. proposed ($10^{-6}m^2/s$)	Transmiss. calibrated ($10^{-6}m^2/s$)
EW1S	12.	12.
EW3	17.	13.6
EW7	15.	12.
NE1	220.	220.
NE2	.12	.80
NE3	320.	300.
NE4N	31.	25.
NE4S	31.	31.
NNW1	8.6	1.1
NNW2	24.	3.
NNW3	20.	20.
NNW4	65.0	11.5
NNW5	4.	4.
NNW6	14.	14.
NNW7	7.5	7.5
SFZ11	3.6	3.6

Grouting for C. D.
NE1, NE3, NNW4
according to proportions
by Rhen 97 (P159)

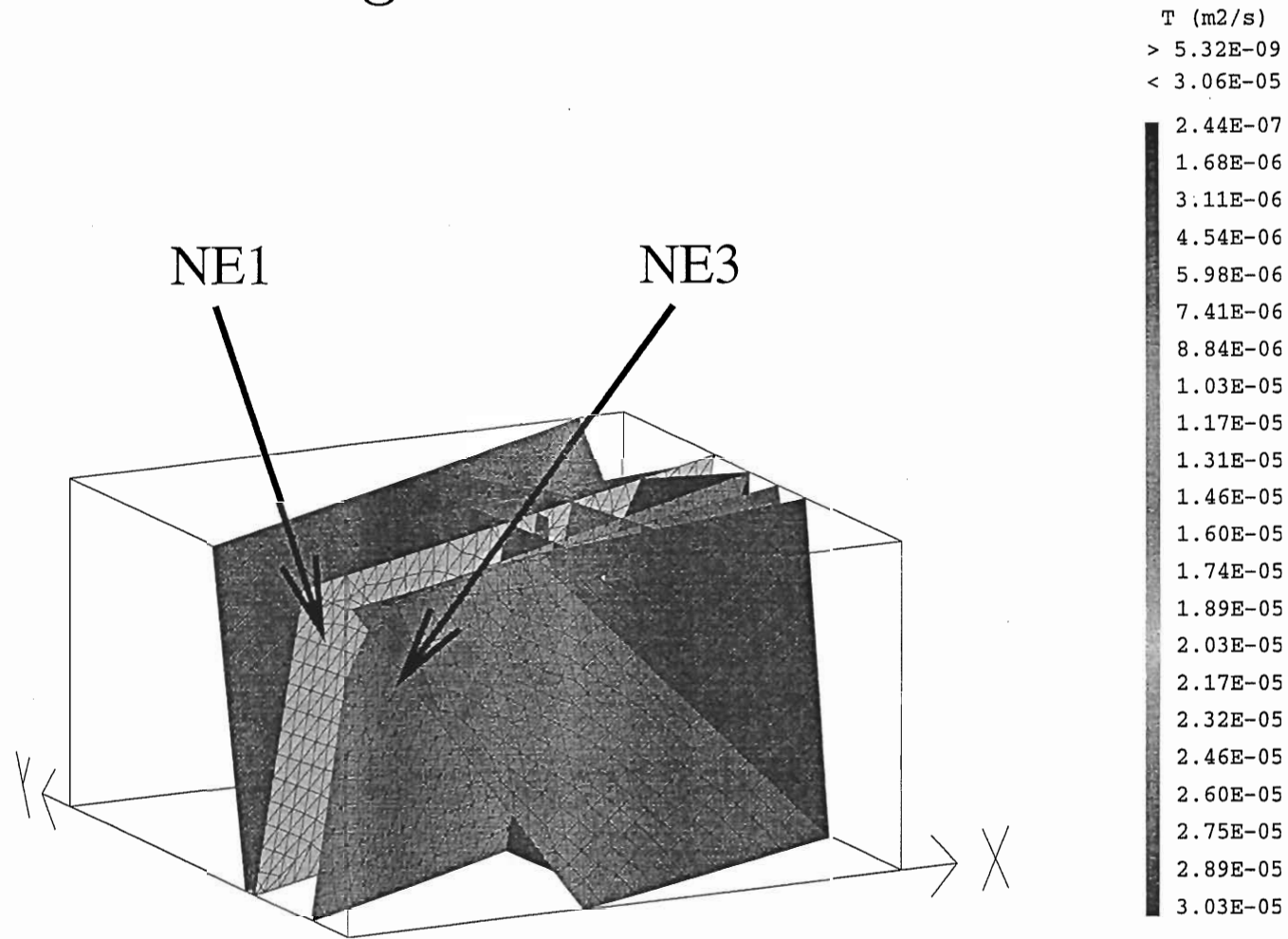


DMT/SEMT/MTMS

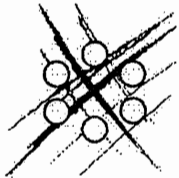


Grenier, february 2000 in Carlsbad

Calibrated transmissivities for hydraulic conducting features



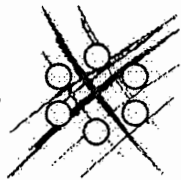
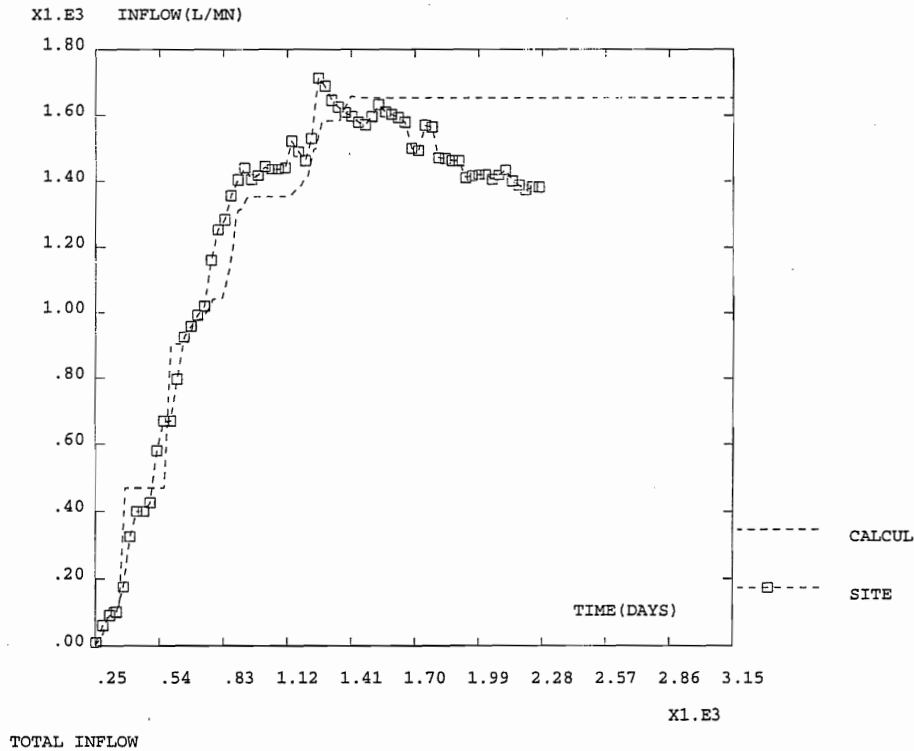
Grenier, february 2000 in Carlsbad



DMT/SEMT/MTMS



Total inflow into tunnel and shaft

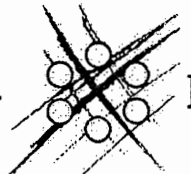
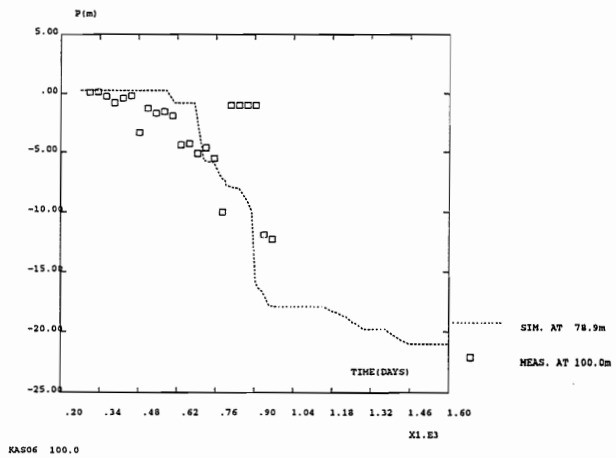
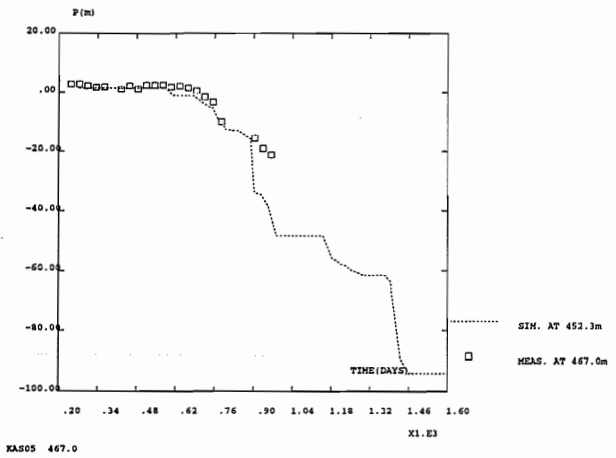
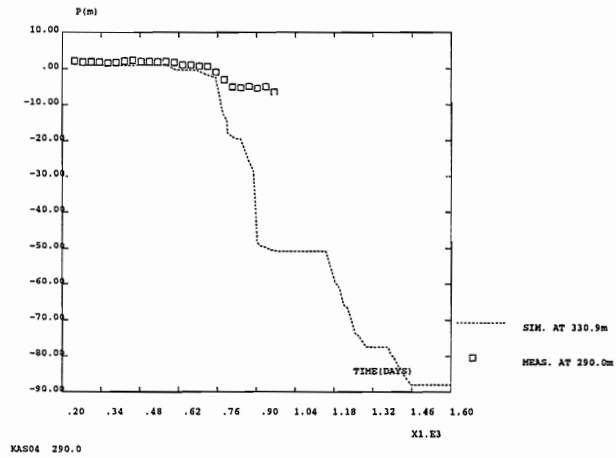
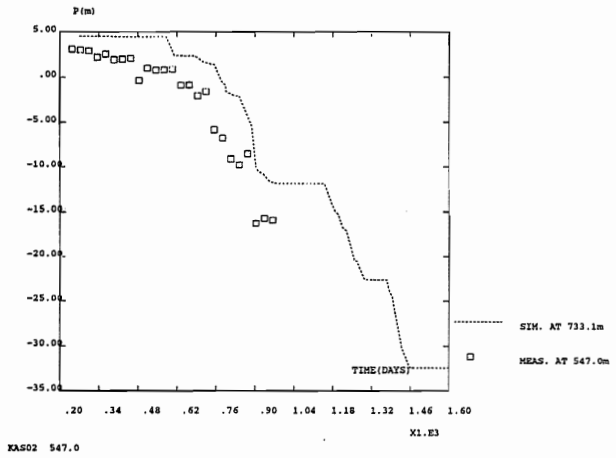


DMT/SEMT/MTMS



Grenier, february 2000 in Carlsbad

Drawdown in the boreholes (1)

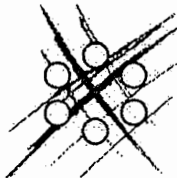
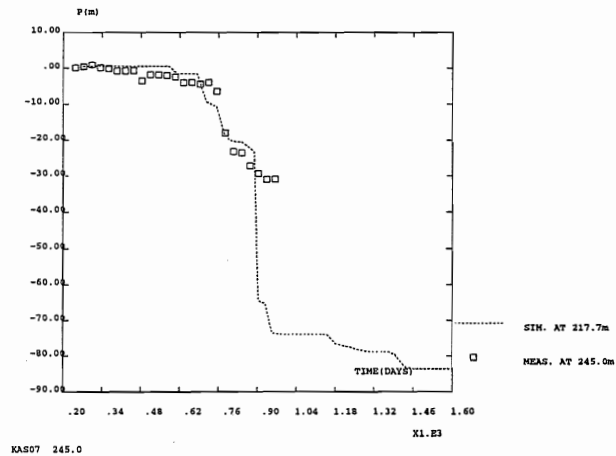
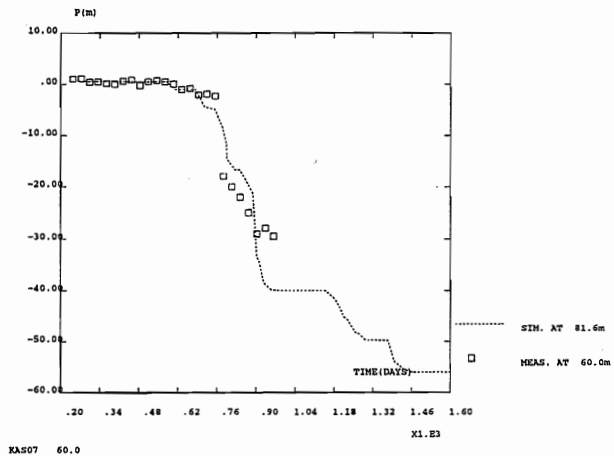
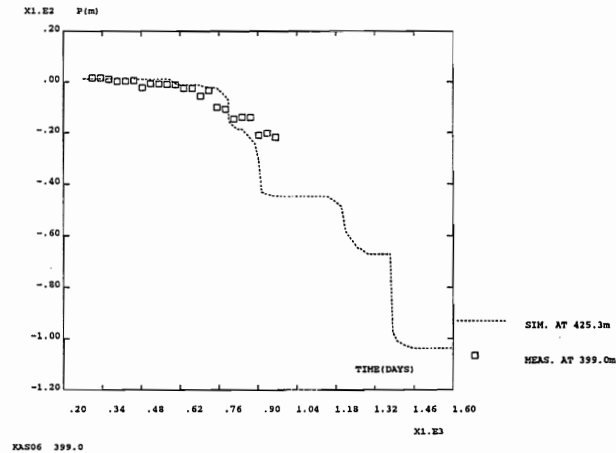
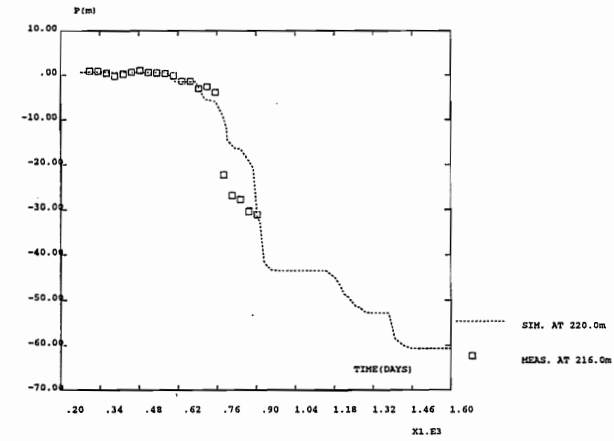


DMT/SEMT/MTMS



Grenier, february 2000 in Carlsbad

Drawdown in the boreholes (2)

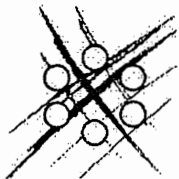
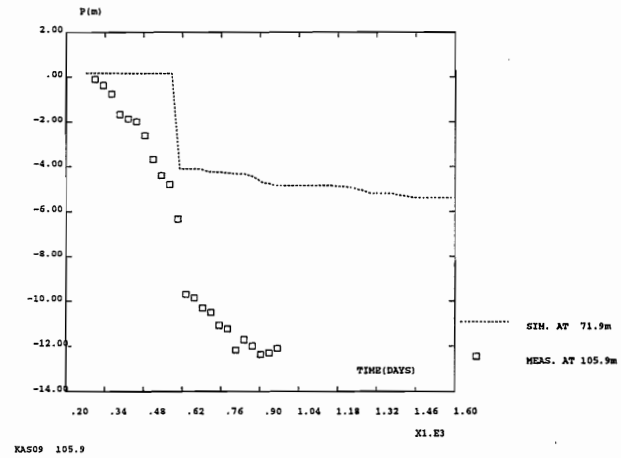
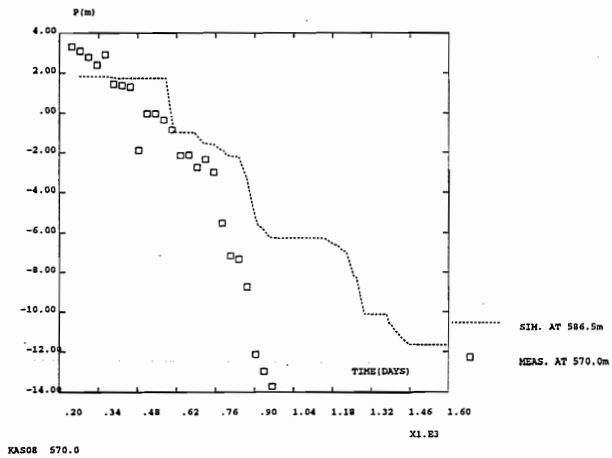
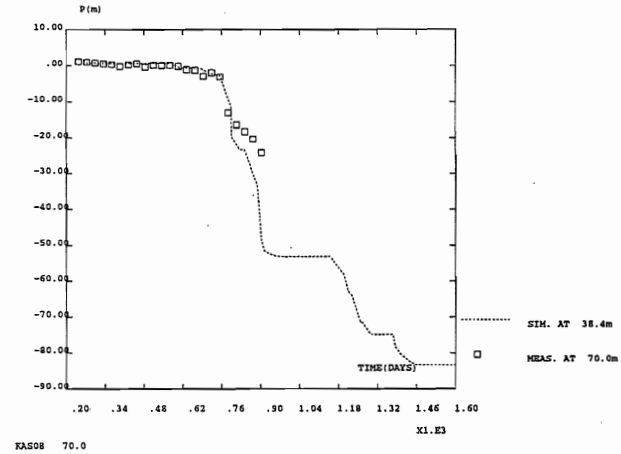
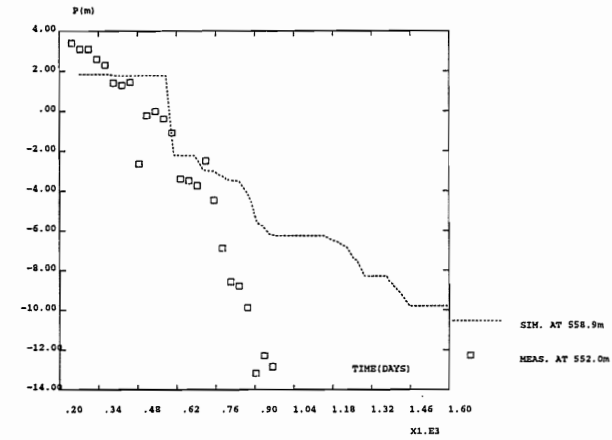


DMT/SEMT/MTMS



Grenier, february 2000 in Carlsbad

Drawdown in the boreholes (3)

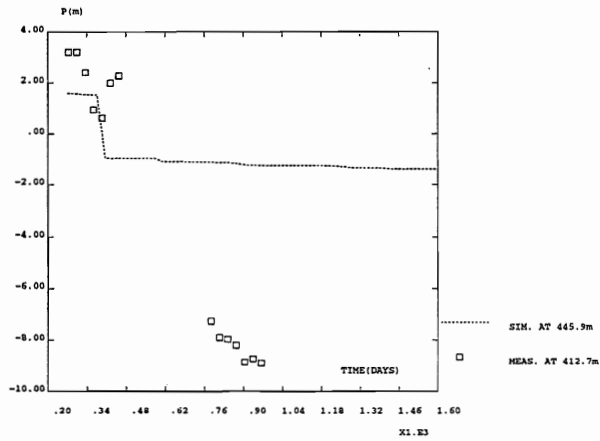


DMT/SEMT/MTMS

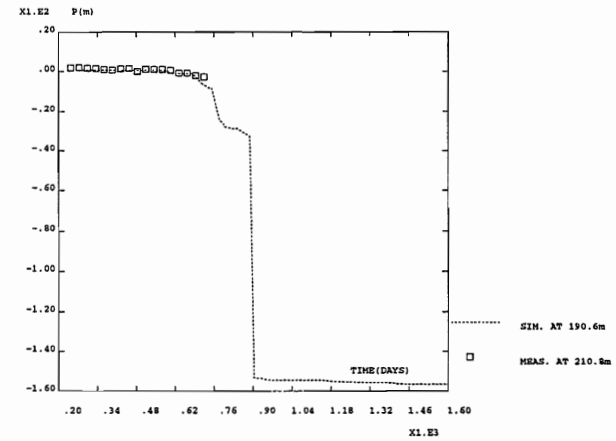


Grenier, february 2000 in Carlsbad

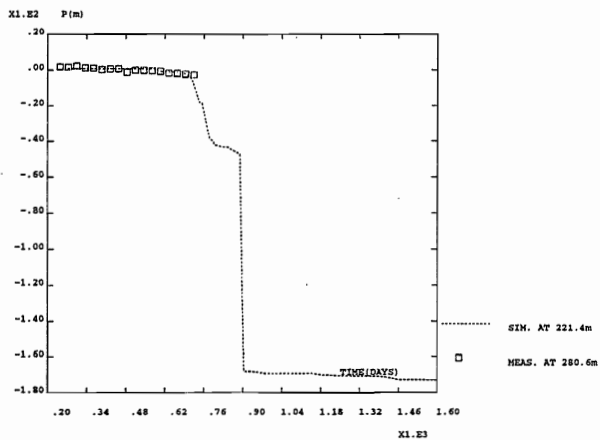
Drawdown in the boreholes (4)



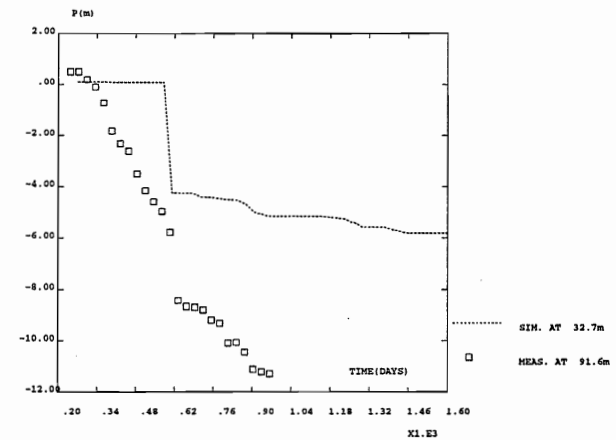
KAS09 412.7



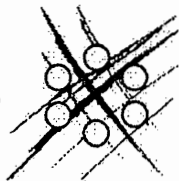
KAS13 210.8



KAS13 280.6



KAS14 91.6

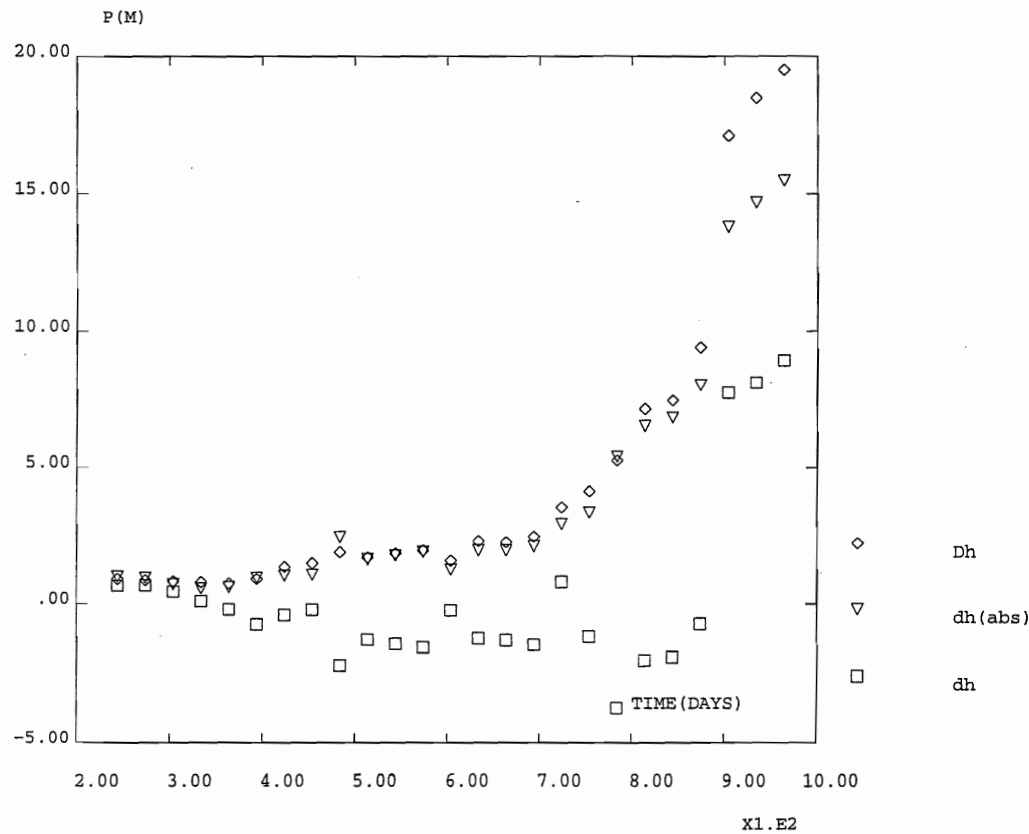


DMT/SEMT/MTMS

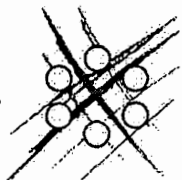


Grenier, february 2000 in Carlsbad

Mean error and accuracy



MEAN ERROR AND ACCURACY



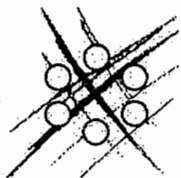
DMT/SEMT/MTMS



Grenier, february 2000 in Carlsbad

Transport of different waters

$$\frac{\partial \omega \chi}{\partial t} + \vec{\nabla} \cdot \chi \vec{U} = \vec{\nabla} \cdot [(D^* + D_{l,t}) \vec{\nabla} \chi]$$

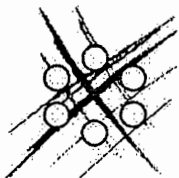
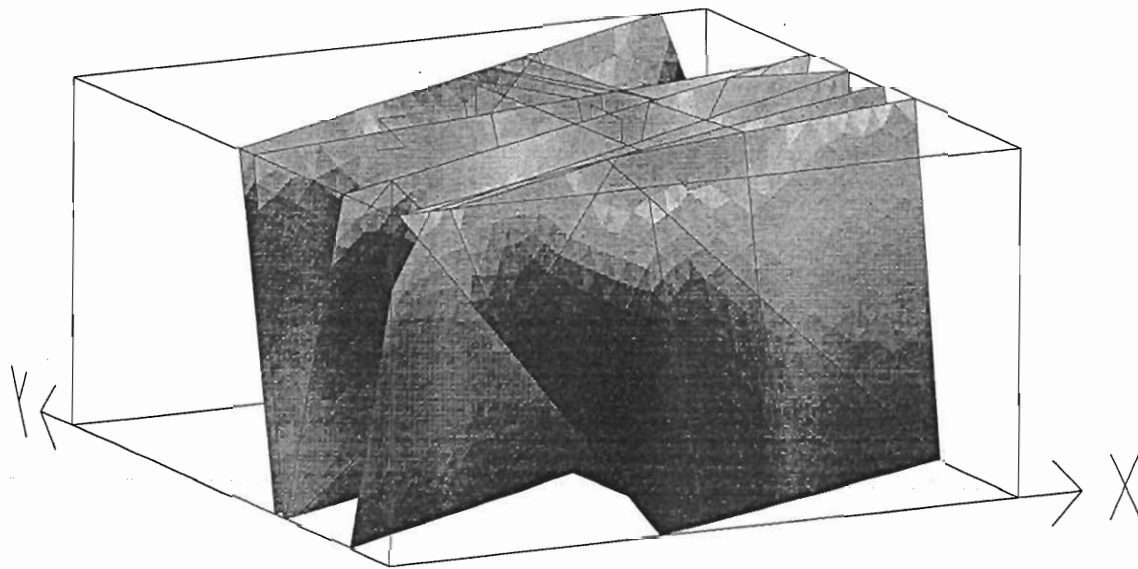
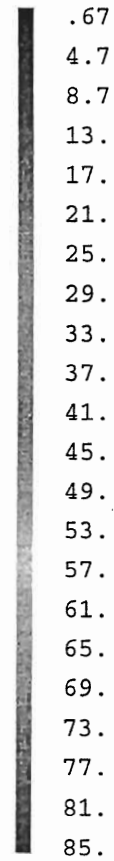


DMT/SEMT/MTMS



Meteoric water proportion (1409 days)

METEORIC (%)
> 5.29E-03
< 8.56E+01

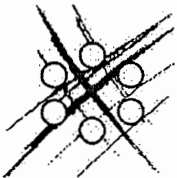
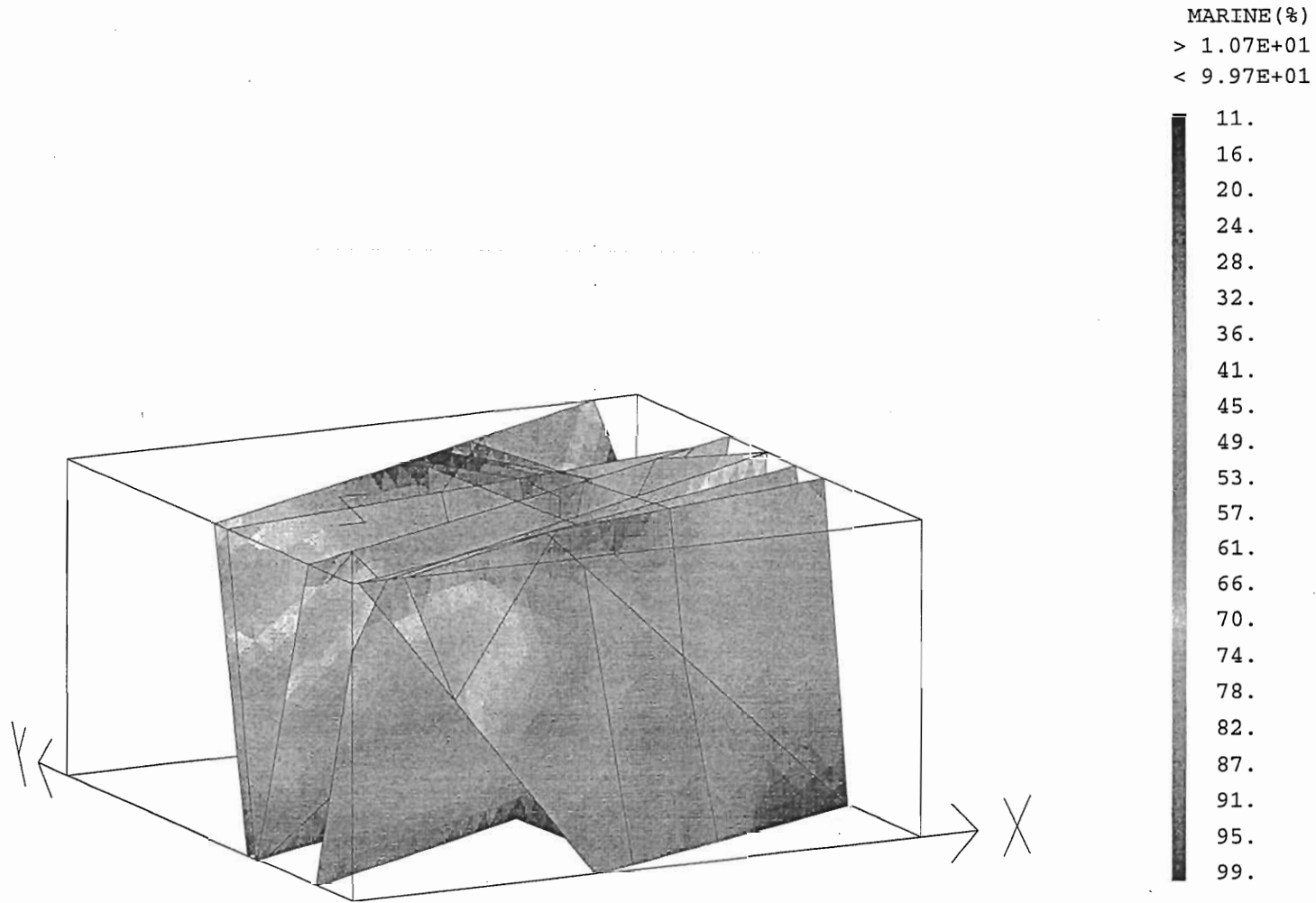


DMT/SEMT/MTMS



Grenier, february 2000 in Carlsbad

Marine water proportion (1409 days)

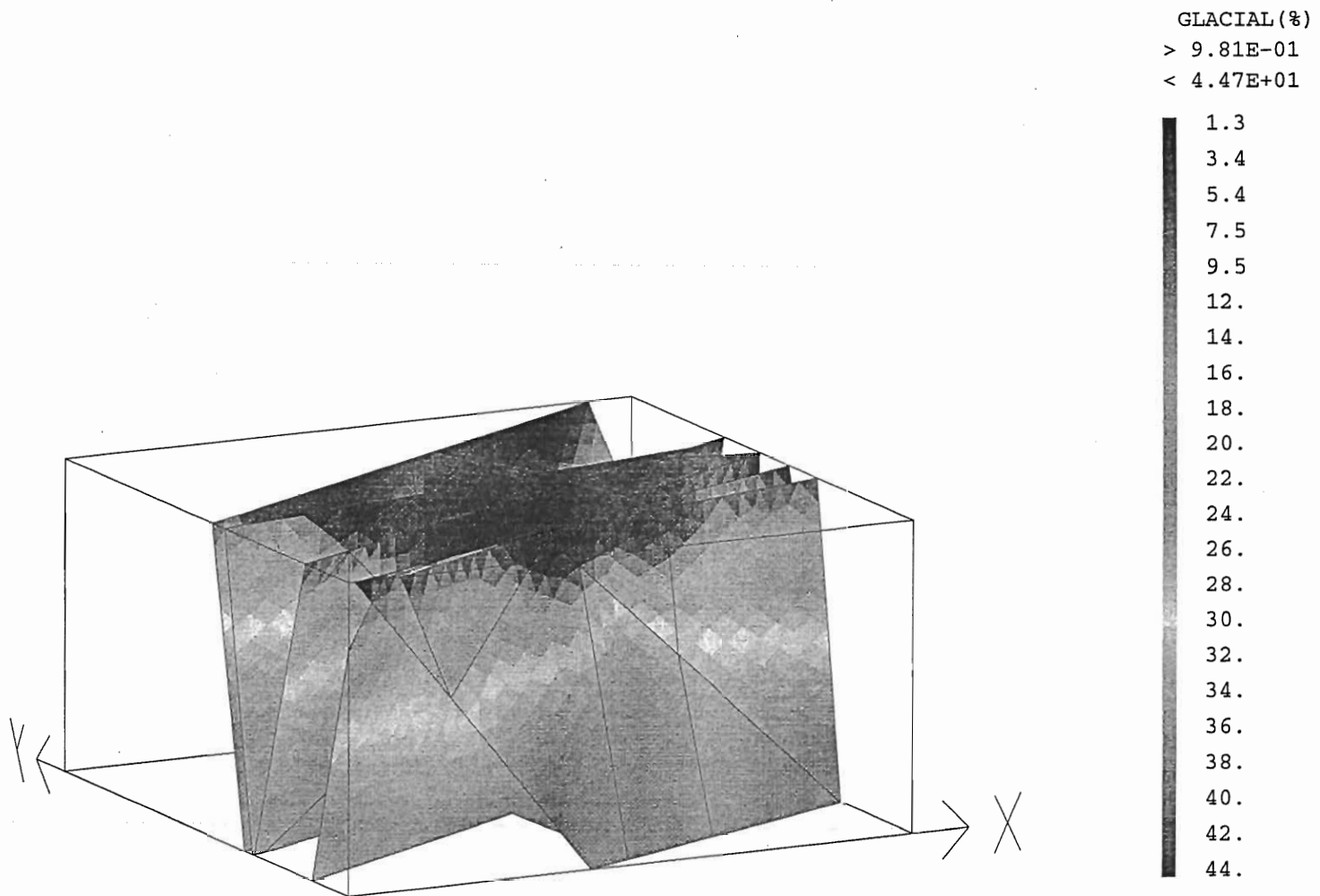


DMT/SEMT/MTMS

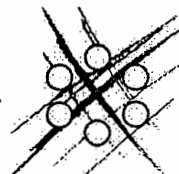


Grenier, february 2000 in Carlsbad

Glacial water proportion (1409 days)



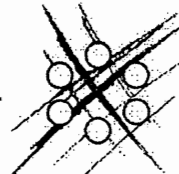
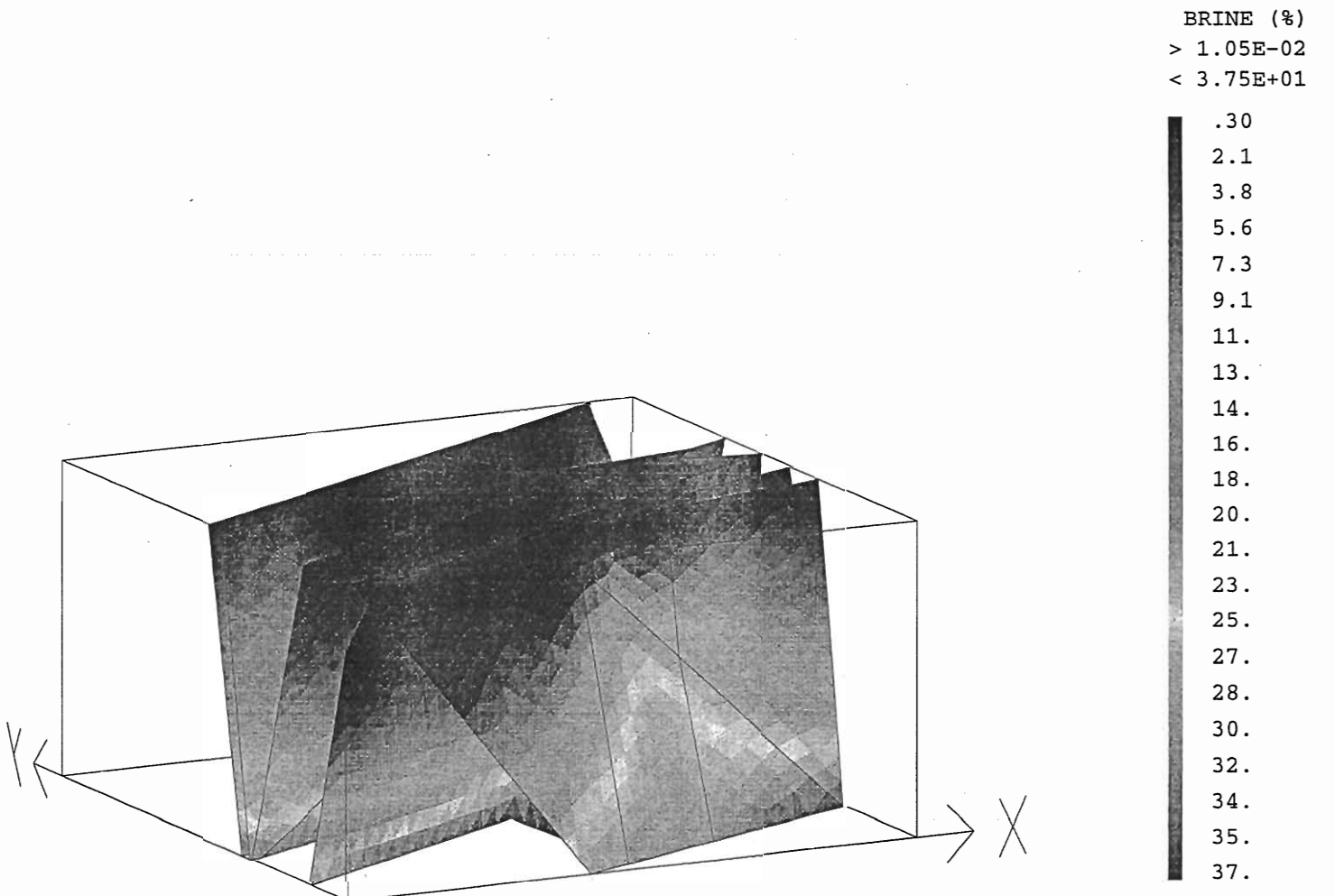
Grenier, february 2000 in Carlsbad



DMT/SEMT/MTMS



Brine water proportion (1409 days)

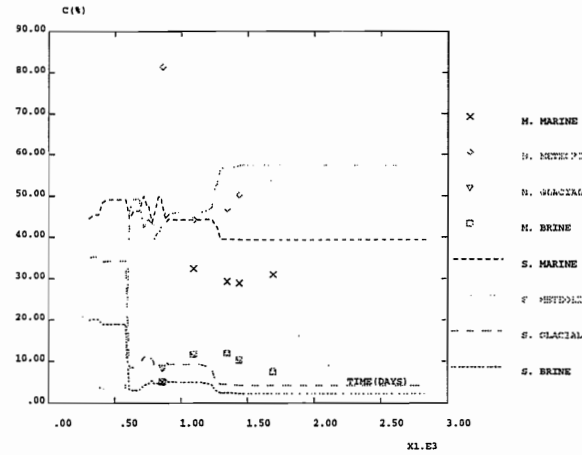
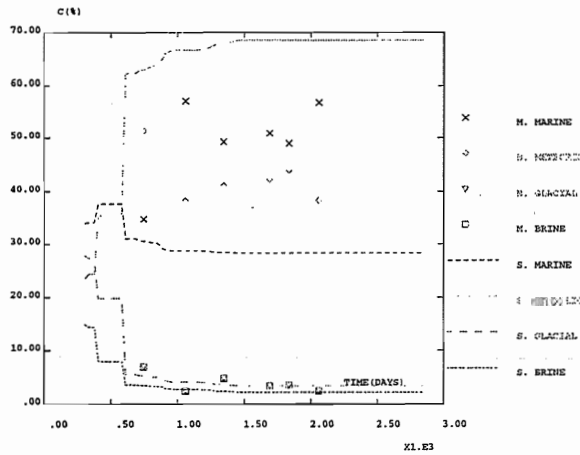
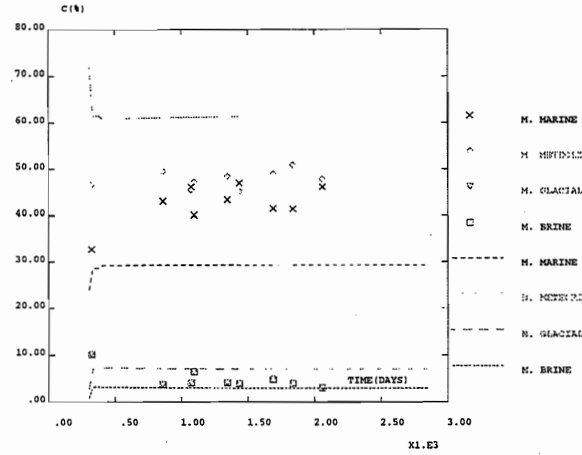
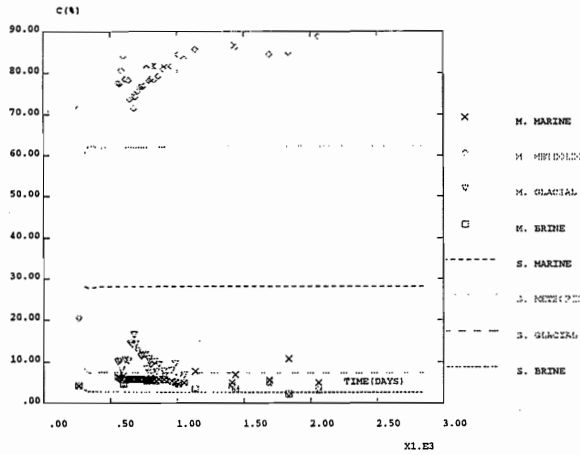


DMT/SEMT/MTMS

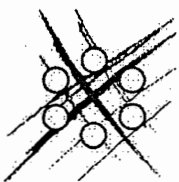


Grenier, february 2000 in Carlsbad

Mixing proportions at control points CP1 to CP4



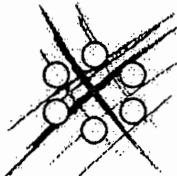
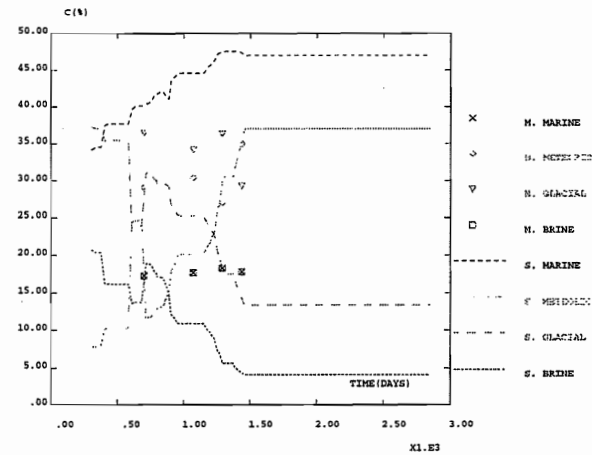
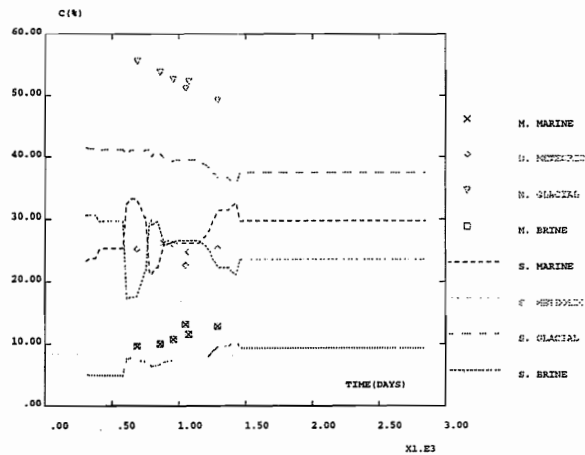
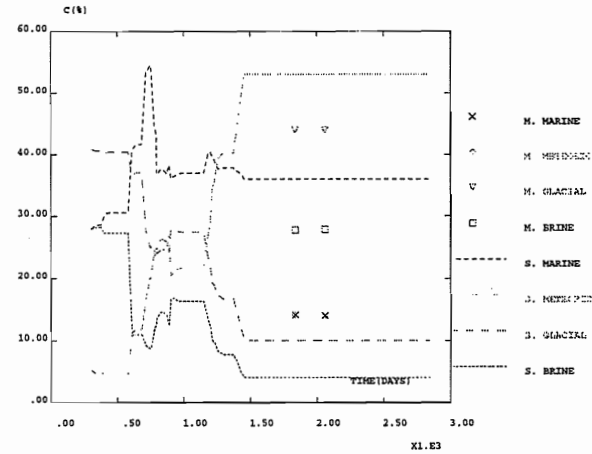
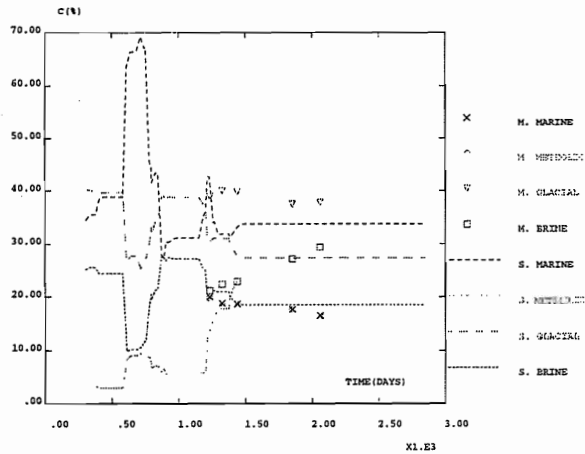
Grenier, february 2000 in Carlsbad



DMT/SEMT/MTMS



Mixing proportions at control points CP5, CP6, CP10, CP11

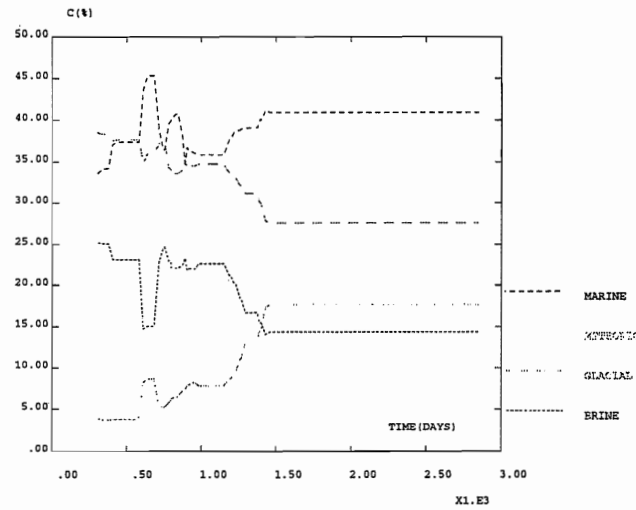
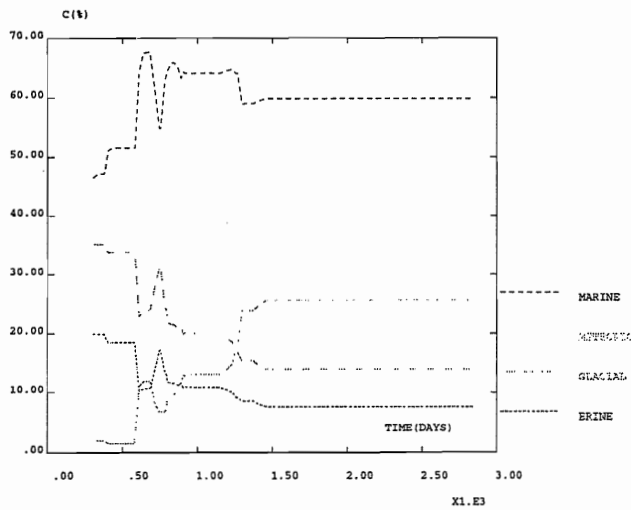


DMT/SEMT/MTMS

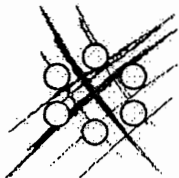


Grenier, february 2000 in Carlsbad

Mixing proportions at predictive control points CP8 and CP9



Grenier, february 2000 in Carlsbad

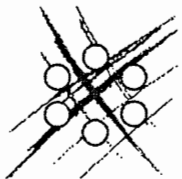


DMT/SEMT/MTMS



Travel time estimation

- Impossible by particle tracking in our geometry
- Implemented a 'back tracking' procedure based on back transport of a concentration pulse in unstationnary velocity field
 - ▷ Rough results due to low number of meshes to exit and boundary condition effects
 - ▷ CP predominantly relate with Aspo or Baltic sea
 - ▷ Boundary conditions are reached rather quickly (tenth to hundredth of days)

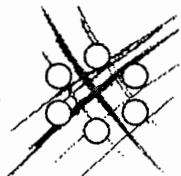


DMT/SEMT/MTMS



Conclusions drawn from mixing results

- ▷ Proportions of Baltic and Meteoric waters are often high
- ▷ Boundary conditions interfere rather quickly (tenth to hundredth of days)

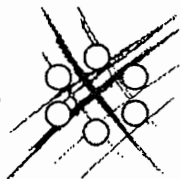


DMT/SEMT/MTMS



Calibration efforts

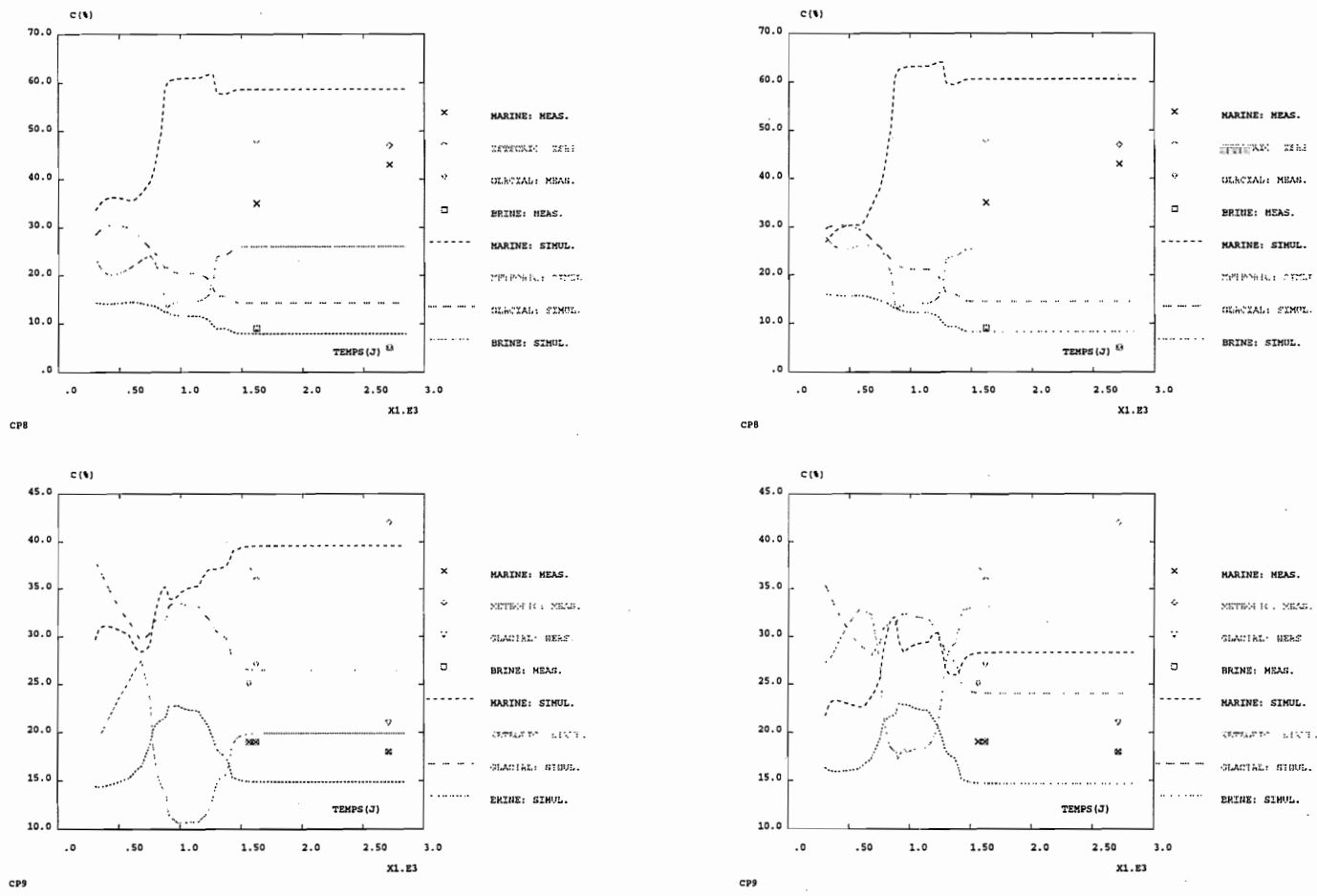
- ▷ Reduce proportions of Meteoric waters through recharge :
not sufficient
 - Requires better modeling of near surface transfers ?
- ▷ Boundary conditions before versus after calibration



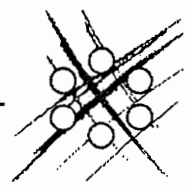
DMT/SEMT/MTMS



Simulations for CP8 and CP9 for different transport boundary conditions (before vs after excavation)



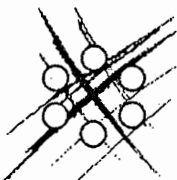
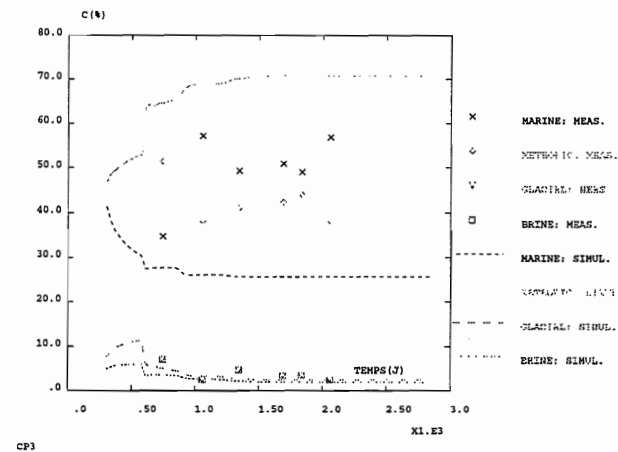
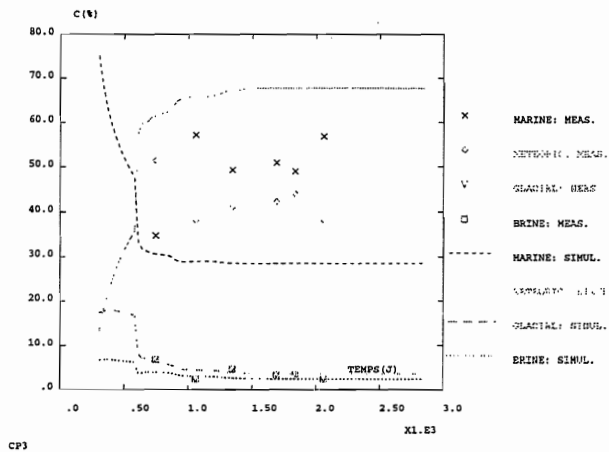
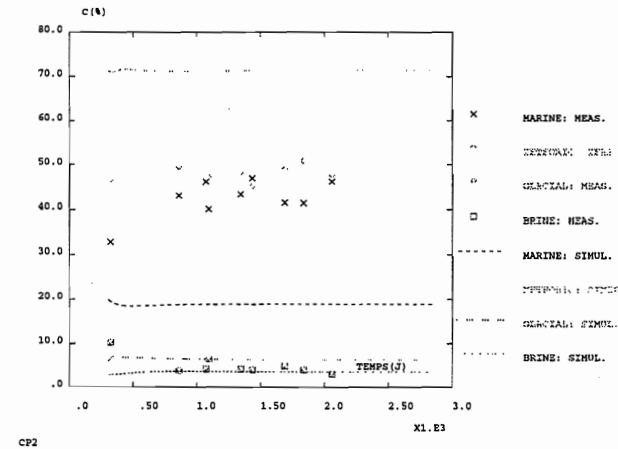
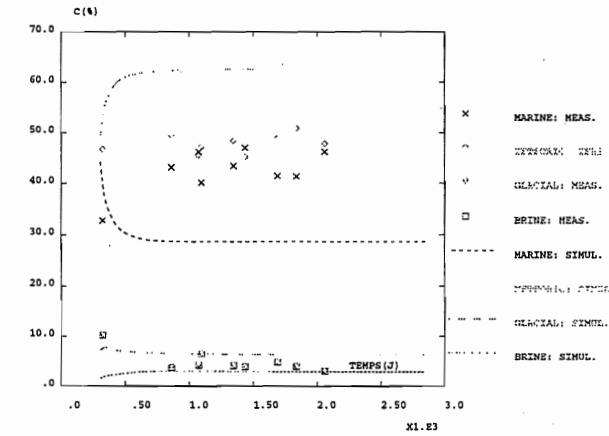
Grenier, february 2000 in Carlsbad



DMT/SEMT/MTMS



Simulations for CP2 and CP3 for different transport boundary conditions (before vs after excavation)

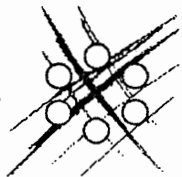
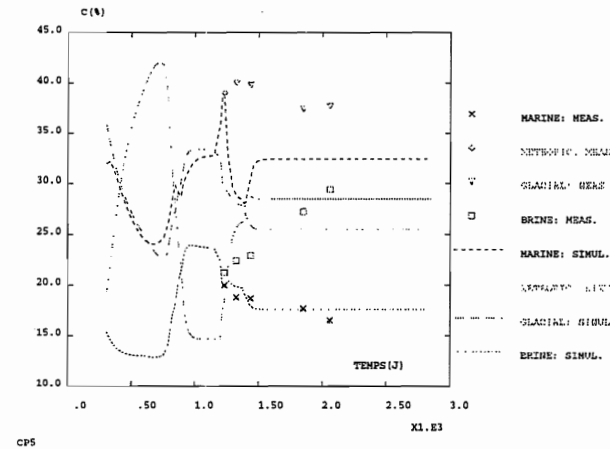
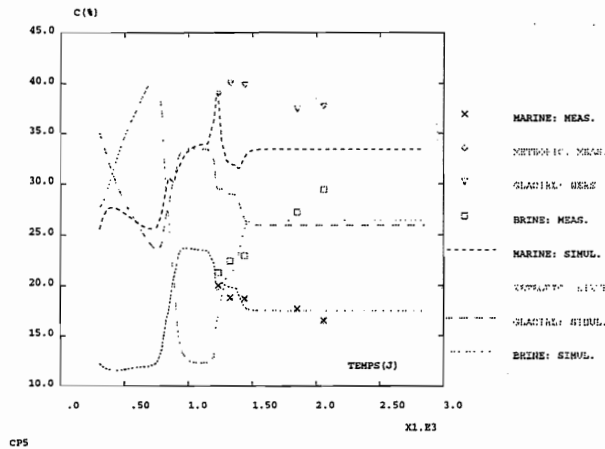
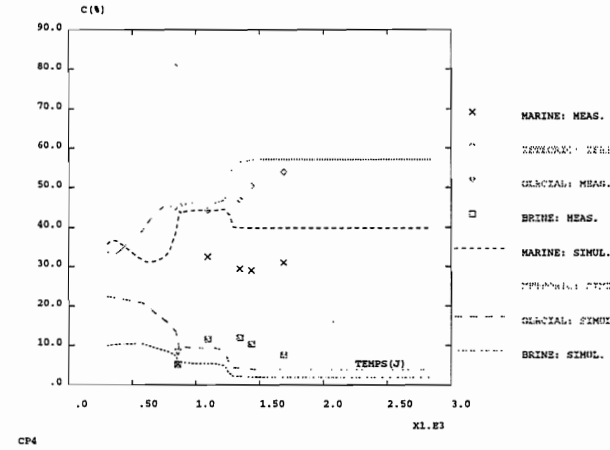
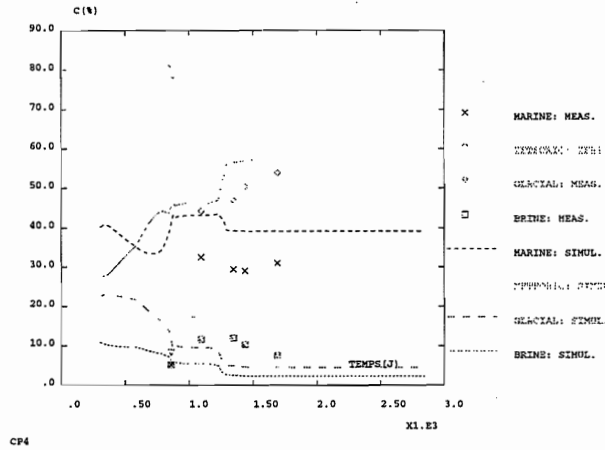


DMT/SEMT/MTMS



Grenier, february 2000 in Carlsbad

Simulations for CP4 and CP5 for different transport boundary conditions (before vs after excavation)

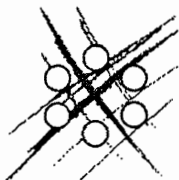
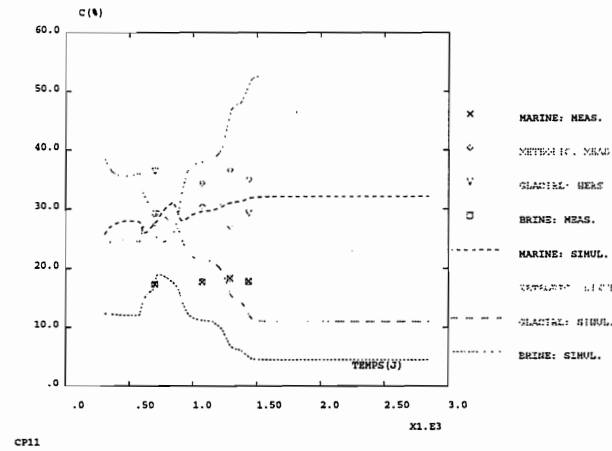
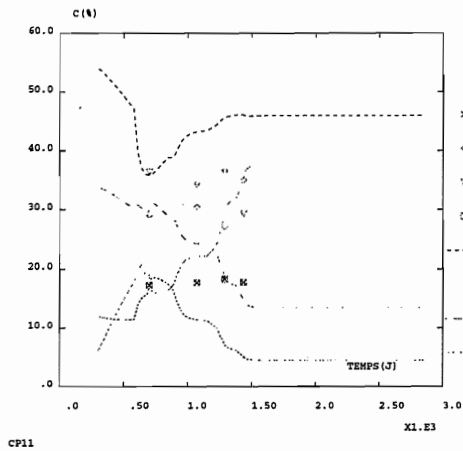
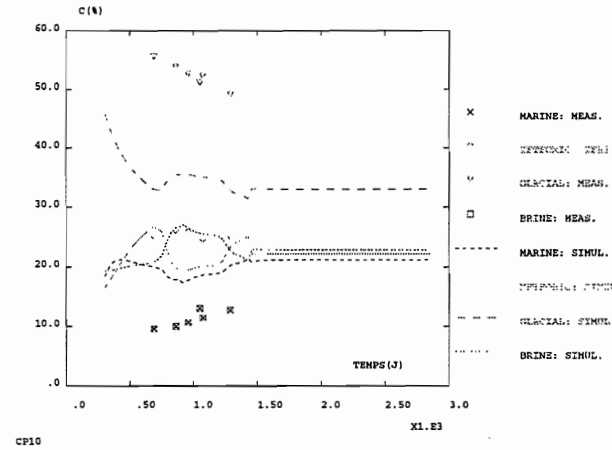
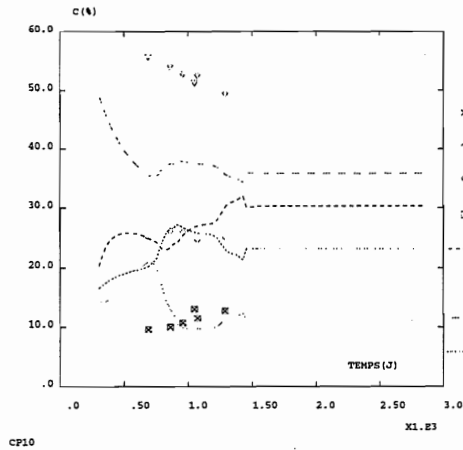


DMT/SEMT/MTMS



Grenier, february 2000 in Carlsbad

Simulations for CP10 and CP11 for different transport boundary conditions (before vs after excavation)



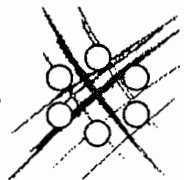
DMT/SEMT/MTMS



Grenier, february 2000 in Carlsbad

Density effects (i.e. Coupling Flow & Transport).

- ▷ No significant density effect was observed neither for flow simulations (pressures along boreholes and inflows) nor for transport results (mixing proportions at CP)



DMT/SEMT/MTMS

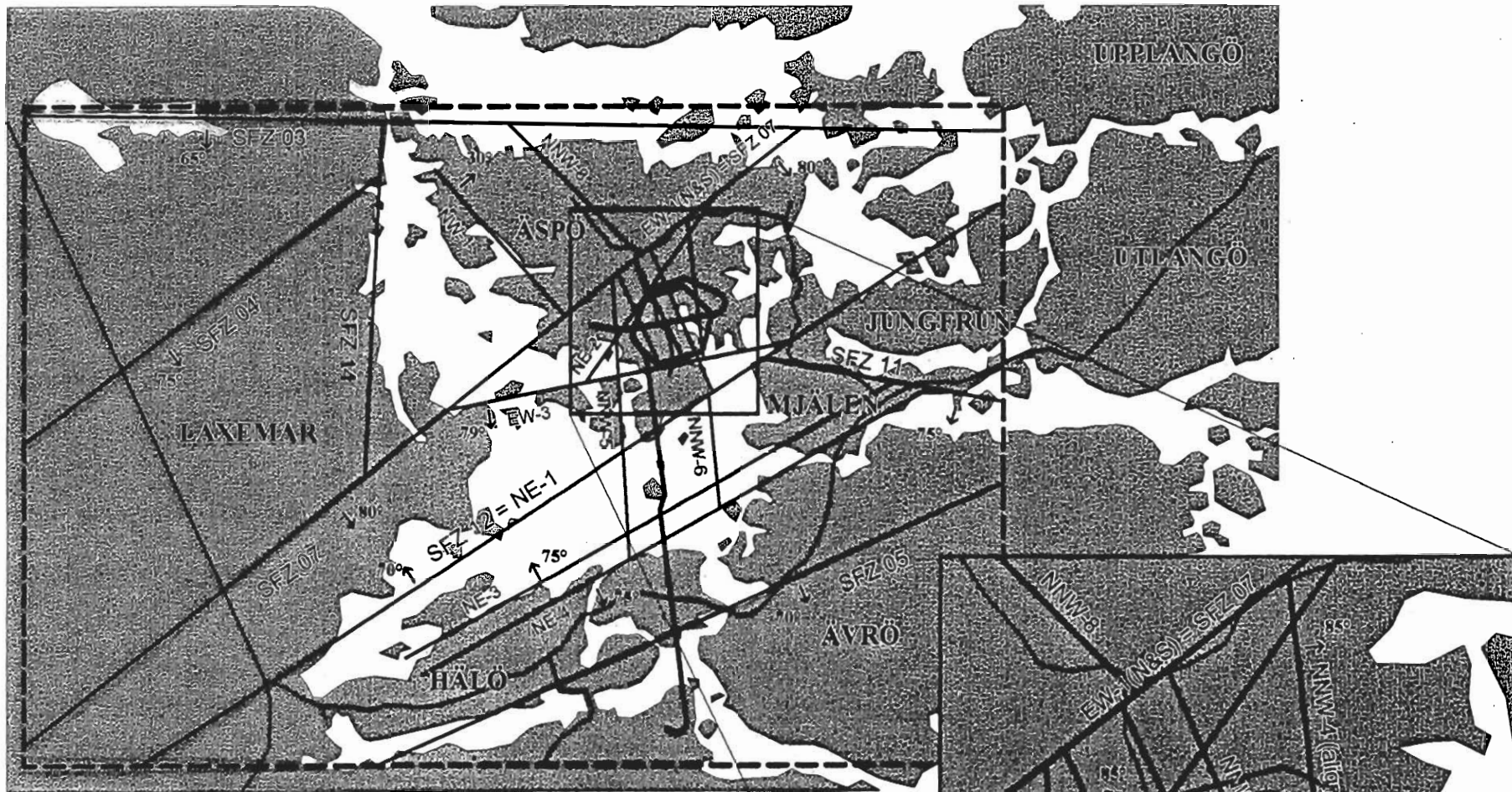


Task 5 modelling

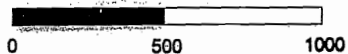
J Wendling (ANTEA)

ÄSPÖ model specifications

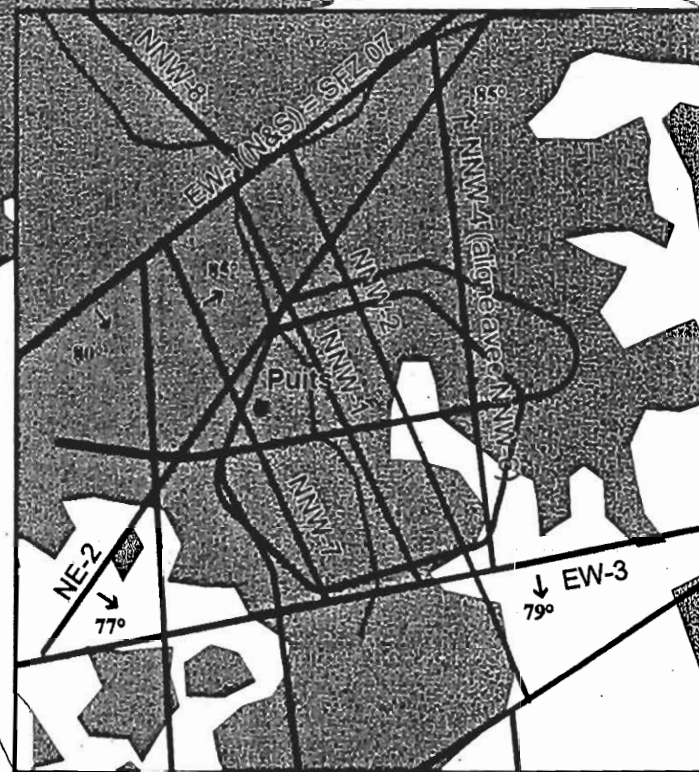
- Mixte Hybrid Finite Element mesh
- Explicit 3D fractures
- Explicit tunnel modelling
- Realistic boundaries conditions
- Conservative transport : mixing
- No density effects



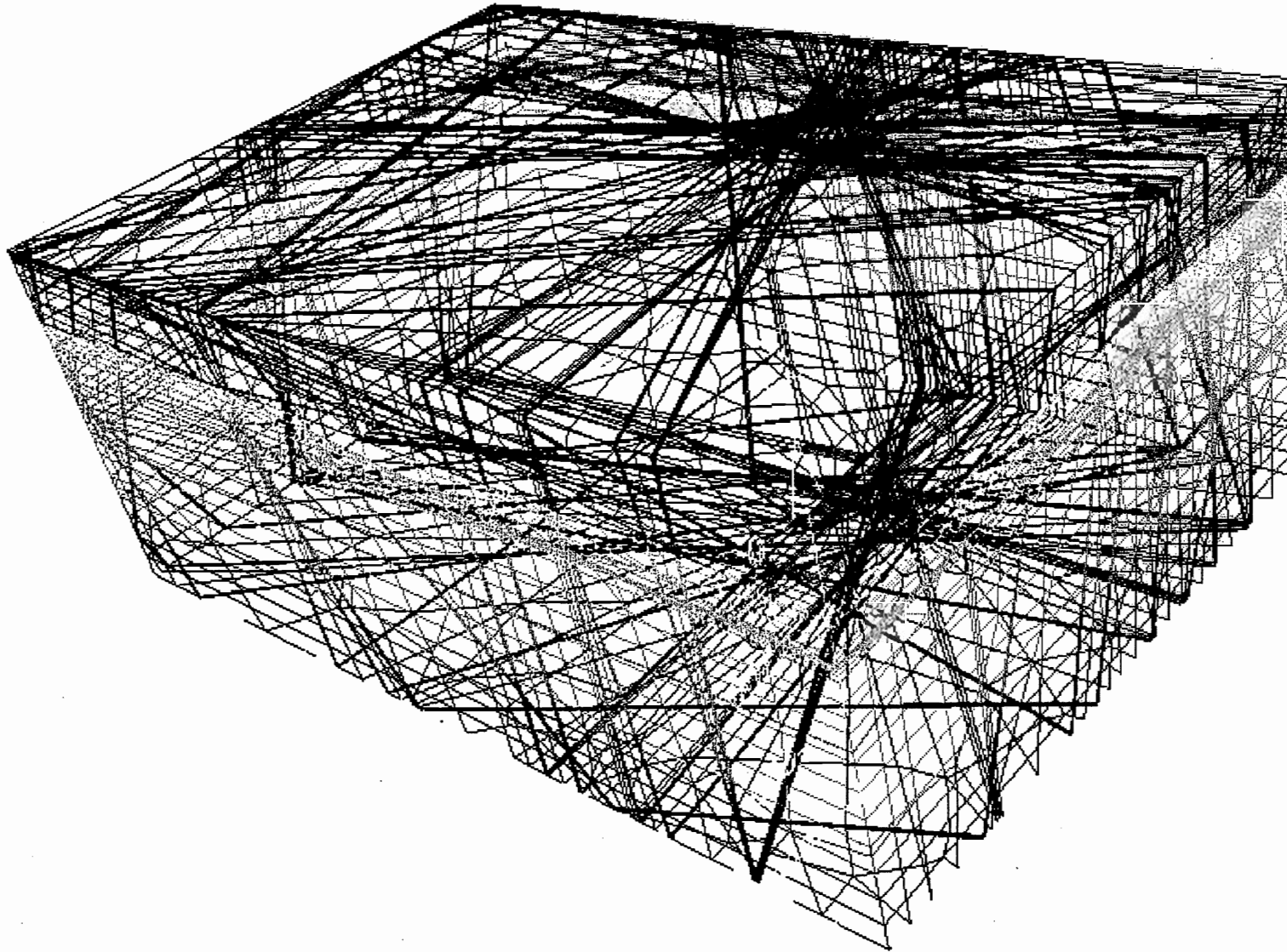
échelle (m)



- Model extension
 - Fractures
 - Tunnel
 - Roads
- 75°
 Dip
 (orientation and value)



3D view of the total mesh
Matrix + Fractures + Tunnels
(South -East view)



PARAMETERS USED FOR THE REFERENCE

Permeability :

Name	Initial Transmissivities (m ² /s)	Final Transmissivities (m ² /s)	Transmissivities SKB ICR 94-16 (m ² /s)	Transmissivities SKB ICR 94-15 (m ² /s)
SFZ 05	10 ⁻⁴	2 10 ⁻⁴		
SFZ12 / NE-1	3 10 ⁻⁴	3 10 ⁻⁴	2 10 ⁻⁵	2 10 ⁻⁴
SFZ 11	3 10 ⁻⁶	3 10 ⁻⁶		
EW-3	2 10 ⁻⁵	2 10 ⁻⁵	1 10 ⁻⁵	3.3 10 ⁻⁵
SFZ-03	3 10 ⁻⁶	3 10 ⁻⁶		
SFZ-14	3 10 ⁻⁶	3 10 ⁻⁶		
SFZ-04	3 10 ⁻⁶	3 10 ⁻⁶		
SFZ-07 / EW-1N&S	2 10 ⁻⁵ / 10 ⁻⁷	2 10 ⁻⁵ / 10 ⁻⁷	2.2 10 ⁻⁵	6 10 ⁻⁵
NW-1	3 10 ⁻⁷	3 10 ⁻⁷	7 10 ⁻⁶	7 10 ⁻⁴
NE-2	3 10⁻⁷	10⁻⁴	4 10⁻⁵	2 10⁻⁴
NNW-5	3 10 ⁻⁶	3 10 ⁻⁶	5 10 ⁻⁵	5 10 ⁻⁷
NNW-7	6 10⁻⁶	10⁻⁴		
NNW-1	10 ⁻⁵	10 ⁻⁵	1.5 10 ⁻⁵	1.5 10 ⁻⁷
NNW-2	4 10 ⁻⁶	4 10 ⁻⁵	4 10 ⁻⁵	4.8 10 ⁻⁵
NE-3	3 10 ⁻⁴	6 10 ⁻⁴	3 10 ⁻⁵	10 ⁻⁴
NNW-4	9 10 ⁻⁵	5 10 ⁻⁴	4 10 ⁻⁴	4 10 ⁻³
NNW-6	10 ⁻⁵	10 ⁻⁵	5 10 ⁻⁵	9 10 ⁻⁷
NNW-8	9 10 ⁻⁶	9 10 ⁻⁶		
NE-4	3 10⁻⁵	2 10⁻⁴	3.2 10⁻⁴	2 10⁻⁴
Fractures intersection	3 10 ⁻⁴	3 10 ⁻⁴		

Storage : formula given in SKB TR 97-06

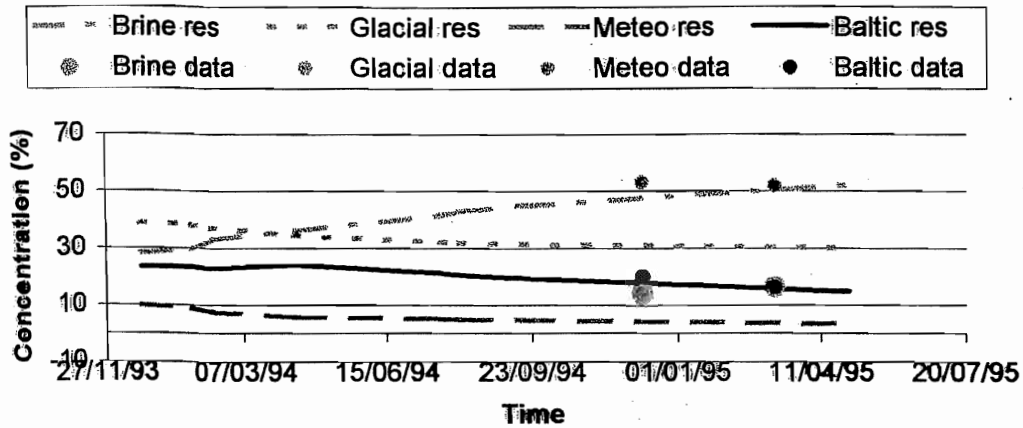
Porosity : Formula given in SKB TR 97-06

Recharge : 5 mm/year

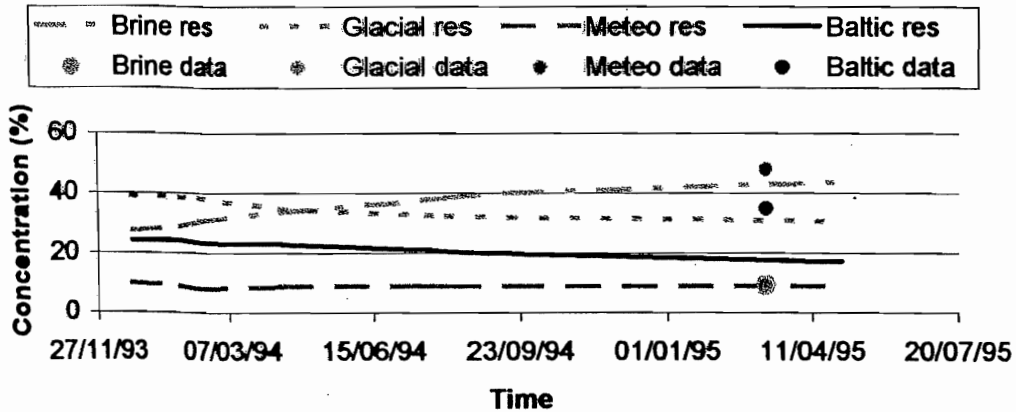
Dispersion : $\alpha_L = 100$ m

$\alpha_T = 10$ m

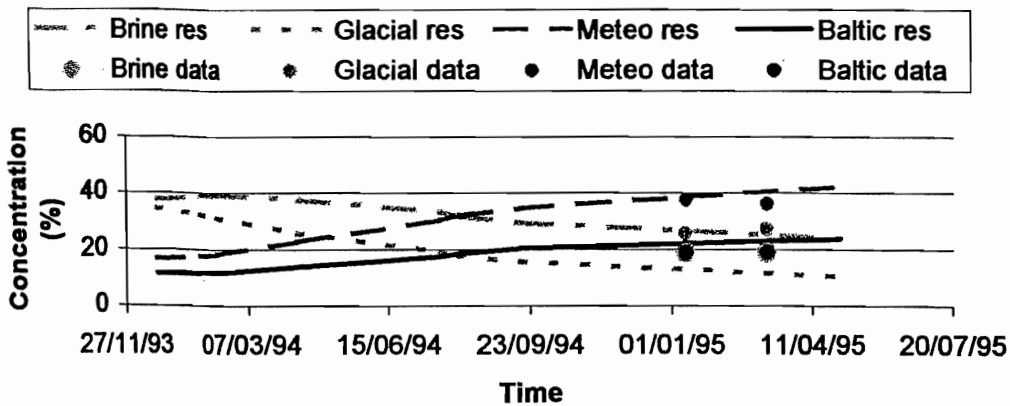
Variation of concentration at KA3005A



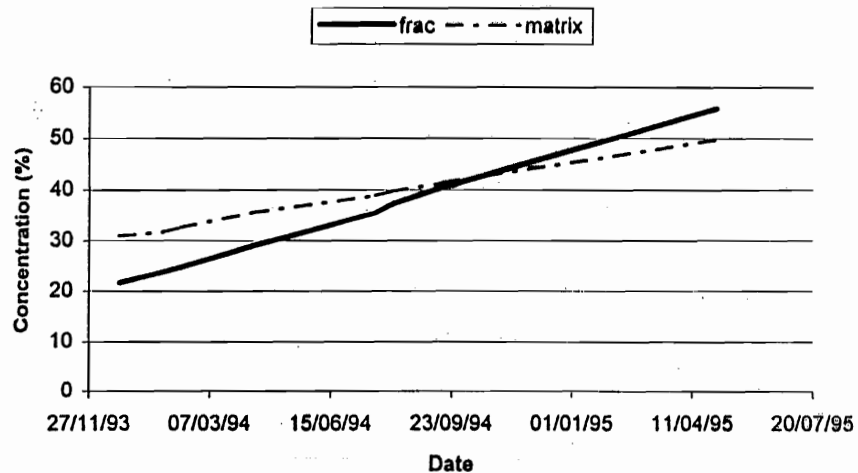
Variation of concentration at KA3110A



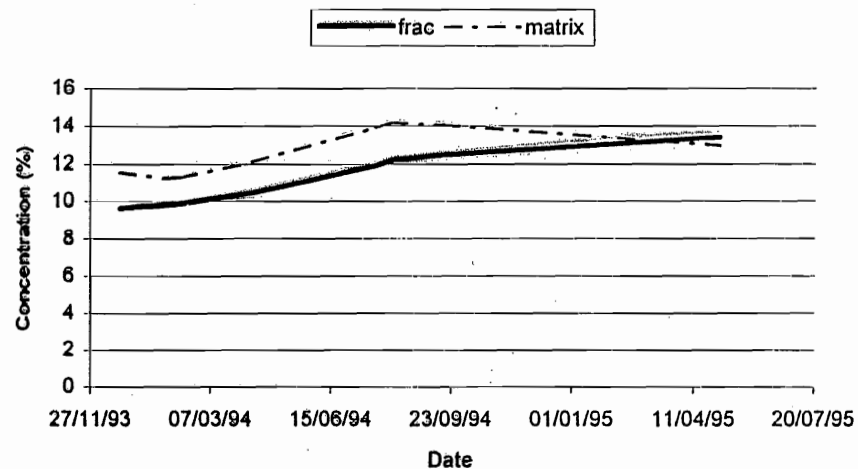
Variation of concentration at KA3385A



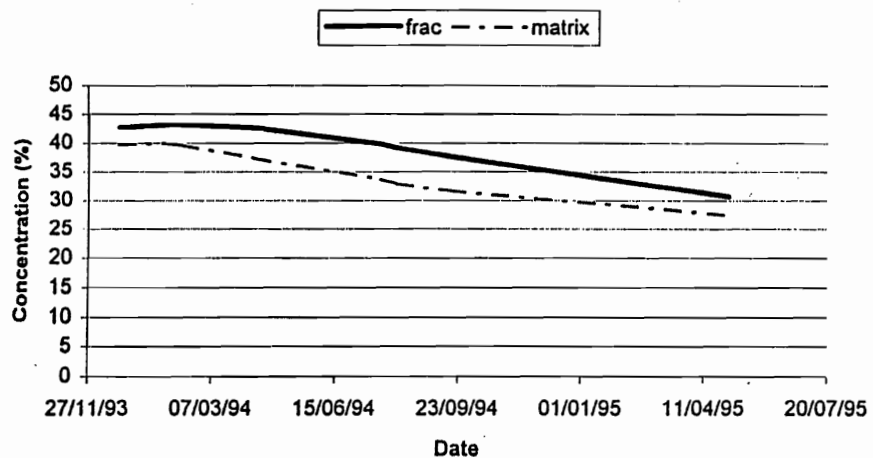
Brine concentration at SA2783A



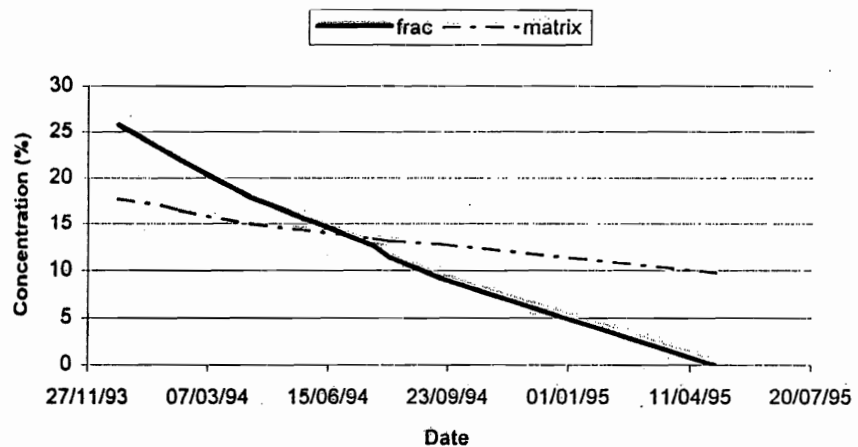
Meteo concentration at SA2783A

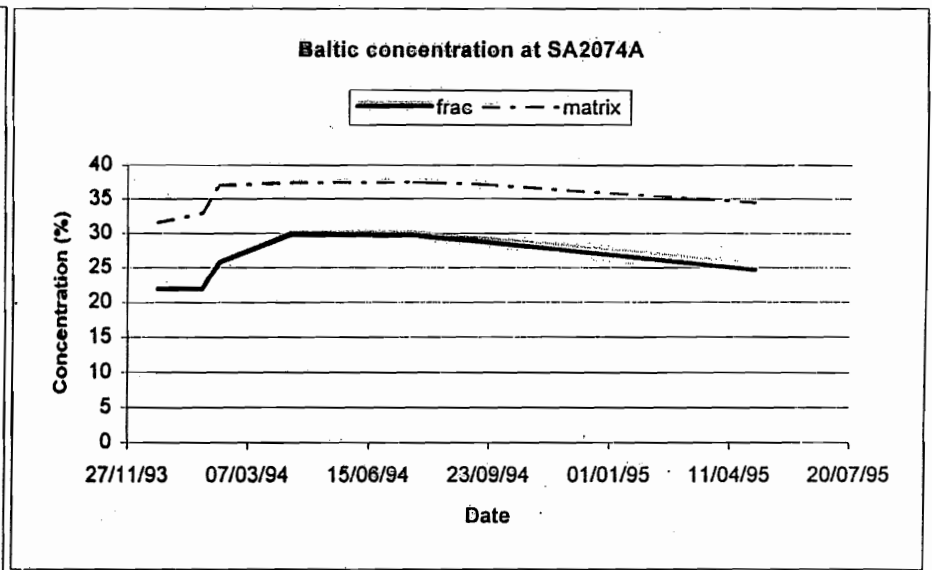
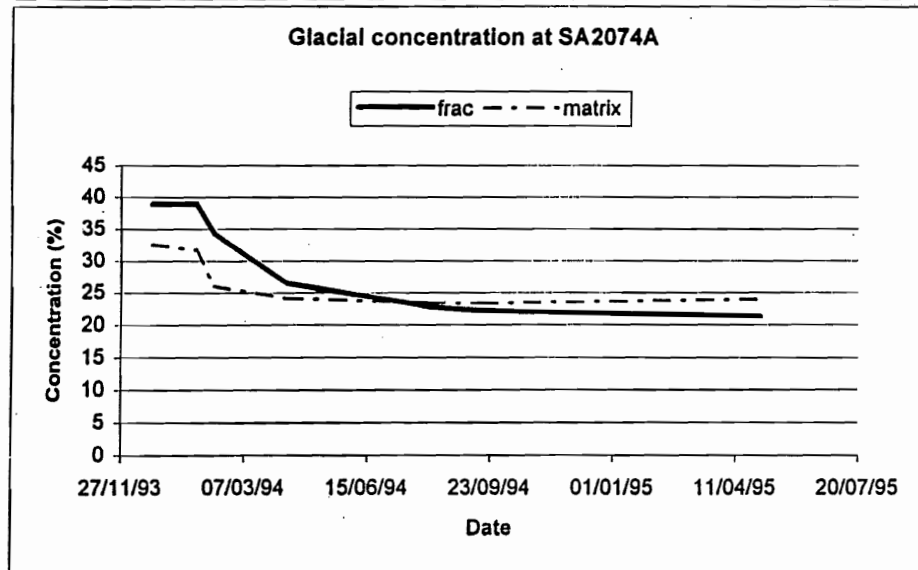
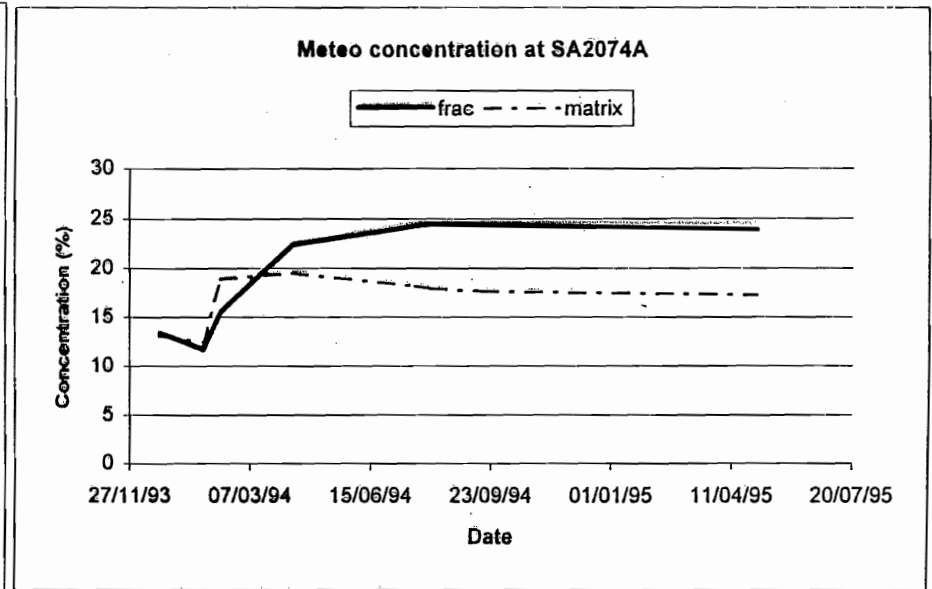
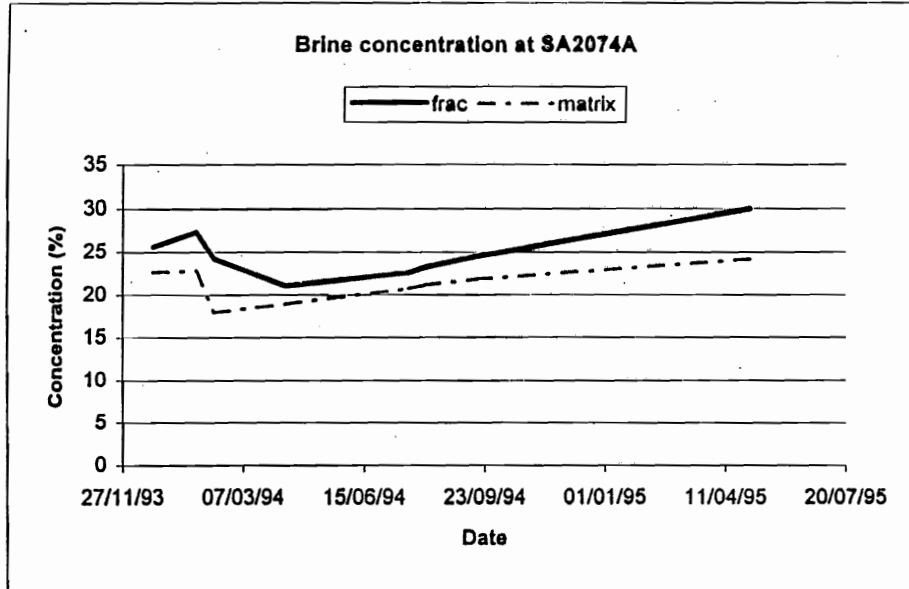


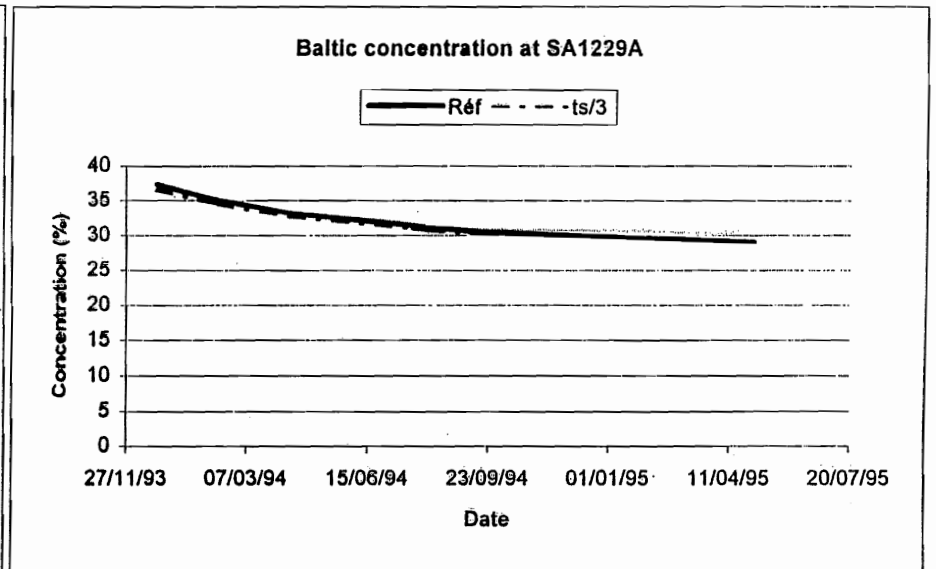
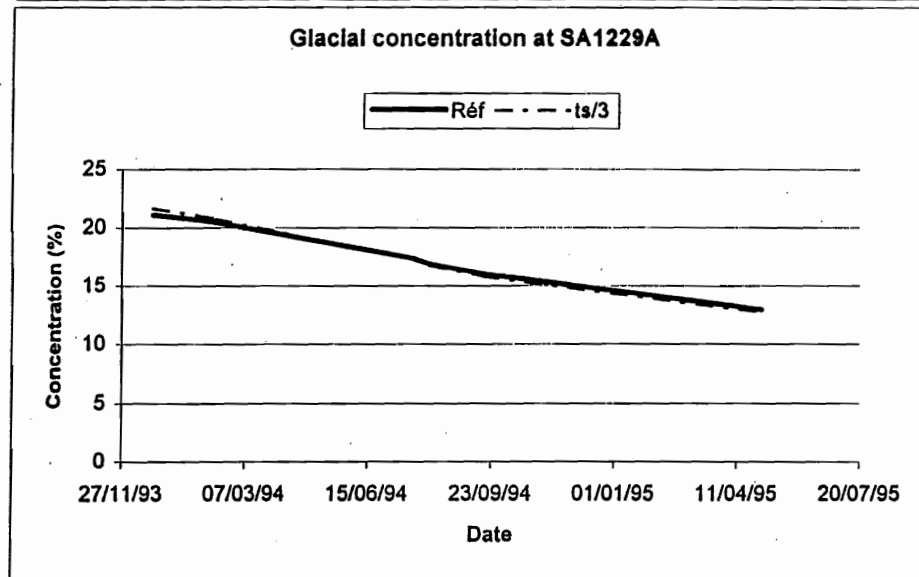
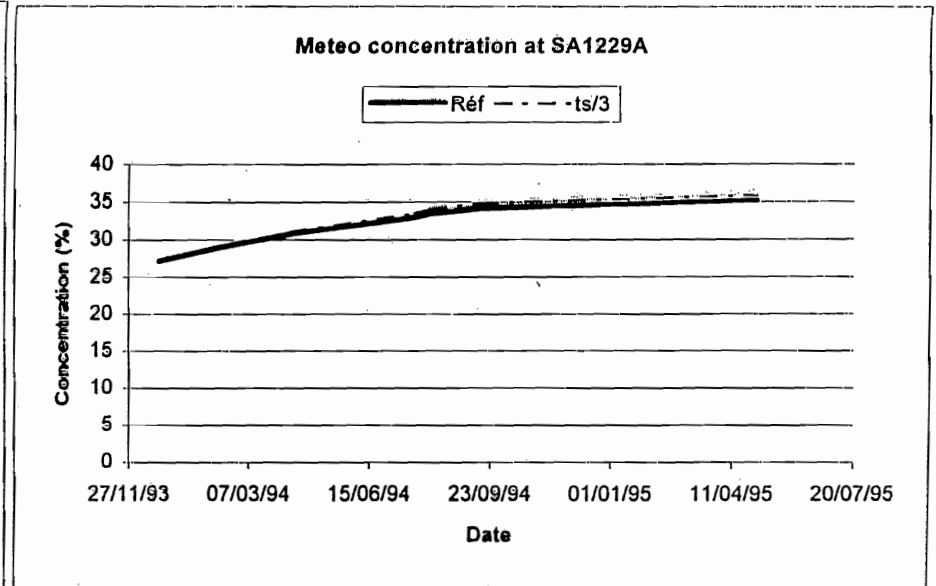
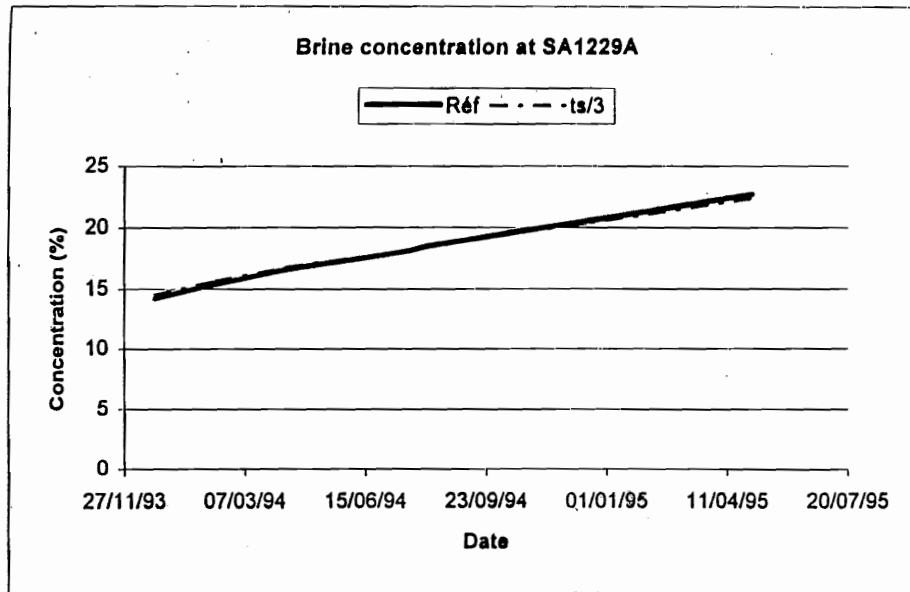
Glacial concentration at SA2783A

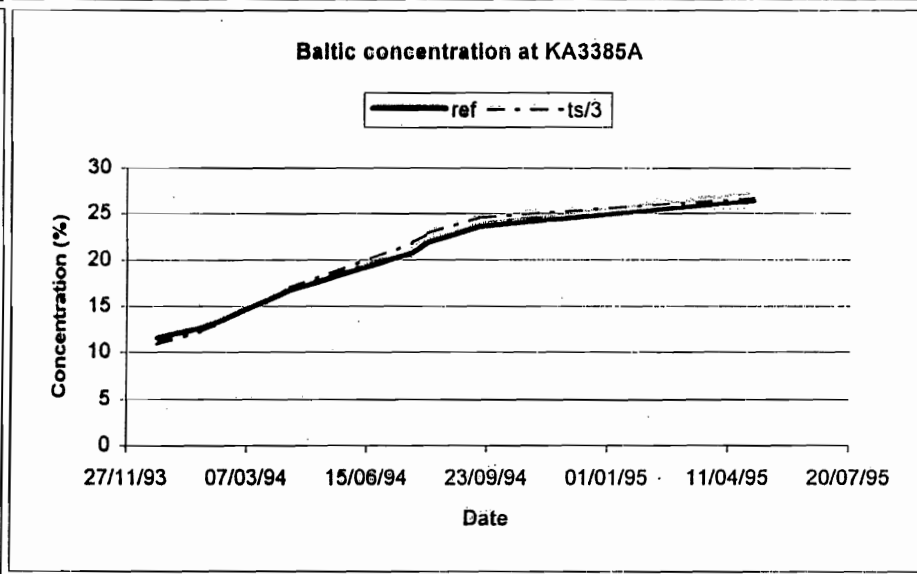
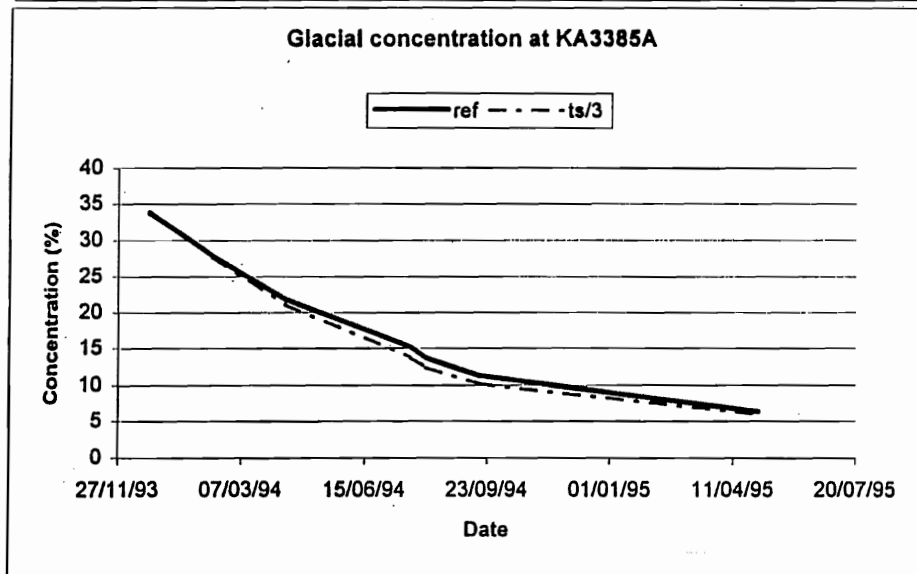
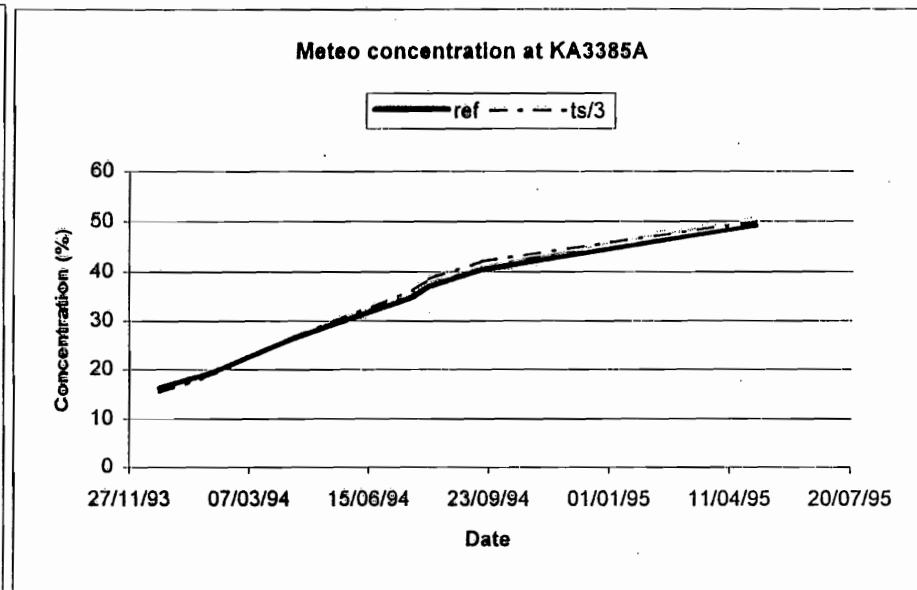
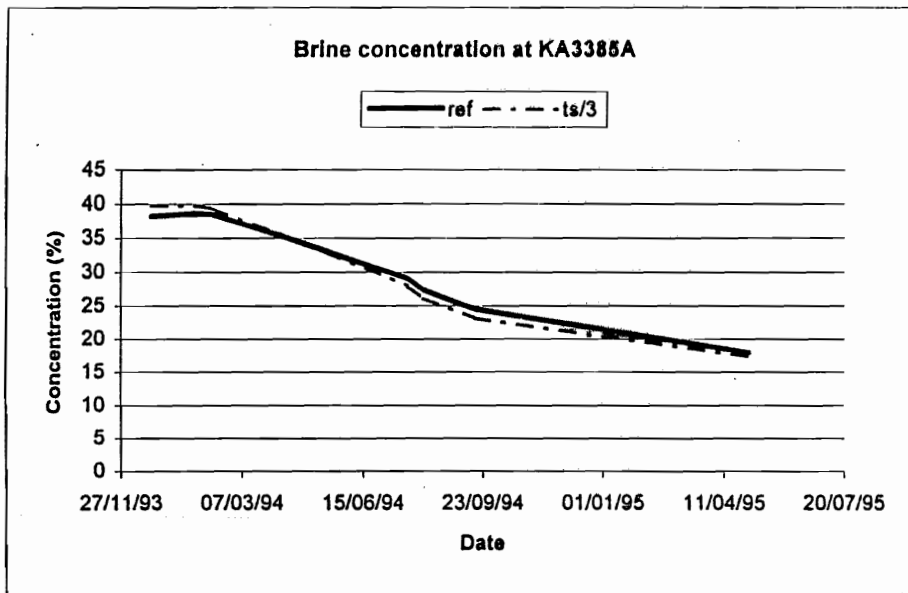


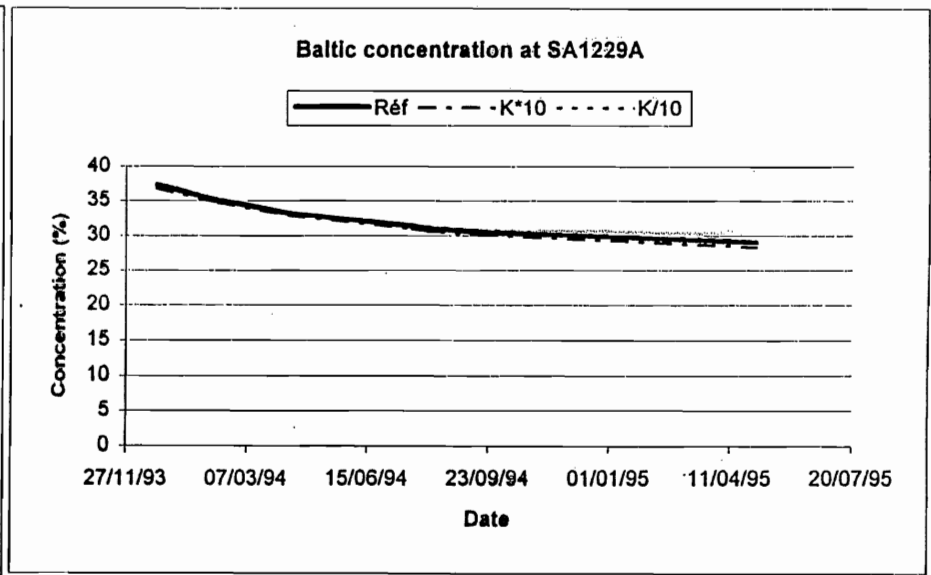
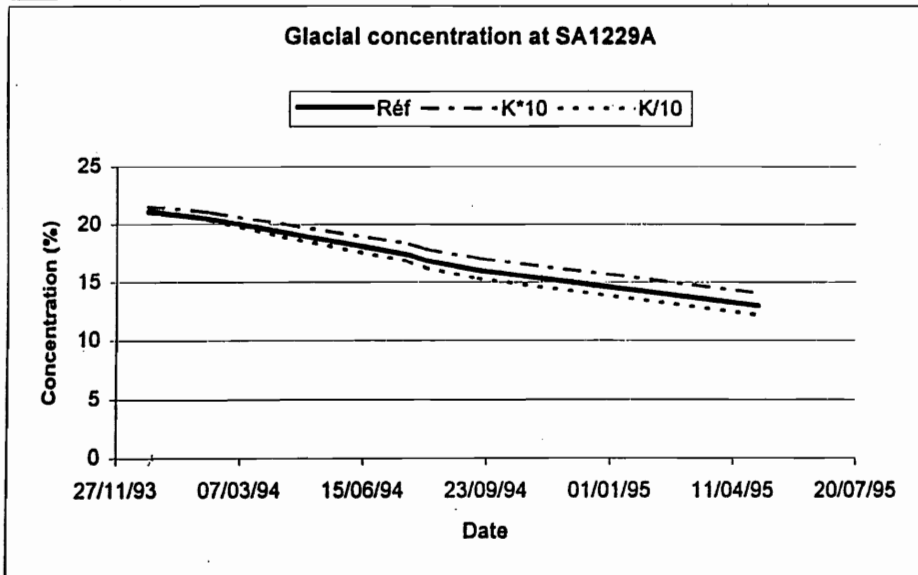
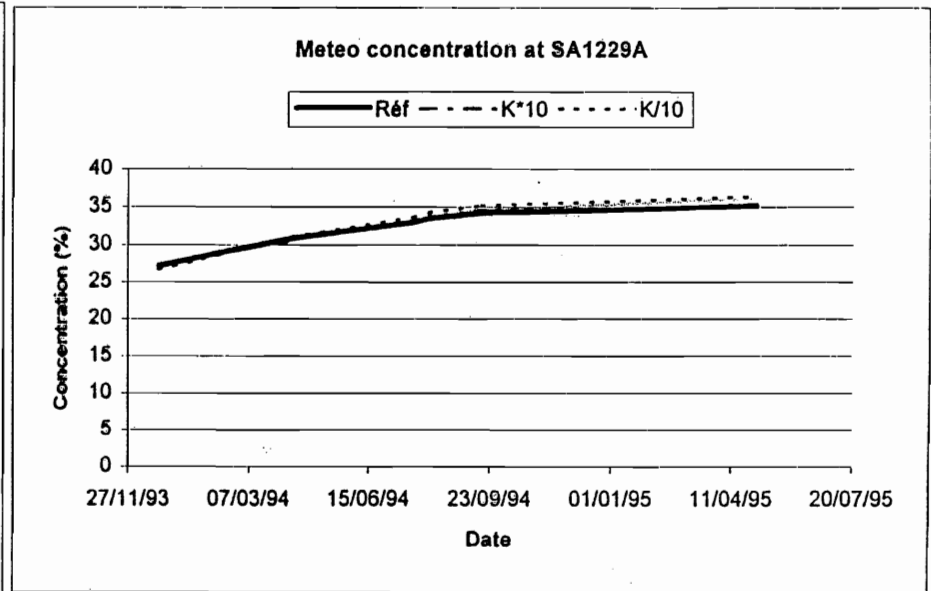
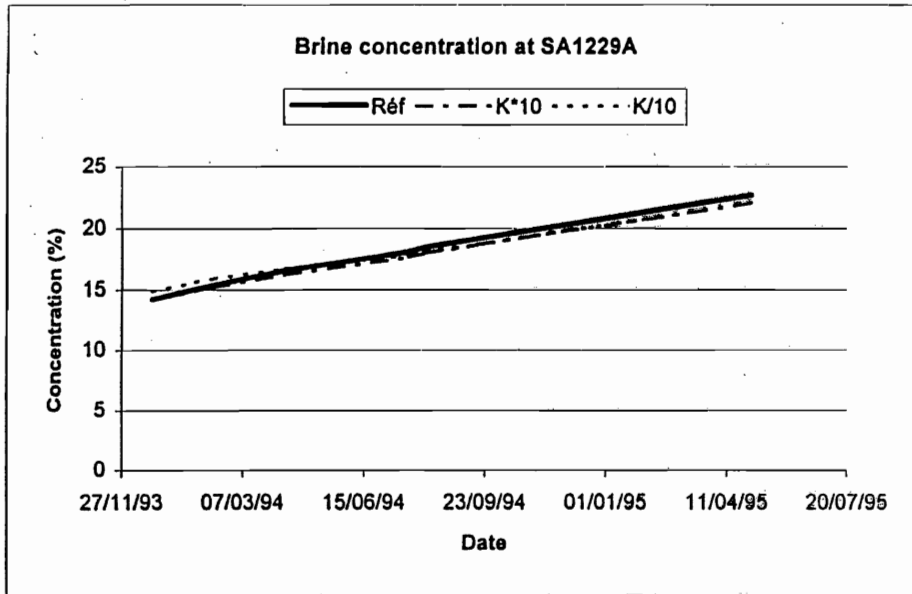
Baltic concentration at SA2783A

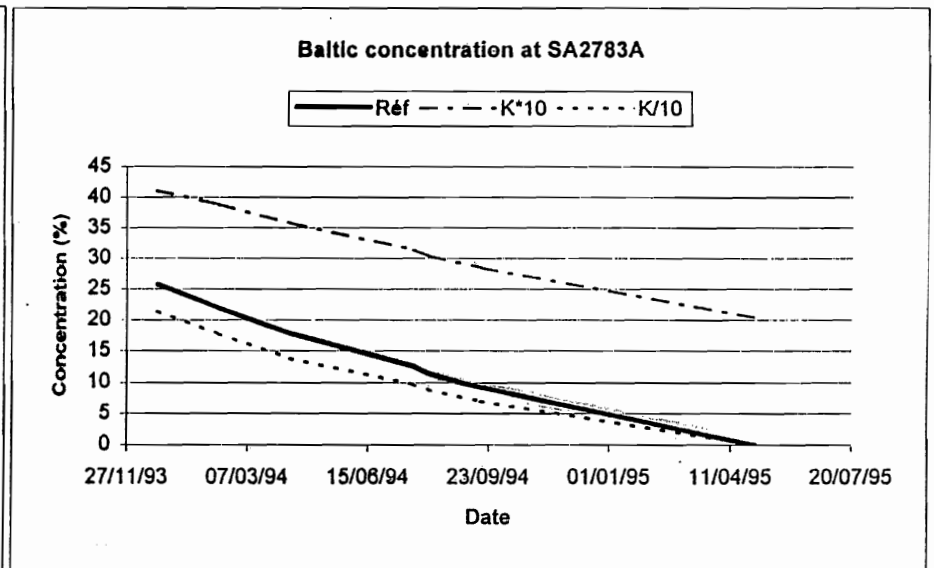
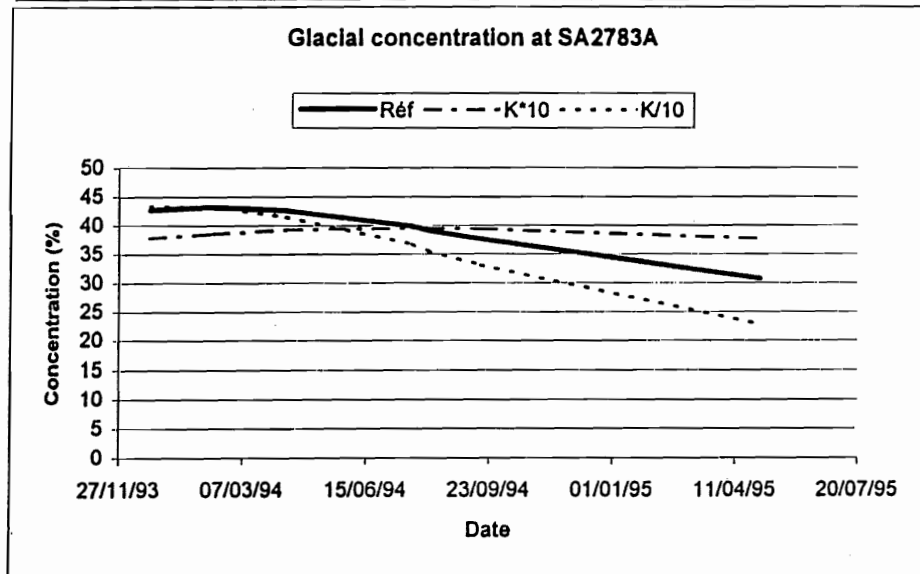
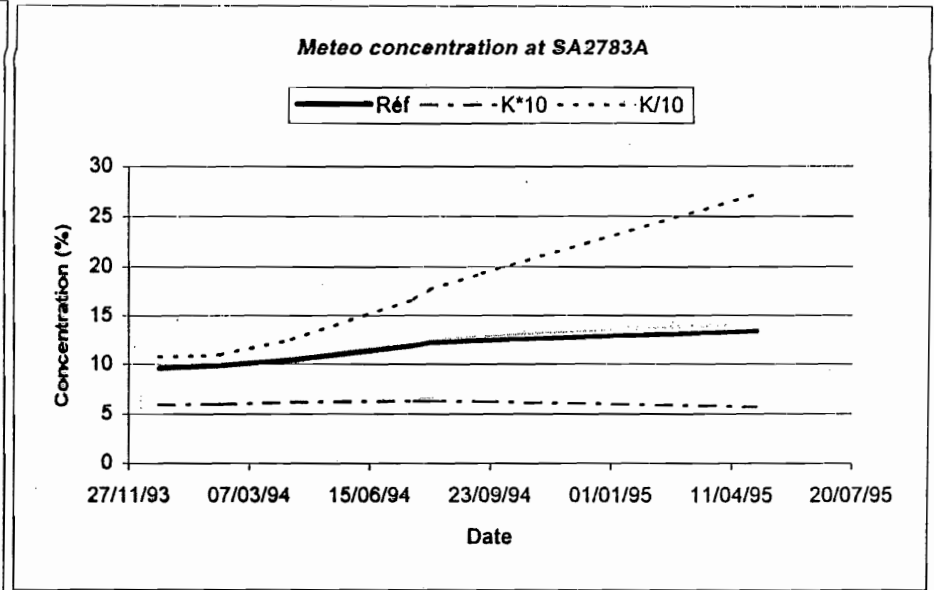
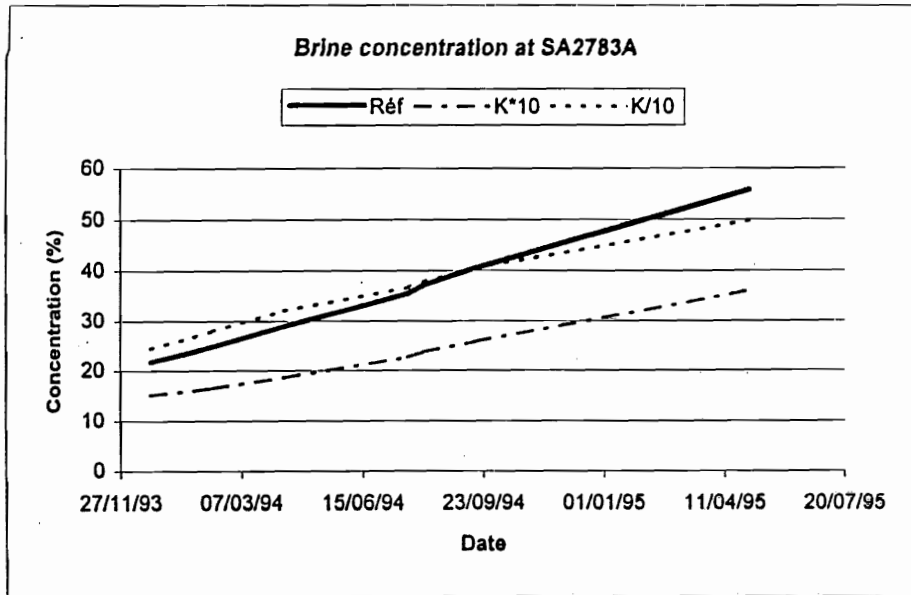




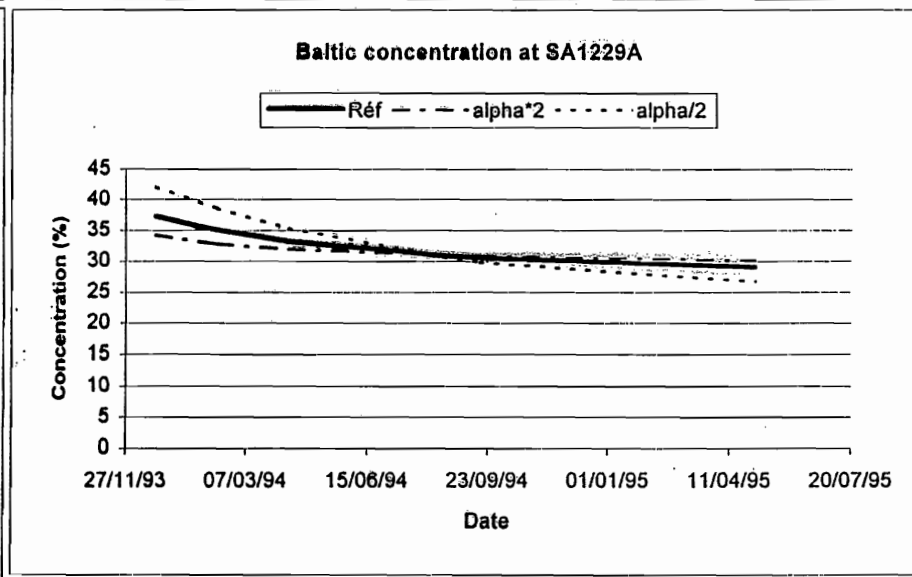
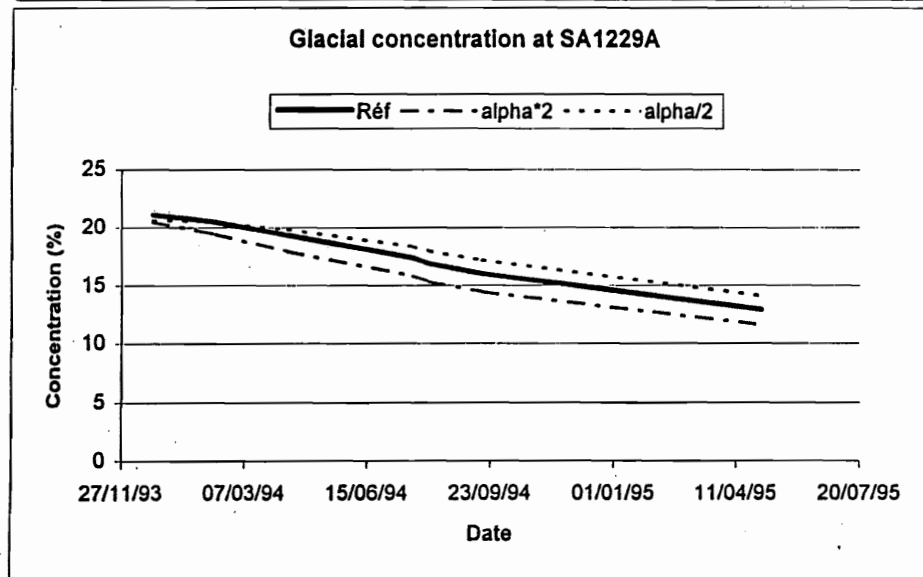
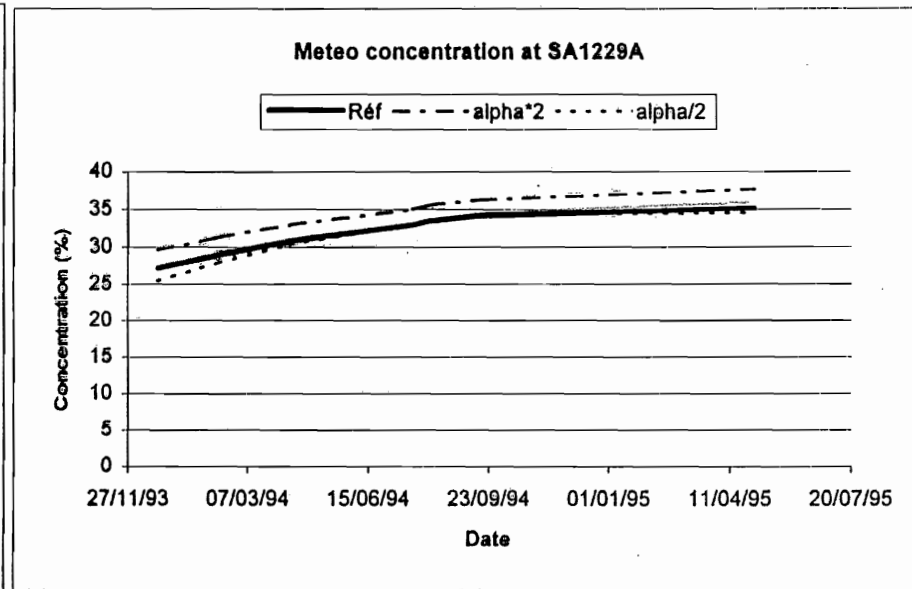
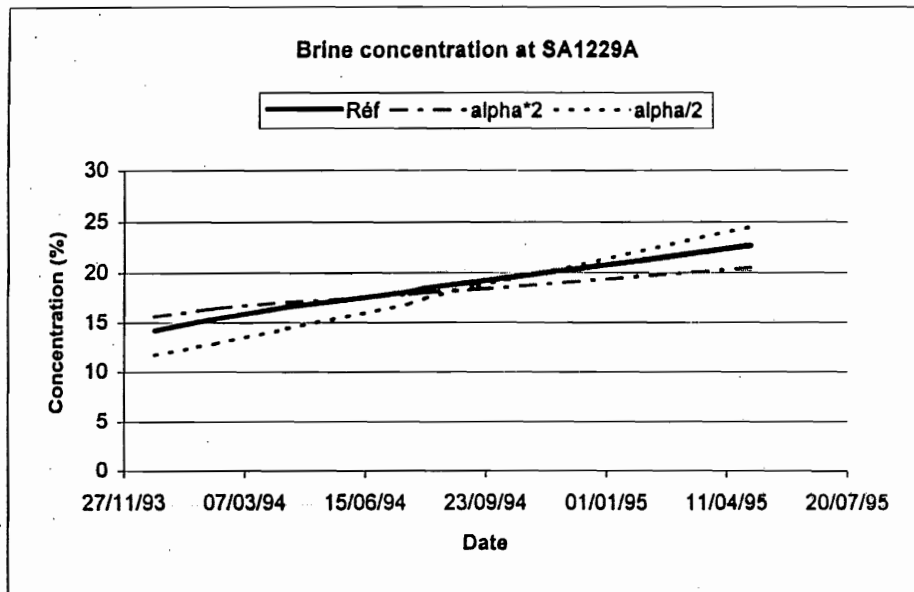




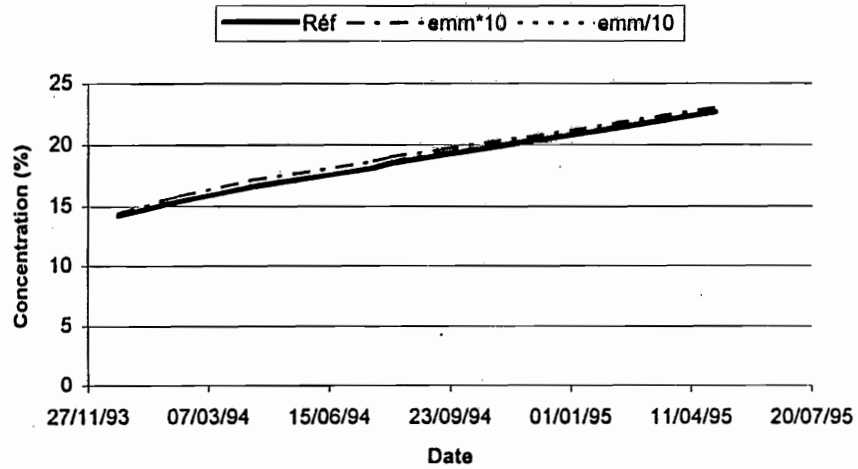




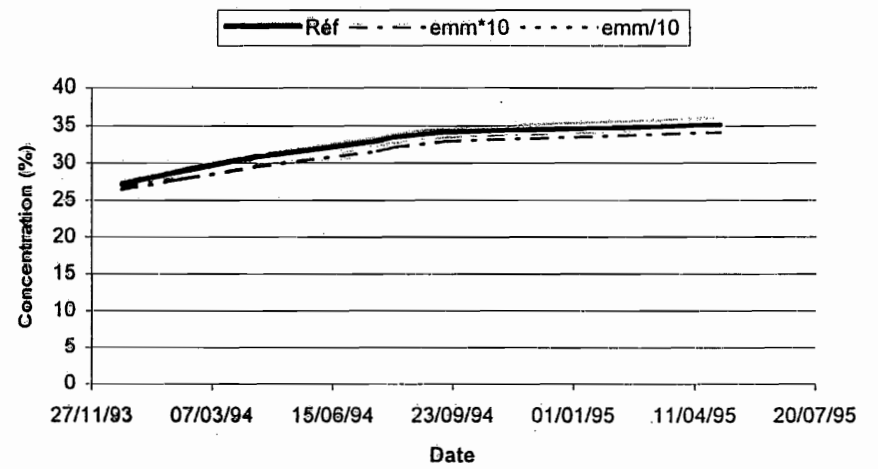
Sensitivity analysis on Disp



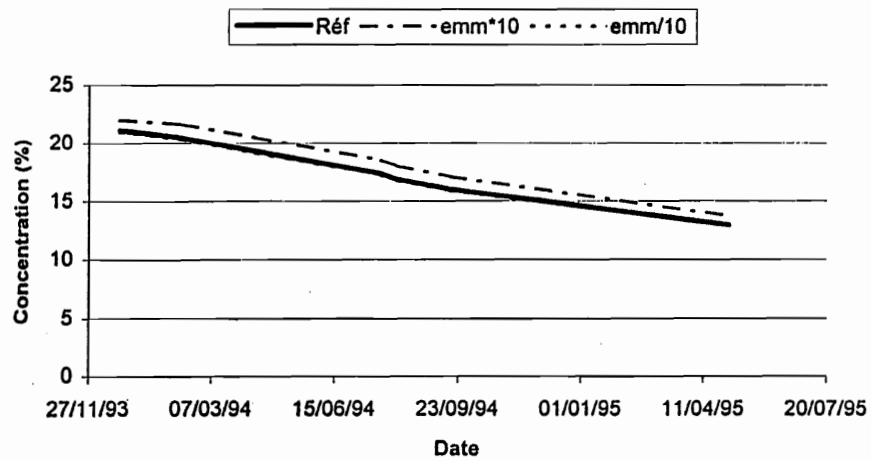
Brine concentration at SA1229A



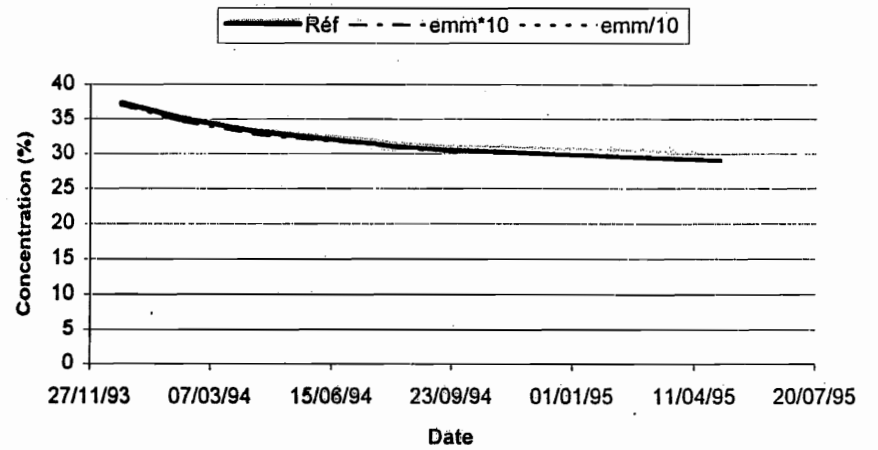
Meteo concentration at SA1229A

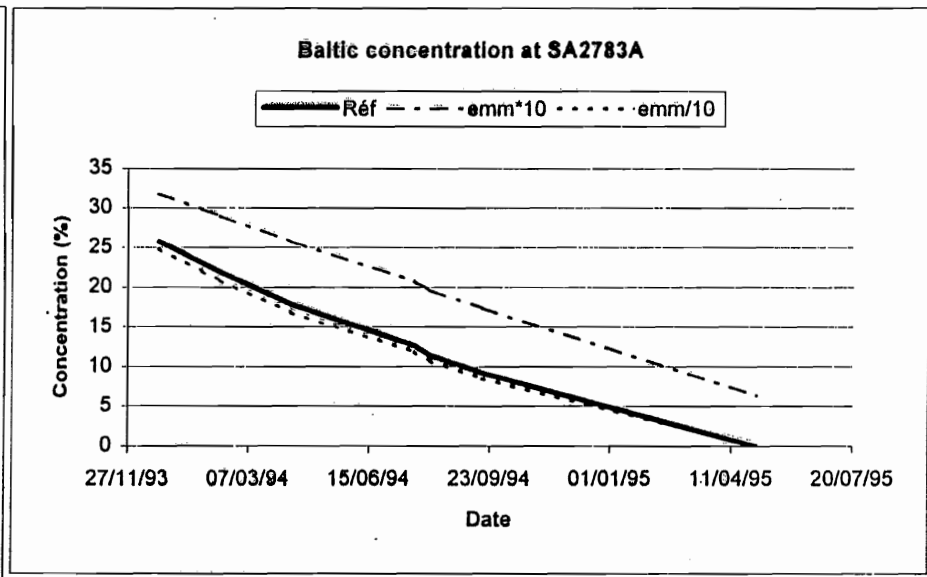
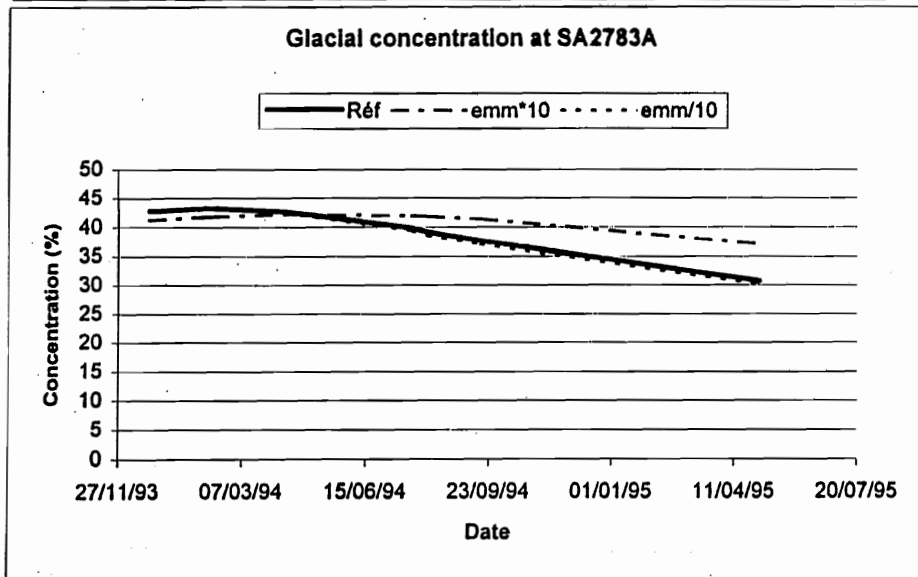
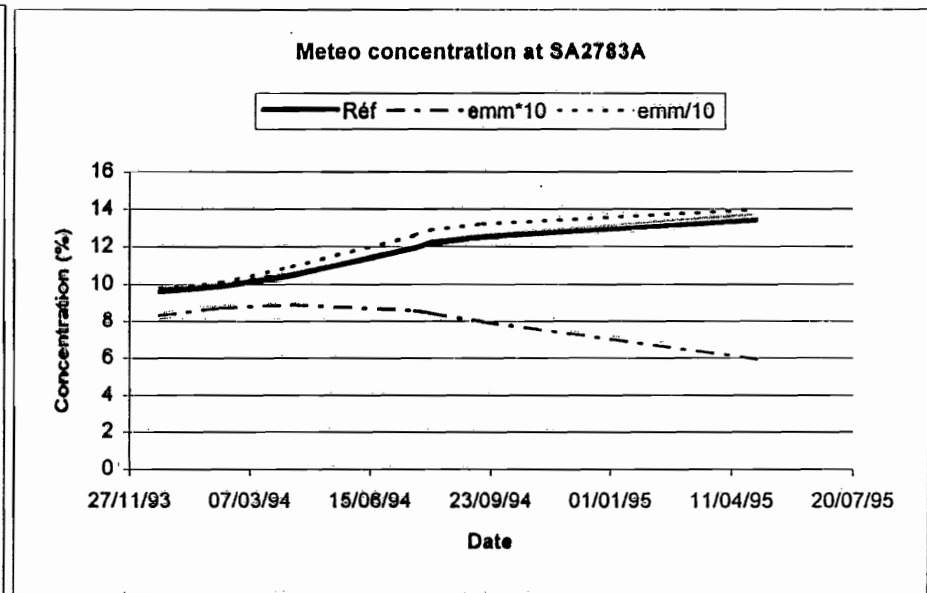
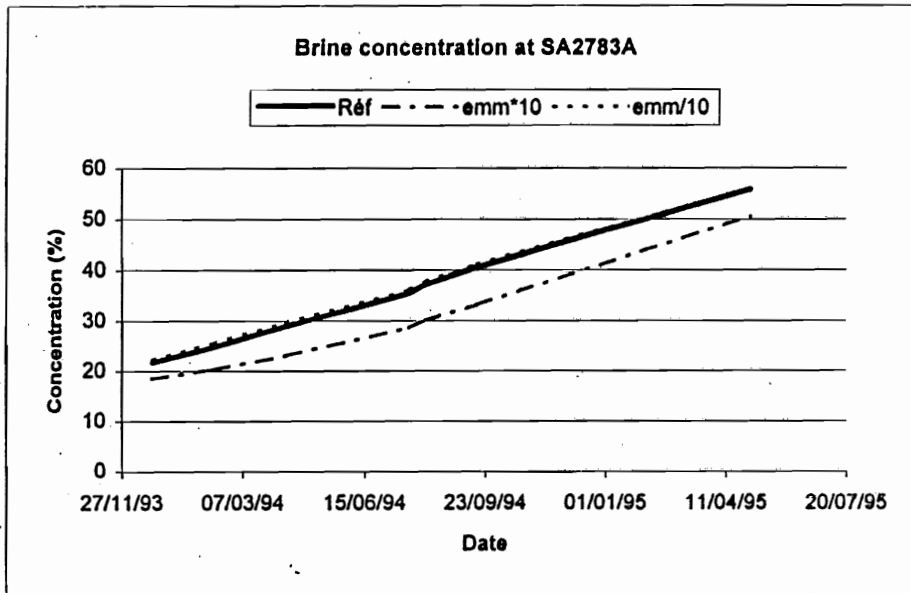


Glacial concentration at SA1229A

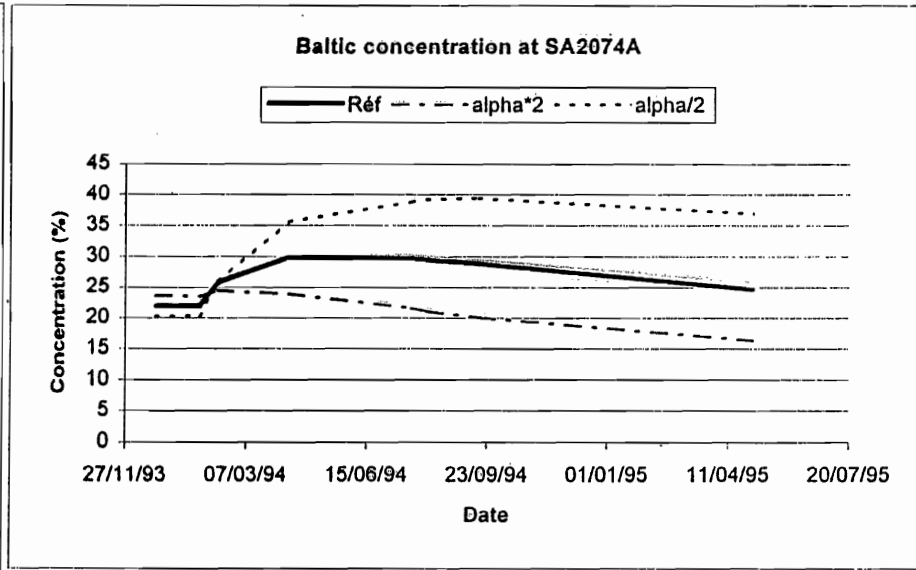
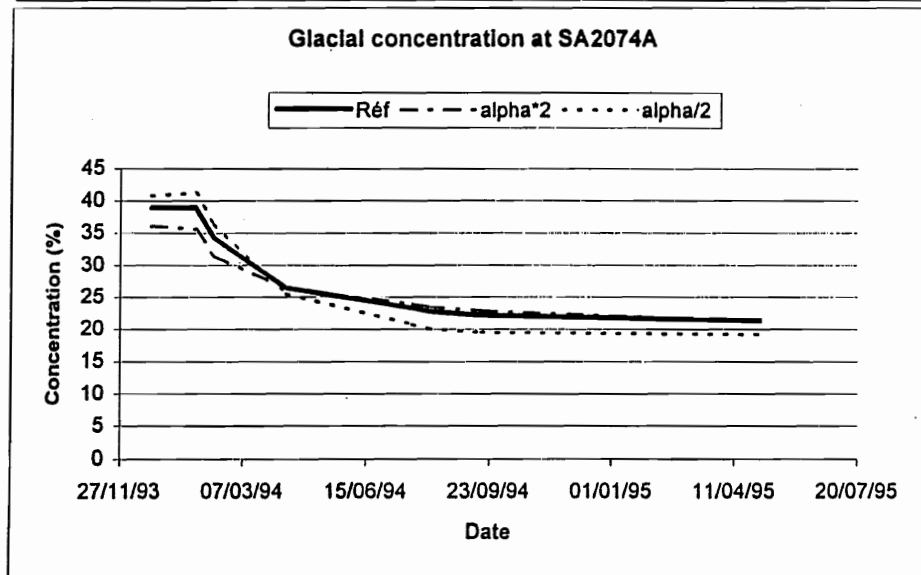
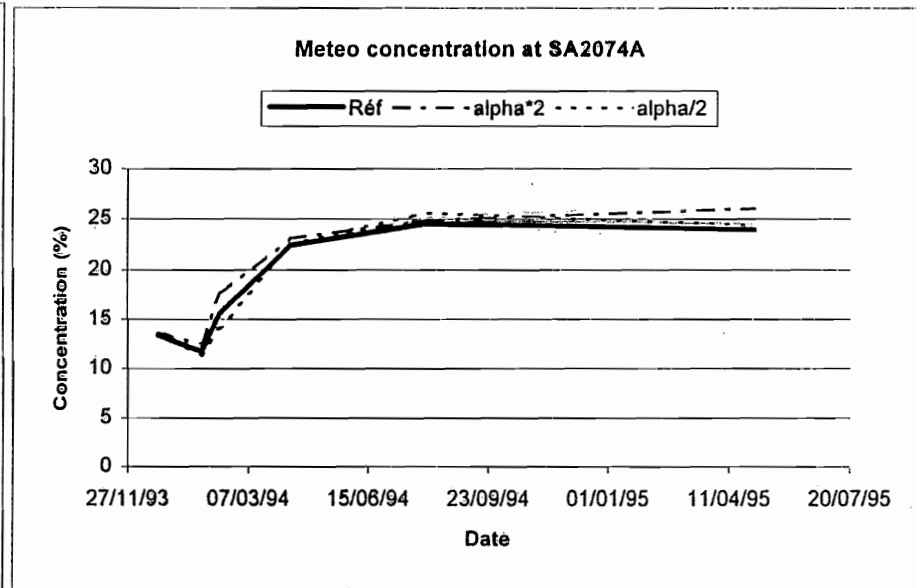
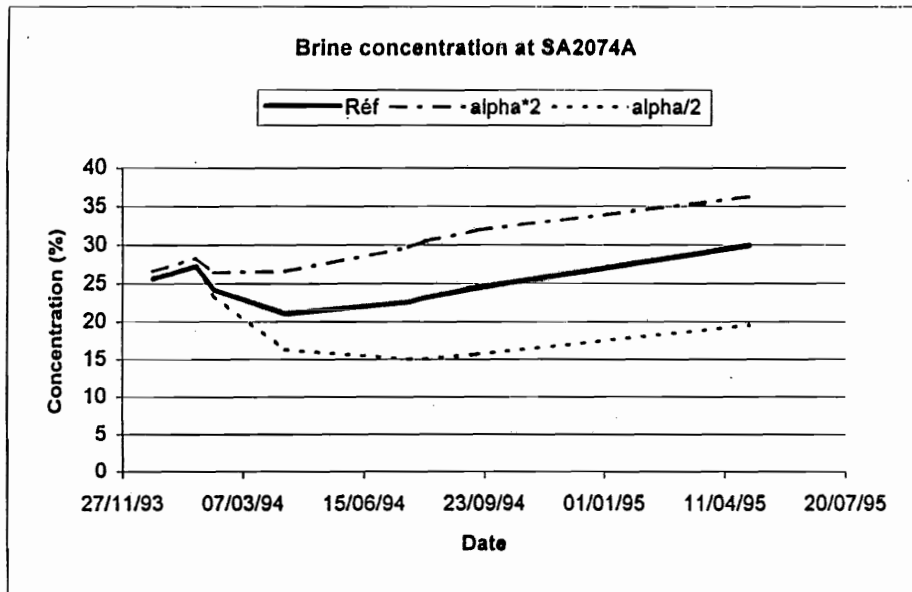


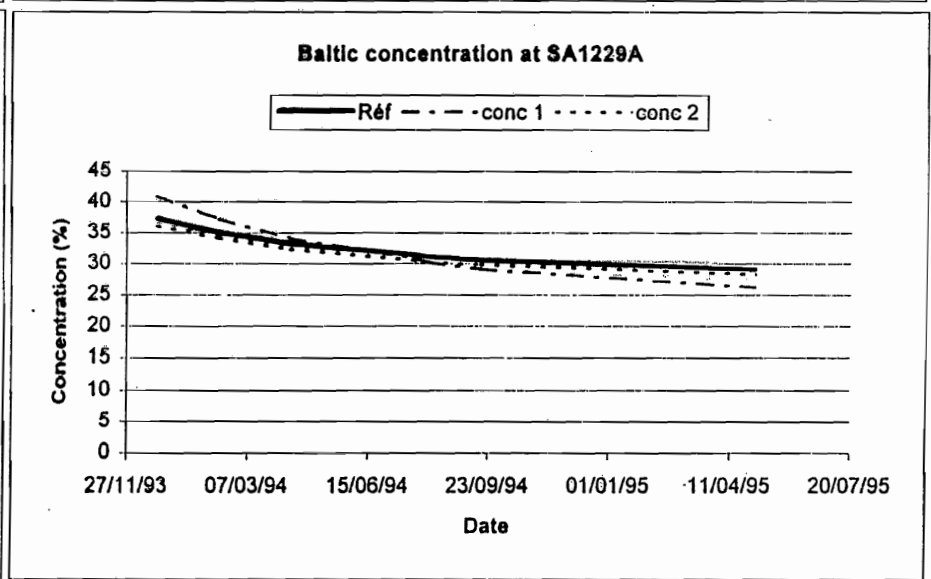
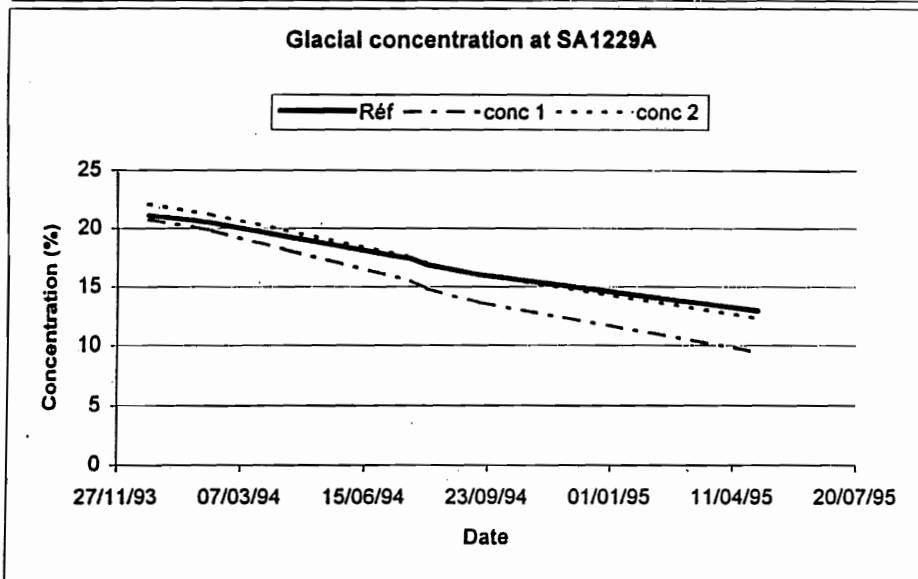
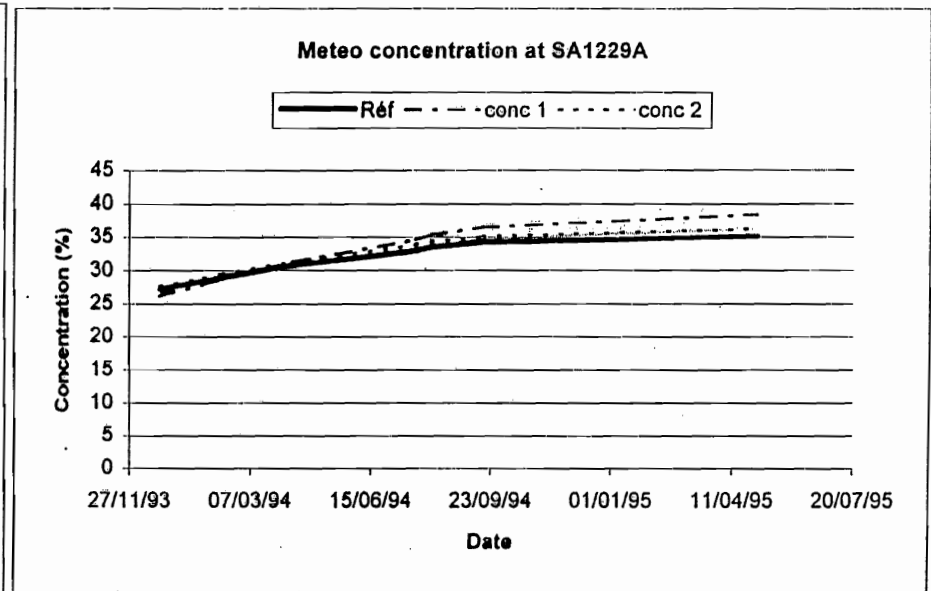
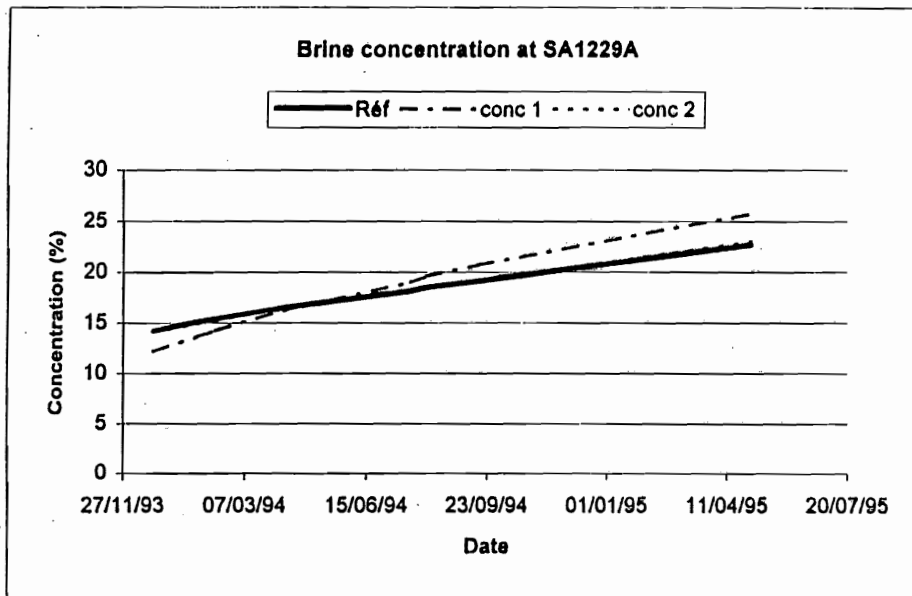
Baltic concentration at SA1229A



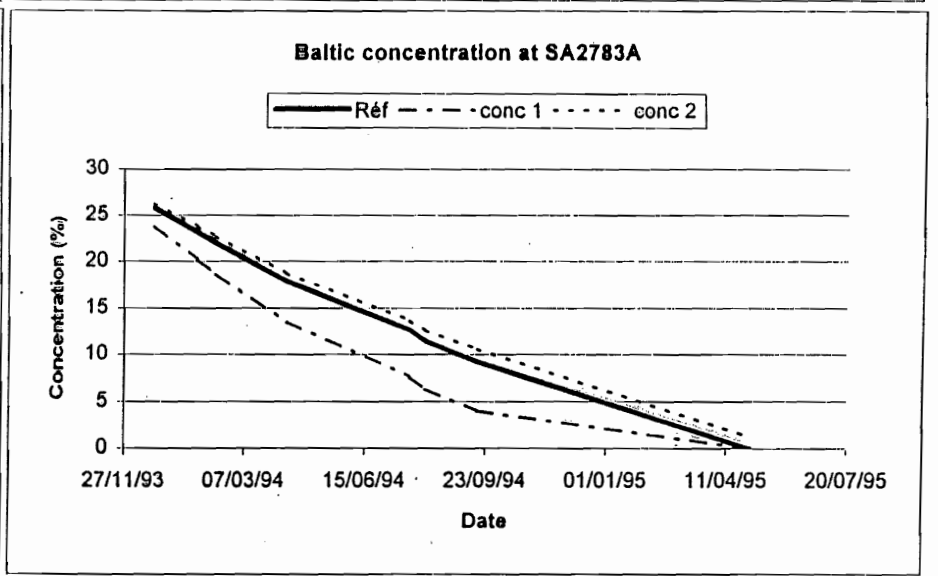
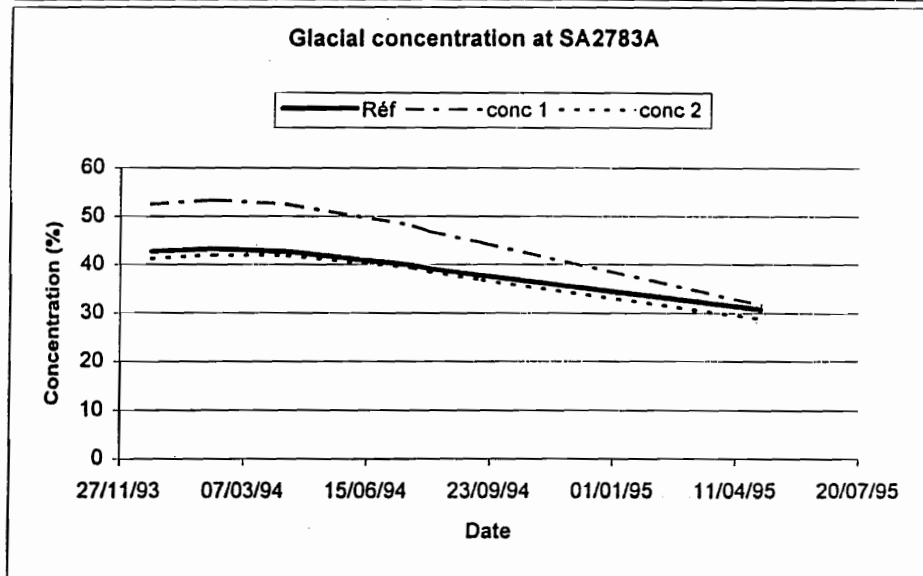
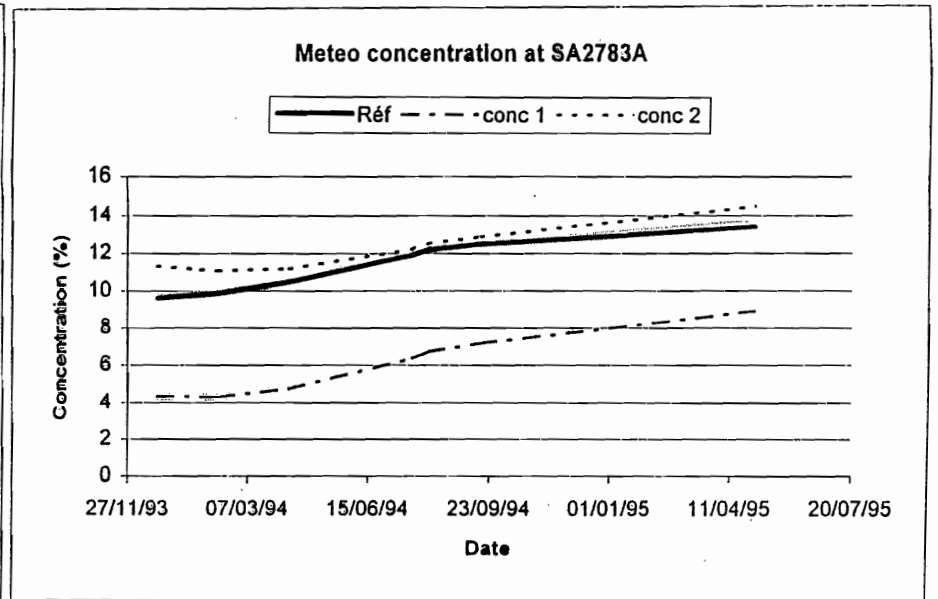
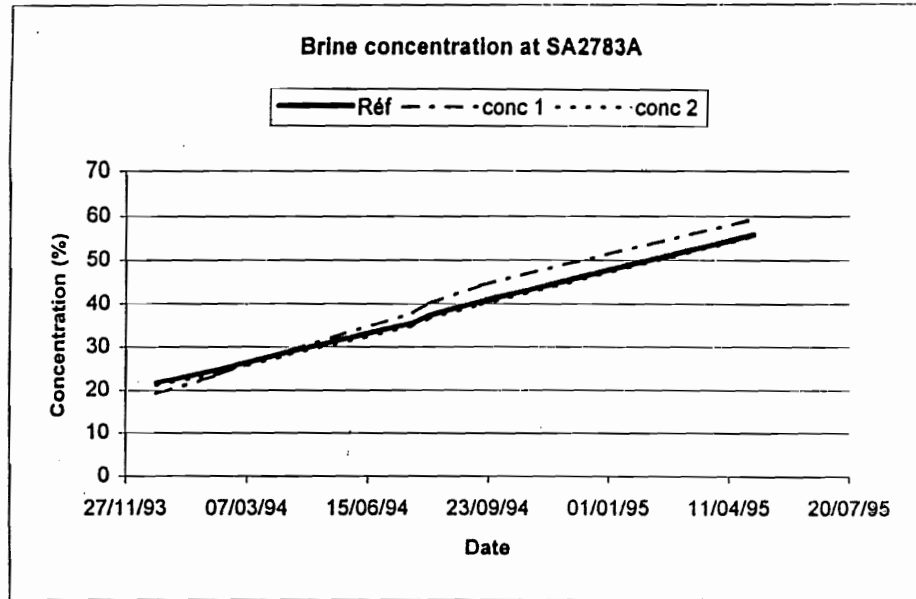


Sensitivity analysis on Disp

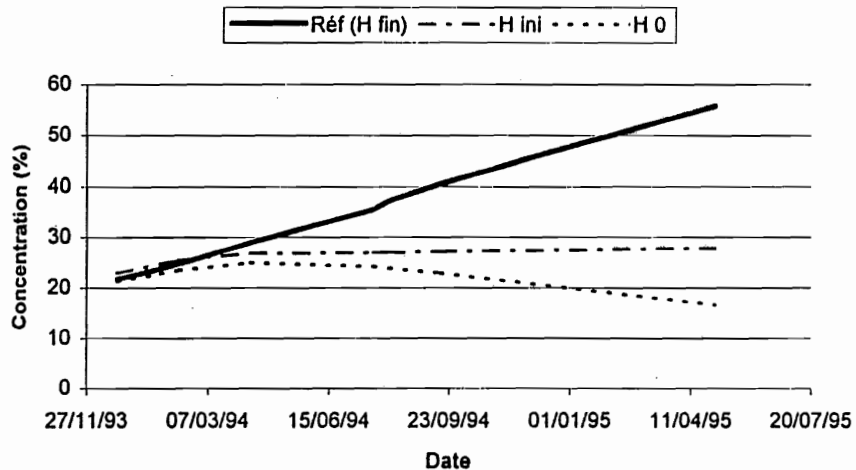




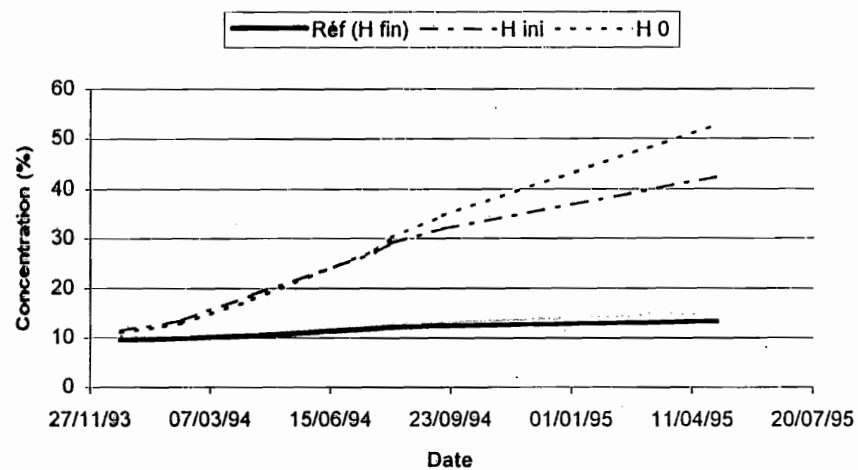
Sensitivity analysis on M3 concentra'



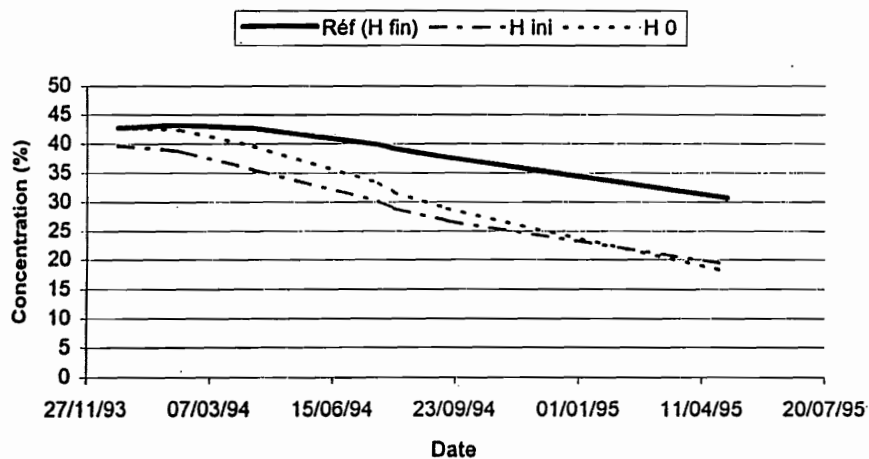
Brine concentration at SA2783A



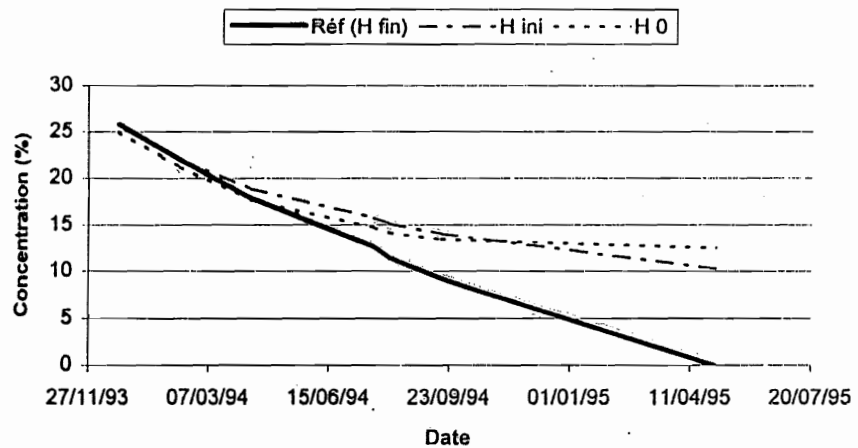
Meteo concentration at SA2783A



Glacial concentration at SA2783A

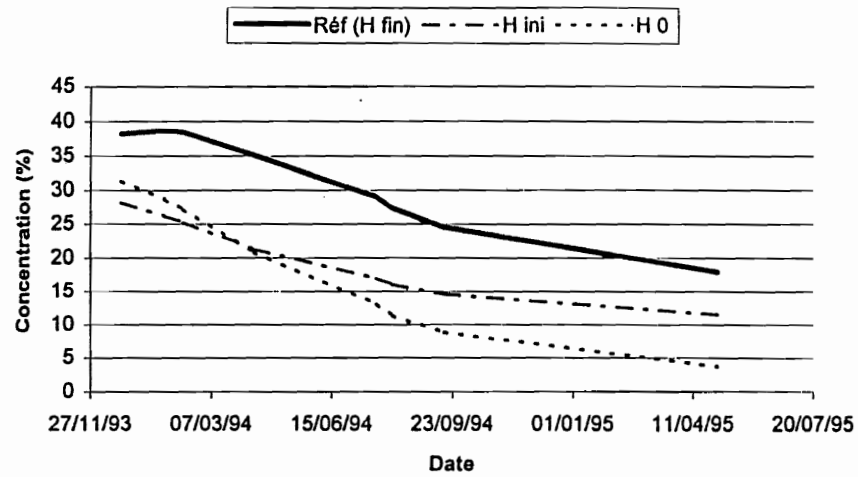


Baltic concentration at SA2783A

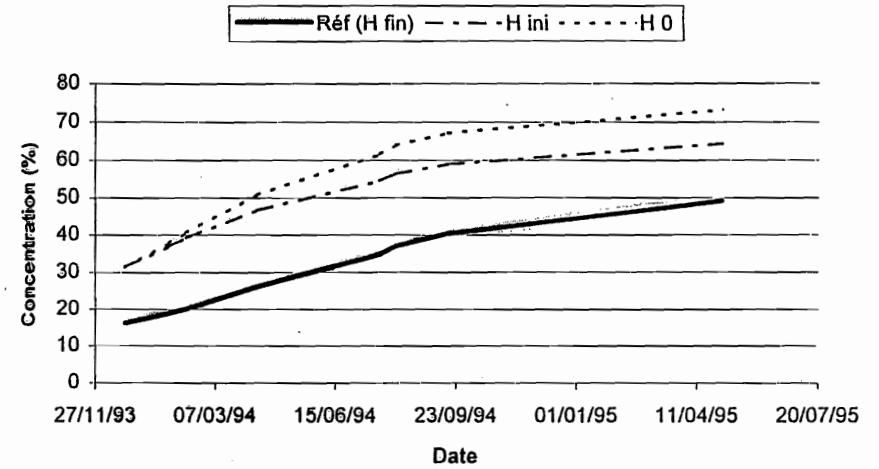


Sensitivity analysis on BC of H

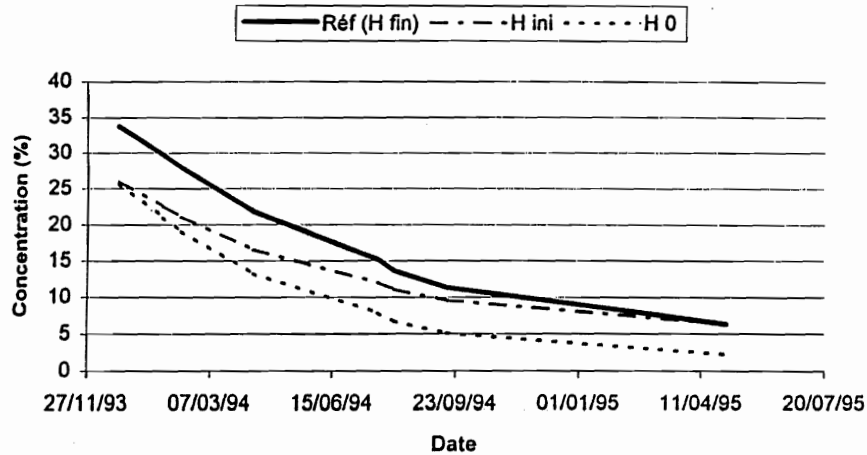
Brine concentration at KA3385A



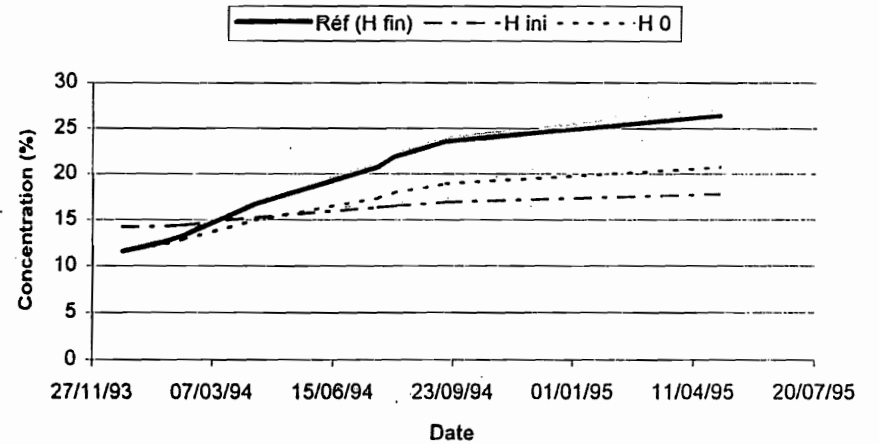
Meteo concentration at KA3385A



Glacial concentration at KA3385A



Baltic concentration at KA3385A



MAIN RESULTS

Influence of limit conditions

In flow : less than 6 months

In concentration : around a year

Matrix

The matrix can account for 10-15 % in concentration calculation

Uncertainties

Uncertainties in	Can account for (variation in end-members concentration, %)
Permeability	5-30
Storage coefficient	0-5
Dispersion	5-15
M3 provided data	0-5
Interpolation	5-30
H limit condition	10-30

Task 5 modelling, Executive summary

D Billaux (ITASCA)

TASK 5 Modeling, Executive Summary
ANDRA/Itasca
D. Billaux
18 February 2000

Objective

The ANDRA/Itasca team participated in Task 5 for the purpose of gaining experience on modelling for a real site, and a first limited approach to coupling of transport and geochemistry. The issues of interest were:

- How can geochemistry help the hydrogeological modelling?
- What kind of complexities are added by looking at geochemistry and hydrogeology at the same time?

Approach - Modelling choices

After a model was constructed, it was first calibrated based upon water flow computations only. The model was then recalibrated using geochemical data. This is a discrete fracture model, with channelized flow in fractures. We consider Darcy's flow, with no density effect. In Äspö coordinates, the model boundaries are ($X = 1000$ to 3000 ; $Y = 6000$ to 8000 ; $Z = -1000$ to 0). The 21 fracture zones (Hydraulic Conductor Domains) as given in the data set are taken into account, whereas rock outside fracture zones is not modelled. The fracture zones are represented as planes, bounded either by the model boundaries or by planar boundaries as specified in the data base. In each fracture plane, flow and transport occur along "channel pipes", i.e. a regular grid of one-dimensional elements. The grid has channels intersecting each other in four directions, at 45° angles.

Transmissivity, width, and storage coefficient are constant for each feature, except at the top boundary under the Baltic, where a "skin factor" is used. The transmissivity values are initialized from the data set, then changed during calibration phase. The specific storage is used as given when data are available (NE-1, NNW-1, NNW-2), and computed from the correlation in TR 97-06 for all other fracture zones. The boundary conditions are :

- constant flux under land, and constant head (with skin factor) under sea at the top surface;
- constant head on vertical faces;
- no flux on the bottom face.

The hydraulic calibration is performed by imposing the flowrates in the tunnel and trying to reproduce the available drawdown histories in boreholes. The calibration parameters are the transmissivities in fracture zones.

Conservative transport is modelled by advective/dispersive particle transport, with spreading due to both longitudinal dispersion in channels and to complete mixing at channel intersections. For end member simulation, the initial mixing ratios in each channel are interpolated from the cubic-grid interpolation at the start of the period, as provided in the data base. These mixing ratios are maintained constant on vertical boundaries throughout the simulation. For the top boundary, we use pure meteoric water under land and pure baltic water under sea.

Mixing ratios at the control points are then used to calibrate the skin factor at the bottom of the Baltic sea. The final skin factor we use is 100, ie we add at the bottom of the sea, above each fracture zone, a 10m-thick layer with a transmissivity equal to 1/100 of the mean fracture zone transmissivity.

Overall, the final model after calibration is relatively close to the initial one. Fracture zone NE2's transmissivity needed a 100-fold increase. This may mean there is another unknown conductor in its vicinity. Otherwise, only NNW1 (divided by 10) and NNW3 (multiplied by 10) had to be modified significantly.

Model sensitivity

Sensitivity studies were performed by doing simulations with modified parameters, testing:

- the effect of the chosen discretization (grid size from 40m to 80m, with either square grids or "four directions" grids).
- Fracture zone hydraulic conductivities (calibration procedure - both "bulk conductivities and skin factor under Baltic sea).
- Fracture zone specific storage (from no storage to ten time the chosen one).
- Longitudinal dispersivity (tenfold increase).

The simulation results had a very small sensitivity to discretization. The hydraulic conductivities used had a high influence on flow patterns, whereas specific storage was not very influential, with relatively fast piezometric response to the tunnel advance. Similarly, dispersion in the model was dominated by the mixing at intersections, so that the longitudinal dispersivity had little effect.

Results

Figure 1 shows a typical result for the hydraulic calibration, while figures 2 to 5 show end member ratios at Control Points computed using conservative transport, after skin factor calibration. The fluctuations in the computed values simply reflect the number of particles used in the model. Generally speaking, the simulations tend to overestimate the amount of Baltic water arriving at the Control Points, despite the skin factor we use at the bottom of the Baltic sea. Note that for simulations performed after hydraulic calibration only, the overestimation is much larger. Figures 6 and 7 show the most important pathways to the Control Points.

Conclusions

By looking at chemical transport, we were able to calibrate the flow parameters in a better way, by adding more constraints to the calibration process. However, uncertainties remain quite large. Specifically, the interpolation of the initial chemical compositions we used is not satisfactory: there is no guarantee that the initial conditions we derive this way are at chemical equilibrium.

A way out of this problem is to compute chemical equilibrium before and during the transport. However, this would be quite intensive numerically, if done over the whole region. Therefore, we are planning to chose a few significant paths on which effectively reactive transport will be simulated, possibly without resorting to end members.

Figure 1. Measured and computed drawdowns in one borehole. Flow-only calibration

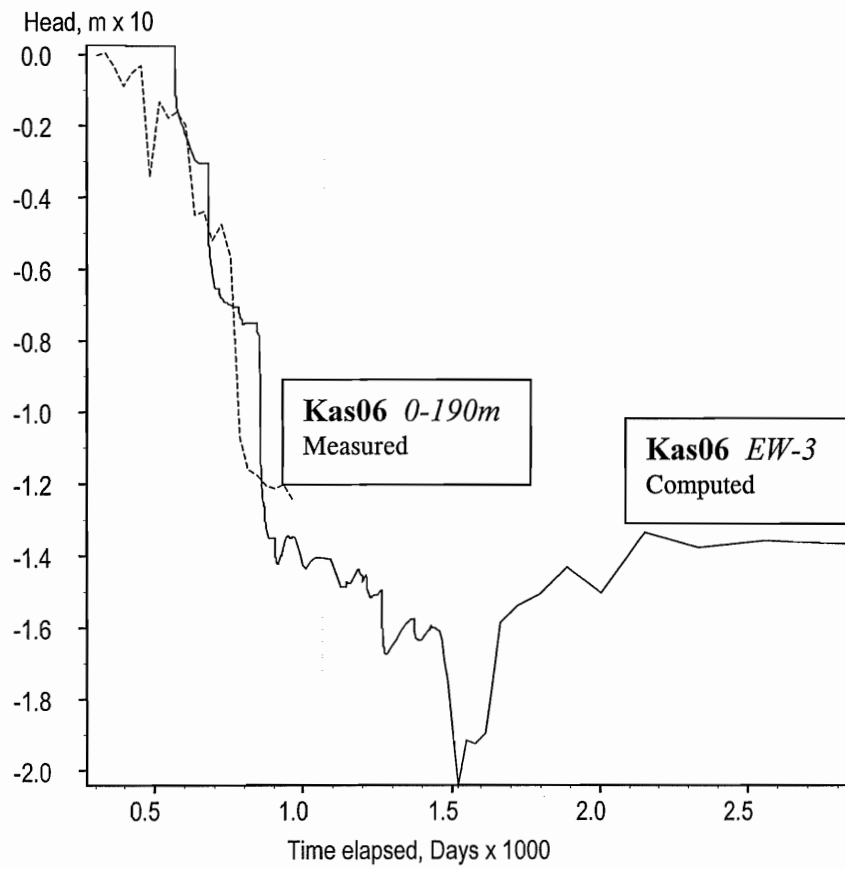


Figure 2. Measured and computed end members ratios in Control Point 2

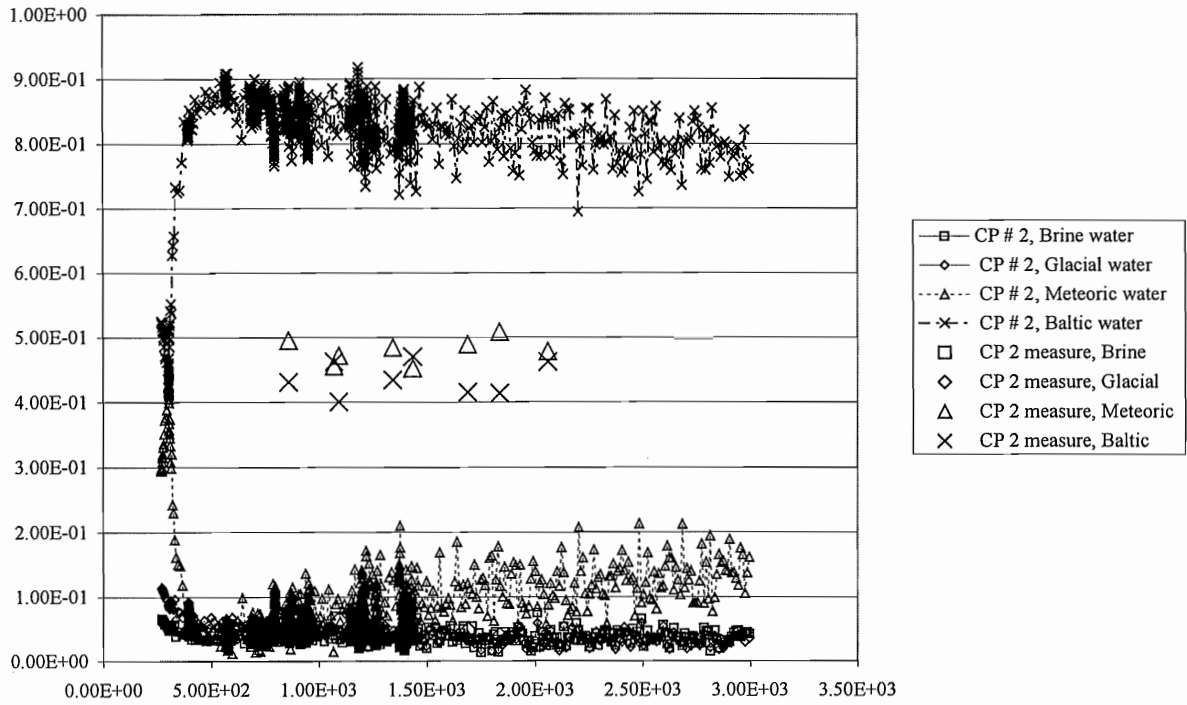


Figure 3. Measured and computed end member ratios in Control Point 3

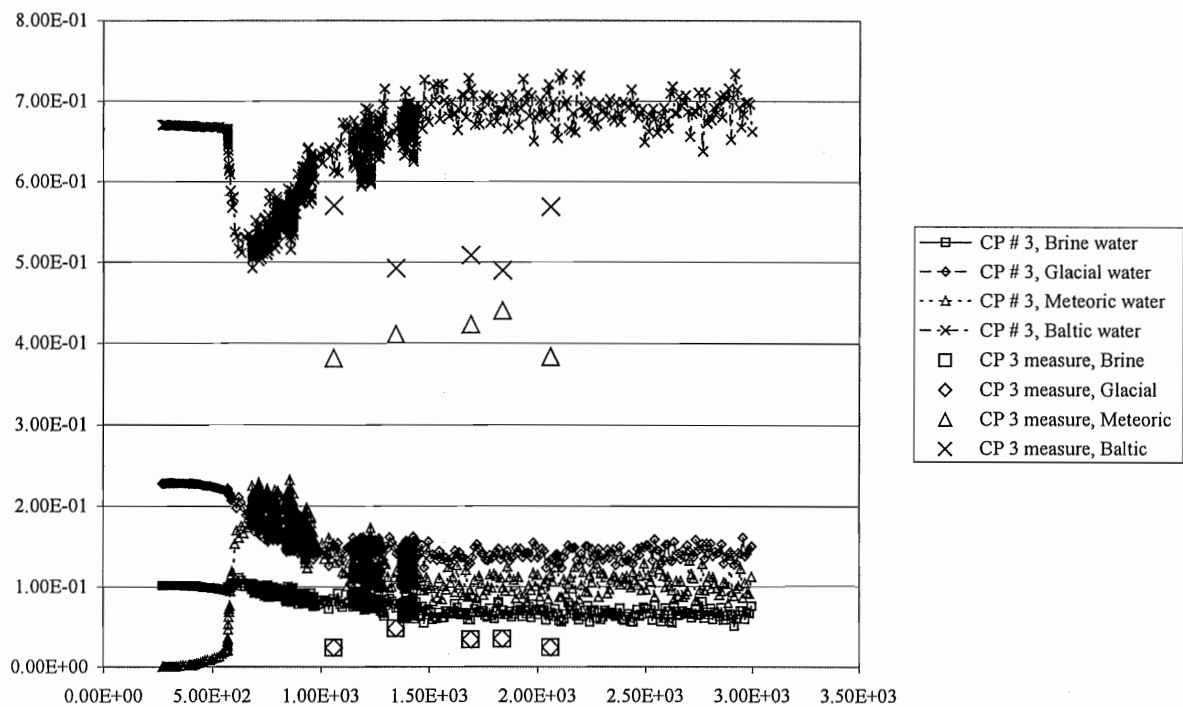


Figure 4. Measured and computed end member ratios in Control Point 5

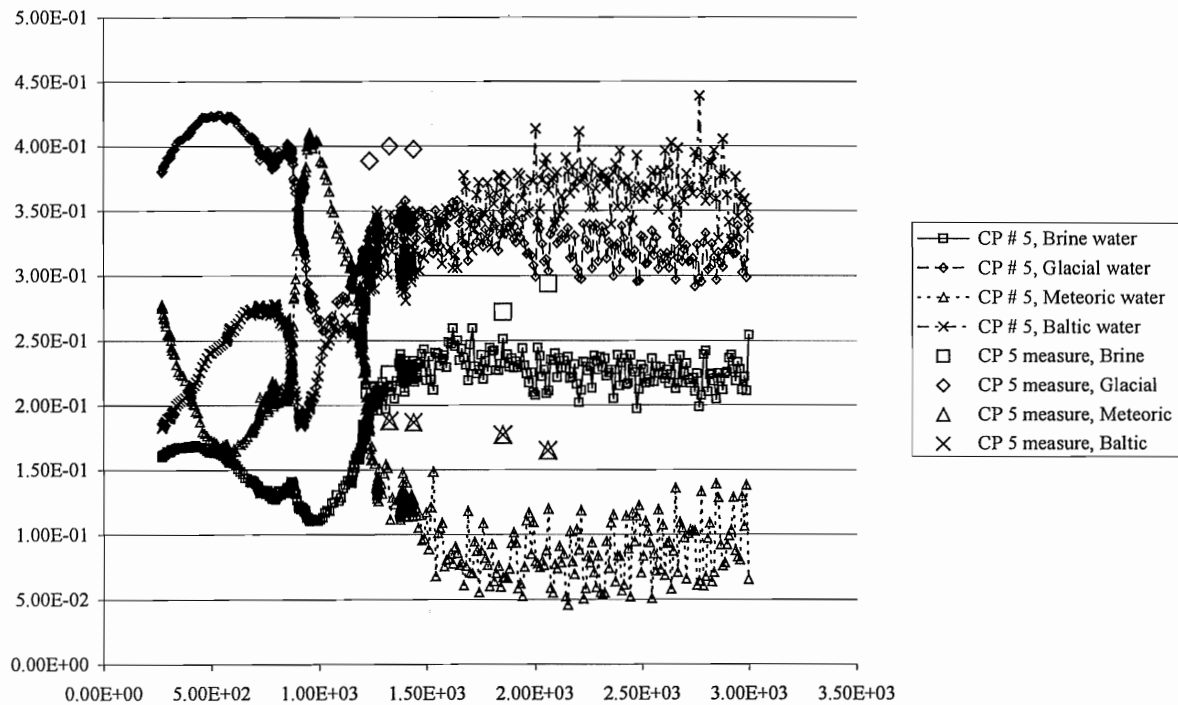


Figure 5. Measured and computed end member ratios in Control Point 11

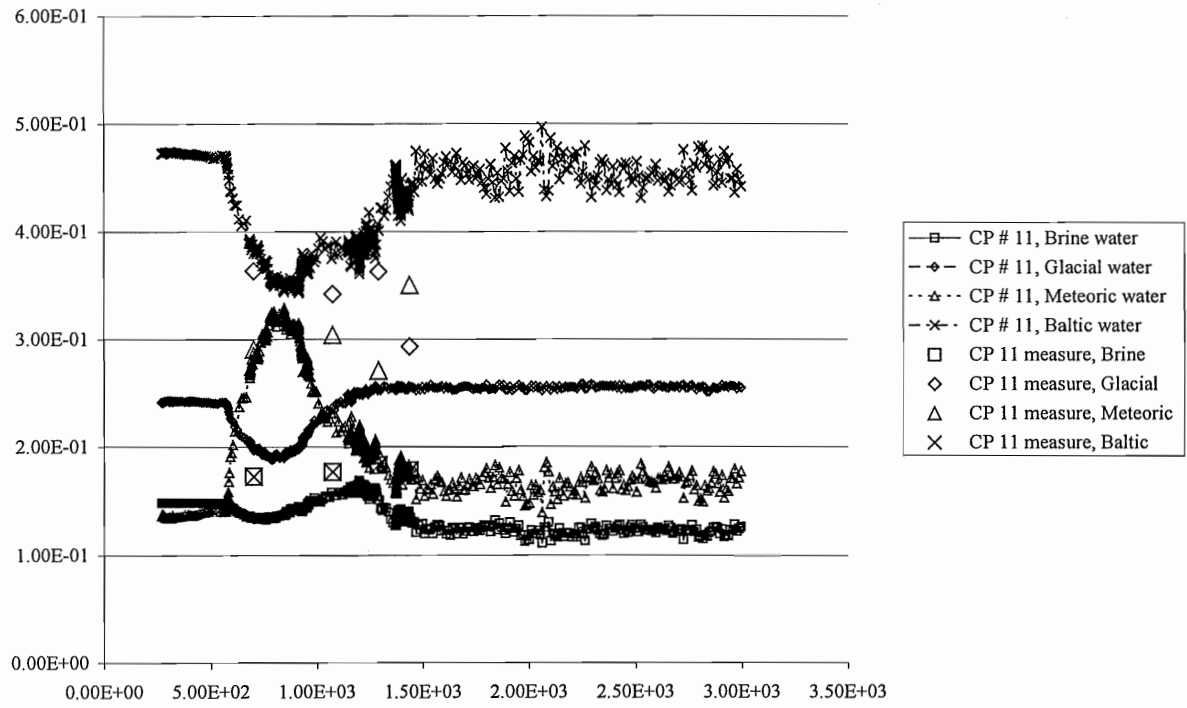


Figure 6. Main transport paths to Control Points, view from top.

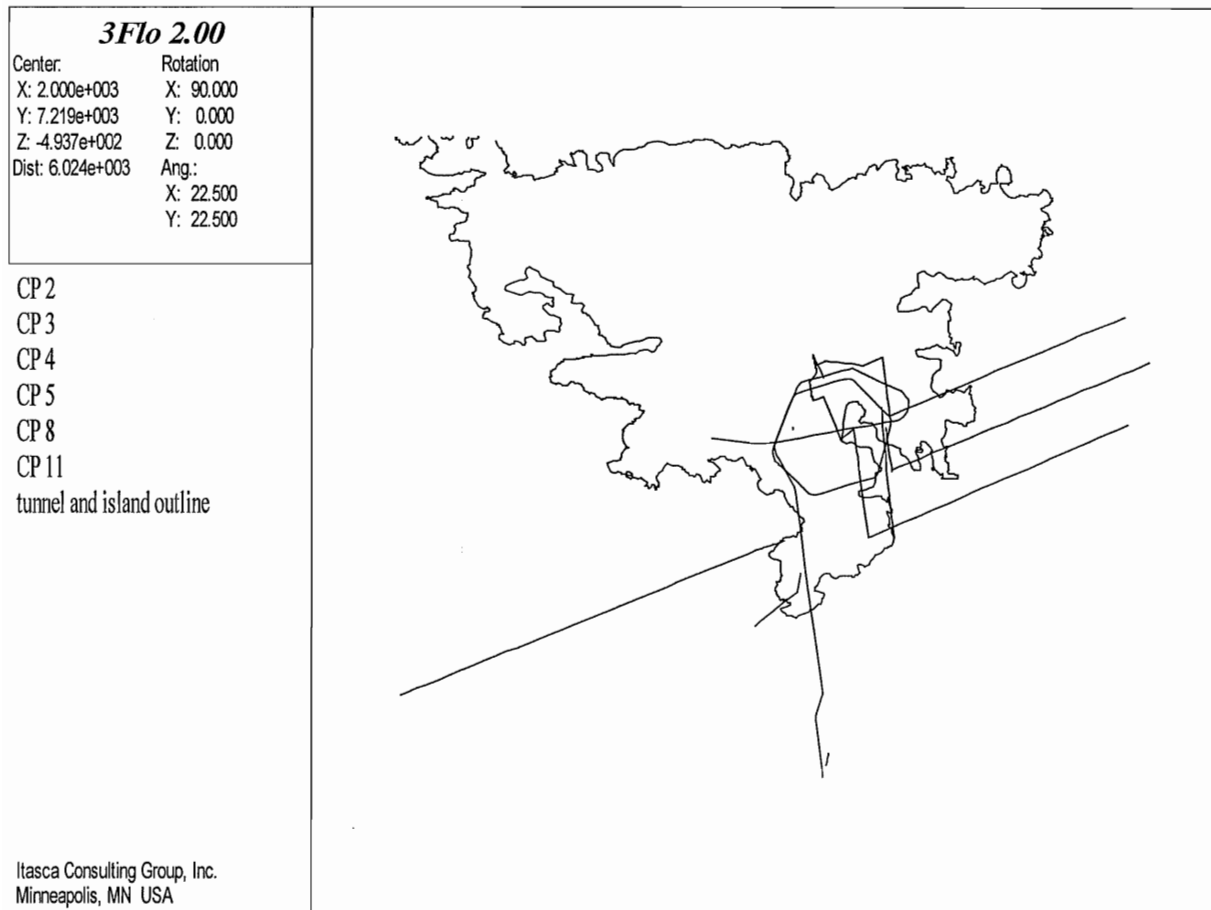
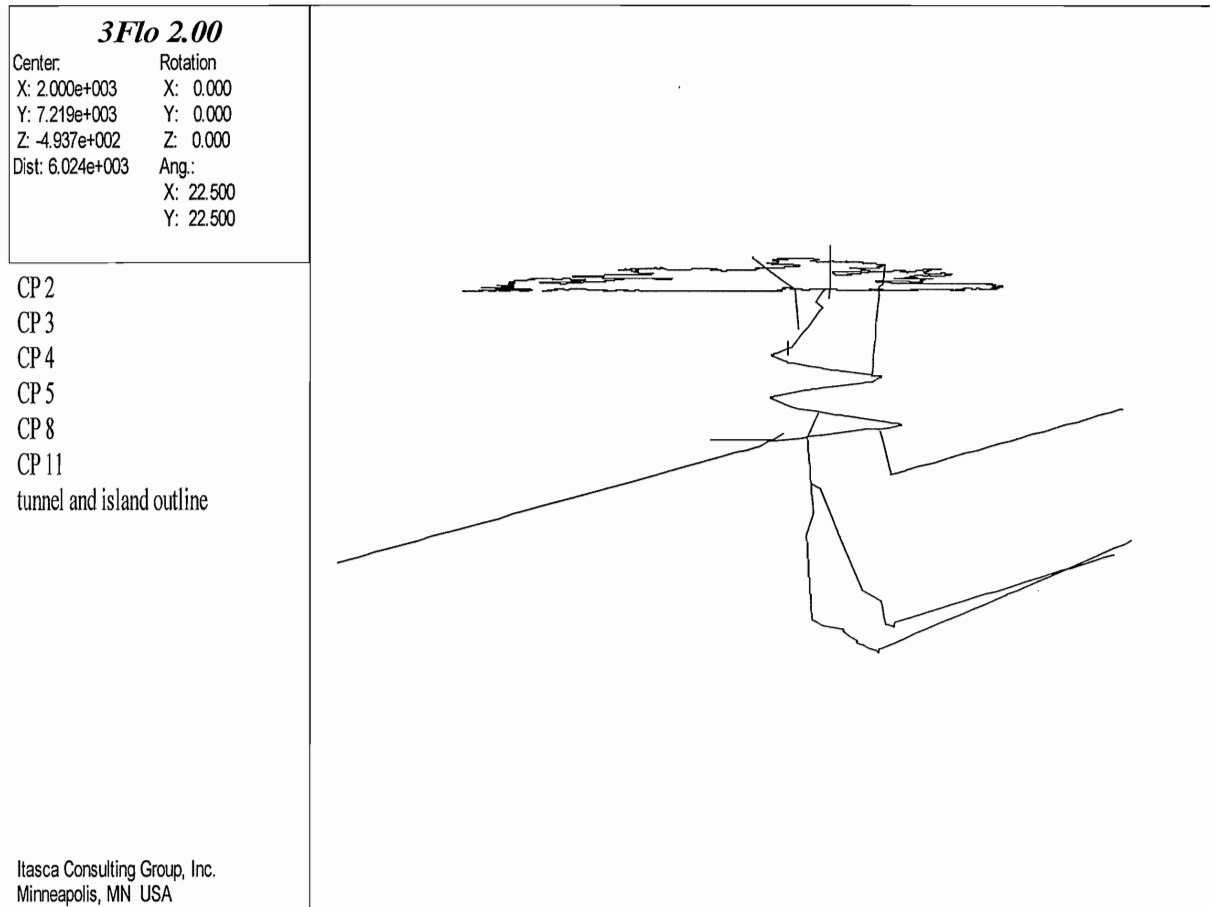


Figure 7. Main transport paths to Control Points, view from south.



Comments on predictions

I Rhén (VBB-VIAK)

Task 5. Comments to the predictions

- Posiva has presented an alternative set of calculated mixing ratios based on different end-members; additionally, chemical reactions have been more widely emphasised
- Modelling of Redox Zone (ENRESA)
- Flow paths - have simulation approaches influenced the results (e.g. increased/decreased the mixing to varying degrees)?
- Flow times – similarities and differences for CPs

Task 5. Summary list of model approaches used by each group

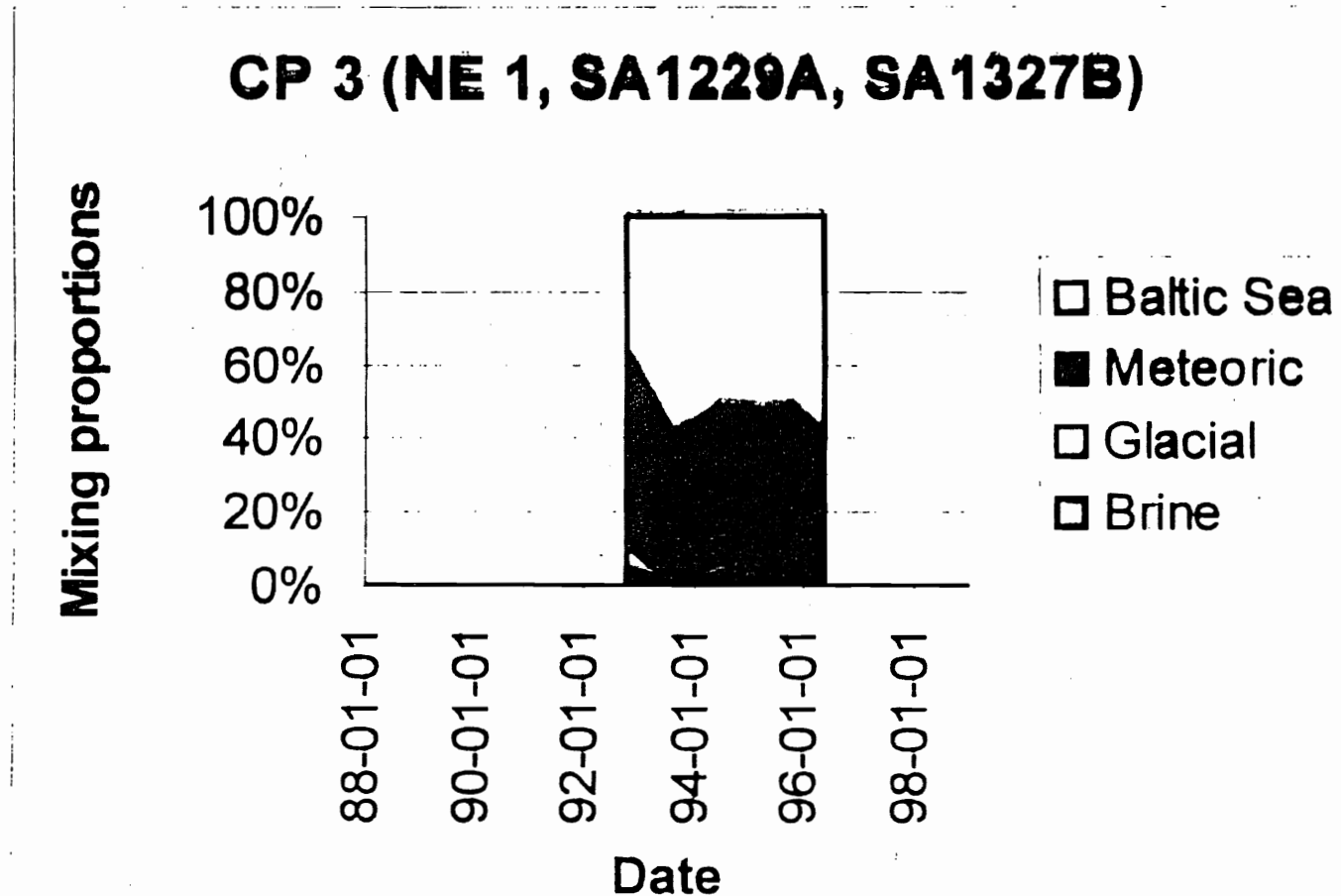
Organisation	Flow modell	Mixing calc.	Reaction modelling
ANDRA-ANTEA	Continuum (FEM) 3D.	^{H3} x	
ANDRA-CEA	Continuum (FEM) (HCD), 9	x	
ANDRA-ITASCA	FEM, DFN ⁿ - chann. flow (HCD)	x	
BMWi	Continuum (FEM) (HCD)	x	x
CRIEPI	Continuum. (FEM) (3D)	x	x
ENRESA	Continuum (FEM) (HCD)	x	x
JNC	FEM, DFN (3D)	x	
POSIVA	FEM - Continuum. (3D)	x x	x
SKB	SC (FDM), F+FDM (3D).9 3D,9	x	x



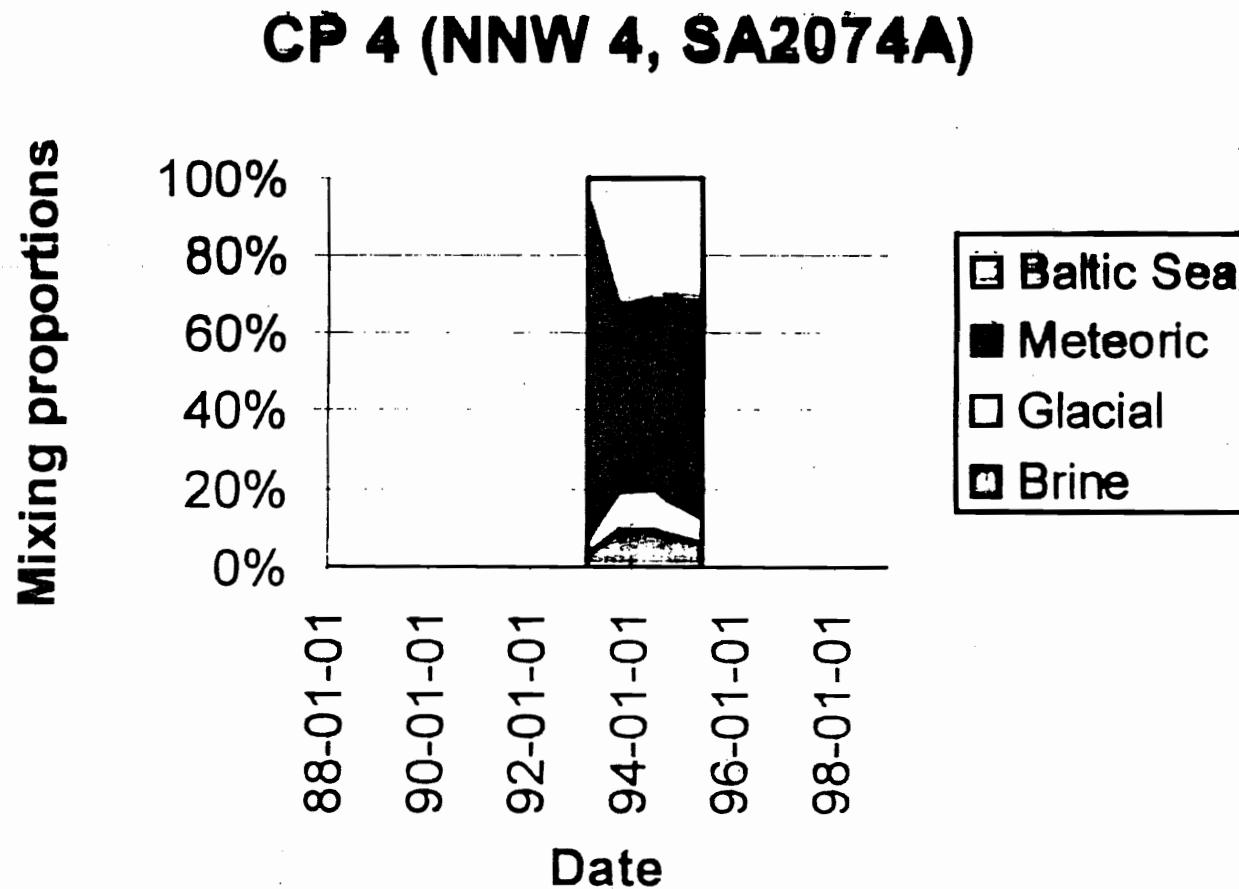
Task 5. Comments to the predictions

- Date May 1991(tunnel face position about 700 m): to indicate the initial conditions in the model
- Date May 1995: to indicate the situation after tunnel construction
- Measured data:
 - Few data available on May 1991
 - Measured data in the diagrams may be 0.5-1 year from May 1995
- Calculated data:
 - Some groups have delivered results for only a few days. Data in the diagrams may be 0.5-1 year from May 1991 and May1995
- (Sometimes a bit unfair comparison in the diagrams)

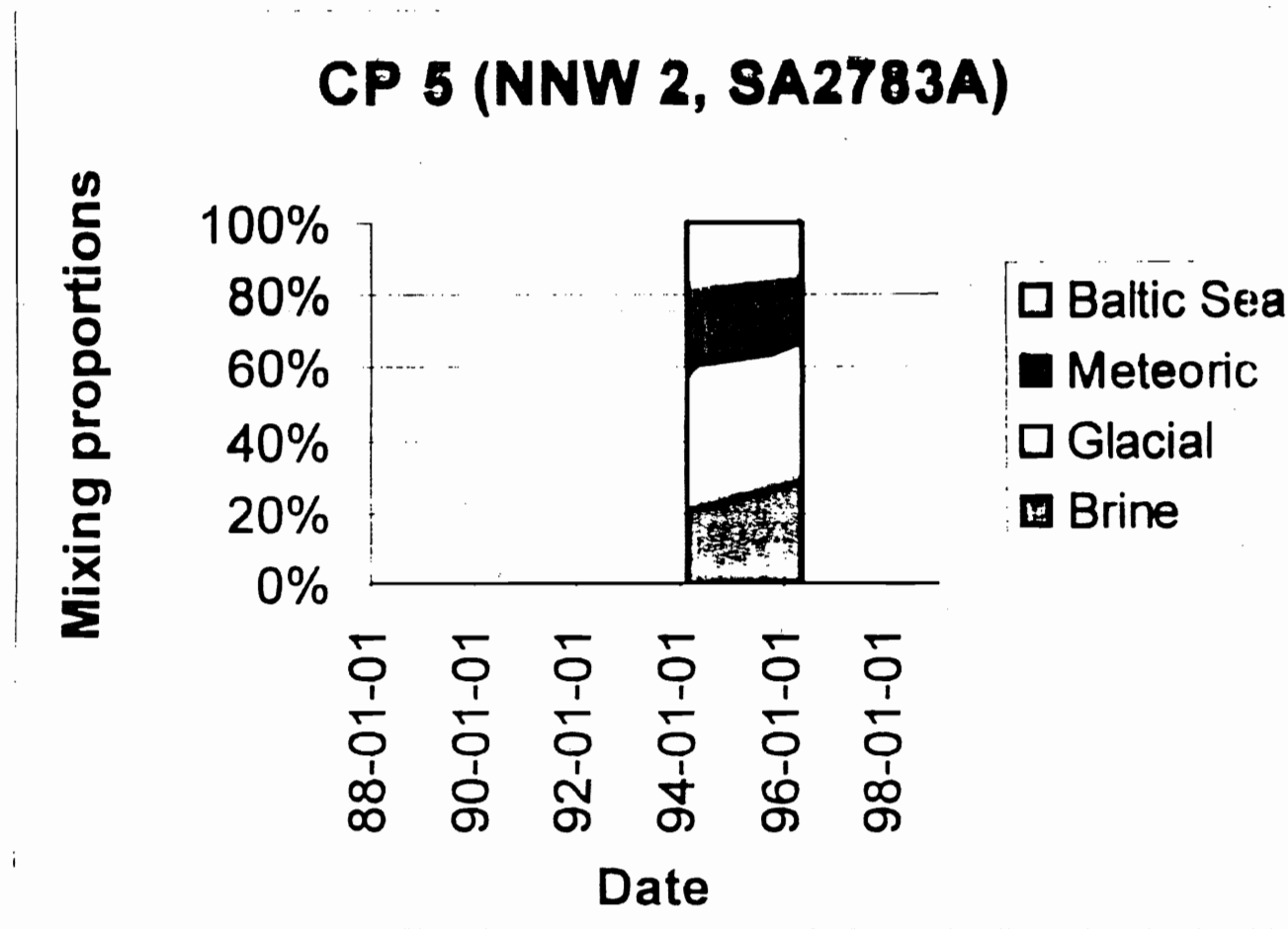
Task 5. Mixing proportions based on measurements at control points



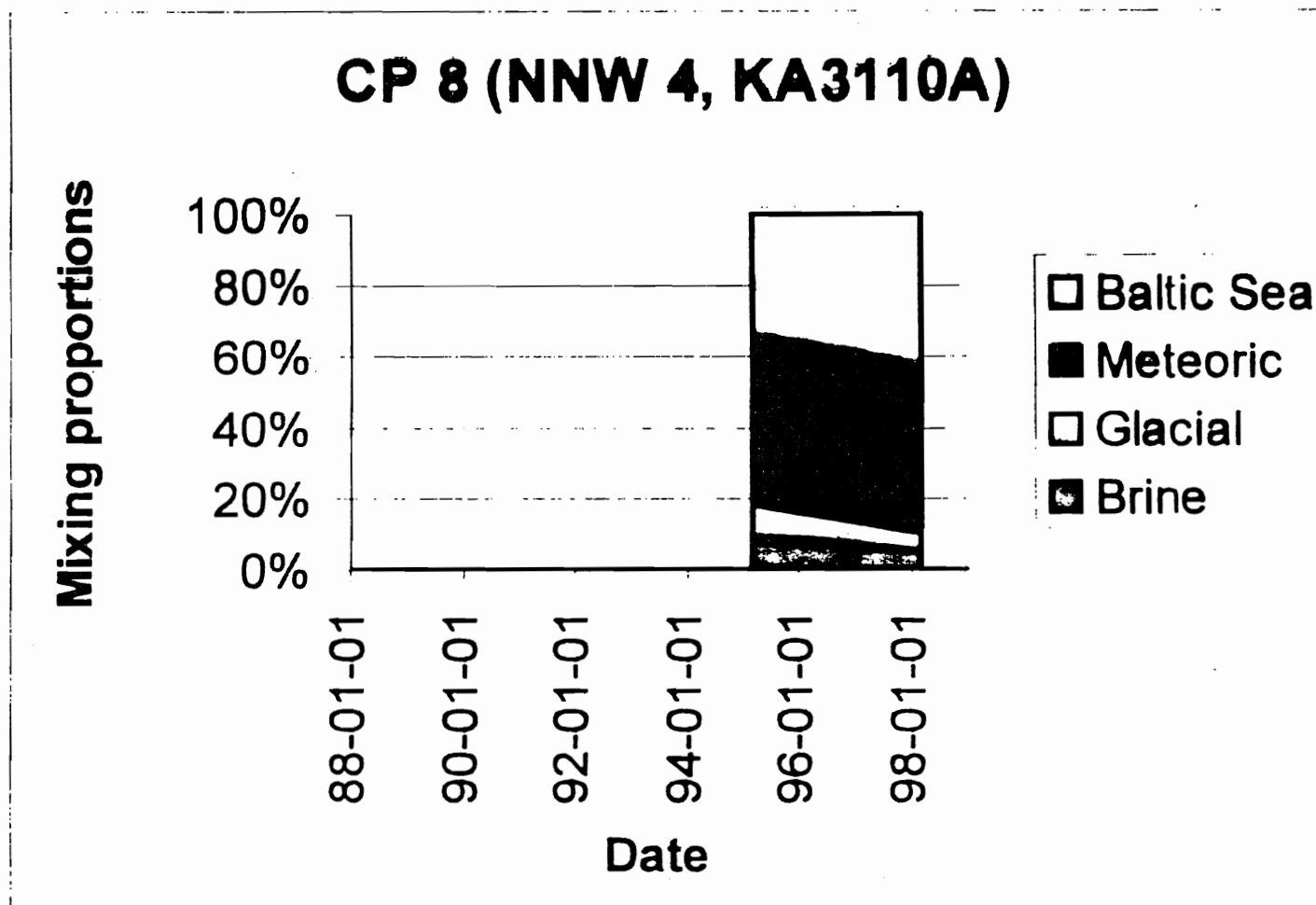
Task 5. Mixing proportions based on measurements at control points



Task 5. Mixing proportions based on measurements at control points



Task 5. Mixing proportions based on measurements at control points

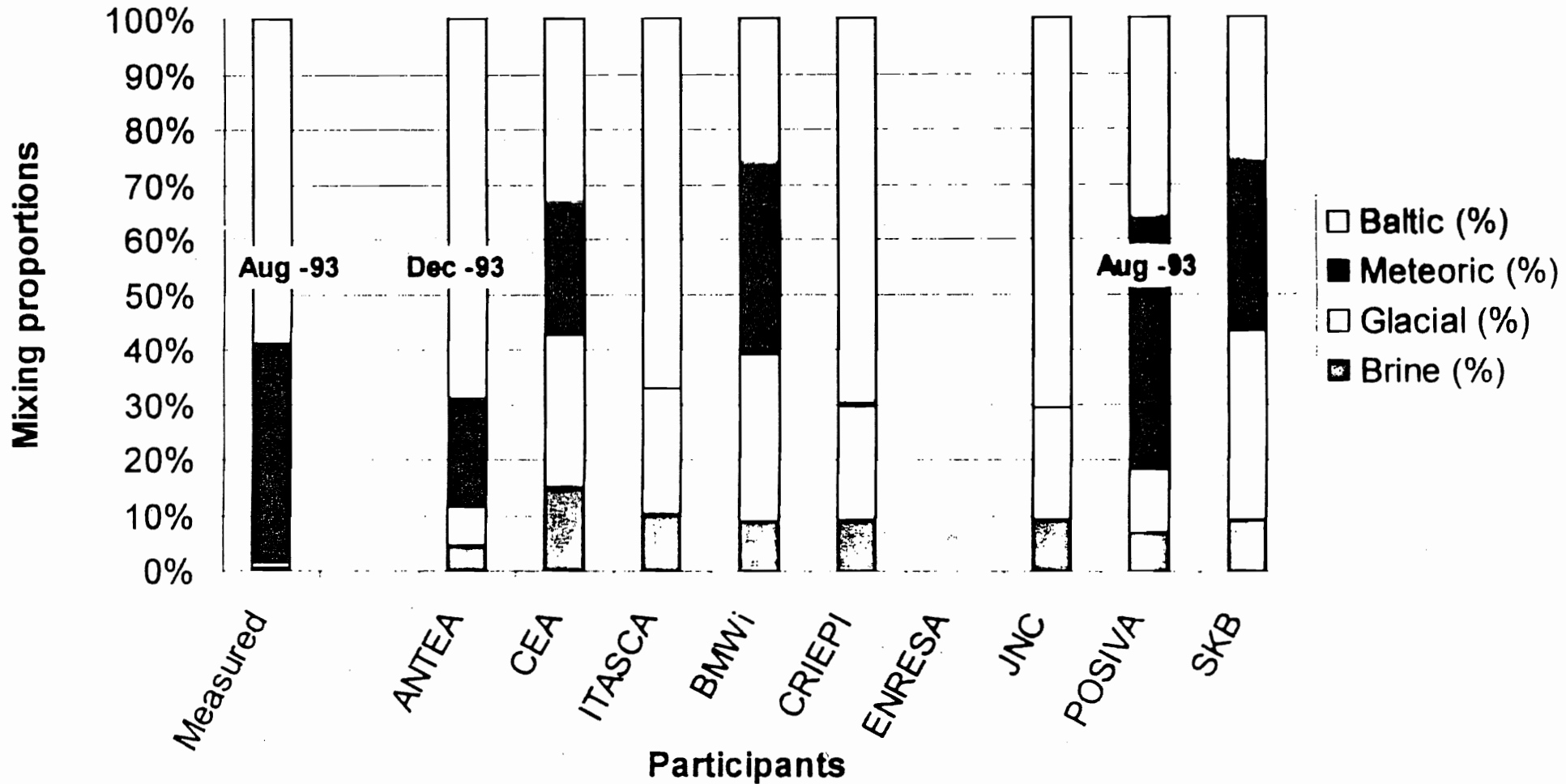


2000-02-04

Task 5. Task Force, Äspö HRL

Task 5. Predictions of mixing proportions

CP: 3 (SA1229A), NE 1, May 1991

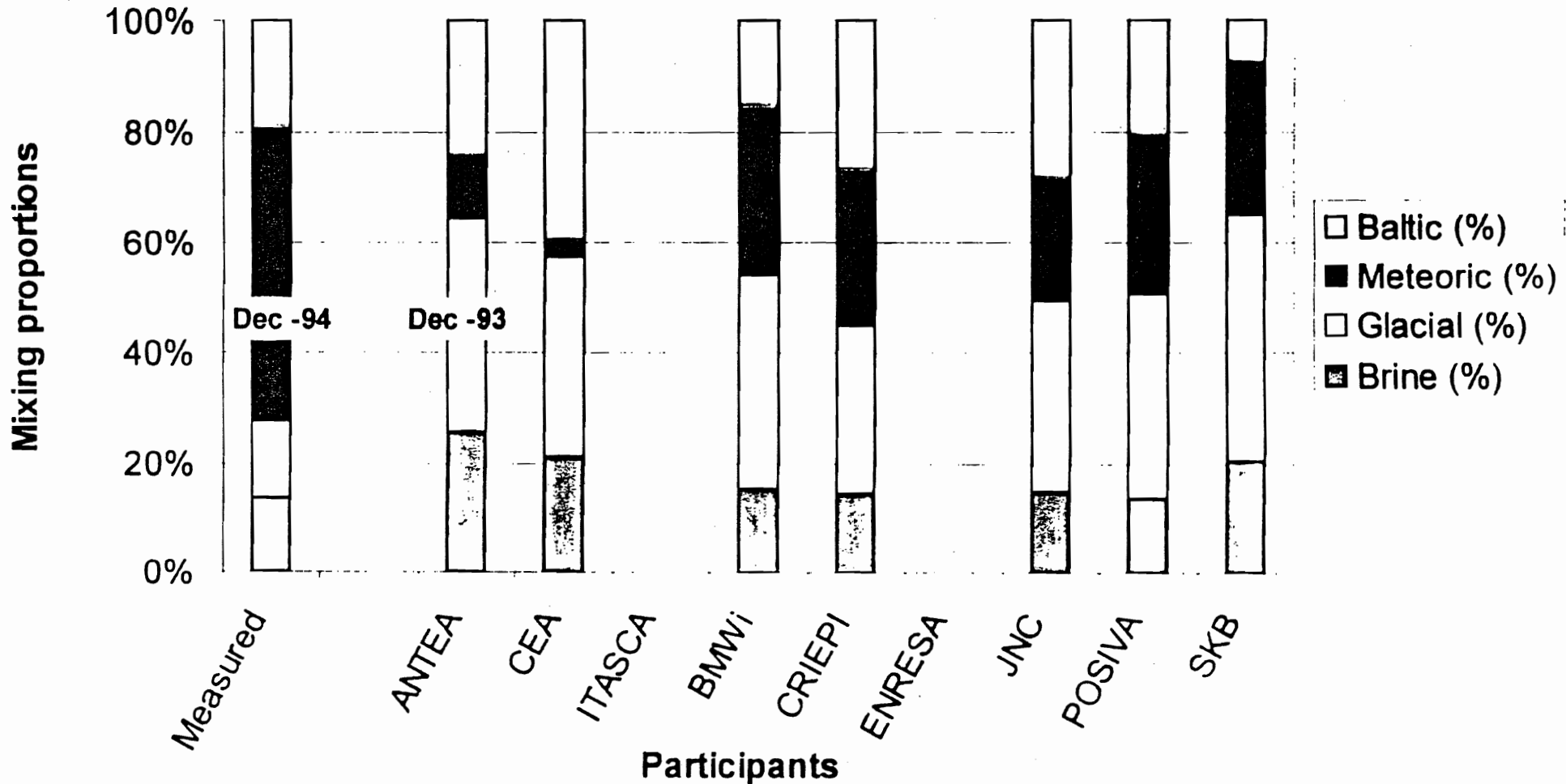


2000-02-04

Task 5. Task Force, Äspö HRL

Task 5. Predictions of mixing proportions

CP: 7 (KA3005A), HRD, May 1991

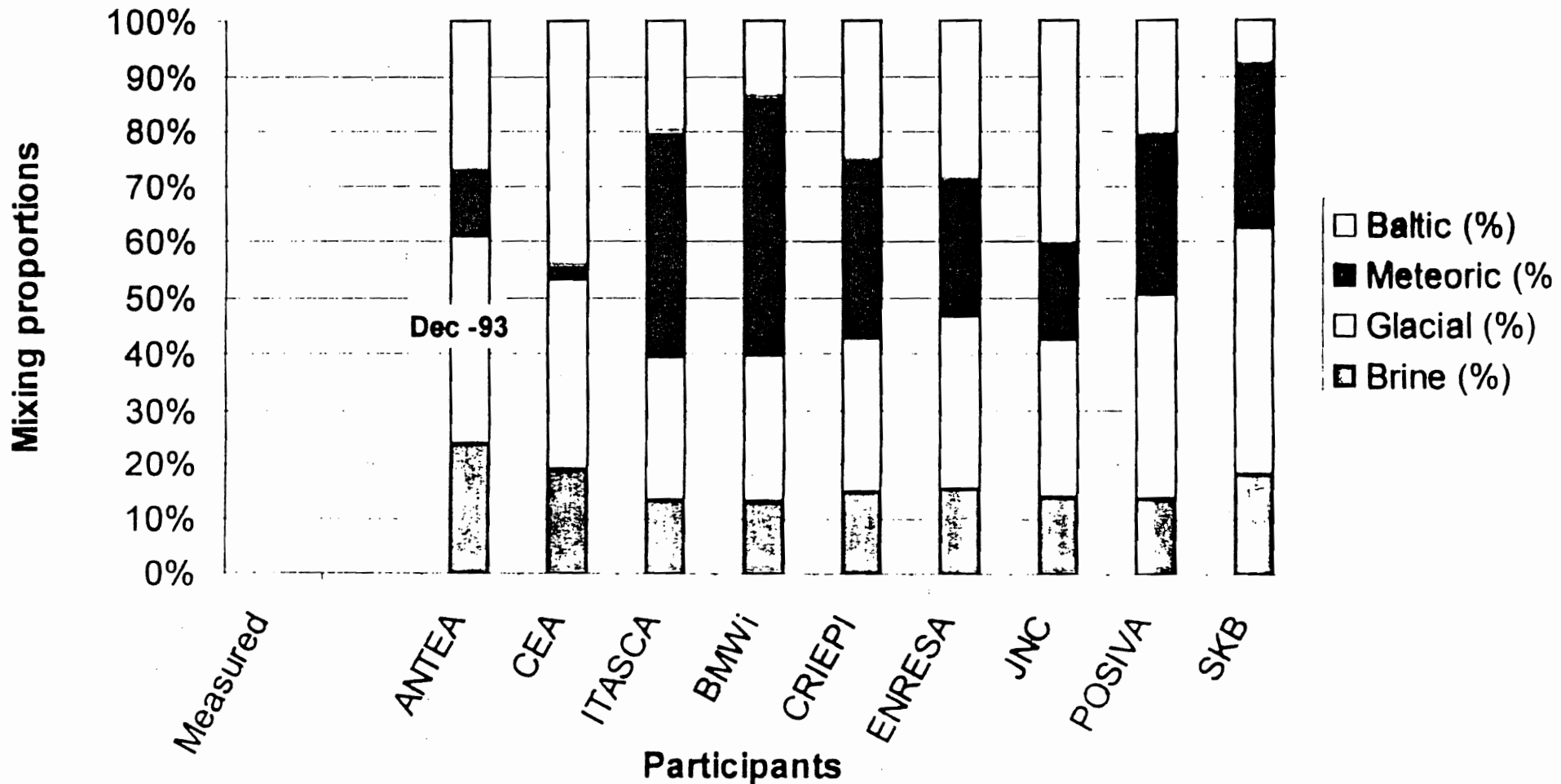


2000-02-04

Task 5. Task Force, Äspö HRL

Task 5. Predictions of mixing proportions

CP: 8 (KA3110A), NNW 4, May 1991

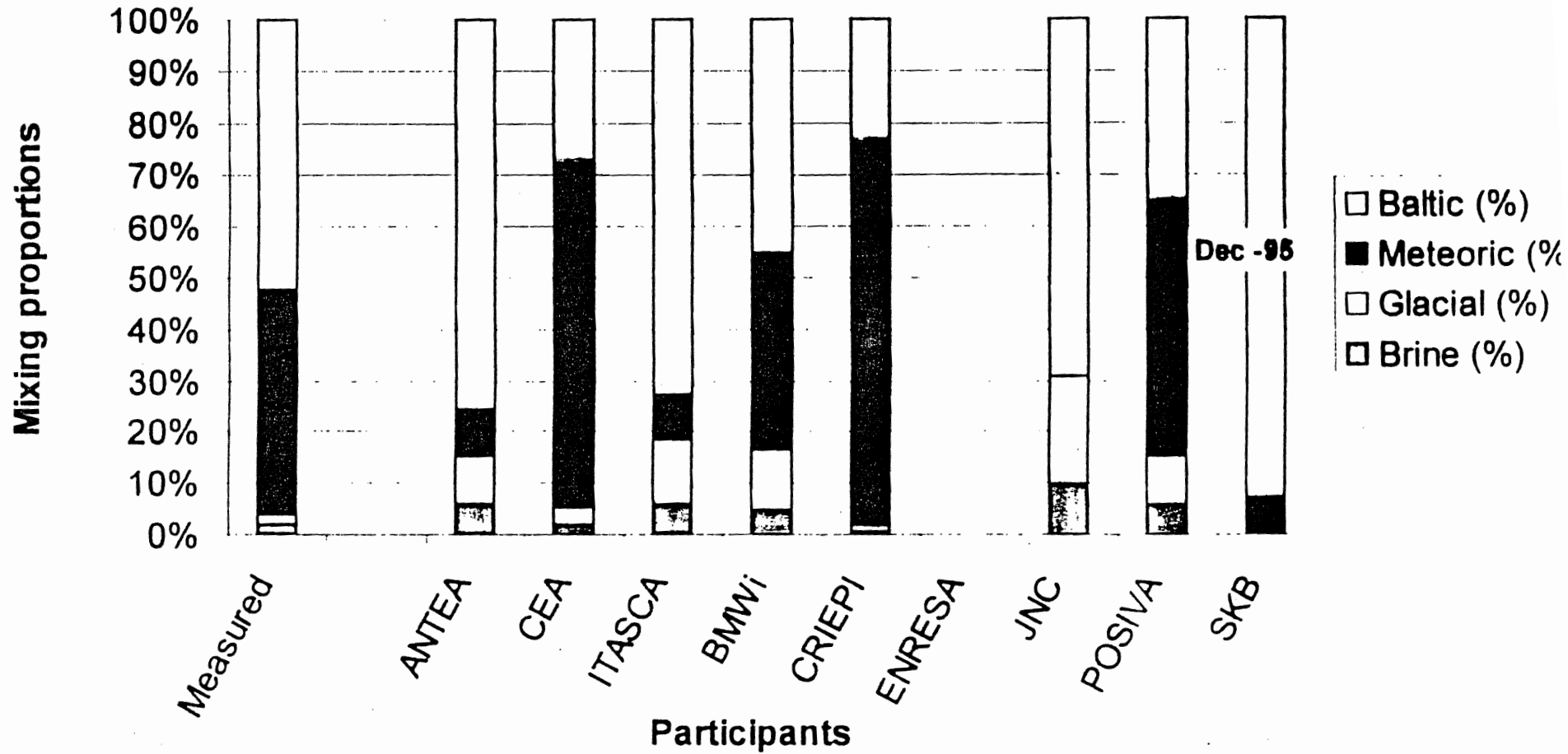


2000-02-04

Task 5. Task Force, Äspö HRL

Task 5. Predictions of mixing proportions

CP: 3 (SA1229A), NE 1, May 1995

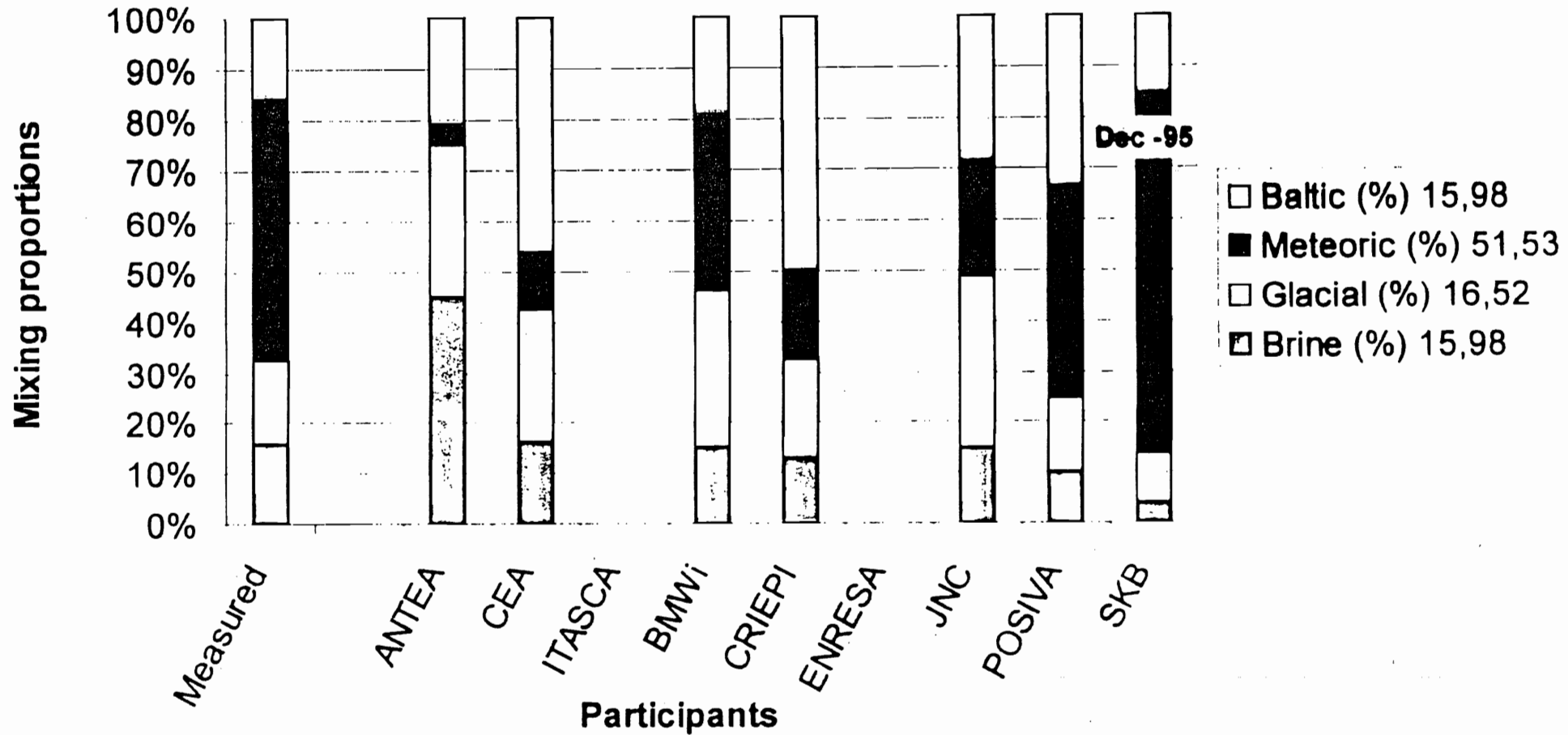


2000-02-04

Task 5. Task Force, Äspö HRL

Task 5. Predictions of mixing proportions

CP: 7 (KA3005A), HRD, May 1995

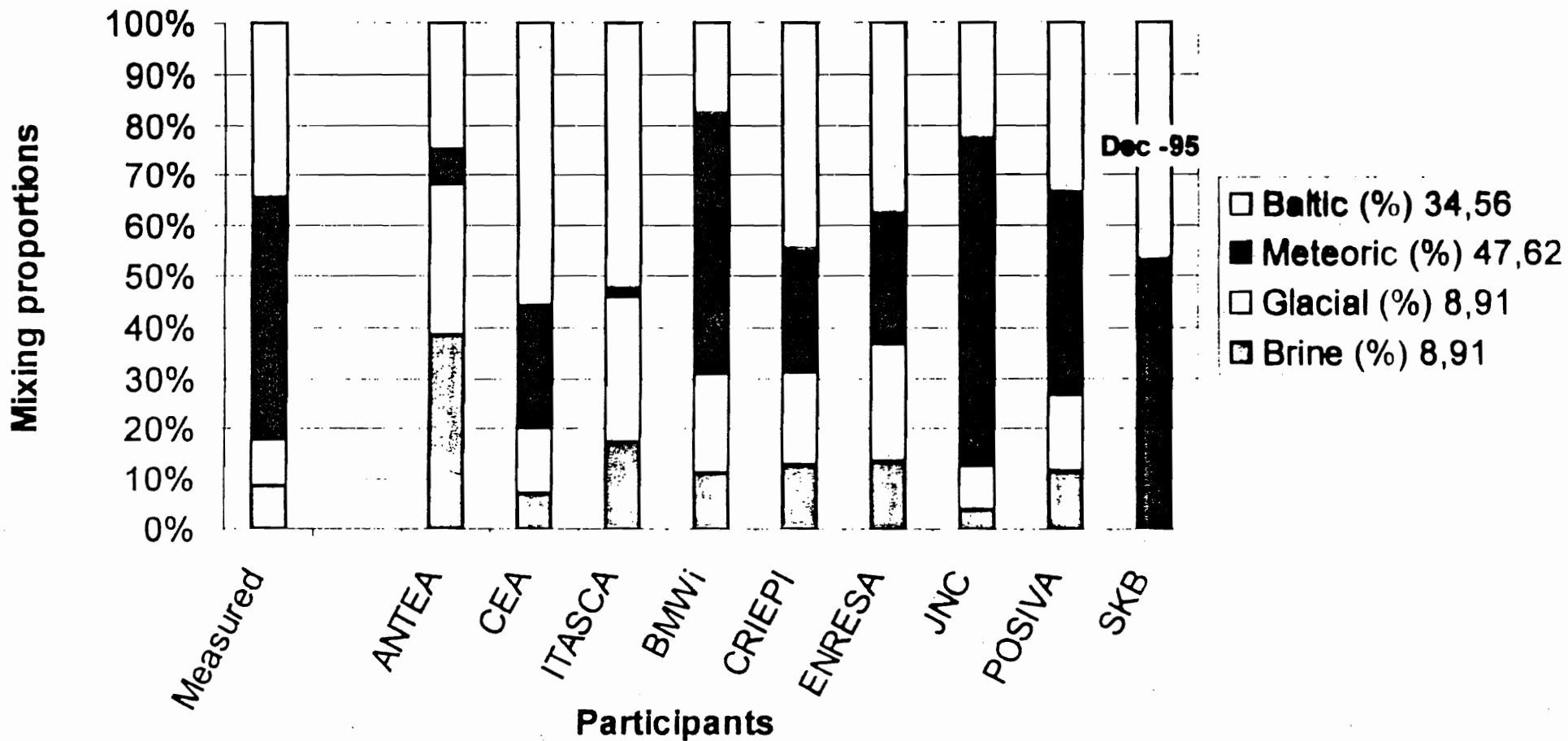


2000-02-04

Task 5. Task Force, Äspö HRL

Task 5. Predictions of mixing proportions

CP: 8 (KA3110A), NNW 4, May 1995

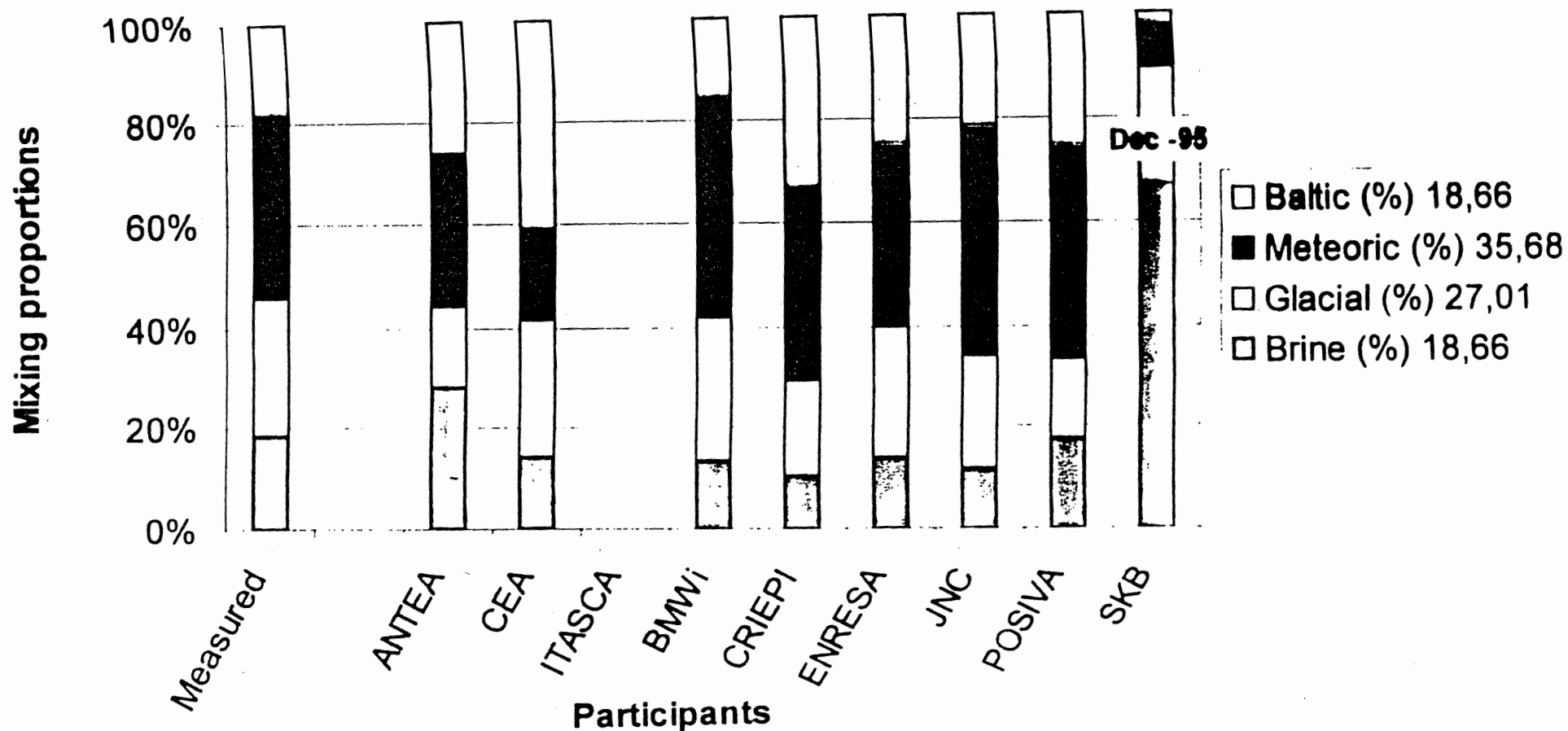


2000-02-04

Task 5. Task Force, Äspö HRL

Task 5. Predictions of mixing proportions

CP: 9 (KA3385A), NNW 7, May 1995



2000-02-04

Task 5. Task Force, Äspö HRL

Task 5. General conclusions

- Level of ambition varies between each of the groups; this is due to:
 - integration of hydrogeology and hydrochemistry is still at a primary stage of development,
 - as a result, few models exist that can integrate successfully the hydrodynamics and hydrochemistry of the groundwater system, and
 - time constraints, especially for those groups (i.e. French participants) who entered the project at a late stage.

Task 5. General conclusions

- Degree of hydrochemical integration mainly restricted to mixing proportions
- This is not so surprising since the modelled system is disturbed
- Consequently, water/rock chemical reactions, normally occurring under equilibrium conditions, have not been addressed
- In any case, the majority of the model approaches chosen could not accommodate such reactions

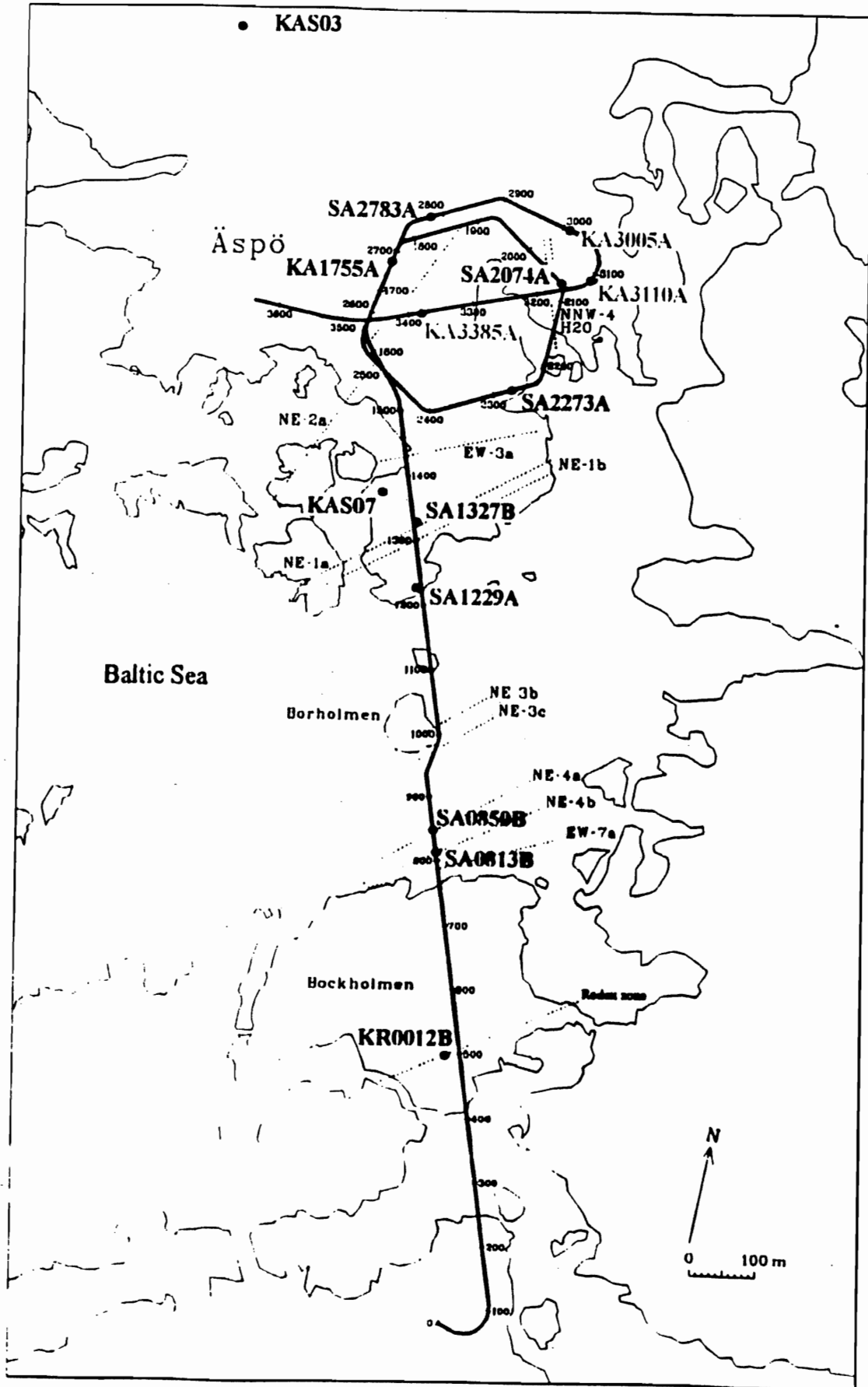
Task 5. General conclusions

- Results essentially validate M3 as being a very useful tool to calculate mixing proportions
- Posiva's mixing proportion calculations using different end-members also provides an alternative approach; the validity could not be fully tested
- Modelling of Redox Zone: Successful integration of hydrodynamics and chemical reactions, but not representative of the Äspö site as a whole

Task 5. Future Issues to be Addressed

- Development of coupled flow and hydrochemical models – particularly involving rapid kinetic reactions more relevant to present Äspö conditions, i.e. equivalent to the repository construction phase.
- Equilibrium water/rock reaction modelling (and PA-related solute transport modelling) is more relevant to repository post-closure conditions when 'equilibrium' groundwater conditions have been restored in the bedrock.

CONTROL POINTS LESS THAN 2900M
CONTROL POINTS MORE THAN 2900M



Comments by appointed Task 5 reviewer

A Bath (IntelliSci)

-
-
-
-
-
-
-
-
-
-

Äspö HRL: Task Force 5



Impact of tunnel construction on the groundwater system at Äspö.

A hydrological - hydrochemical model assessment



-
-
-
-
-
-
-
-

•
•
•

Preliminary review comments

- What are the objectives?
- Are objectives being met?
- What are the impacts and do the models predict them?
- Some comments
- Issues for the results integration

• • • • • • • •

•
•
•

Objectives

- To assess consistency of groundwater flow models and hydrochemistry mixing-reaction models through integration and comparison of hydraulic and hydrochemical data obtained during tunnel excavation.
- To develop procedure for integration of hydrogeological and hydrochemical data which could be used in assessment of potential sites.

• • • • • • • •

•
•
•

Consistency of Flow and Mixing Models

- Credible consistency and improvement of flow models
 - independently constrained by transmissivity versus inflows calibration (?)
 - success is measured in terms of 4 reference waters: is this adequate?
 - large variance among flow/mixing models

•
•
•

Development of procedure for sites

- Water mass deconvolution is only meaningful if dominant process is mixing i.e. more important than reaction;
- Baseline data and early-perturbation data are important for model testing;
- If reaction dominates over mixing, then flow model calibration is independent.

• • • • • • • •

-
-
-

Modelling impact of tunnel construction

- What could be the key impacts?
 - Up-coning and draw-down fluxes
 - Chemical draw-down (e.g. O_2)
 - Microbial/organic ingress, biofilms
 - Salinity increase
 - Rock property changes: dissolution, oxidation, etc
 - Outgassing

-
-
-

Modelling spatial distribution of impact

- Flow and flow/mixing impact is located around tunnel.
- Chemical impact may initially be located away from tunnel, e.g. at compositional interfaces or at reaction fronts (but mass transfers are low).

•
•
•

Some comments

- Heterogeneity and anomalies are significant
 - block scale flow and M3 analysis are likely to be inconsistent!
 - pathways and SC analyses are interesting, but new pathway versus storage concepts need to be tested - different implications for connectivity!
 - inverse reaction-mixing modelling seems to address problem explicitly.

• • • • • • • •

-
-
-

Further comments

- Undisturbed groundwater ‘masses’ distribution and boundary conditions are key uncertainties in comparison of flow and M3:
 - groundwater ‘masses’ distribution is a conceptual site-scale or regional issue;
 - boundary conditions are more problematic where the M3 method works well.

•
•
•

Integrating the results

- Are M3 reference compositions the final measure of consistency or an intermediate test? Why the wide range of modelled compositions at control points?
- To what extent is hydrochemistry an additional constraint on transmissivities or is it only a constraint on conceptual model, flow paths and boundary conditions?

• • • • • • • • •

-
-
-

Integrating results

- Other indicators of impact:
 - travel times from surface and seabed in drawdown cone
 - radius of mass transport versus pressure effects of tunnel (and anisotropy)
 - reactions: ion exchange, dissolution, redox
 - would additional hydrochemical parameters (conservative & reactive) be useful?

-
-
-

Final comment

- Terminology needs to be uniform
- M3 method and components need to be explained
- Be clear about modelled versus measured/interpreted groundwater mixtures
- Sort out the mass balance issues

Modelling of the Redox zone experiment

J Molinero (ULC)

enresa

**NUMERICAL MODELING OF GROUNDWATER FLOW
AND REACTIVE TRANSPORT IN A FRACTURE ZONE**

**THE REDOX ZONE EXPERIMENT OF THE ÄSPÖ
HARD ROCK LABORATORY**

FINAL REPORT Version 0.

Jorge MOLINERO, Javier SAMPER & Luis MONTENEGRO

**E.T.S. Ingenieros de Caminos. University of La Coruña.
Campus de Elviña, 15192-La Coruña (SPAIN)
Tel: +34 (9)81 16.70.00
Fax: +34 (9)81 16.71.70
<http://hydra.udc.es>**



ABSTRACT

This report contains the results of the coupled modeling of water flow and multicomponent reactive transport through the fracture zone of the Redox Zone at Aspo (Sweden). Available hydrogeological and hydrochemical data were first compiled and analyzed taking into account previous interpretations of the hydrochemistry and isotopes. Given the lack of previous hydrogeological models of the Redox Zone, a preliminary flow model was constructed which revealed the need to extend the modelling domain up to natural flow boundaries. A detailed review of topographic sources revealed relevant changes in land use near the experiment zone. This and other aspects and hypotheses about the Redox Zone Project were reviewed and analyzed. This analysis provided the basis for a second stage numerical flow and reactive transport model. Numerical modelling of chemical processes has been pursued by steps of increasing complexity. First, a hydrochemical model of mixing of recharge fresh and saline waters was constructed. Numerical analyses of mixing reveal some interesting conclusions regarding hydrochemical processes which are expected to take place during mixing of fresh shallow water and deep saline water. Mixing alone cannot explain the observed hydrochemical patterns during the experiment. Reactive transport modelling has been carried out both under 1- and 2-D conditions. First, a 1-D vertical numerical model of water flow and reactive transport was performed. Although this 1-D numerical model oversimplifies the flow system near the Redox Zone Experiment, it saves a lot of CPU time when compared to the 2-D numerical model. The 1-D model has been found useful for testing the convergence of numerical solutions and comparing various hydrochemical conceptual models. Once tested under 1-D conditions, conceptual models were solved under general 2-D conditions.

EXECUTIVE SUMMARY

EXECUTIVE SUMMARY

The Äspö HRL is located on the Baltic Sea coast near the town of Oskarshamn in S.E. Sweden. The access tunnel to the HRL starts at the coast line and proceeds approximately 1Km out under the sea floor and terminates under the island of Äspö. This access tunnel intersected a fracture zone at a depth of 70 m below the Baltic sea. The Redox Zone Project was launched in order to evaluate the effect of tunnel construction on the redox conditions of a deep granitic formation. TO that purpose this fracture zone was characterized prior, during and after the tunnel intersected the fracture. Hydrogeological, mineralogical, hydrochemical and isotopic studies were performed in order to understand and evaluate the evolution of redox conditions in the vicinity of the tunnel with special emphasis on the development of an oxidizing front. Available data have been extensively analyzed and interpreted qualitatively and using simple pure-mixing models and mass balance methods (Banwardt et al., 1999). The large availability of hydrochemical information in this experiment provides a unique opportunity to the validation of current numerical tools for coupled water flow and reactive solute transport such as the code CORE2D developed at the University of La Coruña. This study aims at evaluating the potential of these numerical models for integrating hydrodynamic and hydrochemical data into a quantitative model of the system.

1. Available data and previous analyses

A systematic sampling of groundwater was done in several boreholes and the tunnel wall during the Redox Zone Experiment. Collected data indicate that three weeks after the start of the experiment a sharp dilution front arrived to the access tunnel. This appeared as a dramatic decrease in Cl⁻ and base cation concentrations, and an increase in HCO₃⁻ concentration in the groundwater flowing from the roof of the tunnel. A short time later dissolved Fe concentrations in

the tunnel inflows decreased to near zero for a period of a few weeks. This could be taken as an indication of the arrival of an oxidation front to the tunnel position. After the initial dilution, the fracture zone at 70 m depth became increasingly saline. After 50 days both the significant dissolved Fe concentrations at all sample locations and the stable and continuously measured redox potentials (in the range $-150 < Eh < -100$) indicate that anoxic conditions prevailed in the fracture zone. pH remained constant near a value of 8 through out the experiment. HCO_3^- and SO_4^{2-} concentrations increase significantly during the experiment at all the sampling points located at 70 m depth while during the last part of the experiment the concentrations of most solutes remain relatively constant.

Dilution of the saline native groundwater by fresh recharge water is the dominant process controlling the hydrochemistry evolution during the experiment. Previous analyses of this experiment (Banward et al., 1999) used a conceptual mixing model in order to explain salinity evolution. Results of a pure mixing model (taking chloride as a conservative mixing fraction tracer) indicate possible significant sources for HCO_3^- , SO_4^{2-} and Na^+ and a sink for Ca^{2+} . The behavior of Na^+ and Ca^{2+} is apparently consistent with cation exchange, with preferential exchange of dissolved Ca^{2+} and displacement of exchanged Na^+ during the dilution process of the saline groundwater. Isotopic and microbiological studies conclusively ruled out SO_4^{2-} reduction, and provided evidence supporting Fe(III) reduction as respiration pathway for oxidation of organic C in the fracture zone. A large increase in ^{14}C activity was measured in both dissolved organic and inorganic C during the experiment, which provide evidence for young organic C being oxidized. Significant amounts of dissolved CH_4 were also found in the fracture zone, suggesting that active methanogenesis occurs.

There is no conclusive explanation for the increase in dissolved SO_4^{2-} . SO_4^{2-} originating from either the sea water, deeper groundwater, atmospheric deposition or Fe mono-sulfide mineral (found in the marine sediments surrounding the site) is not consistent with sulfur isotope data. Anion exchange due to

adsorption competition between HCO_3^- and SO_4^{2-} may occur, with HCO_3^- dominating the surfaces almost completely at the near neutral pH. Although the hypothesis of anion exchange is attractive it remains to be tested. An unknown source of groundwater with high SO_4^{2-} concentration entering the fracture zone during the experiment has been hypothesized. In spite of the fact that isotopical studies ruled out the dissolution of calcite as being the main process responsible for the increase in HCO_3^- concentrations, thermodynamic calculations show that shallow groundwater (0-15 m) is unsaturated with respect to calcite. Then, dissolution of this mineral could be expected to take place during the experiment.

2. Coupled groundwater flow and reactive transport modelling of the Redox Experiment

A coupled groundwater flow and reactive transport model entails modelling simultaneously groundwater flow, solute transport and hydrochemical reactions. A reliable solute transport model must rely on a sound groundwater model. For that reason, the construction of the coupled groundwater flow and reactive transport model of the Redox Zone Experiment was pursued in several stages:

- 2.1) Hydrogeological conceptual model and numerical groundwater flow model
- 2.2) Hydrochemical conceptual model
- 2.3) Solute transport model
- 2.4) Reactive transport model

Inasmuch as the purpose of the Redox Zone Experiment was mainly the evaluation of redox conditions, more emphasis was given to hydrochemical aspects than to hydrodynamic processes. This means that the previous hydrodynamic model at the redox zone was mostly qualitative with some limited hydrodynamic data (transmissivities and storativities).

The lack of a previous detailed and sound hydrogeological model for this fracture zone motivated the need to devote a lot of time to the construction of a groundwater flow model. Although the general flow patterns around the experiment are quite predictable, the construction of a flow model consistent with both hydrodynamic and salinity data is far from obvious. First of all, the flow and transport model must be able to explain the native salinity conditions at the site which exhibit the presence of a fresh-saline water interface. While it was simple to construct a flow model which could reproduce observed drawdowns, the same was not true for a flow and transport model which could explain simultaneously drawdowns and salinities measured at the tunnel and boreholes. The main difficulties found in constructing a sound flow and transport model were associated to boundary conditions, especially for the bottom boundary. In addition, the lack of sufficient hydrodynamic data did not allow a good representation of spatial heterogeneity. Sensitivity analyses performed with the flow and transport model indicate clearly the relevance of heterogeneity. Computed concentrations are very sensitive to changes in transverse dispersivities.

Once calibrated the flow and transport model, it was used to perform reactive transport simulations. Numerical analysis of mixing of fresh water and saline water were performed. They reveal some conclusions regarding hydrochemical processes which are expected to take place during mixing of fresh shallow water and deep saline water. Mixing alone cannot explain the observed hydrochemical patterns. Reactive transport modelling has been done in two steps. In the first step, a 1-D vertical numerical model of water flow and reactive transport is used. This 1-D model, which oversimplifies the flow system near the Redox Zone Experiment, saves a lot of CPU time when compared to the 2-D numerical model. The 1-D model has been useful for testing the convergence of numerical solutions and exploring and comparing various hydrochemical conceptual models. The reactive solute transport model accounts for aqueous complexation, acid-base reactions, redox processes, cation exchange and dissolution /precipi-

tation of quartz, goethite, pyrite and calcite. Mixing of fresh shallow waters with deeper saline waters induces calcite and pyrite dissolution and goethite precipitation.

Once tested under 1-D conditions, conceptual models were solved under general 2-D conditions. The basic reactive transport model accounts for aqueous complexation, acid-base reactions, redox processes, cation exchange and dissolution /precipitation of quartz, goethite, pyrite and calcite. Other alternative hydrochemical models were proposed which include: 1) anion exchange, which unfortunately cannot be accounted for by CORE2D, 2) oxidation of organic matter by a Fe(III) solid phase, this hypothesis is thermodynamically inconsistent with available redox potential data, 3) presence of gaseous phases (CO₂, O₂) their partial pressures being modified by tunnel and borehole construction. This hypothesis has been tested for CO₂ and has been discarded, 4) methane production processes which require redox potentials much more reducing than those measured at the boreholes, and 5) additional sources of sulfate and calcium which could come from alkaline sulfate-rich waters leaching from the nearby landfill. This hypothesis was tested, but severe convergence problems were found which prevented to draw a sharp conclusion.

The reactive transport model is able to reproduce the observed trends of chloride, potassium, lithium, bromide, calcium and strontium. As expected, differences are observed in dissolved bicarbonate, sulfate and sodium.

Appendix C - Task 5 Data deliveries

Data delivered to Task 5 modelling groups up to TF#13

Delivery No	Type of data	Delivery data
1	Hydrochemical data	February 1998
2	Meteorological, tunnel and zone geometry, excavation history and hydrochemical tunnel data	March 1998
3	Piezometric levels and salinity in borehole sections, borehole coordinates	March 1998
4	Hydrochemical initial and boundary conditions	June 1998
5	Topographical data for the site	August 1998
6	Hydraulic interference tests including LPT2 (Task 1&3 deliveries)	November 1998
7	Update on hydrochemical initial and boundary conditions	October 1998
8	Performance measures and control points	November 1998
9	Water flow into the Äspö tunnel	February 1999
10	Topographical data of Äspö and surroundings, larger area than in data delivery No 5.	(May-99)
11	Boundary and initial conditions for pressure and salinity from regional model (TR-97-09).	(June-99)
12	Transport parameters from four in-situ experiments at Äspö	(June-99)
13	Control points outside the tunnel	(June-99)
14	Chemical groundwater reactions encountered at Äspö HRL	(June-99)
15	Updated control points outside the tunnel. Supersedes Data delivery No 13 and part of No 8.	(Oct-99)
16	Tunnel drilled boreholes with inclination and declination	(Nov-99)
17	Comments on tritium values	
18	Piezometric level in surface drilled boreholes measured during excavation of Aspo HRL. Data for calibration and prediction periods, approx. up to Dec-96.	(Jan-00)
19	Hydrochemistry data before and during excavation of Aspo HRL. Data for calibration and prediction periods, approx. up to 1998.	(Jan-00)

Appendix D Task 4 bibliography

Winberg, A. (ed), 1996. First TRUE Stage - Tracer Retention Understanding Experiments. Descriptive structural-hydraulic models on block and detailed scales of the TRUE-1 site. SKB International Cooperation Report ICR 96-04

Dershowitz, W. et al, 1996. Discrete fracture analysis in support of the Äspö Tracer Retention Understanding Experiment (TRUE-1). SKB International Cooperation Report ICR 96-05

Tanaka, Y., et al, 1997. Numerical analysis with FEGM/FERM for TRUE-1 non-sorbing tracer tests. SKB International Cooperation Report ICR 97-07

Gylling, B et al, 1998. Modelling of the Tracer Retention Understanding Experiment Task 4C-D using the channel network model. SKB International Cooperation Report ICR 98-01

Liedtke, L. & Shao, H., 1997. Modelling of tracer experiments in feature A at Äspö HRL. SKB International Cooperation Report ICR 98-02

Poteri, A., 1998. Modelling of the tracer tests in radially converging and dipole flow fields in the first phase of the TRUE project. SKB International Cooperation Report ICR 98-03

Worraker, W., Holton, D., Cliffe, K.A., 1998. Modelling TRUE-1 (RC-1) tracer tests using a heterogeneous variable aperture approach. Äspö Task Force, Task 4C. SKB International Cooperation Report ICR 98-06

Selroos, J-O., Cvetkovic, V. 1998. Prediction of the TRUE-1 radially converging and dipole tracer tests. Äspö Task Force, Tasks 4C and 4D. SKB International Cooperation Report ICR 98-07

McKenna, S.A., 1999 Solute transport modelling of the Äspö STT-1b tracer tests with multiple rates of mass transfer. Task 4E - Äspö Task Force on Modelling of Groundwater Flow and Transport of Solutes. SKB International Cooperation Report ICR-99-02